Spring 5-31-2021

The Synthesis of Heterogeneous Catalysts: Transition Metal Nanoparticles Encapsulated in Halloysite and Applications in Organic Transformations

Jumanah Hamdi
University of New Orleans, New Orleans, jhamdi@uno.edu

Follow this and additional works at: https://scholarworks.uno.edu/td

The Synthesis of Heterogeneous Catalysts: Transition Metal Nanoparticles Encapsulated in Halloysite and Applications in Organic Transformations

A Dissertation

Submitted to the Graduate Faculty of the
University of New Orleans
in partial fulfillment of the
requirements for the degree of

Doctor of Philosophy
in
Chemistry

by

Jumanah Hamdi

B.S. University of New Orleans, 2015
M.S. University of New Orleans, 2019

May, 2021

Dedication

The completion of this project would not have been accomplished without the support of my family and friends. I would particularly like to dedicate my dissertation work to my two beautiful and very patient boys Gavin and Noah Mitchell. They both probably think that mommy will have a dissertation to work on for the rest of their lives, considering I have been working on it a large part of theirs. Thank you, my boys, for being so patient with me and understanding when I had to stay at work so many late nights and miss out on family time. Thank you for always telling me how proud you are of me. I cannot wait to start this new chapter of my life with you two always by my side. I love you both with all my heart, and you are an inspiration for everything I do.

I want to give a special thank you to my only best friend, Brooke Diehl. Her continuous support and care are what kept me going even when I felt like burying my head in the sand and pretending that it did not exist. She was there through it all. From mental breakdown days to her and me "just doing some science" days. She kept my spirit up and reminded me each day that I am strong, bright, and beautiful and that I got this. Her famous quote, "My baby so smart," put a smile on my face each day, and having her by my side is what kept me going. She was my rock through it all. I love you, Brookie, and thank you for everything.

A special thank you to the father of my children, Joseph Mitchell. He supported my decision to join the Ph.D. program. He believed in me more than I believed in myself. Regardless of what life has in store for us both, I owe him a huge thank you for this. I genuinely appreciated everything he did for me to help make this happen.

I would also like to thank all my friends and family for all their support over the years. My twin Kati Keegan, my sister Brittany Pineda for being there for me through it all. Without you two in my life, I would not have been able to keep pushing through each day, so thank you for being my family always and forever. I would also like to thank other family members who helped me reach this goal. Elizabeth Murillo, Carla Gendusa, Anthony Mitchell, John Mitchell, Shelley Mitchell, and Nicole Kittok for constantly babysitting my children to have the time to get all my research and writing done. Thank you for being there for me through it all. The support I received from you all will never be forgotten and will always be appreciated.

One extraordinary person that has a significant influence on me and the reason I am here today is my mentor and friend, Dr. Stacey Lomenzo. Thank you for mentoring me and taking me under your wing as an undergraduate student and giving me the chance to learn so much from you. I was uncertain about my plans after my B.S. degree, and working with you that summer was an experience I will always cherish and remember. I remember falling in love with research just only after three days of working with you that summer. It helped me make my decision to pursue a Ph.D. in chemistry. I wanted to be just like you. Our friendship grew so much over the years, and I could not have asked for a better mentor and friend. Thank you for everything, and I appreciate everything you have done for me.

Finally, I would like to thank the man who made my dream come true, Dr. Mark Trudell. You took a chance on me when you accepted me into the program. I probably did not sound like the ideal candidate on paper, but you saw a flame in me and decided to take me on and give me this fantastic opportunity that many do not get in life. I want to say thank you from the bottom of my heart because that chance you took changed my life forever. You believed me and knew that you just needed to spark my flame to start a fire in me. You pushed me every day to be the best that I

can be. You put your trust in me to get things done. Thank you for taking that chance years ago

and accepting me into the Trudell group. The support I received from you was beyond my

expectations. I could not have asked for a better mentor and now company partners but mostly a

friend. The friendship we now have will be one I cherish for the rest of my life.

Acknowledgment

I want to express my sincerest gratitude to all the individuals and entities who directly and indirectly impacted my career as a researcher. I want to thank my advisor first, Dr. Mark Trudell, who has never failed to support my research endeavors. His proficiency in organic chemistry, organometallic, and, more importantly, his willingness to help me understand some of our study's most complex aspects was essential to my success.

I want to thank every single old and new member of the Trudell group members for the continuous support. I would also like to thank the other committee members, Dr. Branko Jursic, Dr. John Wiley, Dr. Victor Poltavets. I want to like to thank Dr. Wiley for providing his insight as an inorganic chemist to my research. A special thanks to Dr. Alexis Blanco for providing all the TEM images presented in this dissertation. I want to thank Dr. Poltavets, his group members for providing the XRD data presented in this dissertation. And a special thank you to Dr. Jursic for all his support throughout my time here. You were always available to help anytime I needed him. The friendship we have is one that I hold dearly. I want to thank Dr. Phoebe Zito for her mental support and friendship.

I thank these individuals for their impact on my professional development and their friendships over the years. Thanks to the Chemistry Department at the University of New Orleans for contributing most of the financial support of my projects. Most importantly, I would like to thank my family for all their unwavering love and support throughout my life. None of this would have ever happened without them.

Contents

List of Schemes

Chapter 4

List of Figures

Chapter 3

Chapter 4

Chapter 5

List of Tables

Chapter 1

Chapter 2

Chapter 3

Chapter 4

Chapter 5

Abstract

The natural scrolled clay, halloysite, was studied as a catalyst and solid support for the development of encapsulated transition metal nanoparticles (M@Hal). With the unique tubular nanostructure, raw halloysite exhibited remarkable chemical reactivity superior to other clays in the esterification of biomass-derived carboxylic acids. Raw halloysite was also effective in the esterification of various aromatic and non-aromatic carboxylic acids. These results indicated that halloysite has the potential utility as a "Green" heterogeneous catalyst for a broad scope of esterification applications.

A novel Pd@Hal nanocomposite was synthesized under ambient conditions. The newly prepared catalyst was applied to the widely used Suzuki-Miyaura cross-coupling reaction. This nanocomposite material produced exceptionally high yields of biaryl compounds under ambient conditions. Complete product conversion was obtained with no byproducts using an alcohol: water solvent system at room temperature. It showed excellent results with both hydrophobic/ hydrophilic substrates. The Pd@Hal nanocomposite was also utilized in the hydrogenation reaction of nitro compounds. It exhibited high reaction yields of the corresponding aniline derivatives under ambient conditions. The catalyst was shown to be recoverable and recyclable in both reaction systems without significant loss of catalytic activity.

A reliable method was developed for the preparation of the Ir@Hal nanocomposite. The Ir@Hal catalyst was very efficient for the hydrogenation and transfer hydrogenation of phenol to furnish cyclohexanol. The Ir@Hal nanocomposite effectively hydrogenated various aldehydes and ketones with a broad scope of substrates under very ambient conditions. The catalyst was shown to

be recoverable and recyclable without significant loss of catalytic activity for both the hydrogenation of phenol and cyclohexanone to yield cyclohexanol.

The M@Hal nanocomposites developed in this study proved robust and stable under various reaction conditions. Furthermore, as catalysts, these M@Hal nanocomposites afforded high yields of the target compounds, were amenable to scalable conditions, and exhibited incredible rate enhancement for various organic transformations. In addition, these M@Hal nanocomposites demonstrated the further utility of halloysite as a support for the development of transition metal-based nanocomposite for heterogeneous catalysis having all the advantages of easy separation, easy recovery, and excellent solubility/dispersion.

Keywords: Transition metals, Halloysite, M@Hal, heterogeneous catalysts, Pd@Hal, Ir@Hal, Organic transformations, recovery, Green Chemistry, Suzuki-Miyaura Cross-Coupling, hydrogenation

Chapter 1

Introduction

1.1   Green Chemistry

Green innovation aims for safer, energy-efficient, reduced waste for products and processes. Such products and procedures are based on renewable materials and have a low net impact on the environment. Green nanotechnology is about manufacturing processes that are economically and environmentally sustainable. Industries can apply green chemistry principles to produce safer and more sustainable nanomaterials and more efficient and sustainable nanomanufacturing processes. There is rising pressure from both society and governments for chemistry-based industries to become more sustainable by developing eco-friendly products and strategies that reduce waste and prevent toxic substances from entering the environment. As is often the case, novel and innovative thinking may solve significant science issues, liberating itself from the old beaten paths on how things were done in the past. Such a new review often results in bold and ground-breaking solutions. [1]

The chemical industry is critically important to the world economy; however, its success has led to environmental damage. A greener approach needs to be adopted to prevent additional environmental and public health damage. Green chemistry promotes the careful design of chemical manufacturing processes to reduce toxic components and reduce or eliminate waste and energy use. Industries, universities, and government agencies worldwide are putting in the necessary work to develop more sustainable and efficient procedures that follow green chemistry's principles. Green chemistry is an approach to chemistry that aims to increase efficiency and reduce hazardous effects

on human health and the environment. While no reaction can be entirely "green," the chemical industry can help reduce the overall negative impact by implementing the 12 principles of Green chemistry whenever possible.[2] Paul Anastas proposed that chemistry should be done by using benign chemicals and processes. The proposed focus was on using harmless chemicals instead of toxic ones, developing new, safer chemical processes, and redesigning the old chemical processes to make them milder.[2]

1.1.1 History of Green Chemistry

Green chemistry was initially established as a response to the Pollution Prevention Act of 1990, which proclaimed that U.S. national policy should reduce pollution by enhancing the design of products and processes. By 1991, the U.S. Environmental Protection Agency (EPA) Office of Pollution Prevention had initiated a research grant program urging the redesign of existing chemical products and processes to reduce impacts on human health and the environment. The EPA provided funding in the early 1990s for basic green chemistry research with the U.S. National Science Foundation (NSF). The 12 Principles of Green Chemistry that we use today were issued in 1998, offering clear guidelines for developing chemicals and processes.[3] The Royal Society of Chemistry launched its Green Chemistry journal in 1999. In 2005, the Nobel Prize in Chemistry was awarded to Yves Chauvin, Robert H. Grubbs, and Richard R. Schrock "for developing the metathesis method in organic synthesis." [4] These discoveries provided a chemical reaction now used daily in the chemical industry to produce environmentally friendly products, such as pharmaceuticals, fuels, synthetic fibers, and many other products. This discovery was a significant step forward for green chemistry.

1.1.2 Twelve Principles of Green Chemistry

1. Waste prevention: prioritize waste prevention rather than cleaning up and treating waste after being created. Plan to minimize waste at every step.[5]

2. Atom economy: reduce waste at the molecular level by maximizing the number of atoms from all reagents incorporated into the final product. Chemists should aim to minimize the E-factor (ratio of all reaction waste mass to the desired product mass). Use the atom economy to evaluate reaction efficiency.[5]

3. Less hazardous chemical synthesis: Design chemical reactions and synthetic routes to be as safe as possible. Consider the hazards of all substances handled during the reaction, including waste.[5] A safer synthesis may reduce the number of isolations and purifications. [2]

4. Designing safer chemicals: minimize toxicity directly by molecular design, predict and evaluate aspects such as physical properties, toxicity, and environmental fate throughout the design process.[5]

5. Safer Solvents and Auxiliaries: choose the safest solvent available for any given step. Minimize the total amount of solvents and auxiliary substances used, as these make up a large percentage of the total waste created. [2, 5]

6. Design for energy efficiency: energy requirements should be established for their ecological and economic impacts and reduced. Synthetic procedures should be conducted at ambient temperature and pressure. [2, 5]

7. Use of Renewable feedstock: use chemicals made from renewable sources rather than other equivalent chemicals originating from petrochemical sources. Another advantage of renewable feedstocks is that the feedstock's oxidation state is often close to its desired product.

8. *Reduce Derivatives:* Avoid derivatives to reduce reaction steps and waste created. [2, 5]

9. *Catalysis:* Use catalytic instead of stoichiometric reagents in reactions. Choose catalysts to help increase selectivity, minimize waste, and reduce reaction times and energy demands. [2, 5]

10. *Design chemicals and products for degradation*: Design chemicals that degrade and can be removed easily from the environment and ensure that both chemicals and their degraded products are not toxic to the environment. This principle is perhaps one of the most challenging principles to apply, despite sound experimental evidence of what groups degrade well in the environment. Products must be stable long enough to be available before and during use. [2, 3]

11. *Real-time to prevent pollution:* Include in-process real-time monitoring and control during syntheses to minimize or eliminate the formation of byproducts.

12. *Minimize the potential for accidents:* Select chemicals and their physical forms to reduce the potential for chemical accidents, avoid substances that are corrosive, reactive, or acutely toxic. [2, 3]

1.2 Nanoscience

Nanotechnology is an evolving field. It is an interdisciplinary science with extraordinary capabilities that have been widely advertised for well over a decade. Nanotechnology, as an emerging technology, offers a significant prospect for the scientific community. The development of both new nanomaterials and production techniques provides a substantial opportunity for designers. Nanotechnology can play an essential role in bringing a pivotal functionality to a product; Nanotechnology may represent a small percentage of a final product whose essential functions hinge on exploiting nanotechnology's size-dependent phenomena. [6, 7]

Today, nanotechnology is a prominent scientific field since it combines knowledge from Physics, Chemistry, Biology, Medicine, Informatics, and Engineering.[7, 8] The application and use of nanomaterials in electronic and mechanical devices, in optical and magnetic components, quantum computing, tissue engineering, and other biotechnologies, with smallest features, widths well below 100 nm, are economically the most essential parts of nanotechnology nowadays and presumably in the future. The number of nanoproducts is rapidly growing, with more nanoengineered materials reaching the global market.[9] The continuous innovation in nanotechnology will result in the fabrication of nanomaterials with properties and functionalities that will positively change human health, the environment, electronics, and many other fields.

Nanotechnology can help solve severe global issues such as energy adequacy, climate change, or fatal diseases. Nanotechnology is an area with up-and-coming prospects for turning fundamental research into successful innovations. It will boost the industry's competitiveness and create new products that will positively influence the medical field and the environment. Nanoscience and nanotechnologies open up new research opportunities and lead to new, useful applications, especially in the medical treatments of fatal diseases, such as brain tumors and Alzheimer's disease.[9] Nanomaterials with unique properties allow for new applications to be discovered. Products containing engineered nanomaterials are already on the market; these include metals, ceramics, polymers, smart textiles, cosmetics, sunscreens, electronics, paints, and varnishes. However, new methodologies and instrumentation are needed to increase the knowledge of the properties of the material. Nanomaterials must be assessed for potential effects on health as a precaution and their possible environmental impacts.[7]

1.2.1 Green Nanoscience

Over the past decade, nanotechnology has made significant advances, moving nanotechnology closer to achieving its green potential. However, some novel solutions could have adverse effects on the economy and environment, such as health and safety (EHS) risks (e.g., high energy manufacturing processes and processes that may rely on toxic materials)[1]. These risks must be lessened in advancing green nanotechnology solutions. Environmentally friendly production can be obtained through nanotechnology by joining nanoscience and green chemistry principles.

Green nanoscience seeks to produce greener nanomaterials and to develop effective synthetic processes. Like green chemistry, green nanoscience aims to reduce or eliminate hazards to human health and the environment through product design and process optimization. Green nanotechnology can have various roles and impacts on a wide variety of products. Green nanotechnology is expected to impact an extensive range of economic sectors. Products incorporating multiple green technological innovations such as biotechnology and energy technologies are being developed and used worldwide.[1] Green nanotechnology aims for energy efficiency, reducing waste and toxicity in the earliest stages of molecular design and production to alleviate the ecological effects and enhance the safety and efficiency of chemical production, use, and disposal. Green nanotechnology can support the development of sustainable solutions to address global issues of environmental concern. It takes a lifecycle approach to minimize the undesirable effects of chemicals and their production.[1]

1.3 Catalysis

Chemical reactions involve changes in the arrangement and bonding of atoms in molecules, characterized by a reduction in free energy, the absorption/release of heat, and changes in the state of ordering the system. The reaction rate is determined by the energy pathway for the conversion of

reactants to products. The use of catalysis can improve the economic processes in both productivity and energy consumption. A catalyst is defined as a substance that increases the rate at which a chemical reaction approaches equilibrium without itself being consumed in the process. The definition above has three key features: **(i)** catalysts increase the rate by reducing the activation energy barrier between reactants and products; **(ii)** catalyst concentrations do not influence positions of equilibrium; and **(iii)** reaction should leave the catalyst in a condition such that it can affect an infinite number of further conversions. However, there are two important implications. The lowered activation energy barrier and the unmodified equilibrium position require that the reverse reaction be catalyzed to the same degree as the forward reaction. Therefore, a good hydrogenation catalyst will also be a good dehydrogenation catalyst under appropriate conditions. Also, that the surface is regenerated after each reaction turnover so that the catalyst has an infinite lifetime. This is particularly important but usually compromised in practical application. The harsh conditions of a chemical reaction and the heat flows may lead to irreversible catalyst morphology changes, such as particle growth with associated loss of surface area or the active catalyst's transformation into less active or inactive material.[10] Furthermore, undesirable side-reactions may lead to the permanent deposition of products such as carbonaceous residues onto the catalyst surface, which act as poisons.[11] The term "catalysts selectivity" is introduced because the reaction products are considered catalyst-dependent and because the reaction path facilitated by a catalyst is conditioned by its surface chemistry. For example, under appropriate conditions, carbon monoxide hydrogenation gives almost entirely methane over a nickel catalyst, almost entirely methanol over promoted copper, and higher hydrocarbons over ruthenium; each process is operated on an industrial scale.[12] The definition is not breached because each of these processes is thermodynamically feasible and the positions of equilibrium being approached are those available in principle for an uncatalyzed reaction. However, each case the unique chemical reactivity of the surface guides the reaction along an energetically

favorable pathway to these specific products. Catalyst selectivity is of paramount importance in the development of industrial processes, both for economic and environmental reasons.[10, 13]

Catalysis has been of high interest for chemists since England's Humphry Davy observed in the early 1800s that water was formed when hydrogen and oxygen react in the presence of a red-hot platinum wire. The early use of catalysis in the industry was demonstrated in 1832 when Peregrine Phillips used platinum to oxidize sulfur dioxide (SO_2) to form sulfur trioxide (SO_3). Frederic Kuhlmann followed this in 1837, in which platinum was used to catalyze the production of nitric acid from ammonia.[14] Early in the twentieth century, catalysis was shown to accelerate the reaction rate, and the activity was influenced by the state of the catalyst surface. From then on, chemical technology has made remarkable progress with the use of catalysts.[15] In early 1900's, there was a burst of new industrial-scale processes. These include the development of the Fischer-Tropsch synthesis of alkanes from carbon monoxide and hydrogen, BASF's use of vanadium oxide to produce sulfuric acid, and the "catalytic cracking" " process of petroleum for the production of toluene, an important precursor to the explosive trinitrotoluene (TNT).[15] Since these early discoveries, catalysts have played an essential role in many industrial processes. Some examples include **(i)** production of ethylene oxide from ethylene, **(ii)** synthesis of hydrogen cyanide and acrylonitrile through ammoxidation, **(iii)** synthesis of formaldehyde from the oxidation of methanol, and **(iv)** the production of plastics, synthetic fibers through polymerization reactions.[15] Oil companies became involved in their catalyst production because they were needed for their refineries, such as ZSM-5 catalysts based on zeolite (a naturally occurring mineral) developed by Mobil.[16, 17] Shell has used its technology to generate the sales of its catalysts for hydrogenation cracking.[17] Other companies such as Johnson Matthey used precious metals for industrial catalysts by using platinum metal to purify gases or treat effluent tail gases.[18]

1.3.1   Catalysis in Pharmaceuticals Based on Metal-Mediated Catalysis

The application of catalysts is ubiquitous in the chemical industry in areas ranging from pharmaceuticals to polymers to petroleum processing. More than 90% of all industrial processes are based on metal-mediated catalysis.[19] The widespread utilization of catalytic processes in the industry reflects the economic and environmental benefits achieved through catalysis. Ibuprofen is one of the most used over-the-counter pain relievers. The traditional (Boot's) synthesis requires six steps that use large volumes of solvent, corrosive reagents, and stoichiometric quantities of materials. This process also displays low atom economy; only 40% of the atoms in the starting materials are incorporated into the product. In contrast, in 1992, BHC Company revealed a new, alternative process of synthesizing ibuprofen that was much more environmentally friendly and a model of atom economy,[19, 20] of ibuprofen is achieved in only three steps **Scheme 1** Catalytic amounts of reagents are used in each step of the synthesis, and greater than 99% of the catalyst is recycled. Atom economy doubles to 80%, significantly reducing the amount of waste generated. **Scheme 1** shows a metal catalyst used in each step, shortening the overall number of steps to obtain the final product (Ibuprofen).

Scheme 1. BHC synthesis of Ibuprofen.
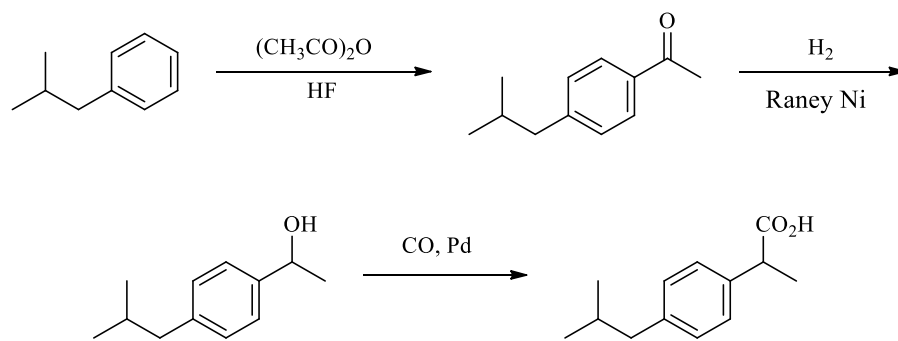
The recently developed three-step catalytic route for ibuprofen, using catalytic acylation, hydrogenation, and carbonylation, represents one of the best examples of catalysis for cleaner processes in pharmaceuticals.[21] Naproxen is another important drug in this category, which is currently manufactured by multistep stoichiometric synthetic routes: **(i)** the Syntex process, starting with α-naphthol and involving stoichiometric bromination, methylation, and alkylmetal coupling reactions to yield naproxen; **(ii)** the Zambon process, involving acylation of nerolin (2-methoxynaphthalene), ketalization, bromination, hydrolysis, and reductive cleavage as the key steps; and **(iii)** asymmetric hydrogenation of 6-methoxy naphthacrylic acid, using the Ru-(S)-BINAP catalyst.[22] Attempts toward the direct synthesis of chiral naproxen via a chiral pool (S)-lactate, and asymmetric hydroformylation followed by oxidation, were also made. These routes suffer from drawbacks such as hazardous reagents and the generation of undesired waste that consists of inorganic salts. Therefore, it is most desirable to develop an environmentally benign catalytic route for the synthesis of naproxen. A detailed study on the two-step hydroformylation-oxidation route for the synthesis of D, L-naproxen (2- MNPA) shown in **Scheme 2**. The proposed hydroformylation-oxidation route to naproxen involves the following reaction steps: **(i)** the hydroformylation of MVN to the regioisomers 2-MNP and 3-MNP, and **(ii)** the oxidation of 2-MNP to D, L-naproxen (2-MNPA), using H_2O_2 as the oxidant. The stoichiometric reactions are shown in **Scheme 2**. Because only 2-MNP is useful for naproxen synthesis, regioselectivity is the most important in the catalytic hydroformylation step. Therefore, the hydroformylation of 6-methoxy-2-vinylnaphthalene (MVN) was investigated using a $Rh(CO)_2(acac)$ catalyst to understanding the role of ligands, reaction conditions, and kinetics. In the second step, the oxidation of 2-MNP with H_2O_2 as the oxidant has been investigated using Na_2WO_4, Na_2MoO_4, Na_2VO_2, PTA, and PMA as catalysts. The improved selectivity through catalysis minimizes or eliminates the need for product separation, reducing the use of solvents and separation agents.[23]

Scheme 2. Synthesis of D, L-Naproxen via a hydroformylation-oxidation route.[23]

CHO

Rh(CO)$_2$(acac)/dppe
CO [B*], H$_2$ [A*]

CHO

+

MeO   MeO   MeO

2-(6-methoxynaphthyl)
propanal

3-(6-methoxynaphthyl)
propanal

Na$_2$WO$_4$ H$_2$O$_2$

COOH

COOH

+

MeO   MeO

2-(6-methoxynaphthyl)
propanic acid

3-(6-methoxynaphthyl)
propanic acid
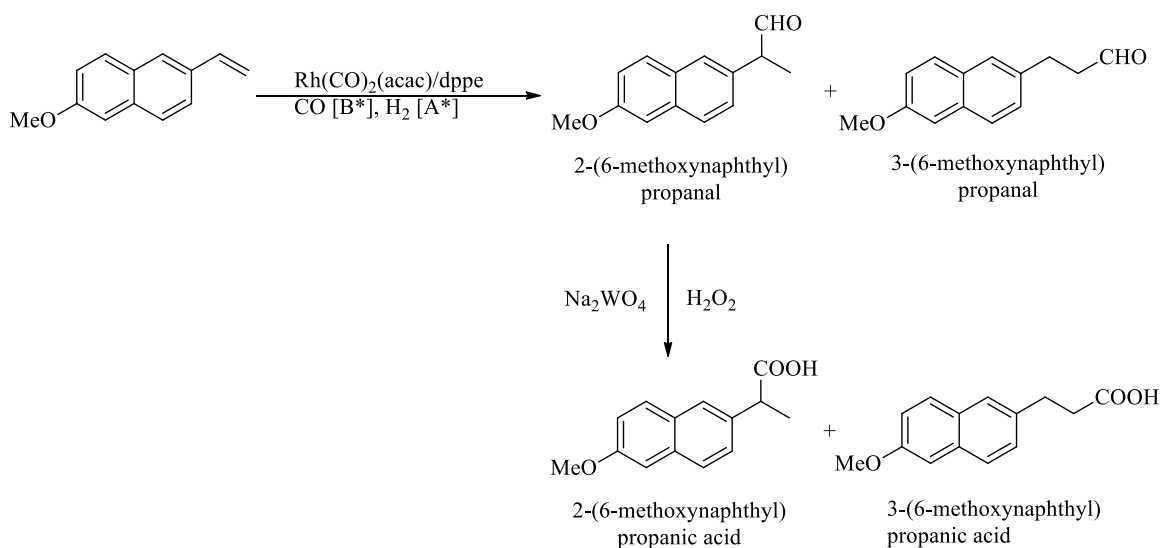
The critical intermediate (bisnoraldehyde) for the production of progesterone and corticosteroids, by Macia and Upjohn, was achieved by switching from a heavy metal oxidant to a bleach and catalyst/co-factor system **Scheme 3**[24] The revised synthesis employs a genetically modified bacterium that uses whole soya sterols, a renewable feedstock, more efficiently than the previous process, increasing feedstock utilization from 15% to 100%. The new catalytic features of the process reduce aqueous waste by 79% and non-recoverable organic solvent waste by 89%.

Scheme 3. Synthesis of bisnoraldehyde.

Whole soya sterols

100% utilization

Fermentation

OH

4-hydroxy-TEMPO
NaOCl, NaHCO$_3$, KBr

H

O

O   O

11
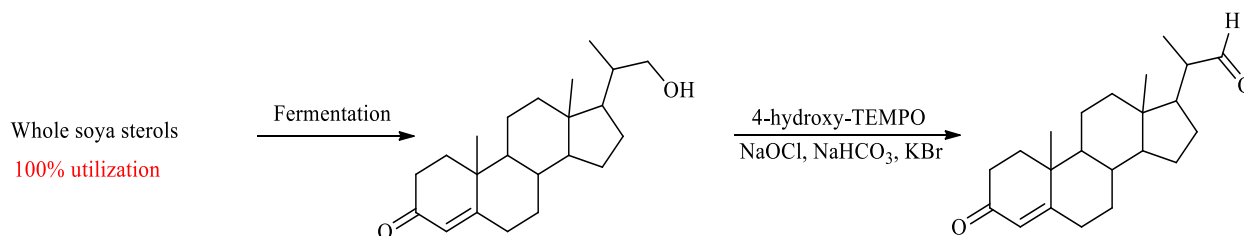
A variety of reactions can be carried out in an aqueous environment by selecting a suitable catalyst. Water is a desirable solvent choice: it is inexpensive and readily available, non-toxic, and non-flammable.[19, 25] An indium catalyst has been employed in several carbon-carbon bond-forming reactions conducted in water. For example, the coupling of a hexose sugar with a 1,3-dicarbonyl compound is efficiently promoted in water using an indium catalyst **Scheme 4.**[26]

Scheme 4. Synthesis of furyl glycosides via InCl$_3$ coupling reaction in water.
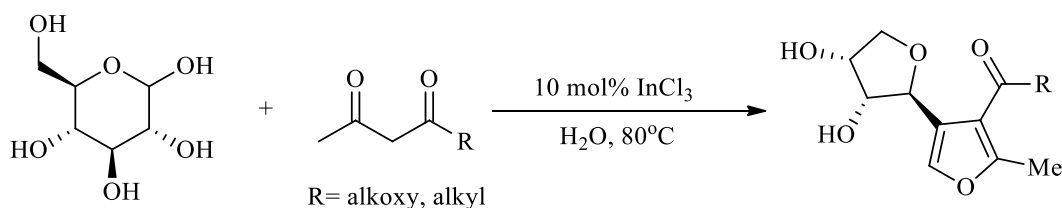
Metal-mediated reactions in water have found applications in cyclization, ring expansion, and isomerization reactions. These examples above show the green chemistry benefits of a less hazardous solvent, reduced energy usage, ease of separation, and selectivity for waste minimization for the preparation of important compounds and intermediates.

1.4 Sustainable Development

The World Commission for Environment and Development, founded in 1983 by the United Nations, was given the task of formulating a report on the perspectives of long-term, sustainable, and environmentally friendly development on a worldwide scale by 2000 and after.[27] The commission defined sustainable development as meeting the present generation's needs without compromising

future generations' ability to meet their own needs. In the succeeding two decades, the concept of sustainability has become the focus of considerable attention both in industry and in society. The 12 principles of green chemistry need to be employed when developing new materials and processes, which can be difficult. These principles distinguish catalysis as one of the essential tools for engaging green chemistry. It allows for the use of less toxic materials.[27] Catalysis is an essential means for the development of a sustainable world and is a key technology in achieving sustainability goals in a broad range of sectors, products, and processes. The focus on catalysis-related research and development activities remains towards sustainability.[28]

Efficiency is the primary driver in catalysis as it directly links to the maximization of the benefits (desired products, profit, etc.) with a minimum of costs in a broad sense. The main properties of industrial catalysts are more than simple inorganic materials (e.g., environmental impact, raw chemicals, materials use, energy consumption, capital investment, etc.). Efficiency is addressed at three levels: **(i)** atom-efficiency- improving efficiency in the use of scarce resources is important through steep reduction of waste and byproducts and use of raw materials, as catalysis impacts the effective use of available feedstocks; **(ii)** cost-efficiency- catalysis has a significant effect on cost-efficiency through improved reaction effectiveness (e.g., reduced separation and waste disposal costs), reduced capital investments (e.g., novel process, one step reactions, and reactor concepts), improved plant and feedstock flexibility, reduction and production time, etc.; **(iii)** energy-efficiency-a key factor in the use of catalysis is the ability to reduce the energy needed to manufacture desired products and operate specific processes.[28] A major challenge for catalysis is to apply its potential towards the improvement of efficiency, which will benefit the end-user through better and cheaper products and processes, the environment through sustainability improvements, and the industry through increased profit margins. Catalysis offers many green chemistry benefits, including lower

energy usage, the use of catalytic amounts of materials, enhanced selectivity, and reduced usage of processing and separation agents.[29, 30]

1.5   Types of catalysis

Catalysis is principally divided into two branches: ***homogeneous catalysis***, when the catalyst is in the same phase as the reaction mixture (typically in liquid phase), and ***heterogeneous catalysis***, when the catalyst is in a different phase (typically solid/liquid, solid/gas or solid/liquid/gas). **Table 1** summarizes a comparison between the main features of homogeneous and heterogeneous catalysis.

Table 1. Comparison between homogeneous and heterogeneous catalysis.

Feature	Homogeneous Catalyst	Heterogeneous Catalyst
Form	*metal complex*	*solid, often metal or metal oxide*
Activity	*high*	*variable*
Selectivity	*high*	*variable*
Reaction Conditions	*mild*	*harsh*
Average Time of Life	*variable*	*long*
Sensitivity to Poisons	*low*	*high*
Problems of Diffusion	*none*	*possible*
Recycling	*difficult (and expensive)*	*easy*
Separation from Products	*difficult*	*easy*
Variations of steric and electronic features	*possible*	*difficult*
Intelligibility of the mechanism	*possible*	*difficult*

One of the main advantages of homogeneous molecular catalysts is that their active sites are spatially well separated when they operate under ideal conditions. Because of such spatial separation and the sites' self-similarity, there is a constant energetic interaction between each active site and the

reactant (substrate). Another advantage, also a direct consequence of spatial isolation and energetic constancy, is that such catalysts are readily amenable to almost all characterization techniques such as time-resolved NMR, FT-IR, X-Ray absorption, and other spectroscopic methods available. Nevertheless, although homogeneous catalysts present, in general, high activity and selectivity values, they show, as a significant drawback, difficult recycling and separation from the products. A heterogeneous system's strengths are easy separation, easy recovery, no solubility, and miscibility issues. Heterogeneous systems help reduce the cost of production and support environmentally benign processes.

Heterogeneous catalysis has a fundamental role in the development of sustainable industrial processes, as it possesses the ability to achieve the objectives of industrial catalysis while paying attention to the principles of sustainable and green chemistry.[31] The usage of heterogeneous catalysis in industrial applications is growing with time and because they can address green chemistry goals by providing the ease of separation of product and catalyst, thus eliminating the need for standard methods of distillation or extraction for catalyst separation, makes them very attractive when compared to homogeneous catalysis. These procedures often have a straining effect on the catalyst, especially when the solubility is difficult (challenging for the extraction procedure) or overly sensitive to temperature. Also, environmentally benign catalysts such as clays and zeolites may replace more hazardous catalysts currently in use. [29, 32] This chemistry domain is even expected to grow due to environmental constraints, which need better selectivity in the reactions and new catalysts for treating pollutants or for depollution issues.

Heterogeneous catalysts take the form of either metals or ionic compounds, which can either be bare or serve as substrates for metal clusters or nanoparticles (NPs). Such catalysts are stable even under relatively harsh reaction conditions (such as high temperatures and pressures) and are readily

separated from reactants and products. By virtue of this robustness, heterogeneous catalysts dominate large-scale industrial processes. Heterogeneous catalysis usually occurs at the surface of a solid catalyst, which ideally has a high surface area to volume ratio. For example, smaller metal particles have a higher fraction of surface atoms than do larger metal particles. This fraction not only has an impact on the fraction of catalytically active metal atoms (metal atom utilization) but also has a substantial effect on selectivity. The metal atom utilization in homogeneous molecular catalysts can reach 100% — a figure that may be orders of magnitude higher than heterogeneous catalysts. Indeed, heterogeneous catalysts might feature non-uniform aggregates of hundreds and/or thousands of metal atoms, only a small fraction of which are exposed to reactants. For example, the reactive, coordinatively unsaturated metal atoms at apices, edges, steps, and corners usually represent less than 20% of the total metal atoms. Increasing the metal atom utilization of a catalyst is particularly important for heterogeneous catalysts composed of a solid substrate decorated with a platinum group metal (PGM) such as Pd, Pt, Rh, Ir, or Ru. Although these metals are among the least abundant of the earth's elements, their presence in catalysts to control vehicle emissions, produce chemicals, refine petroleum, and serve in fuel cells is required. Thus, there exists a long-standing interest in fabricating heterogeneous metal catalysts that feature atomically dispersed metal atoms as robust active centres (100% atom utilization efficiency). Such an approach would combine the advantages of typical homogeneous and heterogeneous catalysts. Heterogeneous catalysts with atomically dispersed metal atoms have been actively studied in the past several years. Further efforts are necessary for the design of new heterogeneous catalysts to reach activity and selectivity values competitive with homogeneous ones.

Understanding structure/reactivity/selectivity relationships in classical metal-based heterogeneous systems is complicated by uncertainties in the active site structure(s) and the large

variety of surface species that are catalytically significant. In general, solid catalysts working heterogeneously possess a broad spectrum of active sites, each with its own energetics, activity, and selectivity. For instance, in a dispersed metal particle, atoms located at surface steps, kinks or terraces, or at the flat exterior surface are stereochemically different from one another, which dramatically influences the variety of energetic situations associated with the adsorption of substrate species.[33, 34] Such a complex problem is encountered with all metal- and alloy-based catalysts and a vast number of other catalysts that are continuous solids, including close-packed oxides, halides, and chalcogenides.

A catalyst's design strives to optimize stability, turnover, solubility, and ease of separation from the product. Changes in ligand design or metal selection can significantly improve selectivity, energy consumption, and solvent utilization. Catalysts also permit the use of more environmentally friendly feedstocks and reagents. In heterogeneous catalysis, three common core areas have to be considered for future catalysis development: **(i)** correlation structure, dynamical rearrangements, transition state, and reaction intermediates; **(ii)** new strategies of catalyst preparation to establish a molecular control of structures (e.g., nanoparticles as most catalysts heterogeneous, homogeneous, and enzymes are NPs); **(iii)** molecular characterization of the active catalysts.[35-37]

1.6 New catalysts

Society demands the development of environmentally friendly products, synthesized by cleaner and more energy-efficient processes require catalysts with different structures and advanced control of active site location and tailored activity.[38] The drivers will be both discovery of new catalyst structures and challenges provided by new resources and new product demands.[39] Molecular-level understanding of structure/performances relationships is necessary to go from novel materials to effective catalysts. Future developments in catalyst synthesis should be directed toward better

integration of green chemistry principles to limit the environmental impact of large-scale catalyst preparation procedures: moderate the energy input, organic solvent uses, limit problematic wastes (i.e., metal nitrates) or toxic exhaust gases (calcination of ammonium salts generates NOx). Research is performed worldwide to discover new catalysts to give better reaction yield or even new catalytic reactions. Although major industrial processes have been discovered and developed by the second half of the last century, progress is still needed, as the major challenges for the future are to reach 100% selectivity and to use less energy.[32]

The last two decades witnessed a tremendous scientific effort to transfer the homogeneous molecular approach to heterogeneous catalysis, leading to single-site heterogeneous catalyst (SSHC) development.[40-45] The main aspect of such catalyst is, by definition, that active sites are identical in chemical composition and their atomic environment, and thus in their interaction with reactants. It could be isolated atoms such as Brønsted H^+ sites in zeolites or molecular complexes, such as multinuclear nanoclusters or organometallic complexes. In many cases, porous materials, such as zeolitic or mesoporous materials of high surface area, favor a good dispersion/isolation of the active entities and may lead to SSHC.[46] Such single-site catalysts, which are common to metal-centered homogeneous catalysts and enzymes, enable the design of new catalysts for various selective oxidations, hydrogenations, hydrations, and other reactions that the "greening" of industrial processes demand.

A single-site heterogeneous catalyst (SSHC) is a solid where the catalytically active sites are well-defined, evenly distributed entities (*single sites*) with a definite chemical surrounding, as in conventional homogeneous systems, but which show all the advantages of heterogeneous systems, in terms of easy separation, recovery, and recyclability.[47] Such single sites are typically located over solid supports with high surface area and present the following general features: **(i)** they consist of

one or few atoms (as in the case of chemically defined metal clusters); **(ii)** are spatially isolated from one another; **(iii)** have all identical energy of interaction between the site itself and a reactant; **(iv)** are structurally well characterized.

SSHC can be compared to those solid catalysts where the active species are present as metal particles or bulk domains of metal or oxidic components whose composition is different from that of the support. In classical heterogeneous catalysts, the catalytically active sites can be surrounded by atoms (or species) of the same nature (e.g., the Ni atoms in a conventional Ni/Al_2O_3 hydrogenation catalyst), whereas the atomic (or molecular) isolation of the active moieties is the distinctive feature of SSHC.[45, 48-50]

The problems presented by both homogeneous and heterogeneous catalysts have triggered intense research over the last few decades in the quest for alternative systems that, ideally, would bridge the gap between these two subdisciplines of catalysis by implementing truly single catalytic sites at the surface of a solid catalyst. The challenge at hand is certainly not trivial: progress in this direction requires the discovery of new materials able to offer sufficient design possibilities as to a Center for Molecular Modeling allow for an exquisite control in the implementation of catalytic functions. Metal-organic frameworks (MOFs) and covalent and porous organic frameworks (POFs) are two relatively new classes of materials that have the potential to become the ideal homo-hetero bridge.[51-57]

MOFs are crystalline compounds consisting of infinite lattices comprised of inorganic secondary building units (SBUs, metal ions, or clusters) and organic linkers, connected by coordination bonds of moderate strength. Distinct from traditional inorganic materials, MOFs can be synthesized from well-defined molecular building blocks and may be understood as molecules arranged in a crystalline lattice.[58]

Porous organic frameworks (POFs) are another class of porous materials that, in contrast to MOFs, are constructed solely from organic building blocks.[59-61] POFs can be classified into two groups depending on the crystallinity of the final solid. Covalent organic frameworks (COFs) are typically synthesized relying on reversible covalent bonds, resulting in highly crystalline materials with mild to low stability. In contrast, amorphous porous organic polymers (POPs) are constructed through irreversible covalent bonds (e.g., C–C bonds). As a result, interpenetrated and non-crystalline structures are typically formed, displaying excellent stability. In both cases, these materials possess high surface area, tunable pore size, and adjustable skeletons, which brings promise to a wide range of applications. Also, POFs can be locally decorated with molecular catalysts that may acquire activities and selectivity comparable to their homogeneous analogs. In clear analogy to MOFs, the vast majority of POFs is synthesized in a modular fashion, making straightforward incorporation of functional groups easy and, therefore, opening a promising playground for using POFs as catalysts. As discussed above, heterogeneous single-site catalysts are isolated, well-defined, active sites which are spatially separated in a given solid and, ideally, structurally identical.

1.6.1 Preparation of Single-Site Heterogeneous Catalysts

Conceptually different approaches have been applied to create catalytically active MOFs and POFs. The host matrixes where single-site centres can be uniformly dispersed have inorganic, organic, or composite nature. Inorganic matrices are typically oxidic solids (silicates, aluminosilicates, aluminophosphates, etc.), often with high porosity and an exceptionally large specific surface area. Organic host matrices have, on the contrary, a carbon-based backbone and are constituted of polymers with different side functionalities that can bind and accommodate the single active site. Then, composite matrices are composed of mixtures of inorganic and organic constituents, in variable proportions and with various morphologies (e.g., co-polymers, multiple-shell materials,

mesoporous hybrid frameworks). Three main approaches to obtaining single sites from their precursors: **(i)** in-matrix synthesis; **(ii)** post-synthetic covalent deposition; **(iii)** post-synthetic non-covalent deposition.

In the in-matrix synthesis approach, the atom-isolated catalytically active sites are homogeneously dispersed in the support matrix and are located at or adjacent to ions that have replaced framework ions of the parent structure. The active species' precursor is already present in the synthesis mixture of the final material, together with the other components, and the single sites are introduced during the synthesis step. The site's chemical environment (hydrophilic/hydrophobic character, surface acidity, steric constraints, etc.) is strongly dependent on the matrix's physical-chemical characteristics. As the main drawback, some centres can be 'buried' within the bulk of the solid, and they cannot be accessible and available for catalysis.[62]

In the post-synthesis covalent deposition approach, the active centre is generally added to the support as a precursor that can be deposited onto the surface (*anchored* or *grafted*) by the formation of covalent bonds. The precursor can be deposited as it is or after functionalization with a side chain (a tether).[63, 64] In the ***anchoring*** technique **Figure 1a**, the active metal (the single site) maintains the definite chemical surroundings as in the parent homogeneous precursor (the covalent deposition takes place only at the opposite end) with all the advantages of heterogeneous systems easy separation, recovery, and recyclability. Conversely, in the ***grafting*** technique **Figure 1b**, the single active site has a different chemical surrounding with respect to the parent precursor; because the coordination shell around the metal centre is partially modified during the covalent deposition, a new reactivity of the active species is expected for this type of catalyst.

Figure 1. (a) Anchoring method. (b) Grafting method.
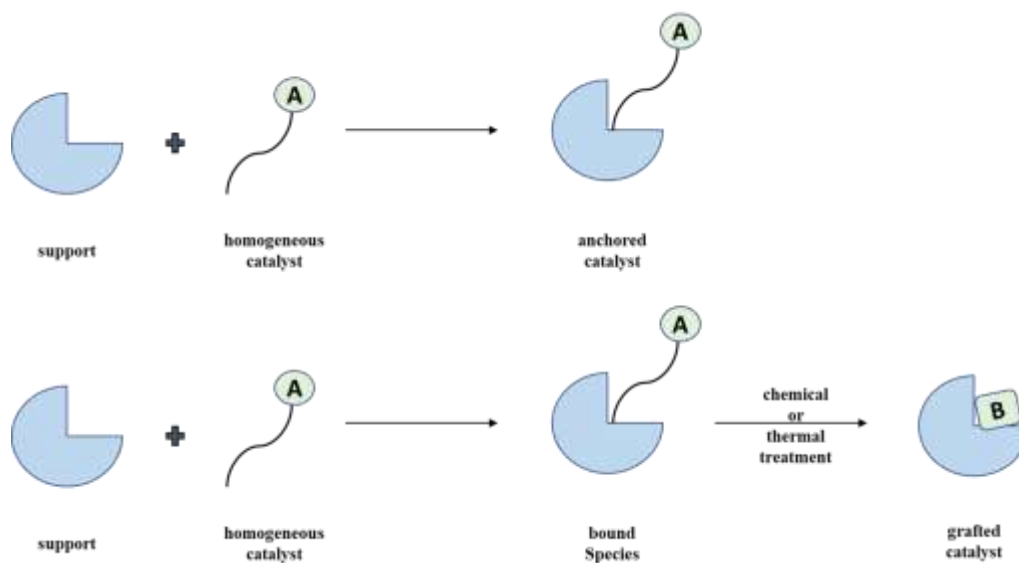
Finally, in the third approach, the homogeneous precursors of the single-site active centres are immobilized onto the surface of solid supports by non-covalent interactions, such as hydrogen bonds, weak van der Waals interactions, or mechanical confinement (trapping or encapsulation) **Figure 2.**

Figure 2. Immobilization of single-site active centres onto the surface of the solid support.
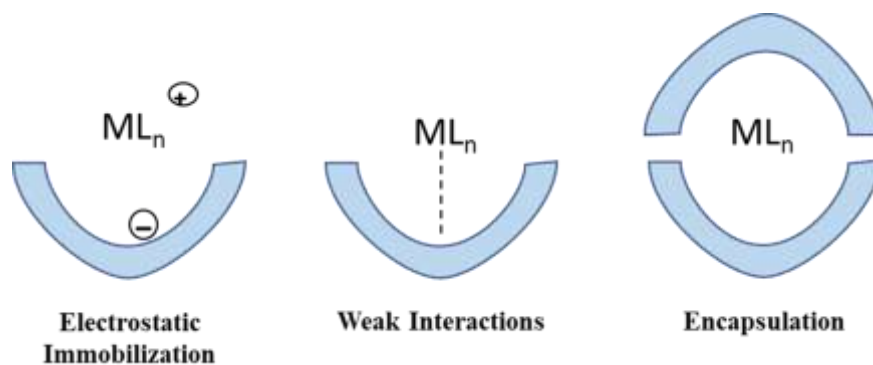
Encapsulation covers a large selection of immobilizing catalytically active species within the pores of inorganic or organic solids. It allows one to keep unaffected the optimal performances of the original homogeneous catalysts. Due to a positive, cooperative effect, it is possible to have a final system with improved characteristics with respect to the parent precursor. These entrapped metal complexes are bulky and cannot diffuse out. In contrast, the reactants and products can freely move through the system.[65-67] These materials frequently display, with respect to the homogeneous parent complex, enhanced: **(i)** activity, adsorption and/or concentration effects; **(ii)** selectivity, as a detrimental free-radical side reaction that occurs in solution, are mostly suppressed in encapsulated systems, and **(iii)** stability, since catalyst deactivation pathways are hindered by local site isolation of the complexes inside the solid matrix.

Encapsulated metal complexes can also easily be separated from the reaction media and reused, with no metal leaching. Many approaches have been created and are being developed for preparing such systems, as it is possible to use different support materials and a wide range of metal precursors of varying nature. Furthermore, there are many possibilities to control and modify the immediate atomic environment and the active site's central atomic structure to tune the catalyst features according to its applications.

1.7 Transition Metal-Catalyzed Reactions: Development and Challenges

Transition metal-catalyzed organic reactions have become indispensable, but there remain numerous challenges:

- Availability of noble transition metals
- The cost of transition metals and the cost of the associated ligand system
- The ability to recover/recycle the catalyst

The development of new catalytic systems that could decrease metal use in chemical reactions or make them recyclable is crucial to these reactions. These new catalytic systems aim to reduce metal usage, improve the transition metal recovery from the reaction media, and increase the catalyst lifetime (recyclability). In addition, easy recovery methods and catalyst recycling would reduce waste streams and reduce the catalyst cost and disposal. These improvements will have a positive impact on both the environment and the economy.

Transition metals continue to play a pivotal role in promoting chemical reactions for laboratory and industrial-scale processes. As initially developed, transition metal catalysts predominantly employed soluble metal complexes with various organic and inorganic co-additives. Such complex homogenous reaction systems present several challenges for scale-up and industrial use, inhibit product purification (metal removal), and have limited catalyst recyclability. Efforts to convert homogenous metal/ligand systems into similarly ligated metal/ligand heterogeneous systems using insoluble supporting materials have had little success. Recent studies aimed at developing robust and recyclable metal heterogeneous systems with catalytic activities comparable to homogeneous systems have focused on the potential use of nanoparticles, metal nanoparticle-supported nanocomposite materials, and single-atom composite materials.[68] However, many of these systems suffer from low reactivity, thermal instability, metal leaching, metal agglomeration, and the need for higher reaction temperatures.[68] Furthermore, the potential of first-row transition metals as heterogeneous catalysts remains to be thoroughly investigated.

Heterogeneous catalysis has been extensively discussed in recent years as a more viable industrial process than homogeneous catalysis. Although homogeneous catalysts offer some advantages, such as soluble metal complexes of various organic and inorganic co-additives, high reactivity, and high selectivity, product purification (metal removal) is a significant issue. Also, poor

ligand recovery and limited catalyst recyclability make these catalytic systems less than ideal for large-scale industrial applications. Heterogeneous catalysts usually solve numerous problems associated with homogeneous media and add advantages such as lower toxicity, the possibility of catalyst recovery, recyclability, ease of handling, and easy separation from the reaction medium. For these reasons, heterogeneous catalysts are referred to as "Environmentally Friendly." Within heterogeneous catalysis, raw and modified clay minerals are widely used in many industrial processes due to their advantageous properties, such as catalytic efficiency, low cost, wide availability, ease of preparation, and high thermal stability.

1.7.1   Element Endangerment

The chemical elements which make up the Earth are limited to 90 natural elements with appreciable abundance. These elements are crucial to fuel all human needs. With the progress in technology, an increase in demand has been observed for numerous elements over the last two decades.[69] The extraction and usage of these elements have increased in recent years due to the high demand for new materials for electronic applications and chemical catalysis. Many of these endangered elements are metals, including transition metals and metalloids, and will be depleted within the next few decades. The elements that have experienced some of the most significant increases in demand and are among the most threatened are palladium, rhodium, and platinum. Changing the present understanding of extraction, consumption, and waste management is needed to maintain the continuous supply of these crucial elements. The risk of these endangered elements is highlighted in **Figure 3**. For some, the threat is higher. The elements that are shown to be remarkably high risk do not mean that they will disappear, but the supply will be overshadowed by demand. Eventually, it will reach a point where it will no longer become economically viable to extract or use a particular element. As the supply of these metals has struggled to keep up with demand, their prices have risen

to a point where the application is no longer economically feasible. As a result, new nanoparticles and nanocomposite technologies have emerged in an effort to minimize endangered element usage.

Figure 3. Endangered elements.
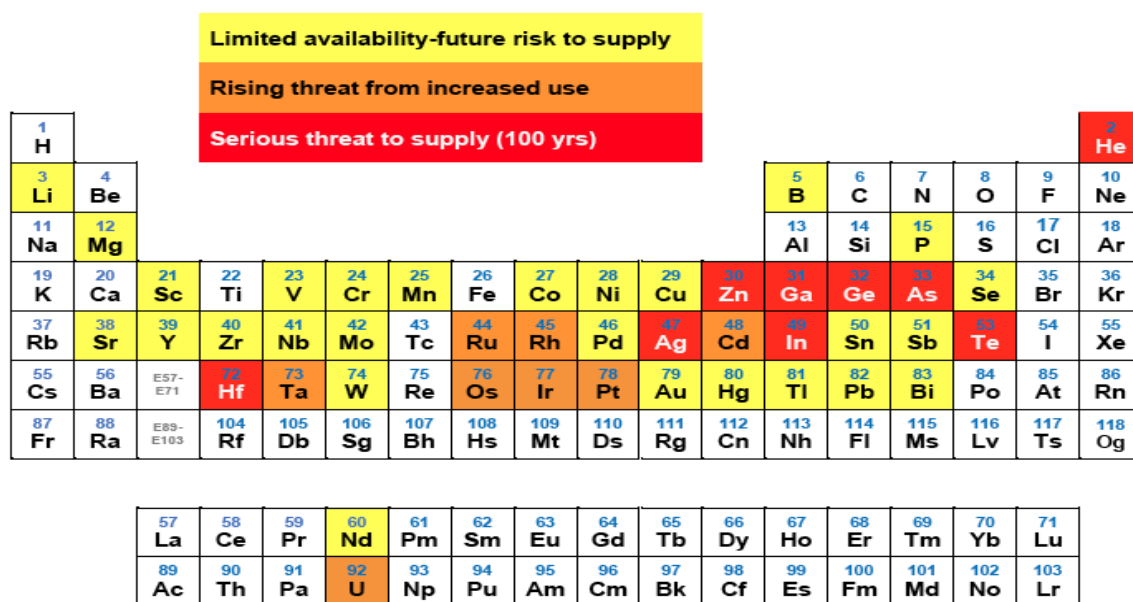
1.8   Clay Science

Clay science has emerged after a few eras of clay use. The two main features that evoke interest in clays are: **(i)** their expected availability and **(ii)** their extraordinary properties. Clay minerals vary in chemical composition, structure, and occurrence modes because they are formed from different parent rocks under variable conditions. Clay minerals are unevenly distributed in the lithosphere, while their concentration steadily increases due to weathering and hydrothermal alterations. Clay minerals in nature also undergo spontaneous modifications and transformations as environmental conditions change. Natural clays are highly heterogeneous in composition and, almost invariably,

contain "impurities" in the form of associated minerals. The particle size also influences the mineralogical composition of clays, the smaller the size, the larger the amorphous x-ray material's contribution. The fineness of clays predetermines both their vulnerability and reactivity. Clay minerals are naturally occurring nanomaterials, abundant, inexpensive, and environmentally friendly. They have a vast potential for the synthesis of clay-polymer nanocomposites with superior mechanical and thermal properties. In industrial applications, clays can be categorized into four types: **(i)** bentonites with montmorillonite as the principal clay mineral constituent, **(ii)** 'kaolin's containing kaolinite, **(iii)** palygorskite and sepiolite, and **(iv)** common clays, which often contain illite/smectite mixed-layer minerals.[70]

1.8.1   Clay Mineral Properties and Structural Information

The structures of phyllosilicates are all based on a tetrahedral (T) and an octahedral (O) sheet. They may condense in either a 1:1 or a 2:1 proportion to form an anisotropic TO or TOT layer shown in **Figure 4.** The 1:1-layer structure consists of the repetition of one tetrahedral and one octahedral sheet. A 1:1-layer structure includes six octahedral sites and four tetrahedral sites. Dioctahedral is when only four of the six octahedral sites are occupied. The 2:1-layer structure is one octahedral sheet sandwiched between two tetrahedral sheets. Six octahedral sites and eight tetrahedral sites characterize the 2:1-layer unit cell. The interlayers are bound together through electrostatic and hydrogen-bonding forces.[70]

Figure 4. 1:1 and 2:1 Clay structure.

1:1 Clay Structure

| Alumina sheet (Octahedral) |
| Silica sheet (Tetrahedral) |

Hydrogen bonding

| Alumina sheet (Octahedral) |
| Silica sheet (Tetrahedral) |

2:1 Clay Structure

| Silica sheet (Tetrahedral) |
| Alumina sheet (Octahedral) |
| Silica sheet (Tetrahedral) |

n H_2O & exchangeable cations

| Silica sheet (Tetrahedral) |
| Alumina sheet (Octahedral) |
| Silica sheet (Tetrahedral) |
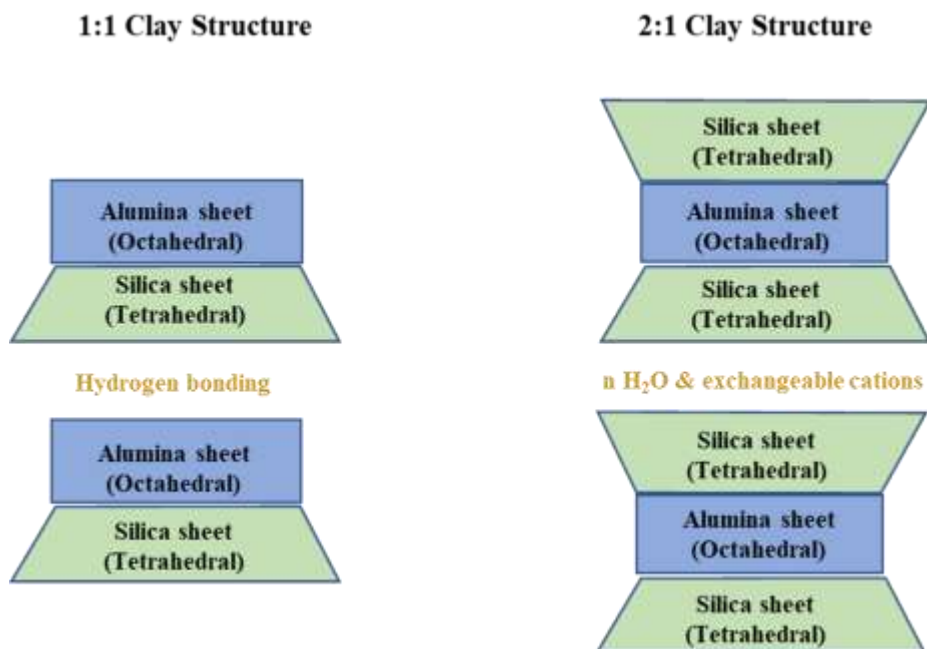
Isomorphic substitution by other metal ions of different valence easily occurs to the central metal ion either in the octahedral (e.g., Mg for Al) or tetrahedral sheets (e.g., Al for Si), thus leading to negative charges on the layers.[71] Consequently, positive-charged cations exist within the interlayer space necessary to compensate negative-charged aluminosilicate layers, and such cations are hydrated like macro-counter anions. In both the 1:1 and 2:1 clay minerals, each layer's broken-edge acts as a second source of charge, generally negative and pH-dependent.[72, 73] Clay minerals have distinctive physicochemical properties. Clays are layered structures. The layers possess a net negative charge neutralized by cations such as Na^+, K^+, Ca^{2+}, etc., which occupy the interlamellar space. Clays' fantastic flexibility for modification is because other cations or other molecules can easily replace these interlamellar cations. Molecules can be covalently attached to layer atoms by straightforward procedures. These modifications offer tremendous scope for altering clay properties

like acidity, pore size, surface area, polarity, and other characteristics that govern their performance catalysts.[70]

1.8.2 Modifications or Functionalization of Clay Minerals

Modification or functionalization of the clay mineral surface and interlayer structure is applied to enhance the clay mineral's endogenous properties. The resulting clay mineral product can be termed as *(designer clay)* because the modification processes provide specially engineered attributes to the material.[16, 74] There are many ways to modify clay minerals:

- Adsorption

- Ion-exchange with inorganic cations and cationic complexes

- Ion-exchange with organic cations

- Binding of inorganic and organic anions, mainly at the edges

- Grafting of organic compounds

- Reaction with acids

- Pillaring by different types of polyhydroxy metal cation

- Interlamellar or intraparticle and interparticle polymerization

- Dehydroxylation and calcination

1.9   Clay Mineral in Catalysis

Engineering clay minerals into catalysts primarily take advantage of the characteristics mentioned above, mainly from their nanoscale layers and interlayer space. These clay-based catalysts can be easily tailored based on the formulations, structure, and surface properties. Historically, clay-based catalysts played a pivotal role in processing crude oil in the 1930s–1960s and ignited a new round of extensive interest in the late 1970s in larger porous materials as a possible catalyst for fluid catalytic cracking (FCC) of heavy oil.[16] Meanwhile, many researchers have been attempting to use them as catalysts in the green synthesis of fine chemicals and the removal of pollutants from the environment by utilizing their peculiar adsorptive capacity and catalytic ability. Several strategies have been used to design new clay catalysts. Methods of acidification, pillaring, and use as supports have been combined to make new catalysts with a specific activity.

Given the design and preparation, herein, the term "clay-based catalysts" refers to the catalytic materials developed from clay minerals using at least one of four approaches: **(i)** the framework of clay minerals itself contains active species; **(ii)** the ions within the interlayer space are judiciously exchanged with active components for catalysis purpose; **(iii)** functional nanoparticles (NPs) or clusters are forged onto or within the clay nanostructure, and **(iv)** clay minerals or their derivatives are used as catalyst supports. In many cases, several interactions and structures are integrated to enhance their performances in separate ways or make them act in a synergic fashion.

1.9.1   Conversion of Biomass-Based Feedstocks using Clay Catalysis

The fossil fuel resources are diminishing, and increasing amounts of planet-warming greenhouse gases like CO_2 and NOx and SOx in the atmosphere require the green production of renewable transportation fuels. In the years ahead, it is expected that the tactical design and formulation of clay-

based catalysts could be targeted to catalyze the conversion of biomass-based and biomass-derived feedstocks.[75] Besides fuels, modern life also depends on the petrochemical industry because most drugs, paints, and plastics are currently derived from oil. The current methods for obtaining fine chemicals and materials are not sustainable in terms of resources and environmental impact. To address this problem, a new focus of clay-based catalysts is on their function as active catalysts for producing fine chemicals from bio-derived feedstocks, like lignocellulose[76] and saccharide[77] lactic acid,[78] and glycerol.[79] An important chemical feedstock derived from plant biomass is γ-valerolactone (GVL). has recently described GVL as an ideal, sustainable liquid used to produce energy and carbon-based consumer products. GVL is renewable, safe to store, and can be employed as a liquid fuel, food additive, solvent, and intermediate to synthesize many fine chemicals. The starting materials for obtaining GVL are levulinic acid and its esters, in turn, acquired by acid hydrolysis of lignocellulosic biomasses. A sustainable process for the hydrogenation of levulinic acid (LA) to γ-valerolactone (GVL) has been reported. GVL can be easily obtained in high yield by adopting mild reaction conditions by hydrogenating an aqueous levulinic acid solution using commercial ruthenium-supported catalyst combined with a heterogeneous acid co-catalyst as the ion exchange resins Amberlyst A70 or A15, niobium phosphate, or oxide.[80]

Scheme 5. Hydrogenation of levulinic acid (LA) to γ-valerolactone (GVL).
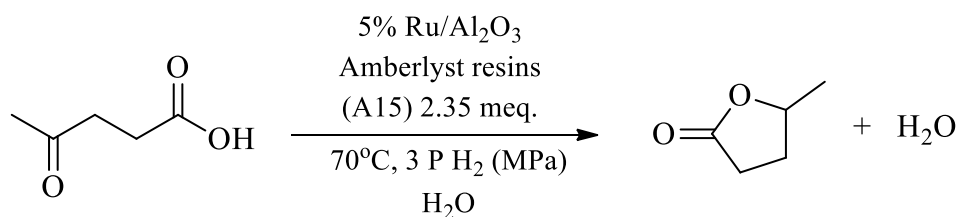
1.9.2 Clay Minerals in Organic Transformations

In addition to their environmental compatibility and cheapness, much effort has been spent exploring newer methods of using clays in their raw and modified forms as catalysts for various organic transformations. Clays have a long history of use as catalysts and support in organic reactions.[81] Recently, the application of clays and clay-supported catalysts in organic synthesis has increased. The use of normal smectites, commercially available montmorillonite K10, and modified forms of these clays have been reported.[82, 83] These modified forms were intercalated with various inorganic and organic ions, metal complexes, and organic compounds. Intercalating clays can optimize their performance by increasing the rates of reactions, yields, product selectivity, and stereoselectivity, including enantioselectivity. Clay-based catalysts can catalyze various types of organic reactions such as addition, oxidation, epoxidation, hydrogenation, allylation, alkylation, acylation, esterification, diazotization, rearrangement, isomerization, cyclization condensation, and polymerization.

In Brønsted and Lewis acids/bases or redox clay species, the clay's strategic modification can enhance the catalytic sites. Integration of acidic properties and basic properties into a solid catalyst, for example, acidic montmorillonite-immobilized primary amines (H-mont-NH$_2$), served as an excellent acid−base bifunctional catalyst for one-pot reaction sequences. This catalyst was the first material with coexisting acid and base sites active for acid−base tandem reactions.[84]

Scheme 6. Acid-base reaction sequences by clay-amine catalysts.
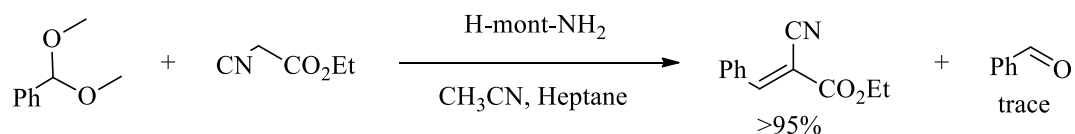
Due to their Brønsted and Lewis acidities, clay minerals in their natural form function as efficient catalysts for certain organic transformations. For example, natural kaolinites were used to catalyze β-keto esters transesterification.[85]

Scheme 7. Transesterification of β-keto esters.

$$RCHO \quad \xrightarrow[\text{montmoillonite k-10, 25}^o\text{C}]{N_2CHCO_2Et, \text{ Pentane}} \quad RCOCH_2CO_2Et + N_2$$
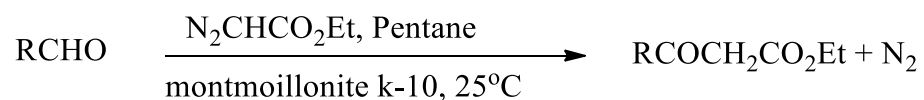
The 2:1 chlorite-group mineral Chamosite was used to catalyze a few different reactions: acylation, cyclization of arylaldehydes, and C-O bond formation reactions.[86]

Scheme 8. Alcohols and amines acylation reactions.
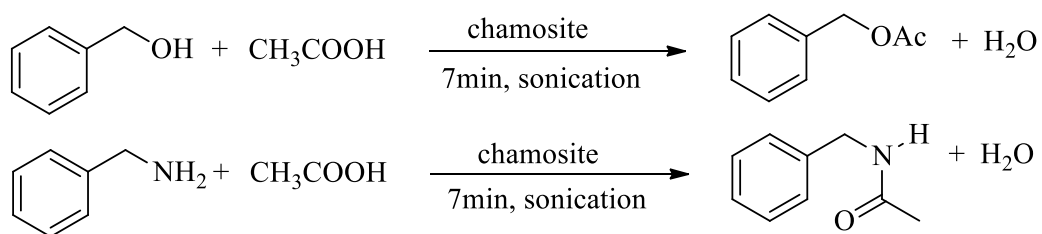
Scheme 9. Cyclization of arylaldehydes with O-phenylenediamines.
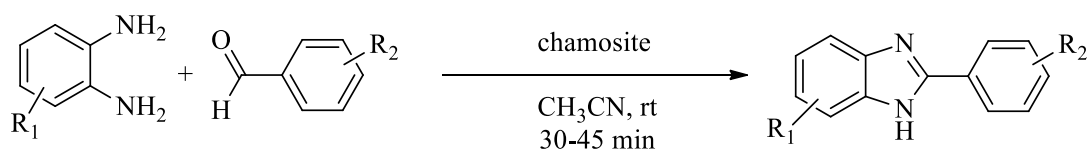
Scheme 10. C—O Bond formation reaction.
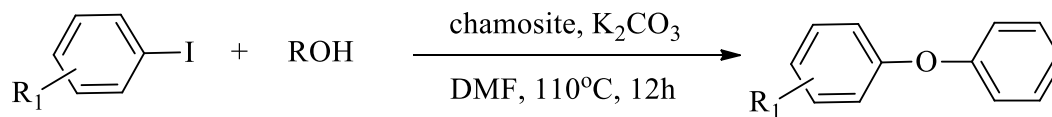
These clay mineral catalysts are non-corrosive and low-cost. In addition, they can be easily separated from the reaction media and reused in a subsequent reaction. Therefore, waste can be minimized. Nevertheless, for catalytic use in many cases, further strategic modifications are necessary to improve and intensify clay-based catalyst performance. Studies directed toward the development of clay-based catalysts will become more prominent as the demand for green processes increases.

1.9.3   Clay Minerals as Supports in Catalysis

Although modified clays can be designed and directly used as a solo catalyst in some reactions, many clay-based solids are used as catalyst support. The surface or inner lumen of clays can be modified by the immobilization or dispersion of catalytically active species. The immobilization of active components on the surface is one way to use clays as support. In this case, the catalytically active species might be immobilized through chemical bonds (grafting) or weaker interactions such as hydrogen bonds or donor-acceptor interactions rather than physical adsorption. Often, the supports and active catalytic components interact and then function through a synergistic effect. This partially explains why the immobilization of costly metal catalysts (e.g., Au, Ru, Pd, and Rh) onto such a support material remarkably enhances the catalytic efficiency. Finally, supported catalysts can minimize commodity catalyst costs due to decreased metal dosage, ease of separation, and catalyst recycling.

Acidified clay properties can be further improved by supporting the clay with Brønsted or Lewis acid compounds, metals, and metal oxides. Numerous metals and metal oxides supported on clay materials that have been used as a catalyst for organic synthesis have been reported in the literature.[87, 88] Clay-supported inorganic reagents (e.g., HNO_3, $ZnCl_2$, $AlCl_3$) were investigated in acid-catalyzed Friedel–Crafts reactions.[87, 89] Clay-supported metal catalysts have been studied for hydrogenation reactions[90, 91] and oxidation reactions.[92] The impregnation of bentonite with potassium hydroxide to catalyze transesterification reactions of fatty oil to biodiesel.[93, 94] However, in supported catalysts, active components are just dispersed on the surface of supports through physical or chemical adsorption. As a result, active components are not stable enough and readily suffer from leaching, especially after repeated use. The use of grafting techniques has been used to help solve leaching issues.

1.9.4 Clay-supported Metal Catalysts (Nanoparticles and Nanocomposite)

Metal nanoparticles have attracted the attention of researchers for many applications. Nano metals are defined as clusters containing tens to thousands of metal atoms. Their sizes vary between one to tens of nanometers.[1, 95-97] Nanoparticles have been considered desirable catalysts due to the acquired large surface area, higher catalytic efficiency, optical and electrical properties.[95, 96, 98] The increased catalytic activity is known to exist in nanoparticles, correlating with their sizes and shapes[99, 100] A variety of synthetic methods such as radiation chemical reduction,[101] chemical reduction in an aqueous solution with or without stabilizing polymers,[102-105] chemical or photoreduction in micelles have been reported for the preparation of metal nanoparticles.[106-108]

The stabilizers for synthesizing nanoparticles play an important role in controlling nano size, shape, and morphology. Various supports/stabilizers like mesoporous solids, organic ligands, polymers, carbon materials, etc., are reported.[109-116] Montmorillonite clay is one of the commonly

suitable supports where metal nanoparticles can be stabilized within the interlayer spacing or into the pores on the surface.[117-120] Identifying a suitable support material for metal-catalyzed heterogeneous catalytic reactions has been a vital study area over decades. Recent awareness in the intercalation chemistry of smectite clays has generated a lot of interest in these minerals as catalysts[88, 121] and support materials for transition metals or metal complexes.[122-126]

Interestingly, clays provide the same effect as that of zeolites to synthesize transition and noble metal nanoparticles. The clay mineral interlamellar space serves as a perfect nanophase reactor due to the swelling property and absorption capacity. Thus, size quantized nanoparticles of catalytically active noble metals can be generated in these clay minerals.[127-130] Clay mineral properties such as swellability and ion exchangeability allow for easy ion exchange of bulky organic cations and simultaneous intercalation of metal atoms in the interlamellar space. The generation of metal nanoparticles in the clay mineral interlamellar space was a favorable method for synthesizing well-dispersed metal particles in nm size. These noble metal-containing clay catalysts played a significant role in the studies of heterogeneous catalytic hydrogenation reactions where clay minerals support the metal catalysts.[131-133] Pd intercalated montmorillonite has been synthesized via the stabilization of Pd nanoparticles in surfactant micelles followed by the intercalation into montmorillonite. Catalysts synthesized by such a method have been used as catalysts in the hydrogenation of various alkenes and alkynes.[134-136]

The selective hydrogenation of only C-O bond in the presence of C=C bond of α, β-unsaturated aldehydes has been a significant challenge in the hydrogenation of carbonyl compounds. Often, either the C=C double bond hydrogenates yielding saturated aldehydes or double bonds hydrogenate, yielding saturated alcohols. Therefore, obtaining high selectivity towards the unsaturated alcohol with high conversion is a challenge. Gyorgy Szollosi reported a 70% selectivity

of cinnamyl alcohol through the hydrogenation of cinnamaldehyde at 4 bar hydrogen at room temperature over a Pt (5 wt.%) impregnated montmorillonite catalyst.[137]

Ir(0)-nanoparticles (Ir-NPs) were synthesized into the nanopores of modified montmorillonite clay by incipient wetness impregnation of the $IrCl_3$ followed by reduction with ethylene glycol. Increasing the montmorillonite clay's surface area was achieved by acid treatment, improving the clay surface to act as a host for the metal nanoparticles. The Ir-NPs showed efficient catalytic activity in aromatic ring hydrogenation under solvent-free conditions with maximum conversion up to 100%. The catalyst was easily separated by simple filtration and remained active for several runs without significant catalytic efficiency loss.[138]

1.10 Halloysite Nanotube Mineral Clay

Much of the research concerning clay minerals is devoted to kaolinite, montmorillonite, and illite. In recent years, halloysite nanotubes (HNTs), a 1:1 dioctahedral natural clay mineral with a unique tubular nanostructure, large aspect ratio, biocompatibility, and high mechanical strength, has arisen as a promising nanomaterial for a variety of applications. Halloysite was first named by Berthier (1826).[139] Raw halloysite is mined from natural deposits, which are then easily ground into a white powder. Halloysite occurs widely in both weathered rocks and soils, especially in wet tropical and subtropical regions and weathered igneous and non-igneous rocks.[140-142] Many countries, such as China, France, Belgium, and New Zealand, have deposits of HNTs. Each deposit is characterized by **(i)** different purity grades. **(ii)** hydration states and **(iii)** characteristic of sizes and shapes. The majority of the natural halloysite clay usually exists with some impurities, such as kaolin, illite, quartz, feldspar, chlorite, gibbsite, salts, and metals. Chemical analysis of many halloysite samples revealed significant amounts (up to 12.8 wt.%) (Fe_2O_3). These findings could be ascribed to the associated Fe oxides such as hematite or maghemite.[143-146] A halloysite sample from a Serbia deposit

was found to have (Cr_2O_3) content varying from 1.96 to 12 wt.%. Small amounts of Ti are also commonly found on the halloysite.[147] Halloysite sizes depend on its specific geological deposit, as reported in the literature based on microscopy[148] and scattering techniques.[149] Typically, the inner diameter, outer diameter, and length of HNTs are 1–30 nm, 30–50 nm, and 100–2000 nm, respectively. The typical morphologies of HNTs are shown in **Figure 5**.[148-150]

Figure 5. TEM Image of tubular halloysite nanoscroll.
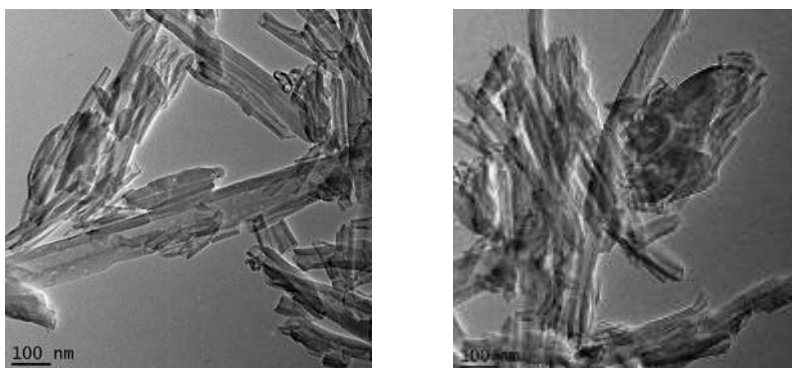
The particles of halloysite can adopt various morphologies, the most common of which is the elongated tubule. However, short tubular, spherical, and platy particle shapes have all been widely reported[143-146] The tubular structure is caused by lattice mismatch between adjacent silicon dioxide and aluminum oxide layers[149, 151] The external and internal diameters are between 60−300 and 10−60 nm, respectively **Figure 6**

Figure 6. Halloysite nanoscroll.

Halloysite Nanoscroll
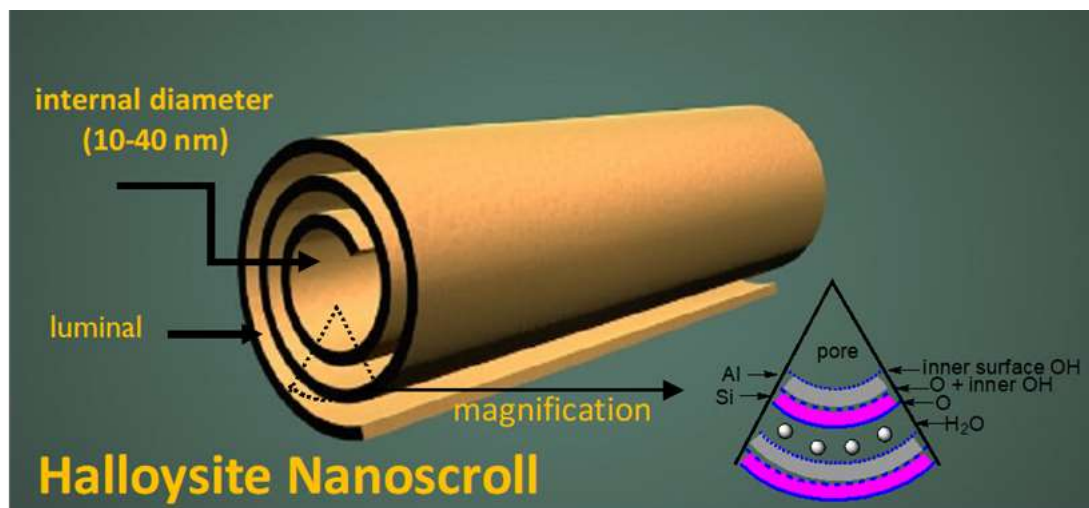
The interlayer distance is 1 or 0.6 nm, depending on the hydration state of the halloysite. The tubules may be extended and thin, short, and stubby, or emerging from other tubes. Tubular halloysite is commonly derived from crystalline minerals, such as feldspars and micas.[152] Formation from micas generally involves crystallization from solution rather than a topotactic alteration. It has also been suggested that the tubular morphology could result from the deformation of platy kaolinite. **Table 2** Summarizes the characteristics of halloysite nanotubes.

Table 2: Physical properties of halloysite nanotubes.

Physical Property	Value
HNTs characteristic surface area	65 m^2/g
HNTs aperture volume	1.25 mL/g
Halloysite specific gravity	2.53 g/cm^3
Refractive index of halloysite	1.54
HNTs internal lumen diameter	15 nm
HNTs mean tube diameter	50 nm

The molecular formula of HNTs is **$Al_2Si_2O_5(OH)_4 \cdot nH_2O$**, where n represents hydration or dehydration. HNTs are hydrated when n equals two and are dehydrated when n equals zero. The hydrated halloysite has a basal (d_{001}) spacing of 10 Å, which is ~3 Å larger than that of kaolinite. Because the interlayer water is weakly held, halloysite (10 Å) can readily and irreversibly dehydrate to give the corresponding halloysite (7 Å) form.[153] Therefore, it is challenging, if not impossible, to handle halloysite (10 Å) without inducing some alteration in its hydration status. The ability of halloysite to hydrate has always been the feature that distinguishes halloysite from kaolinite. The interlayer water content of halloysite (10 Å) is ~12.3 wt.%, corresponding to two water molecules per formula unit. In 1990 Bailey proposed that the interlayer water in halloysite (10 Å) is associated with exchangeable cations that balance the layer charge from some substitutions of Al^{3+} for Si^{4+} in the tetrahedral sheet.[154] The presence of interlayer water may be explained in terms of water activity as proposed for kerolite. This fine-grained phyllosilicate is characterized by extreme layer-stacking disorder, a small, if any, negative charge, and a remarkable ability to hold water molecules. Most of

the water associated with kerolite is weakly bound to layer surfaces and edges, only a minor amount being more strongly bound within the interlayers.[155] Hendricks & Jefferson (1938) and Brindley (1961) proposed that the interlayer water molecules in halloysite (10 Å) form hydrogen bonds with **(i)** one another, **(ii)** oxygens of the siloxane plane, and **(iii)** hydroxyls of the (opposite) aluminol plane. Halloysite (10 Å) dehydrates continuously, stabilizing at a basal spacing near 7.2 Å. This is because halloysite (10 Å) is more disordered, and the two types of water are not distinguished. This model would explain the dynamic properties of interlayer water in halloysite (10 Å).[156, 157] In 1999, Smirnov & Bougeard have made a molecular dynamics study of water structure concerning the silicate layers in halloysite.[158] In 1982 Costanzo identified two types of water: **(i)** "hole water" adsorbed on the clay surface and characterized by two different main orientations, and **(ii)** "associated water" or ice-like configuration forming an intermediate water layer in the halloysite interlayer.[159-161]

1.11 Applications of Halloysite Clay

Until recently, the main application of halloysites was an alternative raw material to kaolinite for ceramics[162] However, since then, there has been an exponential increase in the applications of halloysite nanotubes. Halloysite is used as a support template in various reactions because of the following:

- Halloysite has predefined tubular geometry and diameter, which efficiently allows the entrance and exit of molecules with specific sizes; this further caters to the catalyst's shape and size selectivity.

- Halloysite has higher reactivity and higher cationic exchange capacity as compared to other clays.

- Halloysite improves the catalytic activity of molecular species by enhancing the separation of substances from reaction media. These features of halloysite make them attractive candidates for support usage for catalyst design.

The readily available and relatively cheap nanotubular forms of halloysite have potential uses as nanocomposites with catalyst immobilization, polymerization, drug delivery, and environmental remediation.[150, 163, 164]

Halloysites have great qualities that can be utilized for immobilization. Silver (Ag) nanoparticles were immobilized onto the HNTs by reducing $AgNO_3$ by the polyol process. These immobilized matrices of Ag nanoparticles were used to reduce aromatic nitro compound, 4-nitrophenol (4-NP), in the presence of $NaBH_4$ in alkaline aqueous solutions.[165-169] Recently, HNTs have been used to support the ammonia decomposition reaction by immobilizing Ru nanocatalysts on HNT support and exploring their potential application in catalysis reactions.[170] HNTs are being used as support catalysts in Au/HNTs with extremely low metal loadings. Nanosized gold has been beneficial in the catalytic performance for the selective oxidation of cyclohexene using molecular oxygen in a solvent-free system.[171, 172] The immobilization of enzymes such as laccase, glucose oxidase, lipase, and pepsin into halloysite clay nanotubes provided enhanced biocatalysts in nanoconfined conditions.[173]

Halloysite is being used for polymerization to facilitate catalyst recovery and recycling. Cationic polymers such as polyvinyl pyrrolidone and chitosan crosslinked with glutaraldehyde bind to halloysite. It can be used to achieve delayed-release. Polyvinyl alcohol[174], chitosan[175], pectins[176], hydroxypropyl cellulose[177], polyethylene glycol (PEG)[178] can be mixed with HNTs solution and cast to form nanocomposite films. HNT alginate nanocomposite gel beads can be prepared by mixing the HNTs in water and crosslinking them using calcium ions.[179] Latex rubber can also be combined with

HNTs, and a co-coagulation process can be utilized to prepare HNTs-rubber nanocomposites.[180] These nanocomposites exhibit significantly enhanced properties, especially mechanical ones. The potential applications of the HNTs-polymer nanocomposites include high-performance plastics for use in structural and packing materials, flame retardant rubber/coatings, and biocompatible materials, such as tissue engineering scaffold and drug delivery vehicle. The goal of drug delivery is to deliver the controlled amount of drug at the target site at a predefined rate. Halloysite has been recognized as a carrier for the delivery of cationic agents either by chemisorption or entrapment.[162] Recently, HNTs have been used for sustained delivery of drugs.[181] Clay minerals offer dispersions below micron level in aqueous media. Entrapment of drug molecules in the nanoparticulate system is a helpful strategy for protecting drugs against enzymes and chemicals and hence reduces the dissolution rate. Numerous medications, such as tetracycline, khellin, and nicotinamide adenine dinucleotide, have been loaded into HNTs by soaking in a saturated drug solution under vacuum.[182]

Due to characteristics such as nanoscale lumens, high length-to-diameter (L/D) ratio, low hydroxyl group density on the surface, etc., HNTs have been focused on by researchers recently, as indicated by the rapid growth in related publications. Scientists and engineers have discovered and developed an extensive range of exciting new applications for these unique, cheap, and abundantly available naturally occurring clays with nanoscale lumens. Numerous aspects of the preparation and the catalytic application of these systems warrant a deeper investigation and action. The ever-improving abilities of 'nanoarchitecture' at a molecular level will provide chemists, in the following years, with new tools to design and construct ideal catalysts for desired reactions rather than adapt existing catalysts according to a traditional trial-and-error approach.\

1.13 References

1.   OECD, *Nanotechnology for Green Innovation*. OECD Publishing, Paris: 2013; p 34.

2.   Ivanković, A., Review of 12 Principles of Green Chemistry in Practice. *International Journal of Sustainable and Green Energy* **2017,** *6* (3).

3.   Gupta, M.; Paul, S.; Gupta, R., General aspects of 12 basic principles of green chemistry with applications. *Current Scicene India* **2010,** *99* (10), 1341-1360.

4.   Casey, C. P., 2005 Nobel Prize in Chemistry. Development of the Olefin Metathesis Method in Organic Synthesis. *Journal of Chemical Education* **2006,** *83* (2), 192.

5.   Kent, J. A., *Kent and riegels Handbook of Industrial Chemistry and Biotechnology*. 11th ed.; Springer Science Business Media, LLC: 2007, 2007; Vol. 1, p 1856.

6.   Behari, J., Principles of nanoscience: an overview. *Indian Journal of Experimental Biology* **2010,** *48* (10), 1008-19.

7.   Whitesides, G. M., Nanoscience, Nanotechnology, and Chemistry. *Small* **2005,** *1* (2), 172-179.

8.   Whitesides, G. M., Nanoscience, nanotechnology, and chemistry. *Small* **2005,** *1* (2), 172-9.

9.   Logothetidis, S.; *Nanostructured Materials and Their Applications*. Springer-Verlag-US 2012, p.1-220.

10.   Somorjai, G. A.; Yang, M., The Surface Science of Catalytic Selectivity. *Topics in Catalysis* **2003,** *24* (1), 61-72.

11.   McHenry Jr., K. W., Catalyst poisoning. By L. Louis Hegedus and Robert W. McCabe, Marcel Dekker, 1984, 128 pp., *AIChE Journal* **1985,** *31* (9), 1581-1581.

12.   Jalama, K., Carbon dioxide hydrogenation over nickel-, ruthenium-, and copper-based catalysts: Review of kinetics and mechanism. *Catalysis Reviews* **2017,** *59*, 1-70.

13.   Speight, J. G., Selectivity In Catalysis Edited by Mark E. Davis and Steven L. Suib American Chemical Society Symposium Series 517 American Chemical Society, Washington, DC 1993 xi + 410 pp. *Fuel Science and Technology International* **1993,** *11* (9), 1313-1313.

14.   Wisniak, J., The History of Catalysis. From the Beginning to Nobel Prizes. *Educación Química* **2010,** *21* (1), 60-69.

15. Aftalion, F., *Recent History of the Chemical Industry 1973 to the Millenium: The New Facts of World Chemicals Since 1973.* Springer-Verlag US, 2007: 2007; Vol. 1, p 1856.

16. Vogt, E. T. C.; Weckhuysen, B. M., Fluid catalytic cracking: recent developments on the grand old lady of zeolite catalysis. *Chemical Society reviews* **2015,** *44* (20), 7342-7370.

17. Alabdullah, M. A.; Gomez, A. R.; Vittenet, J.; Bendjeriou-Sedjerari, A.; Xu, W.; Abba, I. A.; Gascon, J., A Viewpoint on the Refinery of the Future: Catalyst and Process Challenges. *ACS Catalysis* **2020,** *10* (15), 8131-8140.

18. Parmon, V.N.; Simagina,V. I.; Milova,L.P.,Precious metals in catalyst production. *Catalysis in Industry* **2010,** *2* (3), 199-205.

19. Anastas, P. T.; Kirchhoff, M. M.; Williamson, T. C., Catalysis as a foundational pillar of green chemistry. *Applied Catalysis A: General* **2001,** *221* (1), 3-13.

20. Trost, B., The atom economy--a search for synthetic efficiency. *Science* **1991,** *254* (5037), 1471-1477.

21. Murphy, M. A., Early Industrial Roots of Green Chemistry and the history of the BHC Ibuprofen process invention and its Quality connection. *Foundations of Chemistry* **2018,** *20* (2), 121-165.

22. Harrington, P. J.; Lodewijk, E., Twenty Years of Naproxen Technology. *Organic Process Research & Development* **1997,** *1* (1), 72-76.

23. Rajurkar, K. B.; Tonde, S. S.; Didgikar, M. R.; Joshi, S. S.; Chaudhari, R. V., Environmentally Benign Catalytic Hydroformylation−Oxidation Route for Naproxen Synthesis. *Industrial & Engineering Chemistry Research* **2007,** *46* (25), 8480-8489.

24. Hogg, J. A., Steroids, the steroid community, and Upjohn in perspective: a profile of innovation. *Steroids* **1992,** *57* (12), 593-616.

25. Sauer, N. N., Green Chemistry: Frontiers in Benign Chemical Syntheses and Processes Edited by Paul T. Anastas and Tracy C. Williamson (U. S. Environmental Protection Agency). Oxford University Press: New York, NY. 1999. 360 pp. ISBN 0-19-850170-6. *Journal of the American Chemical Society* **2000,** *122* (22), 5419-5420.

26. Mahato, S. K.; Acharya, C.; Wellington, K. W.; Bhattacharjee, P.; Jaisankar, P., InCl3: A Versatile Catalyst for Synthesizing a Broad Spectrum of Heterocycles. *American Chemical Soceity: Omega* **2020,** *5* (6), 2503-2519.

27. Khan, S. H., Green Nanotechnology for the Environment and Sustainable Development. In *Green Materials for Wastewater Treatment*, Naushad, M.; Lichtfouse, E., Eds. Springer International Publishing: Cham, 2020; pp 13-46.

28.   Wells, P. B., Catalysis. In *Encyclopedia of Materials: Science and Technology*, Buschow, K. H. J.; Cahn, R. W.; Flemings, M. C.; Ilschner, B.; Kramer, E. J.; Mahajan, S.; Veyssière, P., Eds. Elsevier: Oxford, 2001; pp 1020-1025.

29.   Anastas, P. T.; Bartlett, L. B.; Kirchhoff, M. M.; Williamson, T. C., The role of catalysis in the design, development, and implementation of green chemistry. *Catalysis Today* **2000,** *55* (1), 11-22.

30.   Sheldon, R. A., Fundamentals of green chemistry: efficiency in reaction design. *Chemical Society Review* **2012,** *41* (4), 1437-1451.

31.   Centi, G.; Perathoner, S., Catalysis and sustainable (green) chemistry. *Catalysis Today* **2003,** *77* (4), 287-297.

32.   Védrine, J. C., 9 - Concluding remarks and challenges of heterogeneous catalysis on metal oxides. In *Metal Oxides in Heterogeneous Catalysis*, Védrine, J. C., Ed. Elsevier: 2018; pp 551-569.

33.   Horvath, J. D.; Gellman, A. J., Naturally Chiral Surfaces. *Topics in Catalysis* **2003,** *25* (1), 9-15.

34.   Yeo, Y. Y.; Vattuone, L.; King, D. A., Calorimetric heats for CO and oxygen adsorption and for the catalytic CO oxidation reaction on Pt{111}. *The Journal of Chemical Physics* **1997,** *106* (1), 392-401.

35.   Peden, C. H.; Ray, D. *Advanced Resources for Catalysis Science; Recommendations for a National Catalysis Research Institute*; PNNL-15423; Other: 8215; United States 10.2172/877063; Pacific Northwest National Laboratory (PNNL), Richland, WA (US), Environmental Molecular Sciences Laboratory (EMSL): 2005; p Medium: ED; Size: PDFN.

36.   Thomas, J. M.; Thomas, W. J., *Principles and Practice of Heterogeneous Catalysis*. Wiley: 2014.

37.   Thomas, J. M., Handbook Of Heterogeneous Catalysis. 2., completely revised and enlarged Edition. Vol. 1–8. Edited by G. Ertl, H. Knözinger, F. Schüth, and J. Weitkamp. *Angewandte Chemie International Edition* **2009,** *48* (19), 3390-3391.

38.   Haller, G. L., New catalytic concepts from new materials: understanding catalysis from a fundamental perspective, past, present, and future. *Journal of Catalysis* **2003,** *216* (1), 12-22.

39.   Thomas, J. M., Heterogeneous catalysis: Enigmas, illusions, challenges, realities, and emergent strategies of design. *The Journal of Chemical Physics* **2008,** *128* (18), 182502.

40. Galarneau, A.; Di Renzo, F.; Fajula, F.; Vedrine, J., *Zeolites and Mesoporous Materials at the Dawn of the 21st Century: Proceedings of the 13th International Zeolite Conference, Montpellier, France, 8-13 July 2001*. Elsevier Science: 2001.

41. Thomas, J. M.; Raja, R., Catalytic significance of organometallic compounds immobilized on mesoporous silica: economically and environmentally important examples. *Journal of Organometallic Chemistry* **2004,** *689* (24), 4110-4124.

42. Climent, M. J.; Corma, A.; Iborra, S., Heterogeneous Catalysts for the One-Pot Synthesis of Chemicals and Fine Chemicals. *Chemical Reviews* **2011,** *111* (2), 1072-1133.

43. Xuereb, D. J.; Raja, R., Design strategies for engineering selectivity in bio-inspired heterogeneous catalysts. *Catalysis Science & Technology* **2011,** *1* (4), 517-534.

44. Maschmeyer, T.; Rey, F.; Sankar, G.; Thomas, J. M., Heterogeneous catalysts obtained by grafting metallocene complexes onto mesoporous silica. *Nature* **1995,** *378* (6553), 159-162.

45. Thomas, J. M.; Raja, R.; Lewis, D. W., Single-Site Heterogeneous Catalysts. *Angewandte Chemie International Edition* **2005,** *44* (40), 6456-6482.

46. Santo, V. D.; Guidotti, M.; Psaro, R.; Marchese, L.; Carniato, F.; Bisio, C., Rational design of single-site heterogeneous catalysts: towards high chemo-, regio- and stereoselectivity. *Proceedings of the Royal Society A: Mathematical, Physical and Engineering Sciences* **2012,** *468* (2143), 1904-1926.

47. Guisnet, M.; Guidotti, M., Problems and Pitfalls in the Applications of Zeolites and other Microporous and Mesoporous Solids to Catalytic Fine Chemical Synthesis. In *Catalysts for Fine Chemical Synthesis*, 2006; pp 39-67.

48. Thomas, J. M., The chemistry of crystalline sponges. *Nature* **1994,** *368* (6469), 289-290.

49. Copéret, C.; Chabanas, M.; Petroff Saint-Arroman, R.; Basset, J.-M., Homogeneous and Heterogeneous Catalysis: Bridging the Gap through Surface Organometallic Chemistry. *Angewandte Chemie International Edition* **2003,** *42* (2), 156-181.

50. Thomas, J. M.; Hernandez-Garrido, J. C.; Raja, R.; Bell, R. G., Nanoporous oxidic solids: the confluence of heterogeneous and homogeneous catalysis. *Physical Chemistry Chemical Physics* **2009,** *11* (16), 2799-2825.

51. Hoskins, B. F.; Robson, R., Design and construction of a new class of scaffolding-like materials comprising infinite polymeric frameworks of 3D-linked molecular rods. A reappraisal of the zinc cyanide and cadmium cyanide structures and the synthesis and structure of the diamond-related frameworks. *Journal of the American Chemical Society* **1990,** *112* (4), 1546-1554.

52.   Batten, S. R.; Hoskins, B. F.; Robson, R., Two Interpenetrating 3D Networks Which Generate Spacious Sealed-Off Compartments Enclosing of the Order of 20 Solvent Molecules in the Structures of Zn(CN)(NO$_3$) *Journal of the American Chemical Society* **1995,** *117* (19), 5385-5386.

53.   Kitagawa, S.; Matsuyama, S.; Munakata, M.; Emori, T., Synthesis and crystal structures of novel one-dimensional polymers. *Journal of the Chemical Society, Dalton Transactions* **1991,** (11), 2869-2874.

54.   Kitagawa, S.; Kawata, S.; Nozaka, Y.; Munakata, M., Synthesis and crystal structures of novel copper(I) co-ordination polymers and a hexacopper(I) cluster of quinoline-2-thione. *Journal of the Chemical Society, Dalton Transactions* **1993,** (9), 1399-1404.

55.   Yaghi, O. M.; Li, H., Hydrothermal Synthesis of a Metal-Organic Framework Containing Large Rectangular Channels. *Journal of the American Chemical Society* **1995,** *117* (41), 10401-10402.

56.   Gardner, G. B.; Venkataraman, D.; Moore, J. S.; Lee, S., Spontaneous assembly of a hinged coordination network. *Nature* **1995,** *374* (6525), 792-795.

57.   Riou, D.; Férey, G., Hybrid open frameworks (MIL-n). Part 3 Crystal structures of the HT and LT forms of MIL-7: a new vanadium propylenediphosphonate with an open-framework. Influence of the synthesis temperature on the oxidation state of vanadium within the same structural type. *Journal of Materials Chemistry* **1998,** *8* (12), 2733-2735.

58.   Wang, C.; Liu, D.; Lin, W., Metal–Organic Frameworks as A Tunable Platform for Designing Functional Molecular Materials. *Journal of the American Chemical Society* **2013,** *135* (36), 13222-13234.

59.   Cooper, A. I., Conjugated Microporous Polymers. *Advanced Materials* **2009,** *21* (12), 1291-1295.

60.   Thomas, A., Functional Materials: From Hard to Soft Porous Frameworks. *Angewandte Chemie International Edition* **2010,** *49* (45), 8328-8344.

61.   Dawson, R.; Cooper, A. I.; Adams, D. J., Nanoporous organic polymer networks. *Progress in Polymer Science* **2012,** *37* (4), 530-563.

62.   Maishal, T. K.; Alauzun, J.; Basset, J. M.; Copéret, C.; Corriu, R. J.; Jeanneau, E.; Mehdi, A.; Reyé, C.; Veyre, L.; Thieuleux, C., A tailored organometallic-inorganic hybrid mesostructured material: a route to a well-defined, active, and reusable heterogeneous iridium-NHC catalyst for H/D exchange. *Angew Chem Int Ed Engl* **2008,** *47* (45), 8654-6.

63.   Campbell, I. M., *Catalysis at Surfaces*. Springer Netherlands **1988**, 2-250.

64.   Ertl, G.; Knözinger, H.; Weitkamp, J., *Preparation of Solid Catalysts*. Wiley: 2008.

65.   Heinrichs, C.; Hölderich, W. F., Novel zeolitic hosts for "ship-in-a-bottle" catalysts. *Catalysis Letters* **1999,** *58* (2), 75-80.

66.   Fukuoka, A.; Higashimoto, N.; Sakamoto, Y.; Sasaki, M.; Sugimoto, N.; Inagaki, S.; Fukushima, Y.; Ichikawa, M., Ship-in-bottle synthesis and catalytic performances of platinum carbonyl clusters, nanowires, and nanoparticles in micro- and mesoporous materials. *Catalysis Today* **2001,** *66* (1), 23-31.

67.   Kozhevnikov, I. V., Heteropoly Acids and Related Compounds as Catalysts for Fine Chemical Synthesis. *Catalysis Reviews* **1995,** *37* (2), 311-352.

68.   Wilson, K., R. A. Sheldon, I. Arends and U. Hanefeld. Green chemistry and catalysis. Wiley-VCH, 2007, 448 pp; ISBN 978-3-527-30715-9. *Applied Organometallic Chemistry* **2007,** *21* (11), 1002-1002.

69.   Chattopadhyay, D., Endangered elements of the periodic table. *Resonance* **2017,** *22*, 79-87.

70.   Valásková, M., Clays, clay minerals and cordierite ceramics - A review. *Ceramics Silikaty* **2015,** *59*, 331-340.

71.   Sainz-Díaz, C.; Timón, V.; Hernandez-Laguna, A., Isomorphous substitution effect on the vibration frequencies of hydroxil groups in molecular cluster models of the clay octahedral sheet. *American Mineralogist* **2000,** *85*.

72.   Tournassat, C.; Neaman, A.; Villiéras, F.; Bosbach, D.; Charlet, L., Nanomorphology of montmorillonite particles: Estimation of the clay edge sorption site density by low-pressure gas adsorption and AFM observations. *American Mineralogist* **2003,** *88*, 1989-1995.

73.   Churakov, S. V., Ab initio study of sorption on pyrophyllite: structure and acidity of the edge sites. *Journal of Physical Chemistry B* **2006,** *110* (9), 4135-46.

74.   Bergaya, F.; Lagaly, G., Surface modification of clay minerals. *Applied Clay Science* **2001,** *19*, 1-3.

75.   Stöcker, M., Biofuels and biomass-to-liquid fuels in the biorefinery: catalytic conversion of lignocellulosic biomass using porous materials. *Angewandte Chemie International Edition* 2**008,** *47* (48), 9200-11.

76.   Regalbuto, J. R., Engineering. Cellulosic biofuels--got gasoline? *Science* **2009,** *325* (5942), 822-4.

77.   Holm, M. S.; Pagán-Torres, Y. J.; Saravanamurugan, S.; Riisager, A.; Dumesic, J. A.; Taarning, E., Sn-Beta catalysed conversion of hemicellulosic sugars. *Green Chemistry* **2012,** *14* (3).

78.   Fan, Y.; Zhou, C.; Zhu, X., Selective Catalysis of Lactic Acid to Produce Commodity Chemicals. *Catalysis Reviews* **2009,** *51* (3), 293-324.

79. Zhou, C. H.; Beltramini, J. N.; Fan, Y. X.; Lu, G. Q., Chemoselective catalytic conversion of glycerol as a biorenewable source to valuable commodity chemicals. *Chemical Society Reviews* **2008,** *37* (3), 527-49.

80. Galletti, A. M. R.; Antonetti, C.; De Luise, V.; Martinelli, M., A sustainable process for the production of γ-valerolactone by hydrogenation of biomass-derived levulinic acid. *Green Chemistry* **2012,** *14* (3).

81. Vogels, R.; Kloprogge, T.; Geus, J. W.; Philips, Catalytic activity of synthetic saponite clays: Effects of tetrahedral and octahedral composition. *Journal of Catalysis* **2005,** *231*, 443-452.

82. Kumar, B. S.; Dhakshinamoorthy, A.; Pitchumani, K., K10 montmorillonite clays as environmentally benign catalysts for organic reactions. *Catalysis Science & Technology* **2014,** *4* (8), 2378-2396.

83. Manikandan, D.; Divakar, D.; Rupa, A. V.; Revathi, S.; Preethi, M. E. L.; Sivakumar, T., Synthesis of platinum nanoparticles in montmorillonite and their catalytic behaviour. *Applied Clay Science* **2007,** *37* (1-2), 193-200.

84. Motokura, K.; Tada, M.; Iwasawa, Y., Layered materials with coexisting acidic and basic sites for catalytic one-pot reaction sequences. *Journal of the American Chemical Society* **2009,** *131* (23), 7944-5.

85. Bandgar, B. P.; Uppalla, L. S.; Sadavarte, V. S., Envirocat EPZG and natural clay as efficient catalysts for transesterification of β-keto esters. *Green Chemistry* **2001,** *3* (1), 39-41.

86. Racha, A.; Bojja, S.; Parthasarathy, G., Chamosite, a naturally occurring clay as a versatile catalyst for various organic transformations. *Clay Minerals* **2010,** *45*, 281-299.

87. Varma, R., ChemInform Abstract: Clay and Clay-Supported Reagents in Organic Synthesis. *Tetra* **2002,** *58*, 1235-1255.

88. Laszlo, P., Chemical Reactions on Clays. *Science* **1987,** *235* (4795), 1473-1477.

89. Clark, J. H.; Kybett, A. P.; Macquarrie, D. J.; Barlow, S. J.; Landon, P., Montmorillonite supported transition metal salts as Friedel–Crafts alkylation catalysts. *Chemical Communications* **1989,** (18), 1353-1354.

90. Pinnavaia, T. J.; Raythatha, R.; Lee, J. G.-S.; Halloran, L. J.; Hoffman, J. F., Intercalation of catalytically active metal complexes in mica-type silicates. Rhodium hydrogenation catalysts. *Journal of the American Chemical Society* **1979,** *101* (23), 6891-6897.

91. Su, F.; Lv, L.; Lee, F. Y.; Liu, T.; Cooper, A. I.; Zhao, X. S., Thermally Reduced Ruthenium Nanoparticles as a Highly Active Heterogeneous Catalyst for Hydrogenation of Monoaromatics. *Journal of the American Chemical Society* **2007,** *129* (46), 14213-14223.

92.   Herney-Ramirez, J.; Vicente, M. A.; Madeira, L. M., Heterogeneous photo-Fenton oxidation with pillared clay-based catalysts for wastewater treatment: A review. *Applied Catalysis B: Environmental* **2010,** *98* (1), 10-26.

93.   Zhou, C.-H.; Beltramini, J. N.; Fan, Y.-X.; Lu, G. Q., Chemoselective catalytic conversion of glycerol as a biorenewable source to valuable commodity chemicals. *Chemical Society Reviews* **2008,** *37* (3), 527-549.

94.   Soetaredjo, F. E.; Ayucitra, A.; Ismadji, S.; Maukar, A. L., KOH/bentonite catalysts for transesterification of palm oil to biodiesel. *Applied Clay Science* **2011,** *53* (2), 341-346.

95.   Narayan, N.; Meiyazhagan, A.; Vajtai, R., Metal Nanoparticles as Green Catalysts. *Materials (Basel)* **2019,** *12* (21), 3602.

96.   Sharma, N.; Ojha, H.; Bharadwaj, A.; Pathak, D. P.; Sharma, R. K., Preparation and catalytic applications of nanomaterials: a review. *Royal Society of Chemistry Advances* **2015,** *5* (66), 53381-53403.

97.   Rodrigues, T. S.; da Silva, A. G. M.; Camargo, P. H. C., Nanocatalysis by noble metal nanoparticles: controlled synthesis for the optimization and understanding of activities. *Journal of Materials Chemistry A* **2019,** *7* (11), 5857-5874.

98.   Khan, I.; Saeed, K.; Khan, I., Nanoparticles: Properties, applications and toxicities. *Arabian Journal of Chemistry* **2019,** *12* (7), 908-931.

99.   Nashner, M. S.; Frenkel, A. I.; Adler, D. L.; Shapley, J. R.; Nuzzo, R. G., Structural Characterization of Carbon-Supported Platinum−Ruthenium Nanoparticles from the Molecular Cluster Precursor $PtRu_5C(CO)_{16}$. *Journal of the American Chemical Society* **997,** *119* (33), 7760-7771.

100.   Schmid, G.; Maihack, V.; Lantermann, F.; Peschel, S., Ligand-stabilized metal clusters and colloids: properties and applications. *Journal of the Chemical Society, Dalton Transactions* **1996,** (5), 589-595.

101.   Henglein, A., Physicochemical properties of small metal particles in solution: "microelectrode" reactions, chemisorption, composite metal particles, and the atom-to-metal transition. *The Journal of Physical Chemistry* **1993,** *97* (21), 5457-5471.

102.   Duff, D. G.; Baiker, A.; Edwards, P. P., A new hydrosol of gold clusters. 1. Formation and particle size variation. *Langmuir* **1993,** *9* (9), 2301-2309.

103.   Glavee, G. N.; Klabunde, K. J.; Sorensen, C. M.; Hadjipanayis, G. C., Borohydride reduction of cobalt ions in water. Chemistry leading to nanoscale metal, boride, or borate particles. *Langmuir* **1993,** *9* (1), 162-169.

104. Toshima, N.; Yonezawa, T.; Kushihashi, K., Polymer-protected palladium–platinum bimetallic clusters: preparation, catalytic properties and structural considerations. *Journal of the Chemical Society, Faraday Transactions* **1993,** *89* (14), 2537-2543.

105. Liz-Marzan, L. M.; Philipse, A. P., Stable hydrosols of metallic and bimetallic nanoparticles immobilized on imogolite fibers. *The Journal of Physical Chemistry* **1995,** *99* (41), 15120-15128.

106. Naoki, T.; Tadahito, T., Colloidal Dispersions of Platinum and Palladium Clusters Embedded in the Micelles.Preparation and Application to the Catalysis for Hydrogenation of Olefins. *Bulletin of the Chemical Society of Japan* **1992,** *65* (2), 400-409.

107. Petit, C.; Lixon, P.; Pileni, M. P., In situ synthesis of silver nanocluster in AOT reverse micelles. *The Journal of Physical Chemistry* **1993,** *97* (49), 12974-12983.

108. Wilcoxon, J. P.; Williamson, R. L.; Baughman, R., Optical properties of gold colloids formed in inverse micelles. *The Journal of Chemical Physics* **1993,** *98* (12), 9933-9950.

109. Campelo, J. M.; Conesa, T. D.; Gracia, M. J.; Jurado, M. J.; Luque, R.; Marinas, J. M.; Romero, A. A., Microwave facile preparation of highly active and dispersed SBA-12 supported metal nanoparticles. *Green Chemistry* **2008,** *10* (8), 853-858.

110. Pande, S.; Saha, A.; Jana, S.; Sarkar, S.; Basu, M.; Pradhan, M.; Sinha, A. K.; Saha, S.; Pal, A.; Pal, T., Resin-Immobilized CuO and Cu Nanocomposites for Alcohol Oxidation. *Organic Letters* **2008,** *10* (22), 5179-5181.

111. Kim, S.-W.; Kim, M.; Lee, W. Y.; Hyeon, T., Fabrication of Hollow Palladium Spheres and Their Successful Application to the Recyclable Heterogeneous Catalyst for Suzuki Coupling Reactions. *Journal of the American Chemical Society* **2002,** *124* (26), 7642-7643.

112. Saikia, P. K.; Sarmah, P. P.; Borah, B. J.; Saikia, L.; Saikia, K.; Dutta, D. K., Stabilized Fe3O4 magnetic nanoparticles into nanopores of modified montmorillonite clay: a highly efficient catalyst for the Baeyer–Villiger oxidation under solvent free conditions. *Green Chemistry* **2016,** *18* (9), 2843-2850.

113. Mekewi, M. A.; Darwish, A. S.; Amin, M. S.; Eshaq, G.; Bourazan, H. A., Copper nanoparticles supported onto montmorillonite clays as efficient catalyst for methylene blue dye degradation. *Egyptian Journal of Petroleum* **2016,** *25* (2), 269-279.

114. Tamura, M.; Fujihara, H., Chiral Bisphosphine BINAP-Stabilized Gold and Palladium Nanoparticles with Small Size and Their Palladium Nanoparticle-Catalyzed Asymmetric Reaction. *Journal of the American Chemical Society* **2003,** *125* (51), 15742-15743.

115. Sharma, V. K.; Yngard, R. A.; Lin, Y., Silver nanoparticles: green synthesis and their antimicrobial activities. *Adv Colloid Interface Sci* **2009,** *145* (1-2), 83-96.

116. Mahata, N.; Cunha, A. F.; Órfão, J. J. M.; Figueiredo, J. L., Hydrogenation of chloronitrobenzenes over filamentous carbon stabilized nickel nanoparticles. *Catalysis Communications* **2009,** *10* (8), 1203-1206.

117. Ahmed, O. S.; Dutta, D. K., Generation of Metal Nanoparticles on Montmorillonite K 10 and Their Characterization. *Langmuir* **2003,** *19* (13), 5540-5541.

118. Sarmah, P. P.; Dutta, D. K., Chemoselective reduction of a nitro group through transfer hydrogenation catalysed by Ru0-nanoparticles stabilized on modified Montmorillonite clay. *Green Chemistry* **2012,** *14* (4), 1086-1093.

119. Borah, B. J.; Dutta, D.; Saikia, P. P.; Barua, N. C.; Dutta, D. K., Stabilization of Cu(0)-nanoparticles into the nanopores of modified montmorillonite: An implication on the catalytic approach for "Click" reaction between azides and terminal alkynes. *Green Chemistry* **2011,** *13* (12), 3453-3460.

120. Patel, H. A.; Bajaj, H. C.; Jasra, R. V., Synthesis of Pd and Rh metal nanoparticles in the interlayer space of organically modified montmorillonite. *Journal of Nanoparticle Research* **2008,** *10* (4), 625-632.

121. Manikandan, D.; Duraiswami, D.; Rupa, A.; Revathi, S.; Preethi, M.; Sivakumar, T., Synthesis of platinum nanoparticles in montmorillonite and their catalytic behaviour. *Applied Clay Science* **2007,** *37*, 193-200.

122. Pinnavaia, T. J., Intercalated Clay Catalysts. *Science* **1983,** *220* (4595), 365-371.

123. Choudary, B. M.; Bharathi, P., Syntheses of interlamellar montmorillonitebipyridinepalladium(II) catalysts: the first examples of chelation in smectite clay. *Journal of the Chemical Society, Chemical Communications* **1987,** (19), 1505-1506.

124. Ravindranathan, P.; Malla, P. B.; Komarneni, S.; Roy, R., Preparation of metal supported montmorillonite catalyst: A new approach. *Catalysis Letters* **1990,** *6* (3), 401-407.

125. Shimazu, S.; Ro, K.; Sento, T.; Ichikuni, N.; Uematsu, T., Asymmetric hydrogenation of α,β-unsaturated carboxylic acid esters by rhodium(I) — phosphine complexes supported on smectites. *Journal of Molecular Catalysis A: Chemical* **1996,** *107* (1), 297-303.

126. Bartók, M.; Szöllösi, G.; Mastalir, Á.; Dékány, I., Hydrogenation reactions on heterogenized Wilkinson complexes. *Journal of Molecular Catalysis A: Chemical* **1999,** *139* (2), 227-234.

127. Király, Z.; Dékány, I.; Mastalir, Á.; Bartók, M., In SituGeneration of Palladium Nanoparticles in Smectite Clays. *Journal of Catalysis* **1996,** *161* (1), 401-408.

128. Szűcs, A.; Berger, F.; Dékány, I., Preparation and structural properties of Pd nanoparticles in layered silicate. *Colloids and Surfaces A: Physicochemical and Engineering Aspects* **2000,** *174* (3), 387-402.

129. Papp, S.; Szücs, A.; Dékány, I., Preparation of Pd0 nanoparticles stabilized by polymers and layered silicate. *Applied Clay Science* **2001,** *19* (1), 155-172.

130. Thiripuranthagan, S.; Tohru, M.; Jun, K.; Yutaka, M., Selective Hydrogenation of 2-Methylbenzaldehyde Using Palladium Particles Generated in situ in Surfactant Exchanged Fluorotetrasilicic Mica. *Chemistry Letters* **2001,** *30* (9), 860-861.

131. Szöllösi, G.; Kun, I.; Mastalir, Á.; Bartók, M.; Dékány, I., Preparation, characterization and application of platinum catalysts immobilized on clays. *Solid State Ionics* **2001,** *141-142*, 273-278.

132. Kun, I.; Szőllősi, G.; Bartók, M., Crotonaldehyde hydrogenation over clay-supported platinum catalysts. *Journal of Molecular Catalysis A: Chemical* **2001,** *169*, 235-246.

133. Sivakumar, T.; Krithiga, T.; Shanthi, K.; Mori, T.; Kubo, J.; Morikawa, Y., Noble metals intercalated/supported mica catalyst - Synthesis and characterization. *Journal of Molecular Catalysis A: Chemical* **2004,** *223*, 185-194.

134. Mastalir, Á.; Király, Z.; Szöllosi, G.; Bartók, M., Preparation of Organophilic Pd–Montmorillonite, An Efficient Catalyst in Alkyne Semihydrogenation. *Journal of Catalysis* **2000,** *194* (1), 146-152.

135. Mastalir, Á.; Kiraly, Z.; Szőllősi, G.; Bartók, M., Stereoselective hydrogenation of 1-phenyl-1-pentyne over low-loaded Pd-montmorillonite catalysts. *Applied Catalysis A-general* **2001,** *213*, 133-140.

136. Király, Z.; Veisz, B.; Mastalir, Á.; Köfaragó, G., Preparation of Ultrafine Palladium Particles on Cationic and Anionic Clays, Mediated by Oppositely Charged Surfactants: Catalytic Probes in Hydrogenations. *Langmuir* **2001,** *17* (17), 5381-5387.

137. Gallezot, P.; Richard, D., Selective Hydrogenation of α,β-Unsaturated Aldehydes. *Catalysis Reviews* **1998,** *40* (1-2), 81-126.

138. Das, P.; Sarmah, P.; Borah, B.; Saikia, L.; Dutta, D., Aromatic Ring Hydrogenation Catalyzed by Nanoporous Montmorillonite Supported Ir(0)-Nanoparticle Composites under Solvent Free Conditions. *New J. Chem.* **2016,** *40*.

139. Keeling, J., The mineralogy, geology and occurrences of halloysite. 2015; pp 96-115.

140. Parfitt, R.; Wilson, A. D., Estimation of allophane and halloysite in three sequences of volcanic soils, New Zealand. *Catena Supplement* **1985,** *7*, 1-8.

141. Ziegler, K.; Hsieh, J. C. C.; Chadwick, O. A.; Kelly, E. F.; Hendricks, D. M.; Savin, S. M., Halloysite as a kinetically controlled end product of arid-zone basalt weathering. *Chemical Geology* **2003,** *202* (3), 461-478.

142.	Chadwick, O. A.; Gavenda, R. T.; Kelly, E. F.; Ziegler, K.; Olson, C. G.; Elliott, W. C.; Hendricks, D. M., The impact of climate on the biogeochemical functioning of volcanic soils. *Chemical Geology* **2003,** *202* (3), 195-223.

143.	Kunze, G. W.; Bradley, W. F., Occurrence of a Tabular Halloysite in a Texas Soil. *Clays and Clay Minerals* **1963,** *12* (1), 523-527.

144.	Santos, P. d. S.; Santos, H. d. S.; Brindley, G. W., Mineralogical studies of kaolinite-halloysite clays: Part IV. A platy mineral with structural swelling and shrinking characteristics. *American Mineralogist* **1966,** *51* (11-12), 1640-1648.

145.	Dixon, J. B.; McKee, T. R., Internal and External Morphology of Tubular and Spheroidal Halloysite Particles. *Clays and Clay Minerals* **1974,** *22* (1), 127-137.

146.	Churchman, G. J.; Carr, R. M., The Definition and Nomenclature of Halloysites. *Clays and Clay Minerals* **1975,** *23* (5), 382-388.

147.	Papoulis, D.; Tsolis-Katagas, P.; Kalampounias, A. G.; Tsikouras, B., Progressive formation of halloysite from the hydrothermal alteration of biotite and the formation mechanisms of anatase in altered volcanic rocks from Limnos Island, northeast Aegean Sea, Greece. *Clays and Clay Minerals* **2009,** *57* (5), 566-577.

148.	Cavallaro, G.; Chiappisi, L.; Pasbakhsh, P.; Gradzielski, M.; Lazzara, G., A structural comparison of halloysite nanotubes of different origin by Small-Angle Neutron Scattering (SANS) and Electric Birefringence. *Applied Clay Science* **2018,** *160*, 71-80.

149.	Du, M.; Guo, B.; Jia, D., Newly emerging applications of halloysite nanotubes: a review. *Polymer International* **2010,** *59* (5), 574-582.

150.	Pasbakhsh, P.; Churchman, G. J.; Keeling, J. L., Characterisation of properties of various halloysites relevant to their use as nanotubes and microfibre fillers. *Applied Clay Science* **2013,** *74*, 47-57.

151.	Vergaro, V.; Abdullayev, E.; Lvov, Y. M.; Zeitoun, A.; Cingolani, R.; Rinaldi, R.; Leporatti, S., Cytocompatibility and Uptake of Halloysite Clay Nanotubes. *Biomacromolecules* **2010,** *11* (3), 820-826.

152.	Singh, B.; Gilkes, R. J., An Electron Optical Investigation of the Alteration of Kaolinite to Halloysite. *Clays and Clay Minerals* **1992,** *40* (2), 212-229.

153.	Alexander, L. T.; Faust, G. T.; Hendricks, S. B.; Insley, H.; McMurdie, H. F., Relationship of the clay minerals halloysite and endellite. *American Mineralogist* **1943,** *28* (1), 1-18.

154.	Bailey, S. W. In *Halloysite -A critical assessment*. Sciences Geologiques, Annee1990, pp. 89-98.

155. Miller, A. K.; Guggenheim, S.; Koster van Groos, A. F., The incorporation of "water" in a high-pressure 2:1 layer silicate; a high pressure differential thermal analysis of the 10 Å phase. *American Mineralogist* **1991,** *76* (1-2), 106-112.

156. Hendricks, S. B.; Jefferson, M. E., Structures of Kaolin and Talc-Pyrophyllite Hydrates and Their Bearing on Water Sorption of the Clays. *American Mineralogist* **1938,** *23* (12), 863-875.

157. Brindley, G. W.; Brown, G., *Crystal Structures of Clay Minerals and their X-Ray Identification*. Mineralogical Society of Great Britain and Ireland: 1980**,** pp.1-400.

158. Smirnov, K. S.; Bougeard, D., A Molecular Dynamics Study of Structure and Short-time Dynamics of Water in Kaolinite. *The Journal of Physical Chemistry B* **1999,** *103* (25), 5266-5273.

159. Costanzo, P. M.; Giese, R. F.; Lipsicas, M.; Straley, C., Synthesis of a quasi-stable kaolinite and heat capacity of interlayer water. *Nature* **1982,** *296* (5857), 549-551.

160. Costanzo, P. M.; Giese, R. F.; Lipsicas, M., Static and Dynamic Structure of Water in Hydrated Kaolinites. I. The Static Structure. *Clays and Clay Minerals* **1984,** *32* (5), 419-428.

161. Costanzo, P. M.; Giese, R. F., Dehydration of Synthetic Hydrated Kaolinites: A Model for the Dehydration of Halloysite(10Å). *Clays and Clay Minerals* **1985,** *33* (5), 415-423.

162. Massaro, M.; Noto, R.; Riela, S., Past, Present and Future Perspectives on Halloysite Clay Minerals. *Molecules* **2020,** *25* (20), 4863.

163. Churchman, G.; Pasbakhsh, P. In *Current Trends in Research and Application of Natural Mineral Nanotubes*, 2015.

164. Yuan, P., Properties and applications of halloysite nanotubes: recent research advances and future prospects. *Applied Clay Science* **2015,** *112-113*, 75-93.

165. Liu, P.; Zhao, M., Silver nanoparticle supported on halloysite nanotubes catalyzed reduction of 4-nitrophenol (4-NP). *Applied Surface Science* **2009,** *255*, 3989-3993.

166. Yu, L.; Shi, Y.; Zhao, Z.; Yin, H.; Wei, Y.; Liu, J.; Kang, W.; Jiang, T.; Wang, A., Ultrasmall silver nanoparticles supported on silica and their catalytic performances for carbon monoxide oxidation. *Catalysis Communications* **2011,** *12* (7), 616-620.

167. Ramnani, S. P.; Biswal, J.; Sabharwal, S., Synthesis of silver nanoparticles supported on silica aerogel using gamma radiolysis. *Radiation Physics and Chemistry* **2007,** *76* (8), 1290-1294.

168. Jin, L.; Qian, K.; Jiang, Z.; Huang, W., Ag/SiO$_2$ catalysts prepared via γ-ray irradiation and their catalytic activities in CO oxidation. *Journal of Molecular Catalysis A: Chemical* **2007,** *274* (1), 95-100.

169. Zhai, H.-J.; Sun, D.-W.; Wang, H.-S., Catalytic Properties of Silica/Silver Nanocomposites. *Journal of Nanoscience and Nanotechnology* **2006,** *6* (7), 1968-1972.

170. Wang, L.; Chen, J.; Ge, L.; Zhu, Z.; Rudolph, V., Halloysite-Nanotube-Supported Ru Nanoparticles for Ammonia Catalytic Decomposition to Produce COx-Free Hydrogen. *Energy & Fuels* **2011,** *25* (8), 3408-3416.

171. Luque, R.; Badamali, S.; Clark, J.; Fleming, M.; Macquarrie, D., Controlling selectivity in catalysis: Selective greener oxidation of cyclohexene under microwave conditions. *Applied Catalysis A-General* **2008,** *341*, 154-159.

172. Raveendran, S.; Guliants, V., Recent developments in catalysis using nanostructured materials. *Applied Catalysis A-general - Applied Catalysis: A-General* **2009,** *356*, 1-17.

173. Tully, J.; Yendluri, R.; Lvov, Y., Halloysite Clay Nanotubes for Enzyme Immobilization. *Biomacromolecules* **2016,** *17* (2), 615-621.

174. Qiu, K.; Netravali, A. N., Halloysite nanotube reinforced biodegradable nanocomposites using noncrosslinked and malonic acid crosslinked polyvinyl alcohol. *Polymer Composites* **2013,** *34* (5), 799-809.

175. Liu, M.; Zhang, Y.; Wu, C.; Xiong, S.; Zhou, C., Chitosan/halloysite nanotubes bionanocomposites: Structure, mechanical properties and biocompatibility. *International Journal of Biological Macromolecules* **2012,** *51* (4), 566-575.

176. Cavallaro, G.; Lazzara, G.; Milioto, S., Dispersions of Nanoclays of Different Shapes into Aqueous and Solid Biopolymeric Matrices. Extended Physicochemical Study. *Langmuir* **2011,** *27* (3), 1158-1167.

177. Cavallaro, G.; Donato, D. I.; Lazzara, G.; Milioto, S., Films of Halloysite Nanotubes Sandwiched between Two Layers of Biopolymer: From the Morphology to the Dielectric, Thermal, Transparency, and Wettability Properties. *The Journal of Physical Chemistry C* **2011,** *115* (42), 20491-20498.

178. Cavallaro, G.; De Lisi, R.; Lazzara, G.; Milioto, S., Polyethylene glycol/clay nanotubes composites. *Journal of Thermal Analysis and Calorimetry* **2013,** *112* (1), 383-389.

179. Cavallaro, G.; Gianguzza, A.; Lazzara, G.; Milioto, S.; Piazzese, D., Alginate gel beads filled with halloysite nanotubes. *Applied Clay Science* **2013,** *72*, 132-137.

180. Du, M.; Guo, B.; Lei, Y.; Liu, M.; Jia, D., Carboxylated butadiene–styrene rubber/halloysite nanotube nanocomposites: Interfacial interaction and performance. *Polymer* **2008,** *49* (22), 4871-4876.

181.   Satish, S.; Tharmavaram, M.; Rawtani, D., Halloysite nanotubes as a nature's boon for biomedical applications. *Nanobiomedicine* **2019,** 6.

182.   Price, R.; Gaber, B.; Lvov, Y., In-vitro release characteristics of tetracycline HCl, khellin and nicotinamide adenine dinucleotide from halloysite: A cylindrical mineral. *Journal of Microencapsulation* **2001,** *18*, 713-22.

Chapter 2

Halloysite Catalyzed Esterification of Bio-mass Derived Acids

2.1 Abstract

Halloysite, a natural clay with a hollow tubular structure, was studied as a catalyst for the

esterification of biomass-derived carboxylic acids (levulinic acid, fumaric acid, maleic acid, and

succinic acid) with four different alcohols (MeOH, EtOH, *n*-PrOH, and *n*-BuOH). Reaction

conditions were optimized (10 mol% halloysite, 170 °C, 24 h) and gave high yields of the

corresponding esters and diesters (> 90%). The halloysite was easily recovered and recycled after

washing and drying.

2.2   Introduction

2.2.1   Biobased Products

Currently, most consumable energy and chemicals are produced from limited fossil fuel-based resources. All developed countries are dependent on these depleting fossil fuels for the production of approximately 80% of their energy and 90% of their chemicals.[1] The large-scale production and use of these fossil fuels have negatively impacted the environment due to the emission of harmful greenhouse gases and toxic materials. With a growing world population, the demand for energy and chemicals increases exponentially; consequently, the amount of waste generated from energy and chemical production is also growing. Case-in-point, the United States generated approximately 258 million tons of municipal solid waste (MSW) in 2014. Approximately 35% of the MSW can be recycled/composted, 13% of it can be utilized for the generation of energy through incineration processes, and about 53% of MSW is discarded into landfills (U.S. EPA 2016). It is imperative to identify alternative resources to produce energy and chemicals to meet the increasing demands on finite fossil fuels and minimize the environmental impact of refining-to-consumption processes. Biomass has been identified as a viable renewable resource for the production of chemicals and energy while also reducing generated waste. Although biomass derives from natural resources, it can also be obtained from various waste sources, such as **(i)** agricultural waste (corn stover, rice husk, and sugar cane bagasse); **(ii)** municipal solid waste (MSW); and **(iii)** industrial waste from pulp and paper mills.

Biomass waste valorization is exceedingly essential for resource recovery within an integrated waste management approach.[2] Nearly all wastes currently have some value biomass-derived byproduct for which supply vastly exceeds demand. For example, glycerol can be a

valuable chemical, but it is being generated in increasing quantities by the biodiesel industry and could become a "waste." By applying even a crude valorization analysis, glycerol's conversion to the chemical epichlorohydrin is economically attractive compared to the alternatives. This conversion's value is three times that of conversion to transportation fuel and ten times that of burning to generate electricity.[3] In the longer term, glycerol could become a platform molecule leading to many different fine chemicals. Still, the establishment of such platforms will require a much more mature bio-based chemical industry.[2] A biorefinery, which utilizes renewable biomass as a feedstock resource, may offer a more sustainable solution for the conversion of harvested and waste biomass into platform chemicals.[4] A biorefinery could also bring about sustainable growth and environmental advantages by reducing overall greenhouse gas emissions (NREL) and air toxins.

The concept of biorefinery evolved in the late 1990s. The US Department of Energy defines a biorefinery as an overall concept of a processing plant where biomass feedstocks are converted and extracted into a spectrum of valuable products.[5] The International Energy Agency (IEA) Bioenergy Task 42 defines a biorefinery as "the sustainable processing of biomass into a spectrum of marketable products (food, feed, materials, chemicals) and energy (fuels, power, heat)." Therefore, a biorefinery can be a facility, a process, a plant, or a cluster of facilities for the conversion of biomass. [6] Furthermore, a biorefinery can be assimilated to a petroleum-based refinery. In the petroleum-based refinery process, fossil-based resources, such as oil and natural gas, produce energy and chemicals. In a biorefinery, biomass is used as the feedstock to produce energy and chemicals. [6-8]

There are two strategic goals for biorefinery development. An energy goal, which is the substitution of imported petroleum in favor of renewable domestic raw materials.[9] The second goal

is an economic goal, which is to create a robust biobased industry. The energy goal is addressed by the current effort on EtOH, biodiesel, and advanced biofuel production (butanol, algal biodiesel, etc.) to replace a portion of a large amount of transportation gasoline and diesel used annually in the US. For example, algal oil holds excellent promise as a biodiesel source. Still, it remains a long-term opportunity for developers to identify additional revenue streams to cover the high cost of growing and processing algal biomass for oil recovery.[10] The cost of bio-based production in many cases exceeds the cost of petrochemical production. New products must also be proven to perform at least as well as the petrochemical equivalent they are substituting and have a lower environmental impact. The recent climb in oil prices, the consumer demands for environmentally friendly products, population growth, and limited supplies of non-renewable resources have now opened windows of opportunity for bio-based chemical production from renewable resources as an attractive investment area. Around the world, small but discernable steps are being taken to move from today's fossil-based economy to a more sustainable economy based on the greater use of renewable resources. The transition to a bio-based economy has many drivers:

- An over-dependency of many countries on fossil fuel imports

- The anticipation that oil, gas, coal, and phosphorous will reach peak production in the near future

- The need for countries to diversify their energy source

- The global issue of climate change

- The need to reduce the emission of greenhouse gases

- The need to stimulate regional and rural development

The return on investment in biofuel-only processes presents a significant barrier to achieving the biorefinery's economic goal. Industries need a financial incentive to justify the use of unfamiliar building blocks, the development of processes to convert these building blocks to final products, and the capital investment needed to take the technology to commercial scale. High-value, lower-volume biobased chemicals provide this incentive.[10, 11] A promising approach to reduce biofuel production costs is to use biofuel-driven biorefinery to co-produce both value-added products (chemicals, material) biofuels from biomass resources in a very efficient integrated approach. The added value of the co-products makes it possible to produce fuels at the market competitive cost at a given biomass resource price. The cost was shown to be reduced by at least 30% using the biorefinery approach.[9] Integrating higher-value chemical/material co-products into the biorefinery's fuel and power output will improve all energy-related product's overall profitability and productivity of all energy-related products. Increased profitability makes it more attractive for new biobased companies to contribute to our domestic fuel and power supply by investing in new biorefineries. Increased productivity and efficiency can also be achieved through operations that lower the overall energy intensity of biorefinery unit operations; reduce overall carbon dioxide emissions; maximize the use of all feedstock components, byproducts, and waste streams; and use economies of scale, common processing operations, materials, and equipment to drive down production costs.

2.2.2 Platform Chemicals

Platform chemicals are defined as a chemical that can serve as a substrate for the production of a variety of higher value-added products. Biorefinery is not a new concept; many traditional users of biomass, sugars, starch, and pulp industries run biorefineries today. However, it is the rapid expansion in biofuel production and the need to derive value from all the co-products driving

modern biorefinery development. Sustainability is the main driver for the establishment of biorefineries. Biorefinery development can be designed for environmental, social, and economic sustainability, impacting the full product value chain. Within the bio-based economy and operation of biorefinery, there are significant opportunities for the development of bio-based chemicals and polymers. Biorefineries can be classified based on a number of their key characteristics. These feedstocks can be processed to a range of biorefinery streams termed platforms. These platforms include single carbon molecules such as biogas and syngas, 5- and 6-carbon carbohydrates from starch, sucrose, or cellulose; a mixed 5-and 6-carbon carbohydrates stream derived from hemicelluloses, lignin, oils (plant-based), and organic solutions from grasses. Six-carbon sugar platforms can be accessed from sucrose or through starch or cellulose hydrolysis to give glucose. Glucose serves as feedstock for (biological) fermentation processes providing access to various essential chemical building blocks. Six- and five-carbon platforms are also produced from the hydrolysis of hemicelluloses. They can also undergo selective dehydration, hydrogenation, and oxidation reactions to give useful products, such as sorbitol, furfural, glucaric acid, hydroxymethylfurfural (HMF), and levulinic acid. [9]

Scheme 1. Six- and five-carbon chemical platforms.
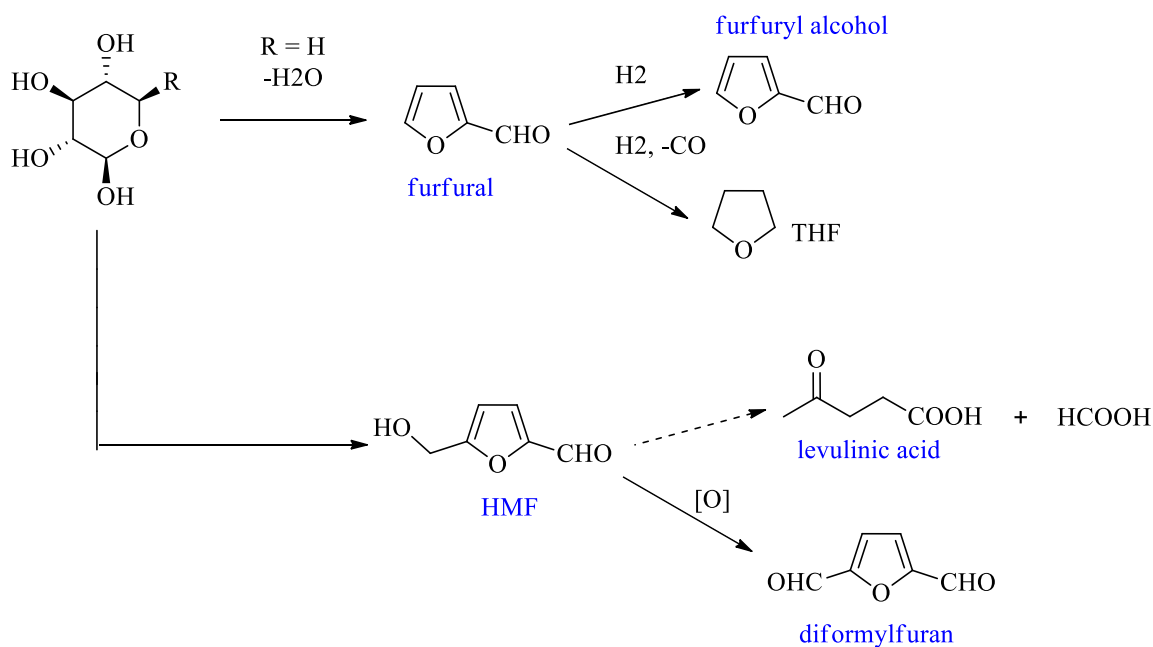
Biorefinery classification includes:

C6 sugar biorefinery yielding ethanol and animal feed from starch crops

Syngas biorefinery yielding FT-diesel and naptha from lignocellulosic residues

C5 and C6 sugars and syngas biorefinery yielding ethanol, FT-diesel, and furfural from lignocellulosic crop

In 2004, the Department of Energy (DOE) identified 12 chemical building blocks from biomass as potential platform chemicals.[12] In 2010, the DOE updated the Platform Chemical List (Bozell and Petersen 2010), including ethanol, furfural, hydroxymethylfurfural, 2,5-furan dicarboxylic acid, glycerol, isoprene, succinic acid, 3-hydroxy propionic acid/ aldehyde, levulinic acid, lactic acid, sorbitol, and xylitol. All these identified platform chemicals, except glycerol and isoprene, can be produced from biomass-derived carbohydrate sources.[12] By developing a list of

specific structures, the report embraced product identification to guide research. The targets

reflected a methodology that included known processes, economics, industrial viability, size of

markets, and a compound's ability to serve as a platform for derivatives production. The evaluation

led to the identification of the products shown in **Table 1**.

Table 1. The DOE top chemical opportunities from carbohydrates, 2010.

Ethanol
Furans
Glycerol and derivatives
Biohydrocarbons
Lactic acid
Succinic acid
Hydroxypropionic acid/aldehyde
Levulinic acid
Sorbitol
Xylitol/arabinitol

Levulinic acid and succinic acid (including the unsaturated analogs fumaric acid and maleic

acid) have been identified as among the top 10 value-added chemicals derived from biomass.[9]

Levulinic acid and succinic acid derivatives have broad applications as chemical building blocks

for fine chemicals. [9, 13] Biomass-derived succinates have been used as monomer precursors for

polyether synthesis, while levulinate esters have been employed as octane boosters for gasoline and

extenders for diesel fuel.[13-19]

2.2.3   Succinic Acid

Succinic acid is currently a high-volume specialty chemical produced by catalytic hydrogenation of

petrochemical maleic acid or anhydride. It is a widely investigated chemical building block

available from a biochemical transformation of biorefinery sugars.[20] Succinic acid offers strong

potential as a platform chemical. Succinate esters are precursors for known petrochemical products

such as 1,4-butanediol (BDO); BDO is currently produced from acetylene or propylene oxide

market size nearly 1 million tonnes. It serves as a raw material for a range of essential chemicals,

including polymer polybutylene terephthalate (PBT) and polybutylene succinate (PBS).

Approximately 40% of BDO is consumed in tetrahydrofuran (THF) products obtained by

homogeneous dehydration of BDO. THF is a solvent for poly(vinyl chloride) (PVC). It is used as a

monomer in the manufacture of polytetramethylene glycol, which is used as an intermediate for

Spandex fibers and polyurethanes.[21] Approximately Succinate esters are also precursors for the

production of γ-butyrolactone and various pyrrolidinone derivatives.[21] A recent publication

describes succinic acid conversion into a new polyester for coating applications upon

polymerization with isosorbide, a renewable building block also available in high yield from

glucose.[22] The production of succinic acid has attracted several industry players. The market

potential for succinic acid and its direct derivatives has been projected to be as much as 275,000

tonnes per year, with an estimated market size for succinic acid-derived polymers being as high as

25 million tonnes per year.[23] The use of succinic acid as a platform chemical is summarized in

Figure 1

Figure 1. Succinic acid as a platform chemical.
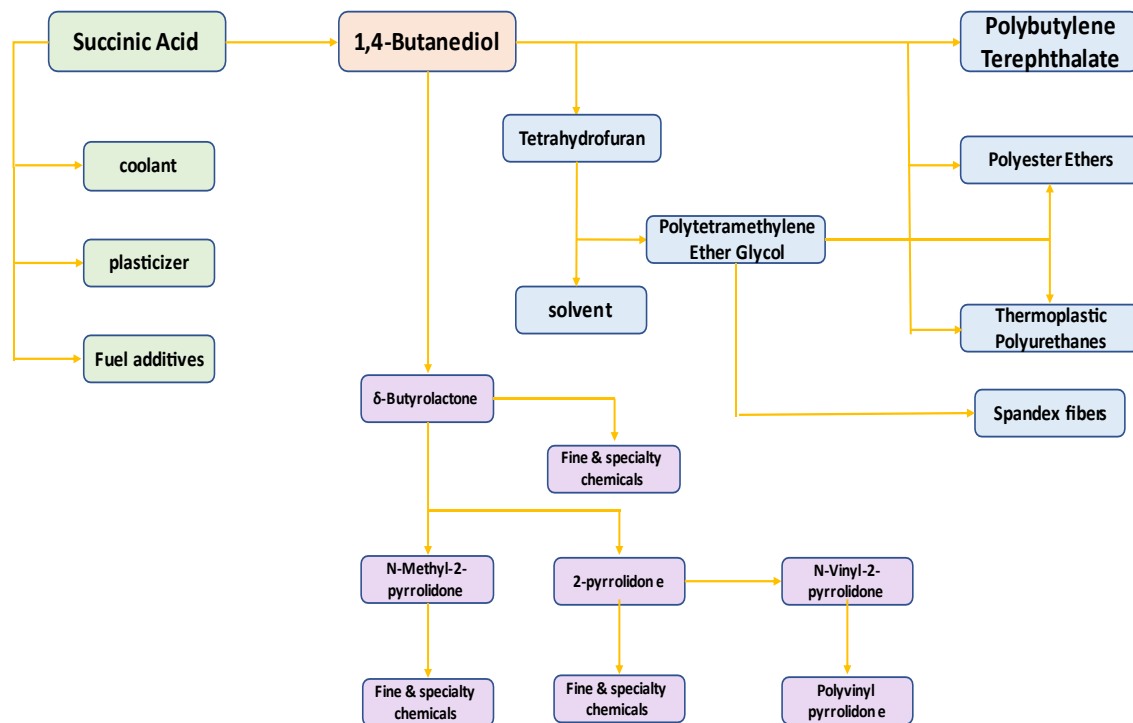
2.2.4 Levulinic Acid

Levulinic acid is of interest as a primary biorefinery building block and platform chemical because of its simple and relatively high yield production from the acid treatment of C6-carbohydrates in lignocellulosic biomass via hydration of HMF, an intermediate in this reaction. It is also possible to obtain levulinic acid from the C5 carbohydrate in hemicelluloses (via furfuryl alcohol) after the acid treatment.[9] Levulinic acid contains two reactive functional groups that allow many synthetic transformations shown in **Figure 2**

Figure 2. Formation and transformation of levulinic acid.
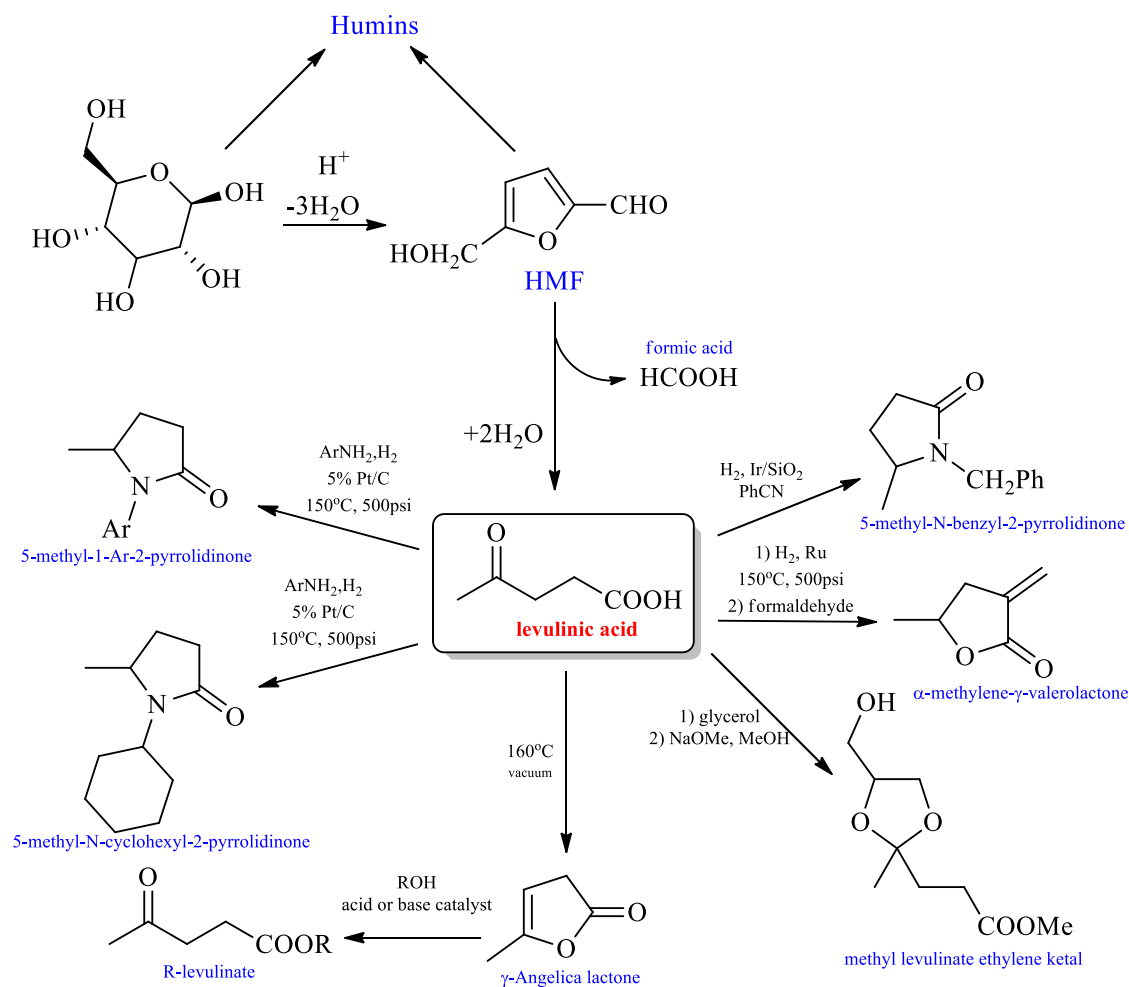
2.2.5 Heterogeneous Acid Catalyst for Esterification

Heterogeneous catalysis has been widely discussed in recent years as a more viable industrial process than homogeneous catalysis to produce biodiesel by transesterification and esterification reactions. Heterogeneous catalysts usually solve various problems associated with homogeneous media and add advantages such as lower toxicity, the possibility of catalyst recovery and recyclability, minimized corrosion capacity, ease of handling, and separation from the reaction

medium [24, 25]. For these reasons, heterogeneous catalysts are often called "environmentally friendly" [26]. Within heterogeneous catalyst technologies, raw and modified clay minerals are already widely employed in many industrial processes due to their favorable properties, such as catalytic efficiency (often displaying product-, regio- or shape-selectivity), low cost, wide availability, ease of preparation, and high thermal stability.[27-30] However, the great majority of these processes use cationic exchanged clay minerals of the 2:1 group and derivatives, which usually present higher activities and catalyze a broader range of reactions than other clay minerals.[31, 32] The use of 1:1 group clay mineral as catalysts has been mostly restricted to kaolinite. Kaolinite use has been limited, serving as a support to the actual catalysts or as a precursor to other catalytic ceramic materials or zeolites.[29] The lack of use of halloysite as a catalyst in organic reactions is no exception, and references to its use are scarce.[33-35]

Esters of levulinic and succinic acid can be readily prepared by various esterification methods from simple alcohols catalyzed by homogeneous and heterogeneous acid catalysts. Mineral acids are cost-effective homogeneous catalysts that produce alkyl levulinates and dialkyl succinates in high yields. However, heterogeneous acid catalysts offer the advantages of easy removal from the reaction media, facilitating product purification and catalyst recyclability. Therefore, various solid acid catalysts derived from many chemically modified solid supports have been investigated as catalysts for this conversion.[36-44] Different zeolites (HUSY, HBEA, HMOR, HZSM-5, HMCM-22) and sulfated oxides (SnO_2, ZrO_2, Nb_2O_5, TiO_2) have been reported as catalysts for the esterification of levulinic acid with bio-ethanol.[36] A novel method for producing sulfonated mesoporous silica–carbon composites made up of a thin layer of carbon with a high density of SO_3H groups covering the internal surface of the pores of three types of mesoporous silica and their successful application as solid acid catalysts in the esterification of several organic

acids (i.e., maleic anhydride, succinic acid, and oleic acid) with ethanol was reported in the literature.[37] Sulfonic mesoporous silicas have demonstrated outstanding catalytic performance in the esterification of levulinic acid with different alcohols to produce alkyl levulinates.[38] Nanohybrids such as Si(Et)Si-Pr/ArSO$_3$H were applied in the synthesis of alkyl levulinates from the esterification of levulinic acid and ethanolysis furfural alcohol.[40] A series of heteropoly acid and ZrO$_2$ biofunctionalized organosilica nanotubes (PW12/ZrO$_2$-Si(Et)Si-NTs) were fabricated and were applied in the synthesis of alkyl levulinates by esterification of levulinic acid and ethanolysis of furfuryl alcohol, and the obtained excellent catalytic activity was explained in terms of the strong Brønsted and Lewis acidity, unique hollow tubular nanostructure, and hydrophobic surface of the hybrid nanocatalysts.[41] Ion exchange resins were also shown to exhibit good catalytic activity for the esterification of levulinic acid with butanol.[42] Many other solid acid catalyst were shown to exhibit good catalytic activity for the esterification reaction of levulinic acid with short-chain alcohols such as sulfonated carbon catalysts, Amberlyst-15 (ion-exchange resin consisting of macroreticular polystyrene with a strong acidic sulfonic group), SAC-13 (SiO$_3$-supported Nafion), mesoporous silica (SBA-15) functionalized with alkyl sulfonic acid groups, zeolite Beta, and HY zeolite.[43]

2.2.6 Halloysite Nanoscroll

Halloysite (Hal) is a natural 1:1 aluminosilicate clay commonly found in weathered rocks and soil. The clay is chemically similar to kaolinite; however, it is commonly found as a hollow tubular nanostructure.[45] **Figure 3**. Since aluminosilicate chemistry is generally not toxic and is exceptionally durable, halloysite has many chemical process advantages.[45, 46] Studies have shown that halloysite has high biocompatibility and high thermal stability, making it much safer to work with than Bronsted or Lewis acids. Also, due to its abundance, halloysite is easily obtained, cheap,

and even reusable.[45] A recent study demonstrated the effectiveness of halloysite as a catalyst for converting lauric acid to corresponding methyl laurate and ethyl laurate esters.[47] With a conversion rate of over 90% for ester formation and an optimum catalyst loading of 12% (w/w), it was of interest to explore this clay's scope, and utility for the development of sustainable conversions of bio-mass derived substrates into fine chemical building blocks and fuel additives. Therefore, as part of an ongoing study in our labs to develop halloysite-based materials, we sought to explore the use of raw halloysite as an esterification catalyst to prepare several critical bio-mass-derived esters.

Figure 3. Halloysite nanoscroll.
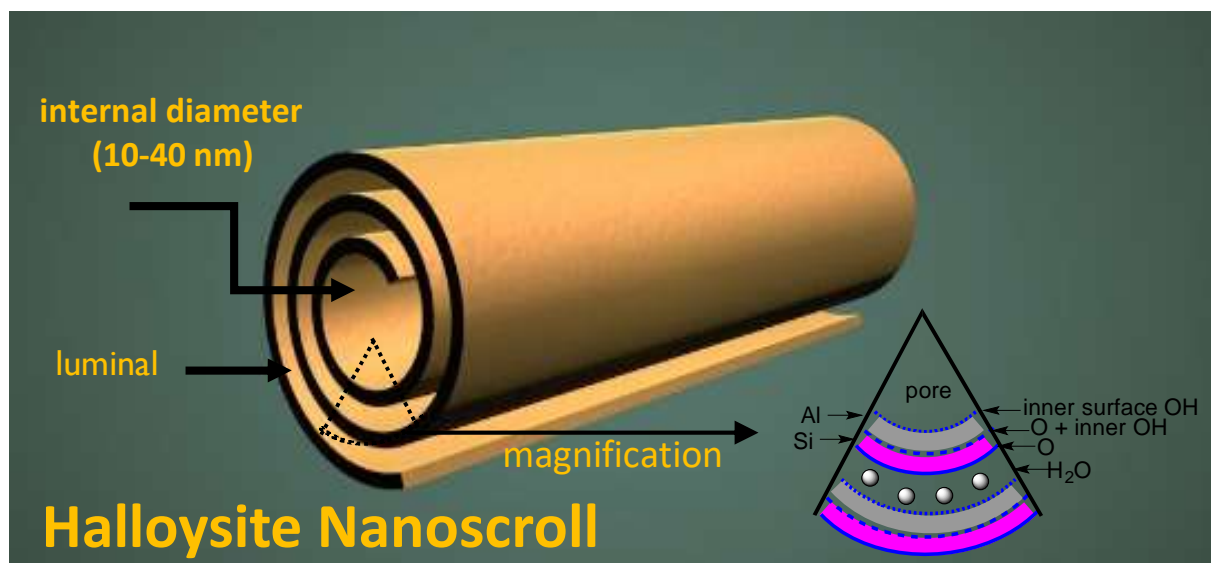
2.2.7 Esterification of Fine Chemicals

Esterification reactions are commonly used in industrial processes. The ester products are primarily used as solvents, plasticizers, synthetic food odorants, scents, and precursors for various pharmaceuticals, agrochemicals, and other compounds.[48] In recent years, these reactions have gained importance due to fossil fuel production from renewable energy sources, especially as an alternative for fossil diesel. The esterification process consists of a reaction between a carboxylic acid and an alcohol in the presence of a catalyst to obtain the corresponding esters[48, 49] Traditionally, strong Brønsted acids like H_2SO_4 are used as homogeneous catalysts in the esterification reaction,[50]. Still, there are significant disadvantages (such as toxicity, corrosion, and environmental problems) that show why it is replaced by a heterogeneous catalyst such as an acid clay.

A significant source of waste in the (fine) chemicals industry is derived from the widespread use of liquid mineral acids (HF, H_2SO_4) and various Lewis acids. They cannot easily be recycled and generally end up, via a hydrolytic workup, as waste streams containing large amounts of inorganic salts. Their widespread replacement by recyclable solid acids would afford a dramatic waste reduction. Solid acids, such as zeolites, acidic clays, and related materials, have many advantages in this respect[31-34] They are often truly catalytic and can easily be separated from liquid reaction mixtures, obviating the need for hydrolytic work-up, and recycled. Moreover, solid acids are non-corrosive and easier (safer) to handle than mineral acids such as H_2SO_4 or HF. Solid acid catalysts are, in principle, applicable to a plethora of acid-promoted processes in organic synthesis.[31-34]

2.3   Results and Discussion

2.3.1   Halloysite Esterification of Platform Carboxylic Acids

Initially, the esterification of levulinic acid with methanol to form methyl levulinate was explored with commercially available raw halloysite. This system was used to identify optimized molar ratios for the reactants/catalyst and identify optimized reaction conditions (°C, h) due to the ease by which simple TLC could monitor the reaction. The product could be isolated and characterized by NMR. The molar amount of the halloysite used in the reaction was based upon the unit cell of $Al_2Si_2O_5(OH)_4 \cdot 2H_2O$ (MW 294.19). In a typical reaction, the acid, alcohol, and halloysite were combined in a sealed stainless steel reaction vessel and heated to an elevated temperature in a silicon oil bath. The reaction vessel was then allowed to cool, and the product ester was isolated and characterized. An optimum molar ratio of acid:alcohol: halloysite of 1:24:0.1 was ideal for the easy handling of the reaction slurry. Although the esterification could be successfully executed with lower alcohol (1:12:0.1) concentrations, less alcohol gave poor dispersion of the halloysite. It made isolation of the product and the recovery of the halloysite more difficult. Alternatively, increasing the amount of halloysite did not significantly improve the yields of the ester. As summarized in **Table 2**, temperature and time seemed to affect the ester yields significantly. Consistent with the earlier report, the high temperature was required to drive the halloysite catalyzed esterification to completion. Our system found it necessary to heat the reaction vessel in an oil bath set to 170 °C. A reaction time of 24 h gave the maximum acid conversion and product yield (99%), while shorter reaction times led to incomplete conversion of the acid.

Table 2. Optimization of esterification conditions for levulinic acid in methanol.
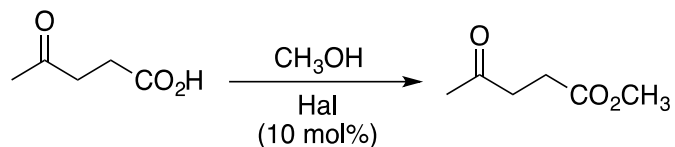
Entry	T (°C)	t (h)	yield (%)[a]
1	150	24	30
2	150	48	48
3	150	72	46
4	160	48	68
5	160	72	66
6	170	12	72
7	170	24	99

[a]Isolated yields.

With optimized conditions established for levulinic acid in methanol, the esterification of levulinic acid with other short-chain alcohols (EtOH, *n*-PrOH *n*-BuOH) was investigated (**Table 2**). Using the optimized conditions established for the methyl ester, the yields of the corresponding ethyl, *n*-propyl, and *n*-butyl levulinates were nearly quantitative. Moreover, the esters exhibited a high degree of purity with little more than filtration required for work-up. This procedure's success prompted a further investigation to confirm halloysite catalyzed esterification as a viable method for converting other biomass-derived acids into esters. As summarized in **Table 2**, methyl esters of the C6-carbohydrate-derived succinic acid and fumaric acid could be prepared using the optimized

conditions in high yields. In a similar fashion to levulinic acid, the dimethyl esters of succinic acid and fumaric acid were obtained in 96% and 92% yield, respectively. The alcohol concentration was maintained for the diacids, and the same molar ratio of diacid:alcohol: halloysite (1:24:0.1) was used. As with levulinic acid, the diacids were readily converted into the corresponding dimethyl, diethyl, di-*n*-propyl, and di-*n*-butyl succinates and fumarates in excellent yield and purity. These conditions were also suitable for converting the *cis*-isomer, maleic acid, into dialkyl maleates in 90-95% yield.[51] It was notable that the carbon double bond's isomerization to give the *trans* fumarate esters was not observed despite the elevated temperature.

Table 3. Biomass-derived esters and diesters.

$$RCO_2H \xrightarrow[\substack{Hal\ (10\ mol\%) \\ 170°C,\ 24\ h}]{R'OH} RCO_2R'$$
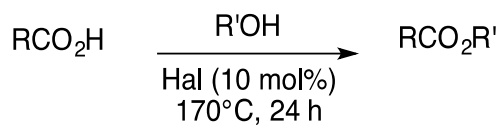
ester R', yield (%) [a]				
acid	**Me**	**Et**	**_n_-Pr**	**_n_-Bu**
levulinic acid (O / CO₂H structure)	99 (99)[b] (63)[c] (48)[d]	99 (99)[b]	97	99
diester R', yield (%)[a]				
diacid	**Me**	**Et**	**_n_-Pr**	**_n_-Bu**
succinic acid (HO₂C...CO₂H)	96	99 (99)[b]	94	95
fumaric acid (HO₂C...CO₂H)	92	99	94	98 (95)[b]
maleic acid (CO₂H / CO₂H)	91	95	90	92
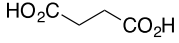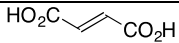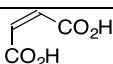
[a]Isolated yield.
[b]Isolated yield of 100 mmol scale reaction.
[c]Isolated yield; reaction with kaolinite.
[d]Isolated yield; reaction with montmorillonite.

The halloysite used in this study has origins from geological deposits at Dragon Mine, Utah (purchased from Sigma Aldrich). The morphology of this polydispersed nanoclay has been well characterized and reported to be 90% halloysite, with the remaining 10% of the material consisting of kaolinite, quartz, and gibbsite.[52] As a catalyst, this halloysite was found to be durable and chemically robust. It was superior to other clay catalysts like kaolite[53] and montmorillonite[54], which under the same conditions gave inferior yields of methyl levulinate (< 65 %, **Table 2**). The halloysite could be recovered from the reaction mixture by simple vacuum filtration and reused without activity loss. There was no apparent structural change to the halloysite after the esterification reaction. Based upon XRD profiles (**Figure 4a**), the positions of the indexed basal reflections (001, 002, and 003) of the raw halloysite (7.23 Å, 3.59 Å, and 2.33 Å) remained unchanged in the recycled halloysite (7.18 Å, 3.57 Å, and 2.34 Å). These results were consistent with the diffraction pattern of the dehydrated form of halloysite (7 Å-form) instead of the clay's hydrated structure (10 Å-form)[55] Further visual inspection of the raw and recycled materials by TEM (**Figure 4b**) revealed no apparent change to the catalyst's tubular structure of the catalyst.

As illustrated in **Figure 5**, recycling studies with halloysite showed that the catalyst could be cycled through at least six consecutive esterification reactions with no loss of activity and excellent isolated yields of the methyl levulinate in each trial. In these studies, the halloysite was collected by vacuum filtration and washed with the corresponding alcohol used in the esterification. The recovered clay was then further rinsed with deionized water and dried at 120 °C overnight. This afforded the recovered halloysite as a free-flowing powder that would be used in subsequent reactions. Using this recovery method, the halloysite could be used in different reaction systems with no observed esters' cross-contamination.

Figure 4. (a) XRD of raw halloysite (red) and recycled halloysite (blue).
(b) TEM image of raw halloysite. (c) TEM image of recycled halloysite.

(a)

(b)

(c)
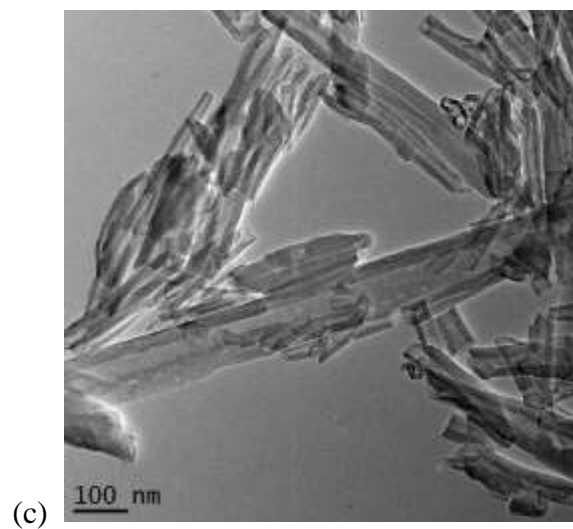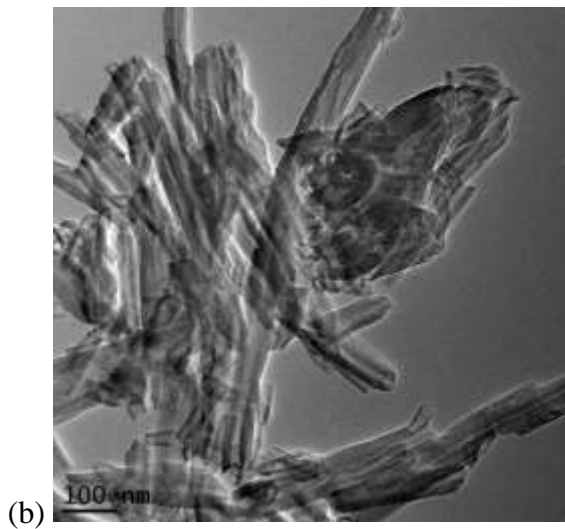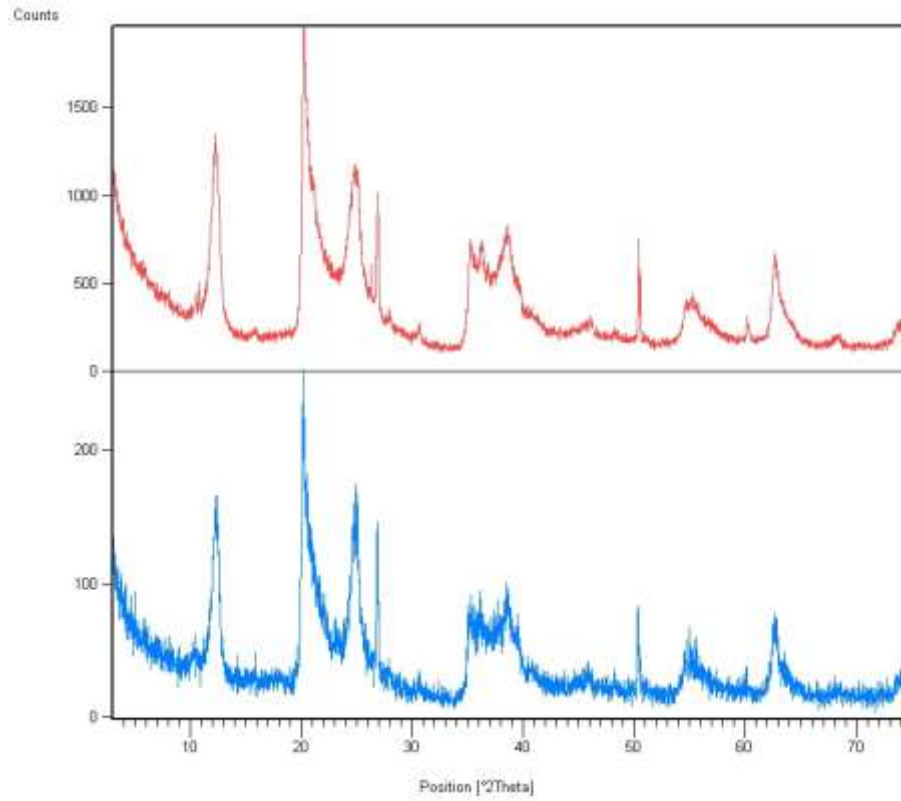
**Figure 5**. Halloysite recycling studies.
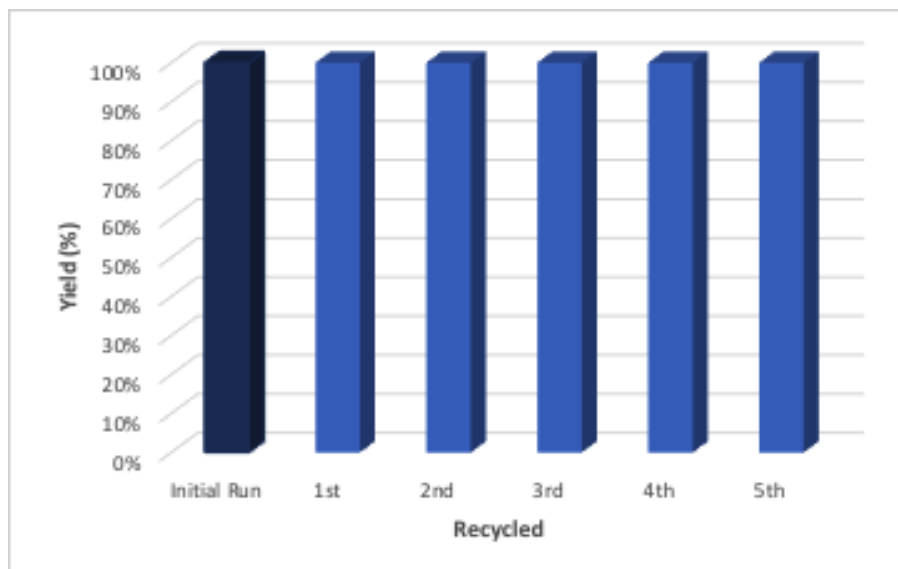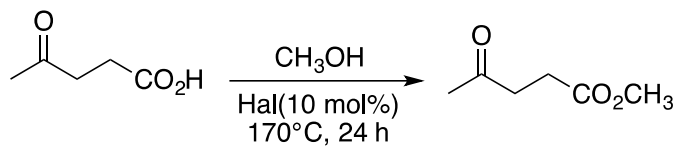
To demonstrate further the utility of halloysite as a catalyst for the esterification reaction, 100 mmol-scale reactions were performed with levulinic acid, succinic acid, and fumaric acid with selected alcohols. The scaled optimized conditions afforded the monoesters methyl and ethyl levulinate in 99% yield. The diesters, diethyl succinate (99% yield), and dibutyl fumarate (95% yield) were obtained in nearly quantitative yields.

2.3.2 Halloysite Catalyzed Fischer Esterification of Aromatic and Non-Aromatic Carboxylic acids

As part of this project's focus, it was of interest to demonstrate the effectiveness of halloysite as a Lewis acid (LA) catalyst for classical organic reactions. An investigation of raw halloysite for the Fischer esterification reaction of fine chemicals was explored.

Figure 6: Fischer esterification.
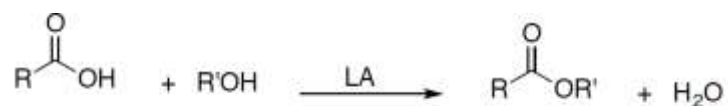
Summarized in **Table 4**, it was demonstrated that raw halloysite could quite effectively promote and catalyze the Fischer esterification of benzoic acid and phenylacetic acid in methanol to produce the corresponding methyl ester.

Table 4: Optimization of halloysite using benzoic acid and phenylacetic acid in methanol

$$\text{R}\overset{\text{O}}{\underset{}{\|}}\text{OH} \quad \xrightarrow[\text{CH}_3\text{OH, heat}]{\text{halloysite}} \quad \text{R}\overset{\text{O}}{\underset{}{\|}}\text{OCH}_3$$
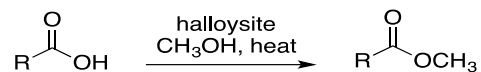
Entry	R	Halloysite loading (mol %)	Temp (°C)	Time (h)	Ester (%)
1	Ph	100	150	3	58
2	Ph	100	150	6	60
3	Ph	100	150	24	64
4	Ph	100	150	48	70
5	Ph	50	150	24	50
6	Ph	50	150	48	54
8	Ph	20	150	48	48
9	Ph	10	150	48	64
10	Ph	10	150	72	53
11	Ph	10	160	48	58
12	Ph	10	160	72	57
13	Ph	10	170	48	78
14	PhCH$_2$	10	150	48	49
15	PhCH$_2$	10	150	72	43
16	PhCH$_2$	10	160	48	68
17	PhCH$_2$	10	170	48	95
18	PhCH$_2$	10	170	72	92
19	Ph	10	reflux	24	NR
20	Ph	10	reflux	48	28
21	Ph	10	110*	2.5	6
222	Ph	10	150*	2.5	11

Using a molar equivalent of raw halloysite (100 mol%) afforded good methyl benzoate

yields (**Table 4**, entries 1-4). An extended reaction time of 48 h provided high yields of the ester

(70%, **Table 4**, entry 4), thus demonstrating the Lewis acid character of the raw halloysite. Further

studies have shown that reducing the raw halloysite (**Table 4**, entries 5-14) still gave good yields of

the methyl benzoate (23-78%). The catalytic activity was found to be effective at loadings as low

as 10 mol %. Optimum catalytic conditions with 10 mol% halloysite was achieved at 170 °C to

furnish methyl benzoate in 78% yield (entry 14). It is noteworthy that conventional reflux or

microwave conditions did not give good yields of the methyl benzoate (entries 20-23). Application

of the optimized condition for the esterification of phenylacetic acid gave excellent yields of

methyl phenylacetate (95% entry 18). Similar to benzoic acid, lower reaction temperatures and

extended reaction times (> 48 h) led to diminished yields of methyl phenylacetate (entries 15-17).

Encouraged by the studies with benzoic acid and phenylacetic acid that demonstrated the

potential effectiveness of raw halloysite as a "Green Catalyst" for the Fischer esterification, the

scope and limitations of the reaction were further investigated using a series of structurally diverse

carboxylic acids and alcohols. These studies are summarized in **Table 5**.

Table 5: Esterification of aromatic and non-aromatic acids
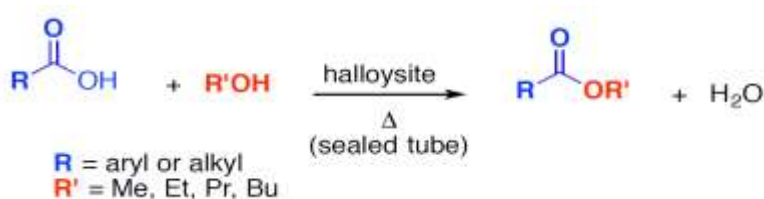
Entry	Aromatic Acids	Alcohol	Ester (%)
1	benzoic acid	MeOH	77
2		EtOH	48
3		n-PrOH	43
4		n-BuOH	52
5	p-toluic acid	MeOH	55
6	p-chlorobenzoic acid	MeOH	55
7	2,3-dichlorobenzoic acid	MeOH	54
8		EtOH	43
9		n-PrOH	33
10		n-BuOH	43
11	4-hydroxy-3-nitrobenzoic acid	MeOH	53
12		EtOH	64
13		n-PrOH	52
14		n-BuOH	43
15	nicotinic acid	MeOH	47
16		EtOH	41
17		n-PrOH	43
18		n-BuOH	54
24	Phenylacetic acid	MeOH	95
25		EtOH	98
26		n-PrOH	92
27		n-BuOH	99
28	Lauric acid	MeOH	97
29		EtOH	95
30		n-PrOH	88
31		n-BuOH	77
32	Palmitic acid	MeOH	98
33	Oleic acid	MeOH	64

Halloysite was dried at 120 °C for 24 h before use to remove any residual surface absorbed water. A 10 mmol% halloysite loading based on the acid gave the optimum yields of the corresponding esters (**Table 5**). The halloysite-catalyzed Fischer esterification reaction proceeded to completion under optimized conditions using various carboxylic acids and dicarboxylic acids. Substituted aromatic acids gave a good yield of the corresponding aromatic ester. The substituents on the aromatic ring seemingly did not affect the yield of the corresponding esters. Activating groups (CH_3-, entry 5) and deactivating groups (4-Cl, and 2,3-Cl_2-; entries 6 and 7) gave moderate yields of the corresponding methyl esters. The heterocyclic nicotinic acid gave diminished yields compared to benzoic acid. Halloysite proved to be a much more effective catalyst for the esterification of non-aromatic acids. Phenylacetic acid and the fatty acids (lauric acid and palmitic acid, entries 24-32). However, unsaturated ester of oleic acid was only obtained in 64% yield.

In general, the alcohol had little effect on the yield of the esters. Methyl ethyl, propyl, and butyl esters were obtained in comparable yields for the same acid. Benzoic acid gave the highest yield of the aromatic esters with methanol (77%), affording modest yields of the ethyl (48%), propyl (43%), and butyl (52%). Non-aromatic acid, lauric acid, gave excellent yields of all the esters.

Halloysite recycling experiments were conducted to establish whether the catalyst could be recovered and reused in subsequent esterification reactions. **Table 6** summarizes that halloysite was used in a five-cycle sequence with two different carboxylic acids without significant activity loss.

Table 6: Recycling investigation.

carboxylic acid/alcohol	cycle	ester (%)
lauric acid/MeOH	1	97
	2	95
	3	95
	4	94
	5	95

2.4   Conclusion

In summary, we have shown that the natural clay, halloysite, is a cost-effective, highly efficient, and easily recyclable catalyst for the esterification of biomass-derived carboxylic acids (levulinic acid, fumaric acid, maleic acid, and succinic acid). The optimized reaction conditions (10 mol% halloysite, 170 °C, 24 h) were scalable and represented a green process for preparing levulinate and succinate esters. Halloysite, with its unique tubular nanostructure, exhibited remarkable chemical reactivity superior to other clays. In addition, we have also shown raw halloysite solid catalyst was an effective catalyst for the esterification of various carboxylic acids using a variety of different carboxylic acid/alcohol systems. The raw halloysite catalytic activity was demonstrated for non-aromatic acids, with exceptionally high isolated yields of the corresponding esters (>90%). Halloysite was less effective with aromatic and unsaturated acids but still gave good yields. The clay catalyst was easily recovered and reused with no loss of activity. Overall, the results indicate

that halloysite has potential utility as a "Green Catalyst" for a broad scope of esterification applications.

2.5   Experimental

2.5.1   Materials and Methods

All reactions were carried out in a stainless-steel reaction vessel suspended in a stirred silicon oil bath. Halloysite clay was purchased from Sigma Aldrich (Source: Applied Minerals, Inc. Dragon Mine, Utah USA) and was used without modification. All other chemicals were purchased from Alfa Aesar, Sigma Aldrich, and VWR. All chemicals were used as received without further purification or modification. Reaction mixtures were filtered prior to work-up using Fisherbrand[TM] filter paper, P2-grade [Porosity: Fine (particle retention: 1-5 µm)]. ^{1}H NMR spectra were recorded at r.t. in DMSO-d_6 or CDCl$_3$ on a Bruker 400 MHz instrument operating at a frequency of 300 MHz for ^{1}H NMR. [1]H chemical shifts were referenced to the DMSO solvent signal (2.50 ppm) or the CHCl$_3$ solvent signal (7.26 ppm). Halloysite XRD measurements were performed on Philips X'Pert diffractometer utilizing Cu Kα radiation (λ = 1.5418 Å) and a curved graphite monochromator at a voltage of 45 kV and a current of 40 mA. Halloysite TEM images were obtained on a JEOL 2010 equipped with an EDAX genesis energy dispersive spectroscopy (EDS) system, operated at an accelerating voltage of 200 kV and an emission current 109 µA.

2.5.2   ^{1}H NMR Characterization of Esters

The ^{1}H NMR spectra of the products of the halloysite catalyzed esterification reactions are shown below to indicate the high purity of the compounds that were obtained with minimal work-up or purification procedures. All the products are known compounds. ^{1}H NMR is shown below for each entry to illustrate the purity of the sample. ^{1}H NMR spectra were identical to spectra in the Spectral

Database for organic compounds. SDBSWeb: https://sdbs.db.aist.go.jp (National Institute of Advanced Industrial Science and Technology)

2.5.3 General Procedure

To a clean, dry stainless-steel reaction pressure vessel was added the carboxylic acid (10.0 mmol), alcohol (240 mmol), halloysite (0.249 g, 1.00 mmol), and a stir bar. The reaction vessel was sealed and placed in an oil bath at 170 °C and allowed to stir for 24h. The reaction mixture was then allowed to cool to room temperature for 30 minutes. The halloysite was filtered using vacuum filtration. The halloysite filter cake was washed with alcohol (10 mL) and set aside for later use. The alcohol from the combined filtrates was removed under reduced pressure. Saturated sodium bicarbonate solution (10 mL) was added to the resulting oil residue, and the mixture was extracted with EtOAc (3 x 20 mL). The combined organic portions were washed with brine, dried over Na_2SO_4, filtered, and the solvent was removed under vacuum to afford the ester (or diester) in pure form as determined by ^1H NMR.

2.5.4 General Procedure: Large-Scale

To a clean, dry stainless reaction pressure vessel was added the carboxylic acid (100.0 mmol), alcohol (2400 mmol), halloysite (2.50 g, 10.0 mmol), and a stir bar. The reaction vessel was sealed and placed in an oil bath at 170 °C and allowed to stir for 24h. The reaction mixture was then allowed to cool to room temperature for 30 minutes. The halloysite was filtered using vacuum filtration. The halloysite filter cake was washed with alcohol (30 mL) and set aside for later use. The excess alcohol from the combined filtrates was removed and recovered on a rotoevaporator under reduced pressure. Saturated sodium bicarbonate solution (100 mL) was added to the resulting oil residue, and the mixture was extracted with EtOAc (3 x 100 mL). The combined organic

portions were washed with brine, dried over Na_2SO_4, filtered, and the solvent was removed under vacuum to afford the ester (or diester) in pure form as determined by ^{1}H NMR.

2.5.5 ^{1}H NMR Data for Biomass Derived Acids.

^{1}H NMR is shown below for each entry to illustrate the purity of the sample. ^{1}H NMR spectra were identical to spectra in the Spectral Database for organic compounds. SDBSWeb: https://sdbs.db.aist.go.jp (National Institute of Advanced Industrial Science and Technology)

methyl levulinate [624-45-3]
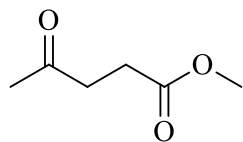
Pale yellow oil (1.29g, 99%)

^{1}H NMR (300 MHz, DMSO-d_6) δ: 3.55 (s, 3H), 2.70 (t, J = 6.0 Hz, 2H), 2.42 (t, J = 6.0 Hz, 2H) 2.08 (s, 3H).
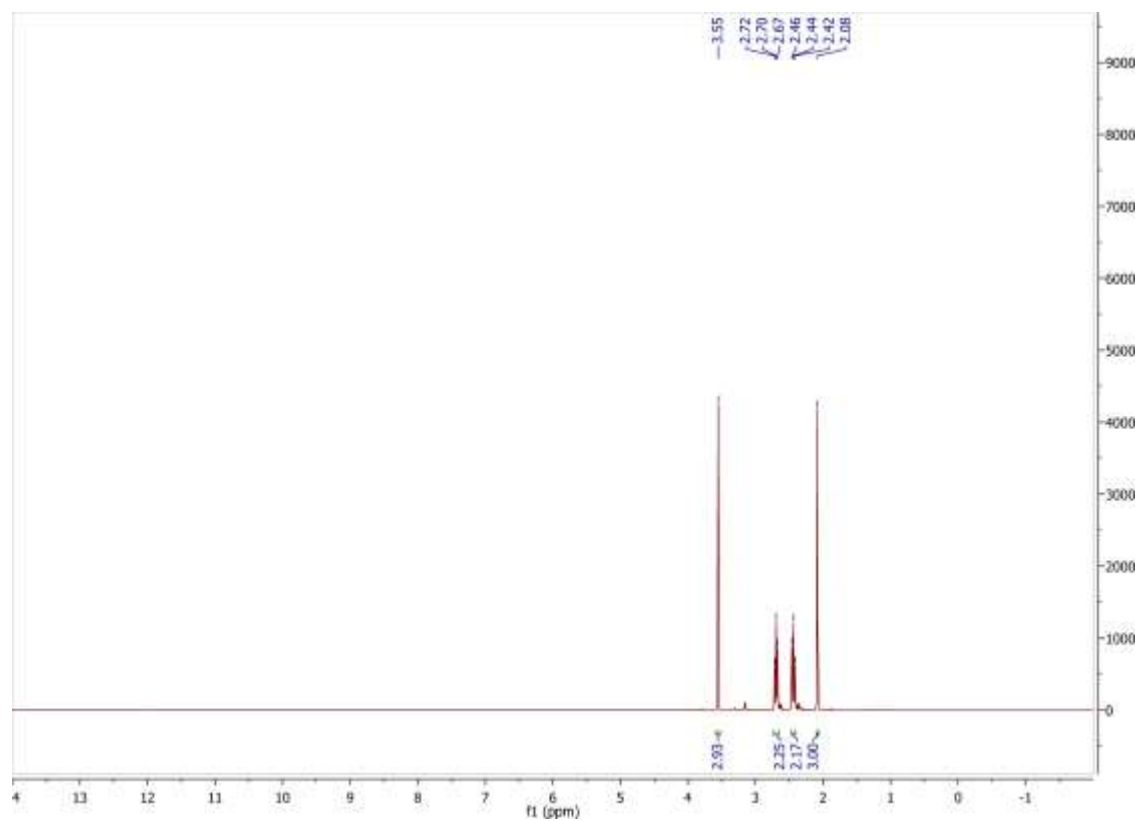
ethyl levulinate [539-88-8]
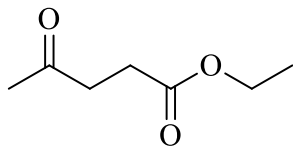
Pale yellow oil (1.43g, 99%)

^{1}H NMR (300 MHz, CDCl$_3$) δ: 4.12 (q, J = 6.6 Hz, 2H), 2.74 (t, J = 6.6 Hz, 2H), 2.54 (t, J = 6.6 Hz, 2H) 2.19 (s,3H), 1.25 (t, J = 6.6 Hz, 3H).
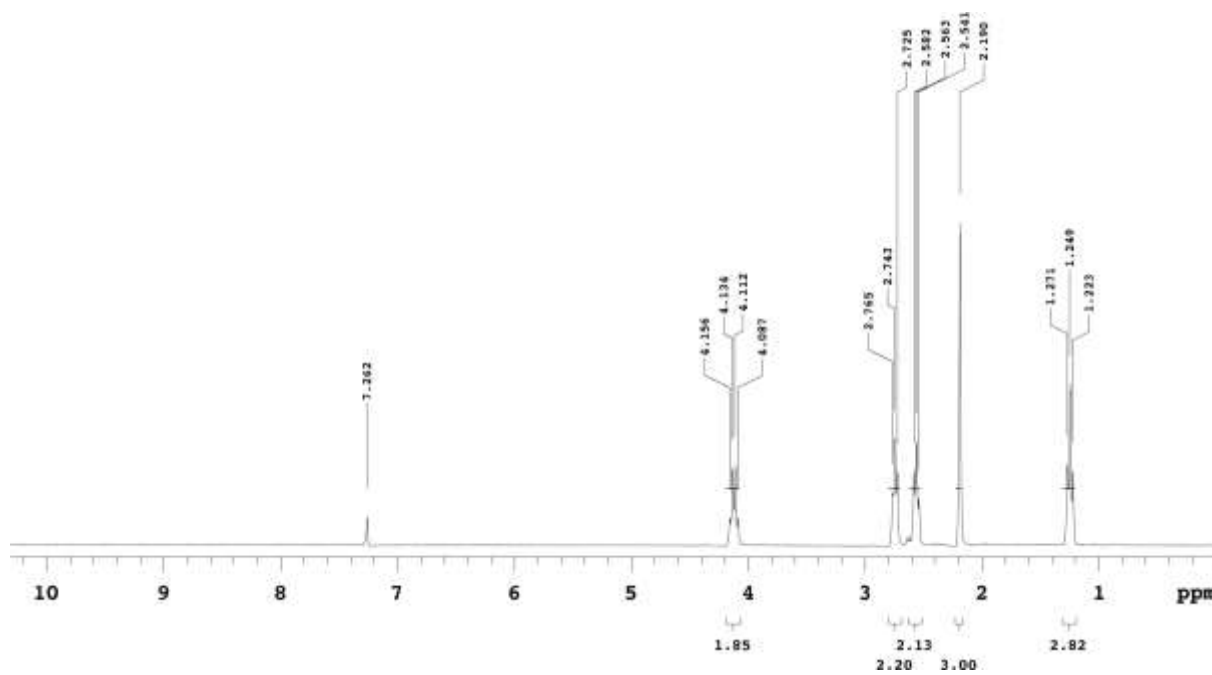
n-propyl levulinate [645-67-0]
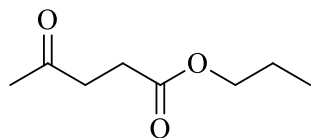
Pale yellow oil (1.54g, 97%)

^{1}H NMR (300 MHz, CDCl$_3$) δ: 4.03 (t, J = 6.6 Hz, 2H), 2.76 (t, J = 6.6 Hz, 2H), 2.57 (t, J = 6.6 Hz, 2H) 2.19 (s,3H), 1.63 (m, 2H), 0.93 (t, J = 6.6 Hz, 3H).
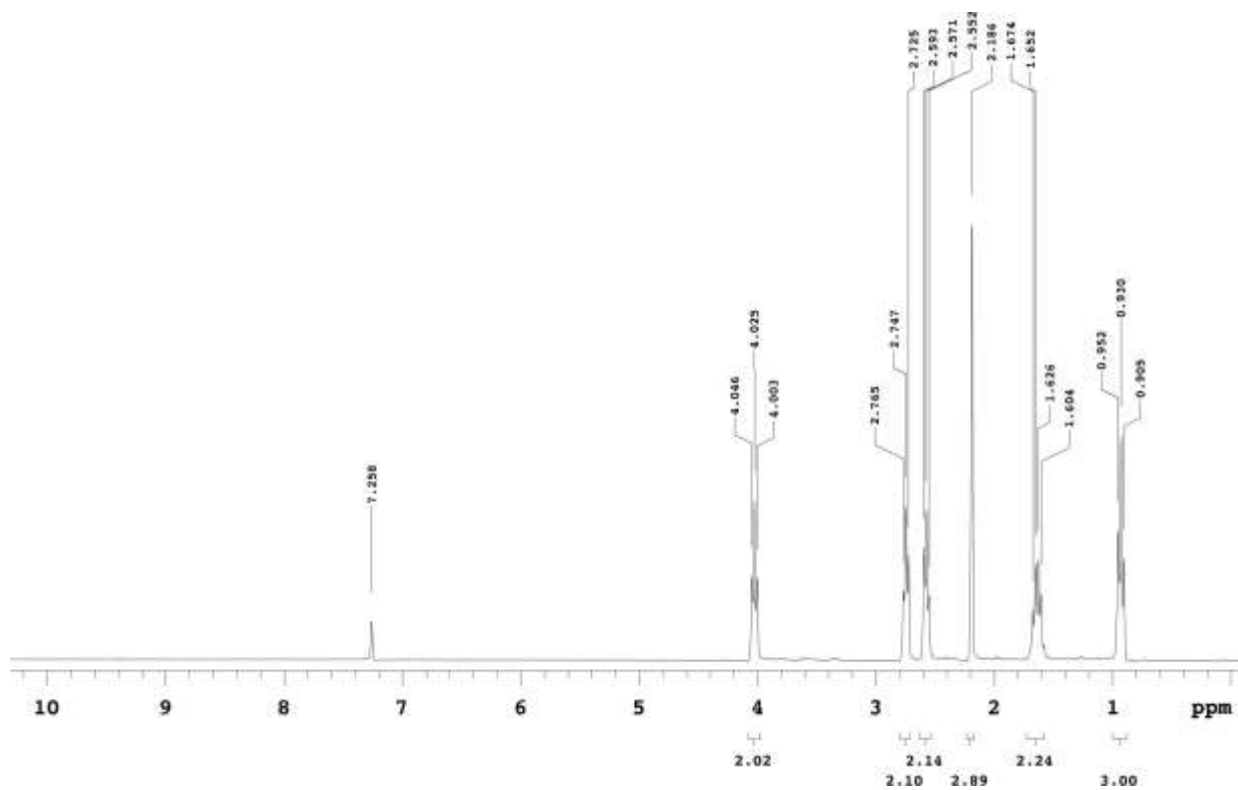
n-butyl levulinate [2052-15-5]
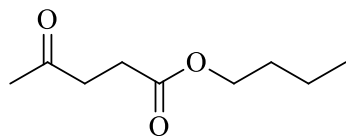
Pale yellow oil (1.71g, 99%)

^{1}H NMR (300 MHz, CDCl3) δ: 4.07 (t, J = 6.6 Hz, 2H), 2.74 (t, J = 6.6 Hz, 2H), 2.56 (t, J = 6.6 Hz, 2H) 2.19 (s,3H), 1.60 (m, 2H), 1.36 (m, 2H), 0.92 (t, J = 6.6 Hz, 3H).
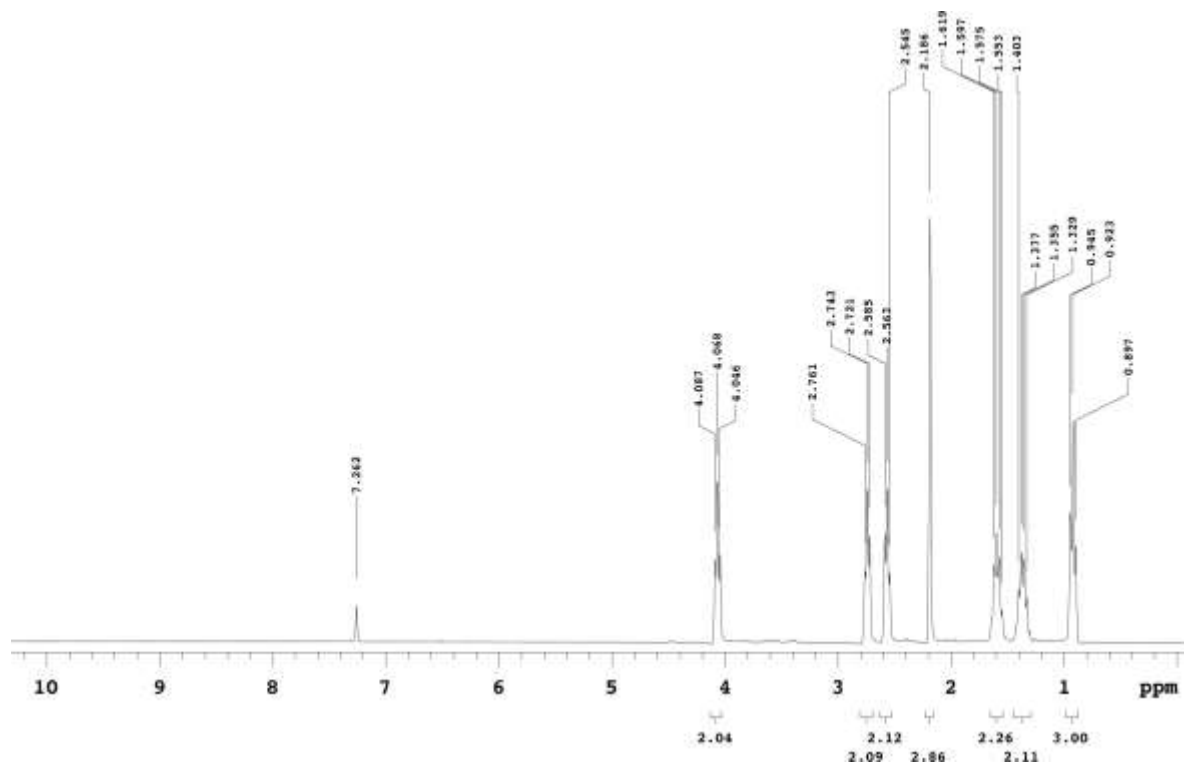
dimethyl succinate [106-65-0]
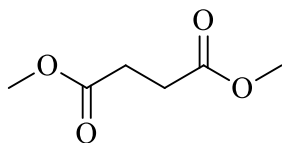
Pale yellow oil (1.40g, 96%)

^{1}H NMR (300 MHz, CDCl$_3$) δ: 3.49 (s, 6H), 2.63 (s, 4H).
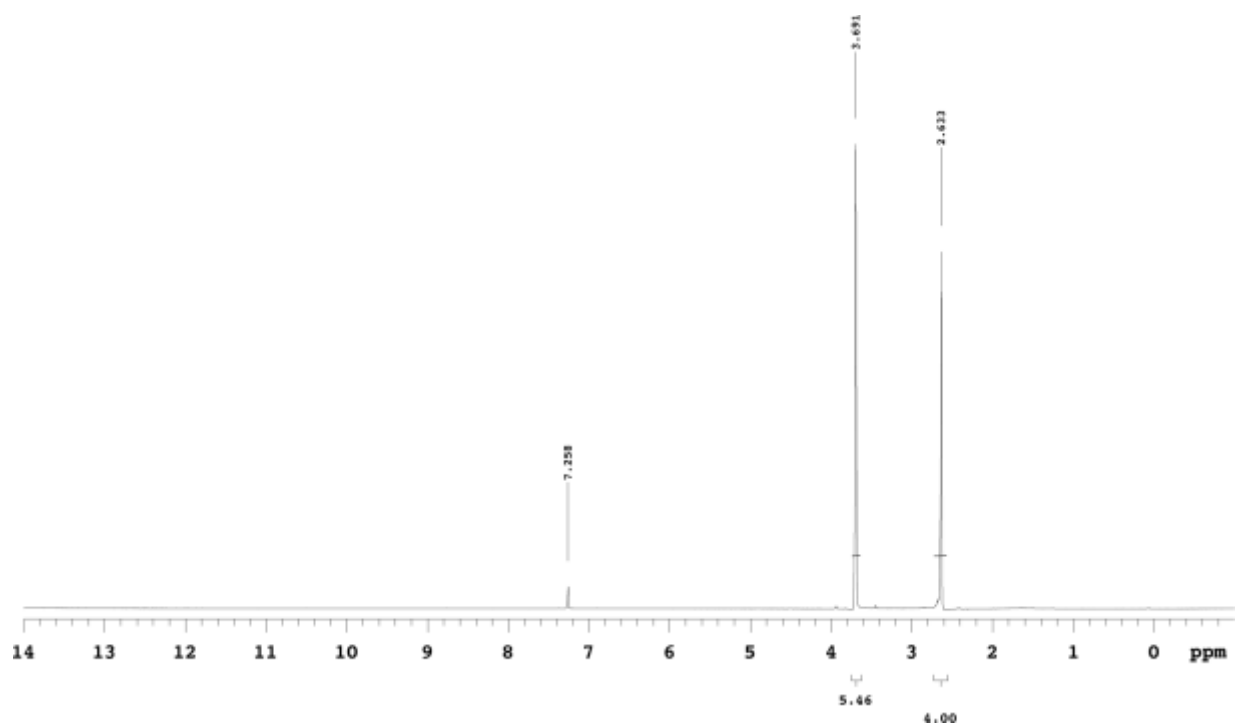
diethyl succinate [123-25-1]
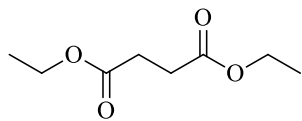
Colorless oil (1.73g, 99%)

^{1}H NMR (300 MHz, CDCl$_3$) δ: 4.14 (q, J = 6.6 Hz, 4H), 2.62 (s, 4H), 1.25 (t J = 6.6 Hz, 6H).
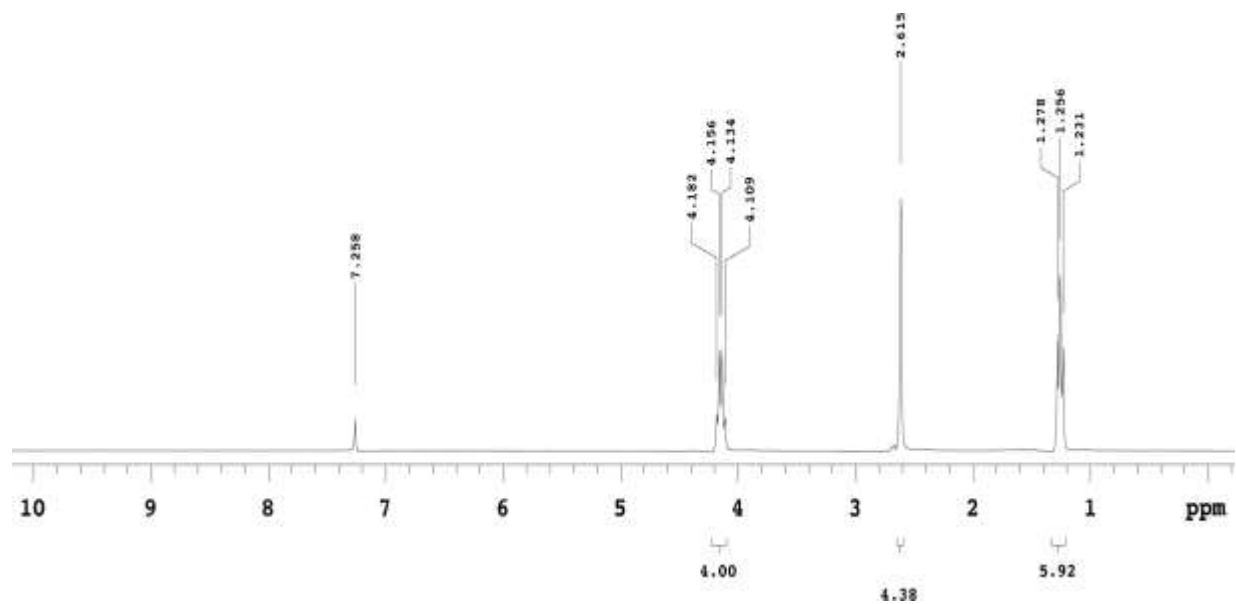
di-n-propyl succinate [925-15-5]
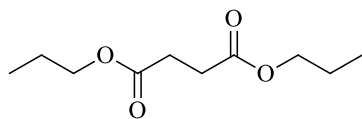
Colorless oil (1.90g, 94%)

^{1}H NMR (300 MHz, CDCl$_3$) δ: 4.05 (t, J = 6.6 Hz, 4H), 2.63 (s, 4H), 1.65 (m, 4H), 0.93 (t, J = 7.8 Hz, 6H).
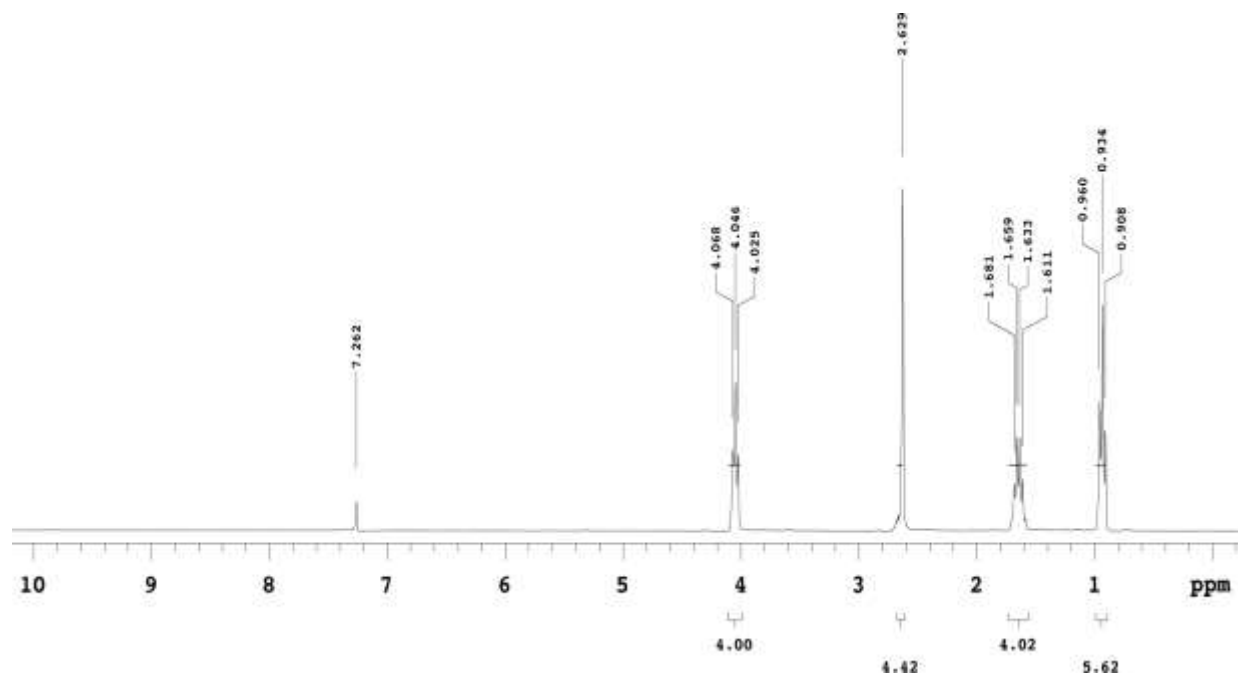
di-n-butyl succinate [141-03-7]
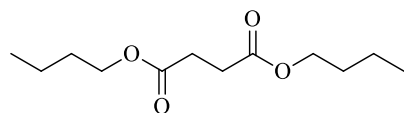
Colorless oil (2.2g, 95%)

^{1}H NMR (300 MHz, CDCl$_3$) δ4.09 (t, J = 6.6 Hz, 4H), 2.62 (s, 4H), 1.60 (m, 4H), 1.37 (m 4H), 0.93 (t, J = 7.8 Hz, 6H).
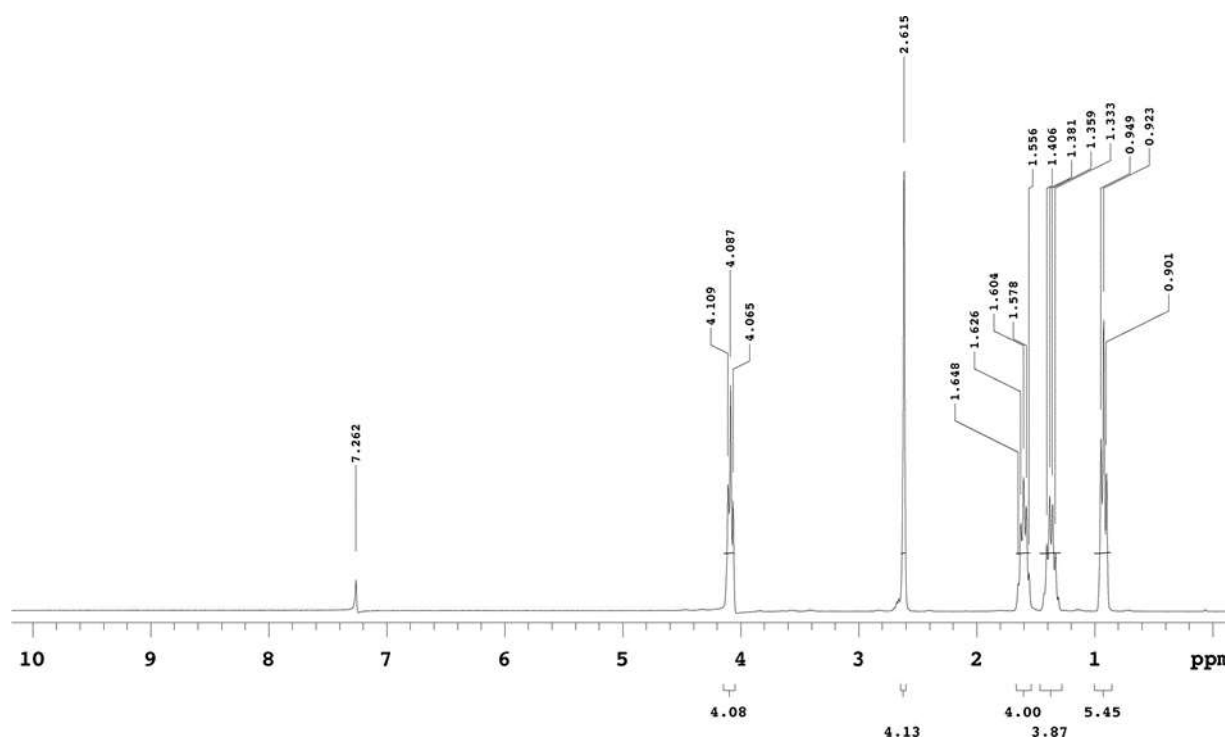
dimethyl fumarate [624-49-7]
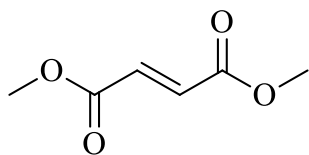
colorless oil (1.32g, 92%)

^{1}H NMR (300 MHz, CDCl$_3$) δ: 6.86 (s, 2H), 3.81 (s, 6H).
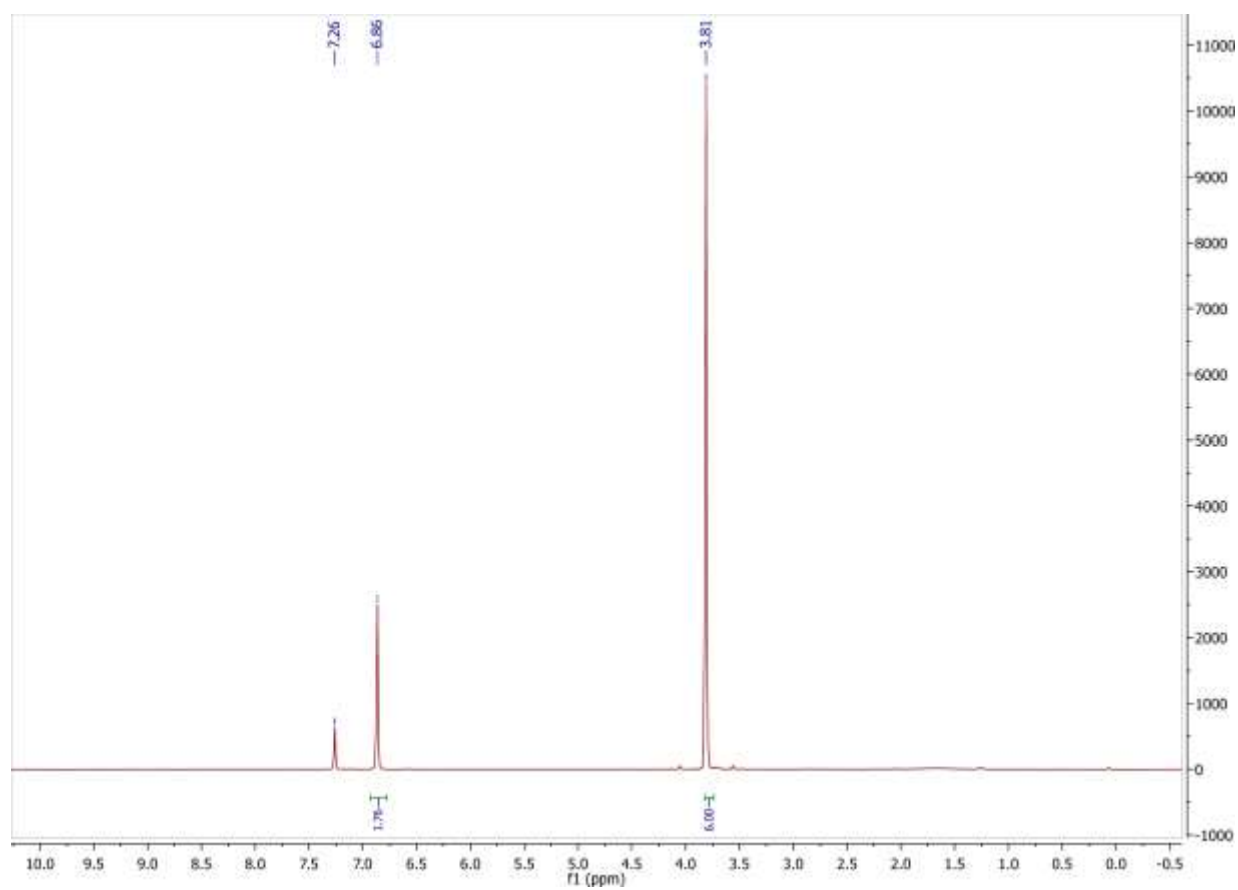
diethyl fumarate [623-91-6]
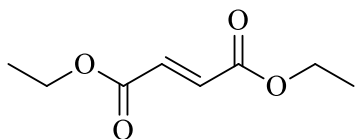
White crystalline powder (1.71g, 99%)

^{1}H NMR (300 MHz, CDCl$_3$) δ: 6.85 (s, 2H), 4.26 (q, J = 6.0 Hz, 4H), 1.31 (t, J = 6.0 Hz, 6H).
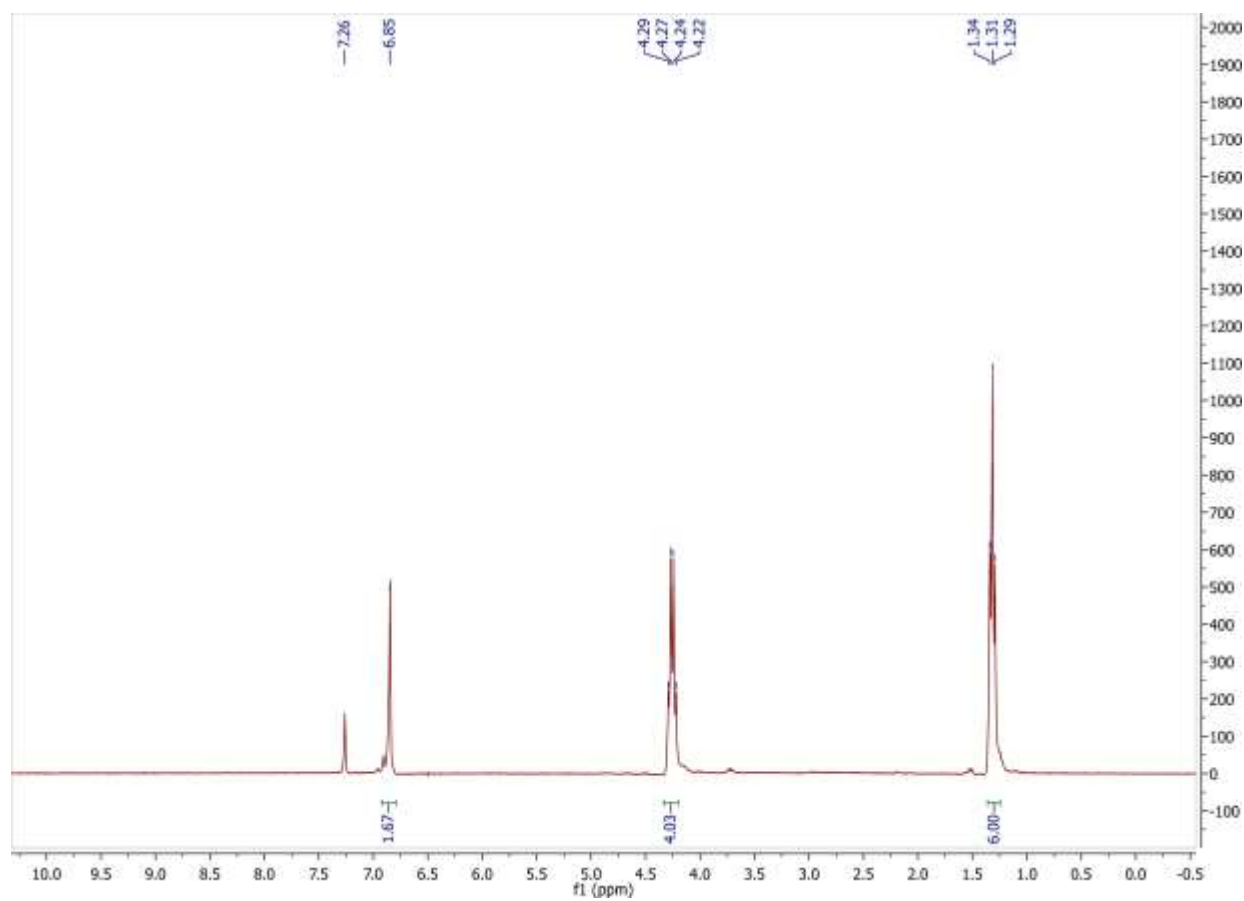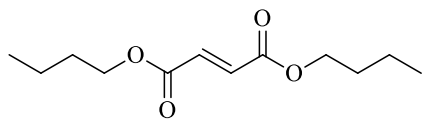
di-n-propyl fumarate [14595-35-8]
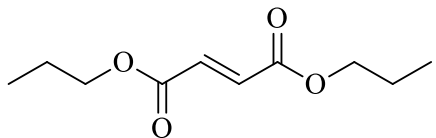
White crystalline powder (1.88g, 94%)

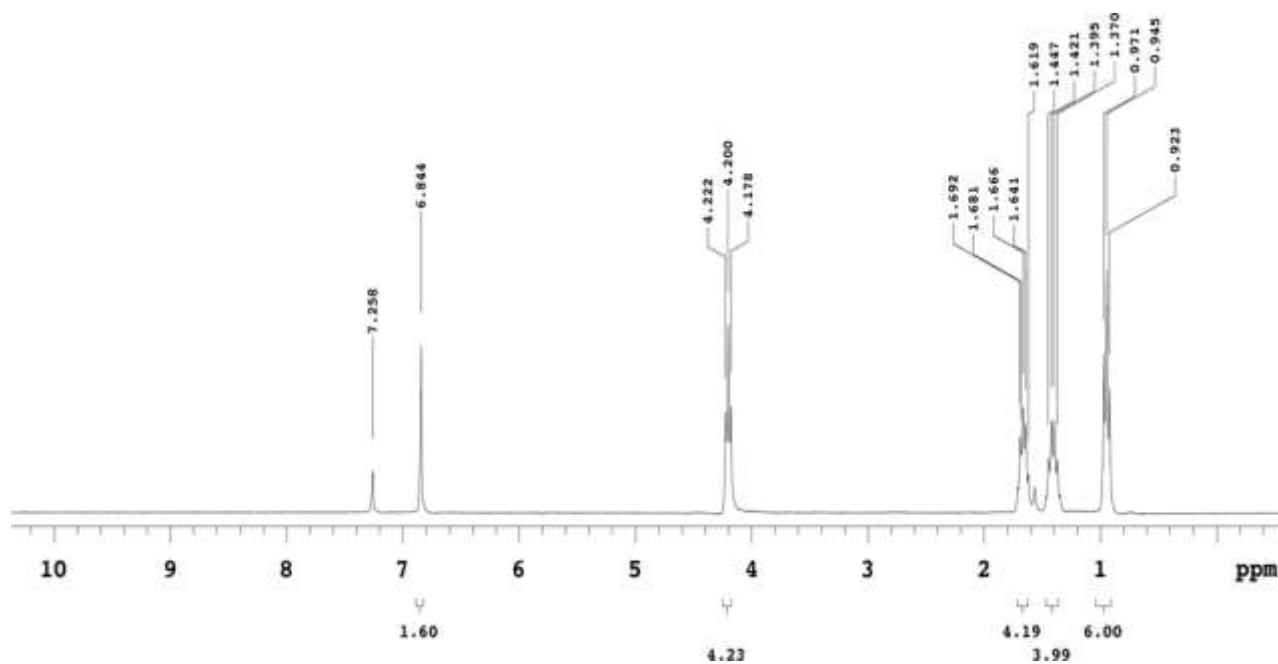^{1}H NMR (300 MHz, CDCl3) δ: 6.86 (s, 2H), 4.16 (t, J = 6.6 Hz, 4H), 1.70 (m, 4H), 0.98 (t, J = 6.6 Hz, 6H).
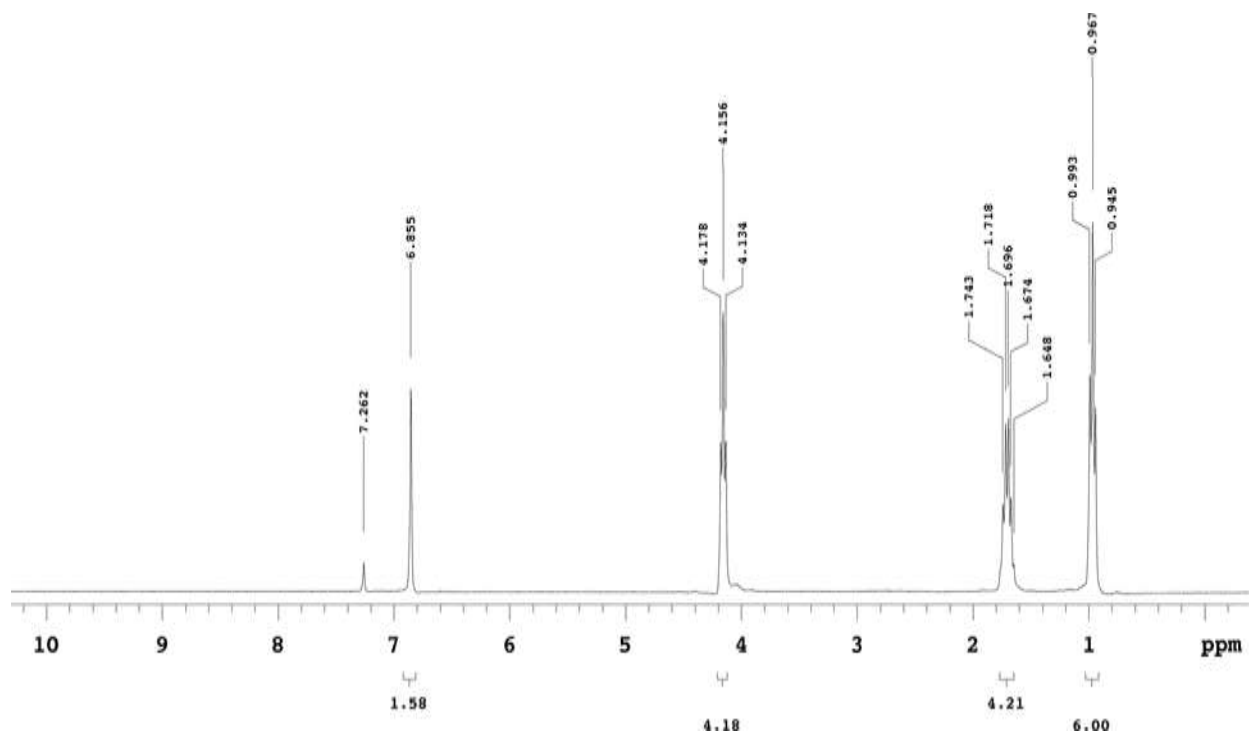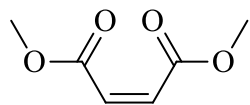
di-n-butyl fumarate [105-75-9]

White crystalline powder (2.2g, 99%)

^{1}H NMR (300 MHz, CDCl$_3$) δ: 6.84 (s, 2H), 4.20 (t, J = 6.6 Hz, 4H), 1.67 (m, 4H), 1.42 (m, 4H), 0.97 (t, J = 6.6 Hz, 6H).
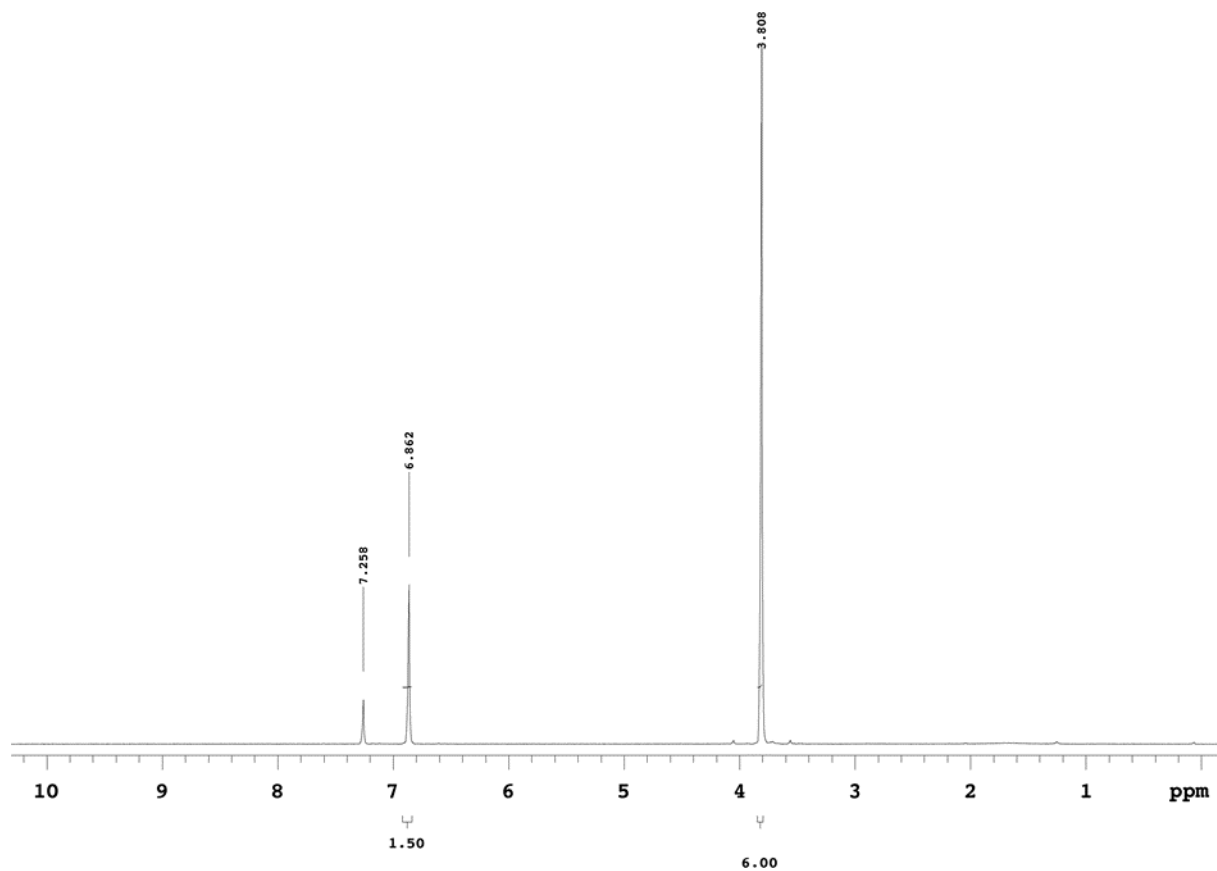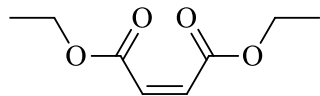
dimethyl maleate [624-48-6]

White solid (1.31g, 91%)

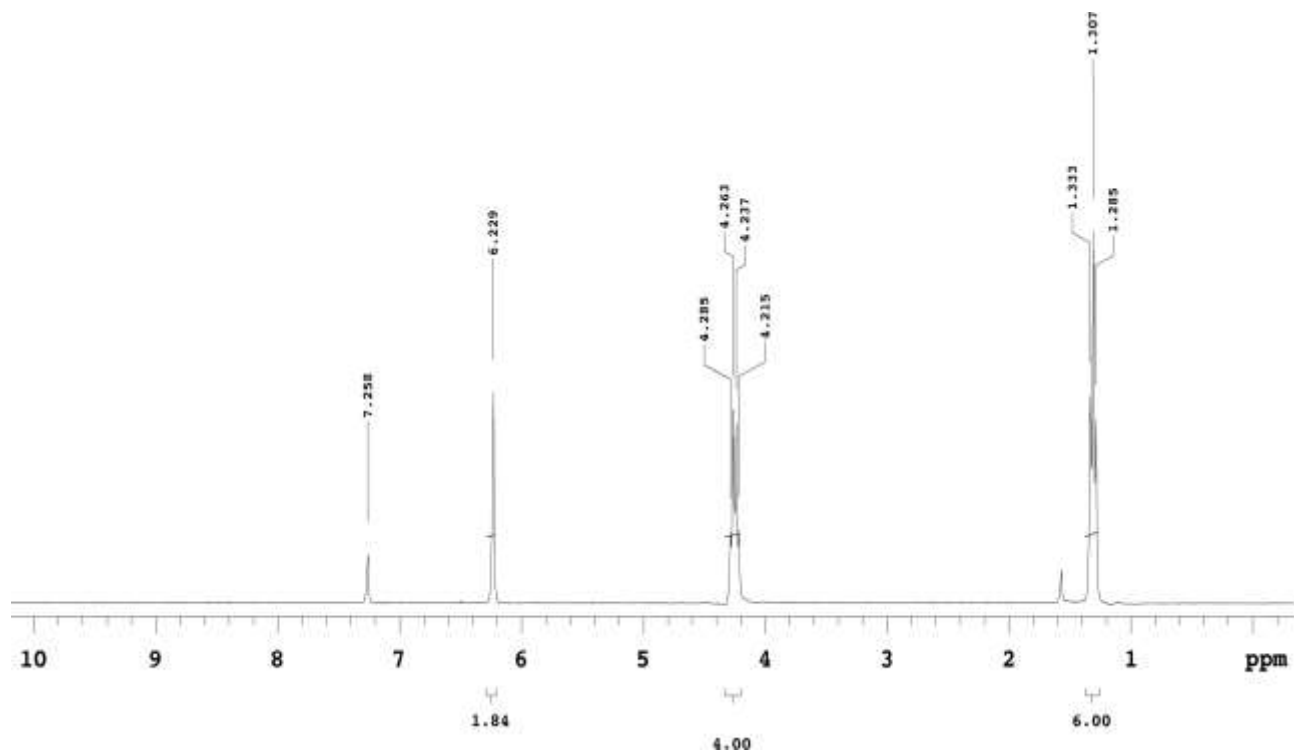^{1}H NMR (300 MHz, CDCl$_3$) δ: 6.86 (s, 2H), 3.81 (s, 6H).

diethyl maleate [141-05-9]

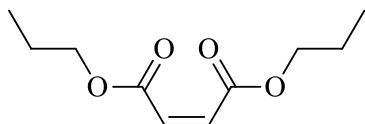Colorless liquid (1.64g, 95%)

^{1}H NMR (300 MHz, CDCl$_3$) δ: 6.22 (s, 2H), 4.25 (q, J = 6.6 Hz, 4H), 1.30 (t, J = 6.6 Hz, 6H).
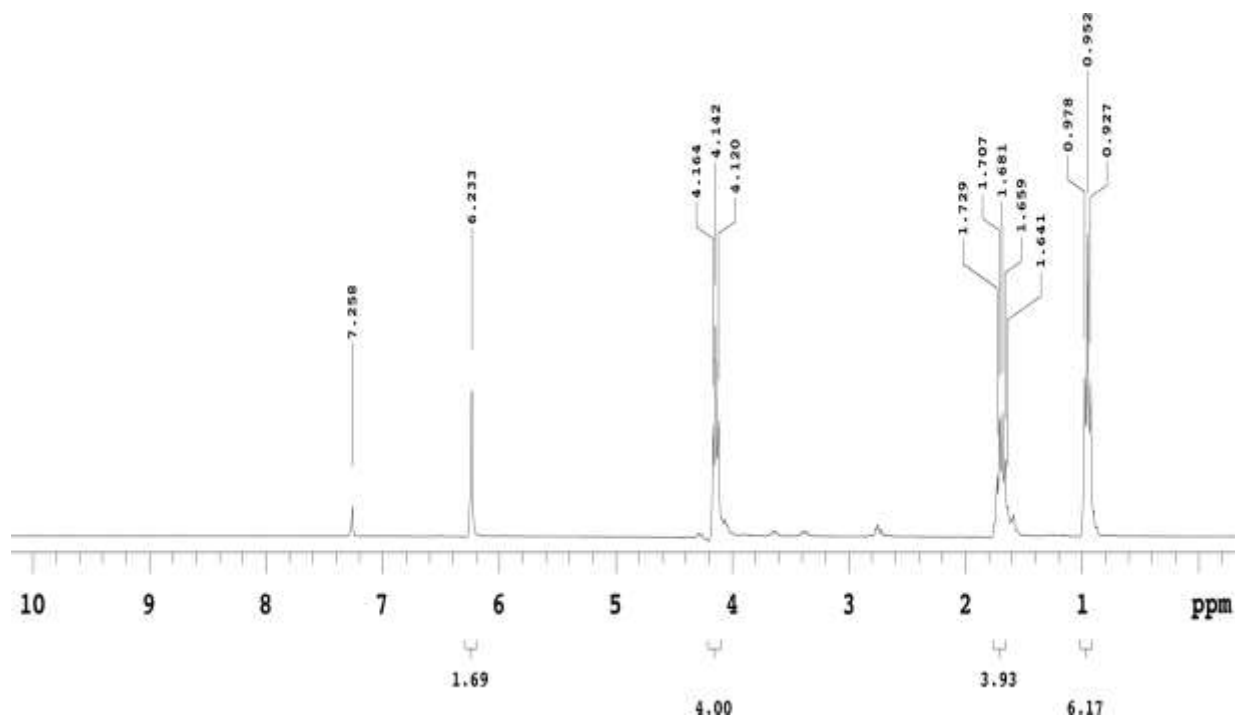
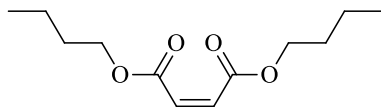**di-n-propyl maleate [2432-63-5]**

Colorless oil (1.8g, 90%)

^{1}H NMR (300 MHz, CDCl$_3$) δ: 6.23 (s, 2H), 4.14 (t, J = 6.6 Hz, 4H), 1.69 (m, 4H), 0.95 (t, J = 7.2 Hz, 6H).
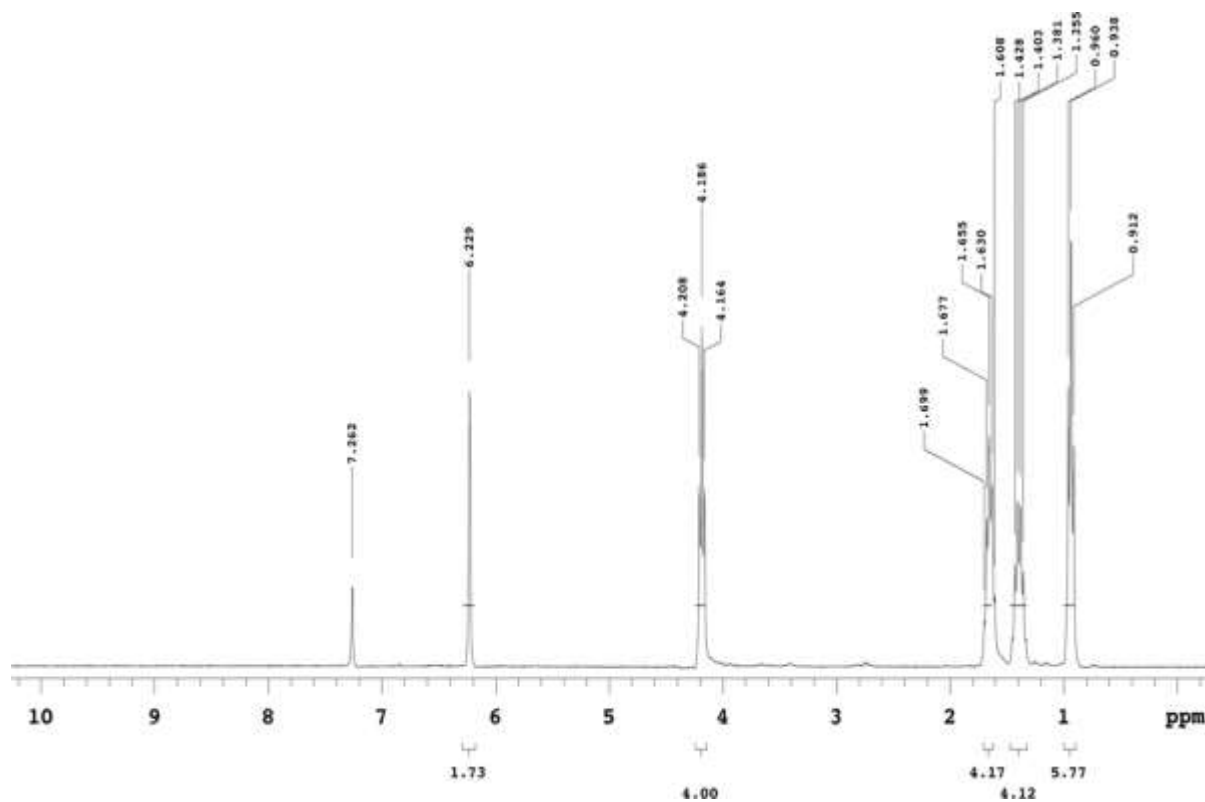
di-n-butyl maleate [105-75-0]

Colorless oil (2.1g, 92%)

^{1}H NMR (300 MHz, CDCl$_3$) δ: 6.23 (s, 2H), 4.19 (t, J = 6.6 Hz, 4H), 1.65 (m, 4H), 1.39 (m, 4H), 0.94 (t, J = 6.6 Hz, 6H).

2.5.6 NMR Data for Esterification of Aromatic and Non-Aromatic Acids

^{1}H NMR is shown below for each entry to illustrate the purity of the sample. ^{1}H NMR spectra were identical to spectra in the Spectral Database for organic compounds. SDBSWeb: https://sdbs.db.aist.go.jp (National Institute of Advanced Industrial Science and Technology)

methyl benzoate [93-58-3]
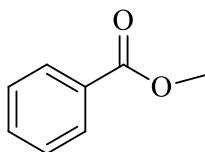
Colorless oil (1.1g, 77%)

^{1}H NMR (300 MHz, DMSO-d_6) δ: 7.96 – 7.88 (m, 2H), 7.61 (d, J = 7.5 Hz, 1H), 7.47 (t, J = 7.6 Hz, 2H), 3.81 (s, 3H).

ethyl benzoate [93-89-0]

Colorless oil (0.73g, 48%)

^{1}H NMR (300 MHz, CDCl$_3$) δ: 8.07 – 8.00 (m, 2H), 7.51 (s, 1H), 7.46 – 7.35 (m, 2H), 4.37 (q, J = 7.1 Hz, 2H), 1.38 (t, J = 7.1 Hz, 3H).

propyl benzoate [2315-68-6]
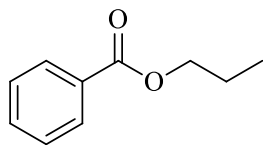
Colorless oil (0.70g, 43%)

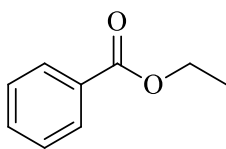^{1}H NMR (300 MHz, DMSO-d_6) δ: 7.95 (d, J = 9.1 Hz, 2H), 7.60 (t, J = 7.4 Hz, 1H), 7.48 (t, J = 8.2 Hz, 2H), 4.19 (t, J = 6.6 Hz, 2H), 3.33 (d, J = 6.6 Hz, 2H), 1.40 (q, J = 7.3 Hz, 2H), 0.81 (t, J = 7.4 Hz, 3H).

butyl benzoate [136-60-7]
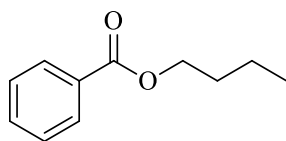
Colorless oil (0.94g, 52%)

^{1}H NMR (300 MHz, DMSO-d_6) δ: 8.47 (d, J = 7.9 Hz, 2H), 8.07 (t, J = 7.3 Hz, 1H), 7.95 (t, J = 7.5 Hz, 2H), 4.75 (t, J = 6.5 Hz, 2H), 2.27 – 2.10 (m, 2H), 1.92 (q, J = 7.5 Hz, 2H), 1.48 – 1.29 (m, 3H).

methyl *p*-toluate [99-75-2]
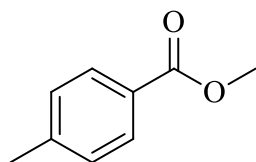
White crystalline solid (0.82g, 55%)

^{1}H NMR (300 MHz, DMSO-d_6) δ: 7.83 (d, J = 8.2 Hz, 2H), 7.30 (d, J = 8.0 Hz, 2H), 3.80 (s, 3H), 2.35 (s, 3H).

methyl *p*-chlorobenzoate [7335-27-5]
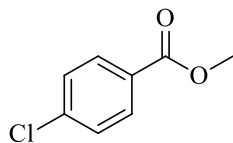
White crystalline solid (0.95g, 55%)

^{1}H NMR (300 MHz, CDCl$_3$) δ: 7.96 (d, *J* = 8.1 Hz, 2H), 7.48 – 7.32 (m, 2H), 3.91 (s, 3H).

methyl 2,3-dichlorobenzoate [2905-54-6]
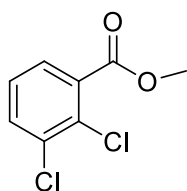
Pale yellow oil (1.1g, 54%)

^{1}H NMR (300 MHz, CDCl$_3$) δ: 7.60 (dd, *J* = 19.9, 7.9 Hz, 2H), 7.32 – 7.13 (m, 1H), 3.93 (s, 3H).

ethyl 2,3-dichlorobenzoate [31273-66-2]
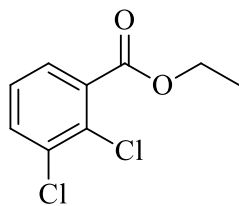
Pale yellow oil (0.93g, 43%)

^{1}H NMR (400 MHz, DMSO-*d$_6$*) δ: 7.73 (d, *J* = 9.6 Hz, 1H), 7.65 (d, *J* = 9.3 Hz, 1H), 7.40 (t, *J* = 7.9 Hz, 1H), 4.30 (q, *J* = 7.1 Hz, 2H), 1.28 (t, *J* = 7.1 Hz, 3H).

propyl 2,3-dichlorobenzoate [25843-11-2]
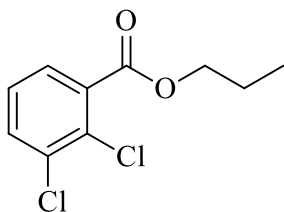
Pale yellow oil (0.77g, 33%)

^{1}H NMR (300 MHz, DMSO-d_6) δ: 7.75 (d, J = 8.0 Hz, 1H), 7.67 (d, J = 7.8 Hz, 1H), 7.42 (t, J = 8.9 Hz, 1H), 4.21 (t, J = 6.5 Hz, 2H), 1.67 (q, J = 7.5 Hz, 2H), 0.91 (t, J = 8.3 Hz, 3H).

methyl 4-hydroxy-3-nitrobenzoate [99-42-3]
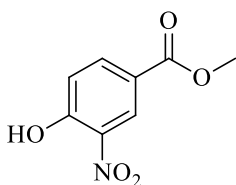
Pale golden/brown solid (1.04g, 53%); mp 75.1-75.9 °C. [Lit. mp 74-76 °C]

^{1}H NMR (300 MHz, CDCl$_3$) δ: 10.89 (s, 1H), 8.82 (d, J = 2.1 Hz, 1H), 8.23 (dd, J = 8.8, 2.1 Hz, 1H), 7.22 (d, J = 8.8 Hz, 1H), 3.94 (s, 3H).

ethyl 4-hydroxy-3-nitrobenzoate [19013-10-6]
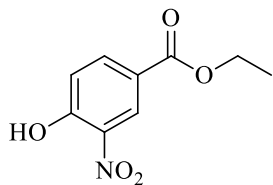
Pale golden/brown solid (1.34g, 64%); mp 70.5-71.2 °C. [Lit. mp 69-71 °C]

^{1}H NMR (300 MHz, CDCl$_3$) δ: 8.79 (d, J = 2.1 Hz, 0H), 8.26 – 8.19 (m, 0H), 7.22 – 7.16 (m, 1H), 4.38 (q, J = 7.1 Hz, 1H), 3.69 (q, J = 7.0 Hz, 2H), 1.39 (t, J = 7.1 Hz, 2H), 1.22 (t, J = 7.0 Hz, 3H).

propyl 4-hydroxy-3-nitrobenzoate [34384-48-0]
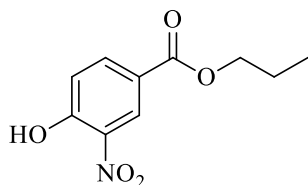
Bright yellow solid (1.0g, 52%); mp 60.2-60.8 °C. [Lit. mp 60-61 °C]

^{1}H NMR (300 MHz, DMSO-d_6) δ: 8.35 (d, J = 2.5 Hz, 1H), 7.64 (dd, J = 9.1, 2.5 Hz, 1H), 6.61 (d, J = 9.1 Hz, 1H), 4.11 (t, J = 6.6 Hz, 2H), 1.72 – 1.60 (m, 2H), 0.93 (t, J = 7.4 Hz, 3H).

butyl 4-hydroxy-3-nitrobenzoate [52791-73-8]
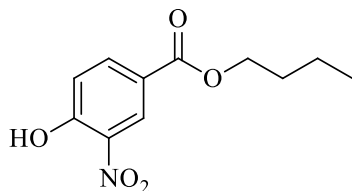
Bright yellow solid (1.0g, 43%); mp 175.3-176.1 °C. [Lit. mp 174-176 °C]

^{1}H NMR (300 MHz, CDCl$_3$) δ: 8.79 (d, J = 2.1 Hz, 1H), 8.26 – 8.19 (m, 1H), 7.20 (d, J = 8.8 Hz, 1H), 4.38 (q, J = 7.1 Hz, 2H), 3.69 (d, J = 7.0 Hz, 2H), 1.39 (t, J = 7.1 Hz, 2H), 1.21 (d, J = 7.0 Hz, 3H).

methyl nicotinate [93-60-7]
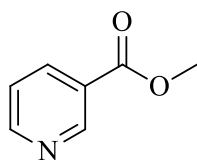
Pale yellow oil (0.64g, 47%)

^{1}H NMR (300 MHz, DMSO-d_6) δ: 9.07 (s, 0H), 8.80 (d, J = 6.1 Hz, 1H), 8.27 (d, J = 8.7 Hz, 1H), 7.58 – 7.46 (m, 1H), 3.86 (s, 3H).

ethyl nicotinate [614-18-6]
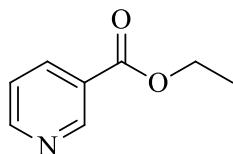
Pale yellow oil (0.62g, 41%)

^{1}H NMR (300 MHz, CDCl$_3$) δ: 9.18 (s, 1H), 8.72 (d, J = 4.8 Hz, 1H), 8.26 (d, J = 7.9 Hz, 1H), 7.43 – 7.29 (m, 1H), 4.38 (q, J = 7.1 Hz, 2H), 1.37 (t, J = 7.1 Hz, 3H).

propyl nicotinate [7681-15-4]
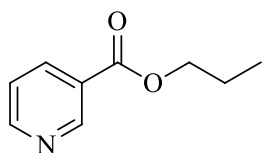
Pale yellow oil (0.72g, 43%)

^{1}H NMR (300 MHz, CDCl$_3$) δ: 9.15 (s, 1H), 8.76 – 8.60 (m, 1H), 8.27 – 8.15 (m, 1H), 7.34 – 7.15 (m, 1H), 4.23 (t, J = 6.7 Hz, 2H), 1.79 – 1.60 (m, 2H), 0.95 (t, J = 7.4 Hz, 3H).

butyl nicotinate [6938-06-3]
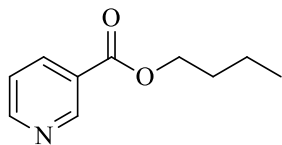
Pale yellow oil (0.92g, 54%)

^{1}H NMR (300 MHz, CDCl$_3$) δ: 9.15 (s, 1H), 8.74 – 8.63 (m, 1H), 8.29 – 8.16 (m, 1H), 7.38 – 7.24 (m, 1H), 4.28 (t, J = 6.6 Hz, 2H), 1.69 (p, J = 6.8 Hz, 2H), 1.45 – 1.30 (m, 2H), 0.90 (t, J = 7.4 Hz, 3H).

methyl phenylacetate [101-41-7]
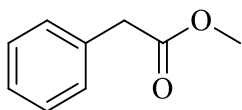
Pale yellow oil (1.4g, 95%)

^{1}H NMR (400 MHz, DMSO-d_6) δ: 7.28 (dt, J = 12.8, 7.2 Hz, 5H), 3.67 (s, 2H), 3.60 (s, 3H).

ethyl phenylacetate [101-97-3]
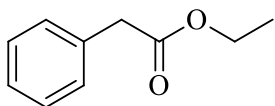
Pale yellow oil (1.6g, 98%)

^{1}H NMR (300 MHz, DMSO-d_6) δ: 7.45 – 7.12 (m, 5H), 4.08 (q, J = 7.1 Hz, 2H), 3.65 (s, 2H), 1.17 (t, J = 7.1 Hz, 3H).

propyl phenylacetate [4606-15-9]
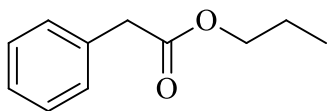
Pale yellow oil (1.6g, 92%)

^{1}H NMR (300 MHz, CDCl$_3$) δ: 7.34 – 7.26 (m, 4H), 4.06 (t, J = 6.7 Hz, 2H), 3.63 (s, 2H), 1.70 – 1.59 (m, 2H), 0.92 (t, J = 7.4 Hz, 3H).

butyl phenylacetate [122-43-0]
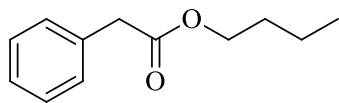
Pale yellow oil (1.9g, 99%)

^{1}H NMR (300 MHz, DMSO-d_6) δ: 7.76 (s, 4H), 4.52 (t, J = 6.6 Hz, 2H), 4.08 (s, 2H), 2.08 – 1.97 (m, 2H), 1.80 (q, J = 7.4 Hz, 2H), 1.35 (t, J = 7.3 Hz, 3H).

methyl laurate [111-82-0]
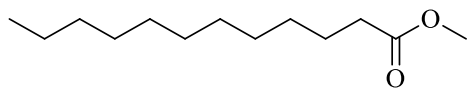
Pale yellow oil (2.1g, 97%)

^{1}H NMR (300 MHz, DMSO-d_6) δ: 3.55 (s, 3H), 2.25 (t, J = 7.4 Hz, 2H), 1.54 – 1.42 (m, 2H), 1.21 (s, 18H), 0.82 (d, J = 6.8 Hz, 3H).

ethyl laurate [106-33-2]
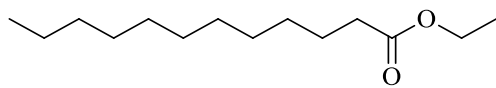
Pale yellow oil (2.2g, 95%)

^{1}H NMR (300 MHz, CDCl$_3$) δ: 4.11 (q, J = 7.1 Hz, 2H), 2.27 (t, J = 7.5 Hz, 2H), 1.69 – 1.56 (m, 2H), 1.24 (s, 18H), 0.91 – 0.81 (m, 3H).

propyl laurate [3681-78-5]
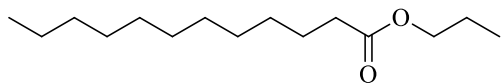
Pale yellow oil (2.1g, 88%)

^{1}H NMR (300 MHz, DMSO-d_6) δ: 3.93 (t, J = 6.6 Hz, 2H), 2.25 (t, J = 7.3 Hz, 2H), 1.53 (dt, J = 14.0, 7.0 Hz, 4H), 1.22 (s, 18H), 0.85 (s, 3H).

butyl laurate [106-18-3]
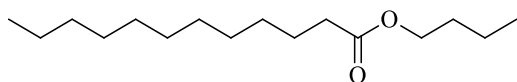
Pale yellow oil (2.0g, 77%)

^{1}H NMR (400 MHz, DMSO-d_6) δ: 3.98 (t, J = 6.6 Hz, 2H), 2.23 (d, J = 7.3 Hz, 2H), 1.51 (s, 2H), 1.27 (s, 6H), 1.09 (s, 3H), 0.83 (t, J = 6.5 Hz, 3H).

methyl palmitate [112-39-0]
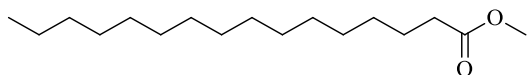
Colorless oil (2.7g, 98%)

^{1}H NMR (300 MHz, DMSO-d_6) δ: 3.55 (s, 3H), 2.25 (t, J = 7.4 Hz, 2H), 1.53 – 1.41 (m, 2H), 1.21 (d, J = 1.7 Hz, 26H), 0.83 (t, J = 6.6 Hz, 3H).

methyl oleate [112-62-9]
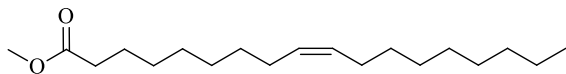
Amber oil (1.8g, 64%)

^{1}H NMR (300 MHz, DMSO-d_6) δ: 5.30 (t, J = 4.6 Hz, 2H), 3.55 (s, 3H), 2.25 (t, J = 7.4 Hz, 2H), 1.98 – 1.91 (m, 3H), 1.54 – 1.43 (m, 2H), 1.22 (s, 20H), 0.87 – 0.78 (m, 3H).

2.6 References

1. Fernando, S.; Adhikari, S.; Chandrapal, C.; Murali, N., Biorefineries: Current Status, Challenges, and Future Direction. *Energy & Fuels* **2006,** *20* (4), 1727-1737.

2. Tuck, C.; Perez Velilla, E.; Horvath, I.; Sheldon, R.; Poliakoff, M., Valorization of Biomass: Deriving More Value from Waste. *Science (New York, N.Y.)* **2012,** *337*, 695-9.

3. McCoy, M., Glycerin Surplus. *Chemical & Engineering News* **2006,** *84*, 7.

4. Esposito, D.; Antonietti, M., Redefining biorefinery: the search for unconventional building blocks for materials. *Chemical Society Reviews* **2015,** *44* (16), 5821-5835.

5. Kamm, B.; Schneider, B.; Hüttl, R.; Grünewald, H.; Dr. Gusovius, H.-J.; Stollberg, C.; Ay, P.; Kamm, M., Lignocellulosic Feedstock Biorefinery - Combination of technologies of agroforestry and a biobased substance and energy economy. *Forum der Forschung* **2006,** *19*.

6. van Putten, R.-J.; van der Waal, J. C.; de Jong, E.; Rasrendra, C. B.; Heeres, H. J.; de Vries, J. G., Hydroxymethylfurfural, A Versatile Platform Chemical Made from Renewable Resources. *Chemical Reviews* **2013,** *113* (3), 1499-1597.

7. Kamm, B.; Kamm, M., Principles of biorefineries. *Applied Microbiol Biotechnol* **2004,** *64* (2), 137-45.

8. de Jong, E.; Jungmeier, G., Biorefinery Concepts in Comparison to Petrochemical Refineries. Industrial Biorefineries and white biotchenology, Elseviers B.V. 2015; pp 3-33.

9. Bozell, J. J.; Petersen, G. R., Technology development for the production of biobased products from biorefinery carbohydrates—the US Department of Energy's "Top 10" revisited. *Green Chemistry* **2010,** *12* (4), 539-554.

10. Chisti, Y., Biodiesel from microalgae. *Biotechnology Advances* **2007,** *25* (3), 294-306.

11. Donaldson, T. L.; Culberson, O. L., An industry model of commodity chemicals from renewable resources. *Energy* **1984,** *9* (8), 693-707.

12. Werpy, T.; Holladay, J.; White, J., Top Value Added Chemicals From Biomass: I. Results of Screening for Potential Candidates from Sugars and Synthesis Gas. **2004**.

13. Balat, M.; Balat, H., Progress in biodiesel processing. *Applied Energy* **2010,** *87* (6), 1815-1835.

14. Davis, R. T., L.; Biddy, M. J.; Beckham, G. T.; Scarlata, C.; Jacobson, J.; Cafferty, K.; Ross, J.; Likas, J.; Knorr, D.; Schoen, P., Process design and economics for the conversion of lignocellulosic biomass to hydrocarbons: Dilute-acid and enzymatic deconstruction of biomass to sugars and biological conversion of sugars to hydrocarbons. *NREL Technology. Rep.* **2013**, 88-101.

15. Wu, L.; Moteki, T.; Gokhale, Amit A.; Flaherty, David W.; Toste, F. D., Production of Fuels and Chemicals from Biomass: Condensation Reactions and Beyond. *Chemical and Biomolecular Engineering* **2016,** *1* (1), 32-58.

16. Delhomme, C.; Weuster-Botz, D.; Kühn, F. E., Succinic acid from renewable resources as a C4 building-block chemical—a review of the catalytic possibilities in aqueous media. *Green Chemistry* **2009,** *11* (1), 13-26.

17. Haas, T.; Jaeger, B.; Weber, R.; Mitchell, S. F.; King, C. F., New diol processes: 1,3-propanediol and 1,4-butanediol. *Applied Catalysis A: General* **2005,** *280* (1), 83-88.

18. Démolis, A.; Essayem, N.; Rataboul, F., Synthesis and Applications of Alkyl Levulinates. *ACS Sustainable Chemistry & Engineering* **2014,** *2* (6), 1338-1352.

19. Ahmad, E.; Alam, M. I.; Pant, K. K.; Haider, M. A., Catalytic and mechanistic insights into the production of ethyl levulinate from biorenewable feedstocks. *Green Chemistry* **2016,** *18* (18), 4804-4823.

20. Bechthold, I.; Bretz, K.; Kabasci, S.; Kopitzky, R.; Springer, A., Succinic Acid: A New Platform Chemical for Biobased Polymers from Renewable Resources. *Chemical Engineering & Technology* **2008,** *31* (5), 647-654.

21. Morgan, M., Butanediol: The evolution continues. **2004,** *81*, 18-20.

22. Noordover, B. A. J.; van Staalduinen, V. G.; Duchateau, R.; Koning, C. E.; van, B.; Mak, M.; Heise, A.; Frissen, A. E.; van Haveren, J., Co- and Terpolyesters Based on Isosorbide and Succinic Acid for Coating Applications: Synthesis and Characterization. *Biomacromolecules* **2006,** *7* (12), 3406-3416.

23. Corma, A.; Iborra, S.; Velty, A., Chemical Routes for the Transformation of Biomass into Chemicals. *Chemical Reviews* **2007,** *107* (6), 2411-2502.

24. Xu, L.; Wang, Y.; Yang, X.; Yu, X.; Guo, Y.; Clark, J. H., Preparation of mesoporous polyoxometalate-tantalum pentoxide composite catalyst and its application for biodiesel production by esterification and transesterification. *Green Chemistry* **2008,** *10* (7), 746-755.

25. Zhou, C.-H., Emerging trends and challenges in synthetic clay-based materials and layered double hydroxides Preface. *Applied Clay Science* **2010,** *48*, 1-4.

26.   Sejidov, F.; Mansoori, Y.; Goodarzi, N., Esterification reaction using solid heterogeneous acid catalysts under solvent-less condition. *Journal of Molecular Catalysis A: Chemical* **2005,** *240*, 186-190.

27.   Okada, K.; Shimai, A.; Takei, T.; Hayashi, S.; Yasumori, A.; MacKenzie, K. J. D., Preparation of microporous silica from metakaolinite by selective leaching method. *Microporous and Mesoporous Materials* **1998,** *21* (4), 289-296.

28.   Hart, M. P.; Brown, D. R., Surface acidities and catalytic activities of acid-activated clays. *Journal of Molecular Catalysis A: Chemical* **2004,** *212* (1), 315-321.

29.   Wilson, I., Applied Clay Mineralogy. Occurrences, processing, and application of kaolin, bentonite, palygorskite sepiolite, and common clays. *Clays and Clay Minerals* **2007,** *55* (6), 644-645.

30.   Zhang, L.; Jin, Q.; Shan, L.; Liu, Y.; Wang, X.; Huang, J., $H_3PWI_2O_4$ immobilized on silylated palygorskite and catalytic activity in esterification reactions. *Applied Clay Science* **2010,** *47* (3), 229-234.

31.   Tateiwa, J.-i.; Horiuchi, H.; Hashimoto, K.; Yamauchi, T.; Uemura, S., Cation-Exchanged Montmorillonite-Catalyzed Facile Friedel-Crafts Alkylation of Hydroxy and Methoxy Aromatics with 4-Hydroxybutan-2-one To Produce Raspberry Ketone and Some Pharmaceutically Active Compounds. *The Journal of Organic Chemistry* **1994,** *59* (20), 5901-5904.

32.   Castellano, M.; Turturro, A.; Riani, P.; Montanari, T.; Finocchio, E.; Ramis, G.; Busca, G., Bulk and surface properties of commercial kaolins. *Applied Clay Science* **2010,** *48* (3), 446-454.

33.   Machado, G.; Castro, K.; Wypych, F.; Nakagaki, S., Immobilization of metalloporphyrins into nanotubes of natural halloysite toward selective catalysts for oxidation reactions. *Journal of Molecular Catalysis A: Chemical* **2008,** *283*, 99-107.

34.   Barrientos-Ramírez, S.; Ramos-Fernández, E. V.; Silvestre-Albero, J.; Sepúlveda-Escribano, A.; Pastor-Blas, M.; Gonzalez, A., Use of natural halloysite as catalyst support in the atom transfer radical polymerization of methy methacrylate. *Microporous and Mesoporous Materials* **2009,** *120*, 132-140.

35.   Liu, P.; Zhao, M., Silver nanoparticle supported on halloysite nanotubes catalyzed reduction of   4-nitrophenol (4-NP). *Applied Surface Science* **2009,** *255*, 3989-3993.

36.   Fernandes, D. R.; Rocha, A. S.; Mai, E. F.; Mota, C. J. A.; Teixeira da Silva, V., Levulinic acid esterification with ethanol to ethyl levulinate production over solid acid catalysts. *Applied Catalysis A: General* **2012,** *425-426*, 199-204.

37.   Valle-Vigón, P.; Sevilla, M.; Fuertes, A. B., Sulfonated mesoporous silica-carbon composites and their use as solid acid catalysts. *Applied Surface Science* **2012,** *261*, 574.

38.   Melero, J. A.; Morales, G.; Iglesias, J.; Paniagua, M.; Hernández, B.; Penedo, S., Efficient conversion of levulinic acid into alkyl levulinates catalyzed by sulfonic mesostructured silicas. *Applied Catalysis A: General* **2013,** *466*, 116-122.

39.   Pileidis, F. D.; Tabassum, M.; Coutts, S.; Titirici, M.-M., Esterification of levulinic acid into ethyl levulinate catalyzed by sulfonated hydrothermal carbons. *Chinese Journal of Catalysis* **2014,** *35* (6), 929-936.

40.   An, S.; Song, D.; Lu, B.; Yang, X.; Guo, Y.-H., Morphology Tailoring of Sulfonic Acid Functionalized Organosilica Nanohybrids for the Synthesis of Biomass-Derived Alkyl Levulinates. *Chemistry-A European Journal* **2015,** *21* (30), 10786-10798.

41.   Song, D.; An, S.; Sun, Y.; Guo, Y., Efficient conversion of levulinic acid or furfuryl alcohol into alkyl levulinates catalyzed by heteropoly acid and ZrO_2 biofunctionalized organosilica nanotubes. *Journal of Catalysis* **2016,** *333*, 184-199.

42.   Tejero, M. A.; Ramírez, E.; Fité, C.; Tejero, J.; Cunill, F., Esterification of levulinic acid with butanol over ion exchange resins. *Applied Catalysis A: General* **2016,** *517*, 56-66.

43.   Ogino, I.; Suzuki, Y.; Mukai, S. R., Esterification of levulinic acid with ethanol catalyzed by sulfonated carbon catalysts: Promotional effects of additional functional groups. *Catalysis Today* **2018,** *314*, 62-69.

44.   Luan, Q.-j.; Liu, L.-j.; Gong, S.-w.; Lu, J.; Wang, X.; Lv, D., Clean and efficient conversion of renewable levulinic acid to levulinate esters catalyzed by an organic-salt of H4SiW12O40. *Process Safety and Environmental Protection* **2018,** *117*, 341-349.

45.   Hillier, S.; Brydson, R.; Delbos, E.; Fraser, T.; Gray, N.; Pendlowski, H.; Phillips, I.; Robertson, J.; Wilson, I., Correlations among the mineralogical and physical properties of halloysite nanotubes (HNTs). *Clay Minerals* **2018,** *51* (3), 325-350.

46.   Kirumakki, S. R.; Nagaraju, N.; Chary, K. V. R., Esterification of alcohols with acetic acid over zeolites Hβ, HY and HZSM5. *Applied Catalysis A: General* **2006,** *299*, 185-192.

47.   Zatta, L.; Gardolinski, J. E. F. d. C.; Wypych, F., Raw halloysite as reusable heterogeneous catalyst for esterification of lauric acid. *Applied Clay Science* **2011,** *51* (1), 165-169.

48.   Barbosa, S. L.; Dabdoub, M. J.; Hurtado, G. R.; Klein, S. I.; Baroni, A. C. M.; Cunha, C., Solvent-free esterification reactions using Lewis acids in solid-phase catalysis. *Applied Catalysis A: General* **2006,** *313* (2), 146-150.

49. Hashemzehi, M.; Saghatoleslami, N.; Nayebzadeh, H., Microwave-Assisted Solution Combustion Synthesis of Spinel-Type Mixed Oxides for Esterification Reaction. *Chemical Engineering Communications* **2017,** *204* (4), 415-423.

50. Xu, L.; Yang, X.; Yu, X.; Guo, Y.; Maynurkader, Preparation of mesoporous polyoxometalate–tantalum pentoxide composite catalyst for efficient esterification of fatty acid. *Catalysis Communications* **2008,** *9* (7), 1607-1611.

51. Rodenas, Y.; Mariscal, R.; Fierro, J. L. G.; Martín Alonso, D.; Dumesic, J. A.; López Granados, M., Improving the production of maleic acid from biomass: TS-1 catalysed aqueous phase oxidation of furfural in the presence of γ-valerolactone. *Green Chemistry* **2018,** *20* (12), 2845-2856.

52. Cavallaro, G.; Chiappisi, L.; Pasbakhsh, P.; Gradzielski, M.; Lazzara, G., A structural comparison of halloysite nanotubes of different origin by Small-Angle Neutron Scattering (SANS) and Electric Birefringence. *Applied Clay Science* **2018,** *160*, 71-80.

53. Konwar, D.; Gogoi, P. K.; Gogoi, P.; Borah, G.; Baruah, R.; Hazarika, N.; Borgohain, R., Esterification of carboxylic acids by acid-activated Kaolinite clay. *Indian J. Chem. Technol.* **2008,** *15* (1), 75-78.

54. Kumar, B. S.; Dhakshinamoorthy, A.; Pitchumani, K., K10 montmorillonite clays as environmentally benign catalysts for organic reactions. *Catalysis Science & Technology* **2014,** *4* (8), 2378-2396.

55. Brindley, G. W.; Brown, G., *Crystal Structures of Clay Minerals and their X-Ray Identification*. Mineralogical Society of Great Britain and Ireland: 1980.

Chapter 3

Room-Temperature Aqueous Suzuki-Miyaura Cross-Coupling Reactions Catalyzed via Recyclable Palladium@Halloysite Nanocomposite
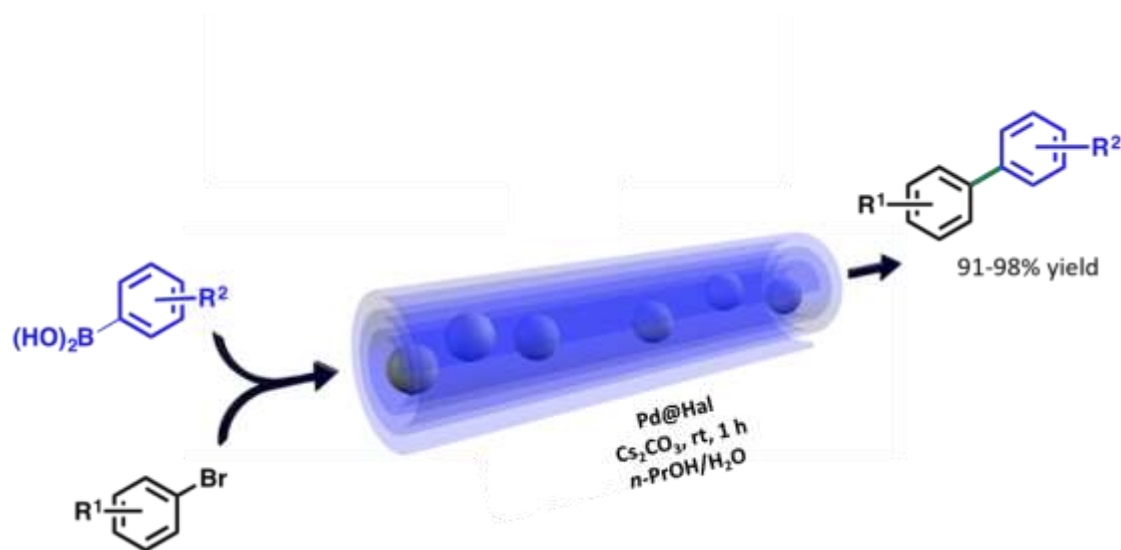
3.1 Abstract

A reliable method for encapsulating palladium nanoparticles (6-8 nm particles) in halloysite (Pd@Hal) has been developed. The Pd@Hal was found to be a highly efficient room temperature catalyst for Suzuki-Miyaura cross-coupling reactions that gave high yields of a diverse array of coupling products in n-PrOH: H_2O (5:2) within 1 h. The catalytic system was remarkably effective with a broad scope of substrates. Further, the catalyst was easily recovered and recycled without significant loss of catalytic activity.

3.2   Introduction

3.2.1   Transition Metals in Synthetic Organic Chemistry

The formation of new carbon-carbon bonds is central to organic chemistry and a prerequisite for all life on earth. Transition metal-catalyzed reactions are one of the most powerful and direct approaches for synthesizing organic molecules. Transition metal-catalyzed cross-coupling reactions to form C-C, C-N, C-O, and C-S bonds are among the most powerful organometallic transformation in organic chemistry. The importance of the synthesis of carbon-carbon bonds is reflected by the fact that Nobel Prizes in Chemistry have previously been given to this area: In 1912 for the Grignard reaction[1], 1950 the Diels-Alder reaction[2], 1979 the Wittig reaction[3], 2005 for the olefin metathesis, and Palladium-catalyzed cross-coupling in organic chemistry (2010)[4]. Transition metal-catalyzed processes have been extensively utilized in the industry for over the past 30 years. They have been employed for library preparations, discovery syntheses, and large-scale preparation of active pharmaceutical ingredients. This use relates to the efficiency of conducting many chemical transformations with a tolerance of numerous functional groups, high enantio-, diastereomer-, and chemo-selectivity. Transition metals play an essential role in organic chemistry. The most applied transition metal-catalyzed applications relate to the transformations that result in a cross-coupling for the formation of carbon-carbon and carbon-heteroatom bonds, asymmetric hydrogenation, oxidation, asymmetric addition, and metathesis. [5, 6]

Transition metals have a unique capability to activate a variety of organic compounds, and because of this activation, they can catalyze the formation of new bonds. This has led to the development of many transition metal-catalyzed reactions. Palladium is one metal that was used early on for organic catalytic

transformations. Generally, transition metals, particularly palladium, have been essential for developing

reactions for carbon-carbon bond formation.[7] Transition metals have been utilized since the mid-1970s. In

1971, Fe (III) complex was shown to catalyze organ magnesium reagents coupling with haloalkenes.[8] The

following year, in 1972, Kumada, Tamao, and Corriu independently reported the cross-coupling of

organo-magnesium reagents with an alkenyl or aryl halides catalyzed by a Ni (II) complex.[9] Since these

seminal reports, palladium and nickel complexes have emerged as the mainstream catalysts employing

organo-boronates, silicon, tin, magnesium, and zinc reagents as the nucleophilic components wherein the

corresponding cross-couplings are referred to as Suzuki-Miyaura, Stille, Kumada, Negishi, Heck

coupling.[4, 10-13]

Scheme 1. Palladium-catalyzed C-X coupling reactions.

124
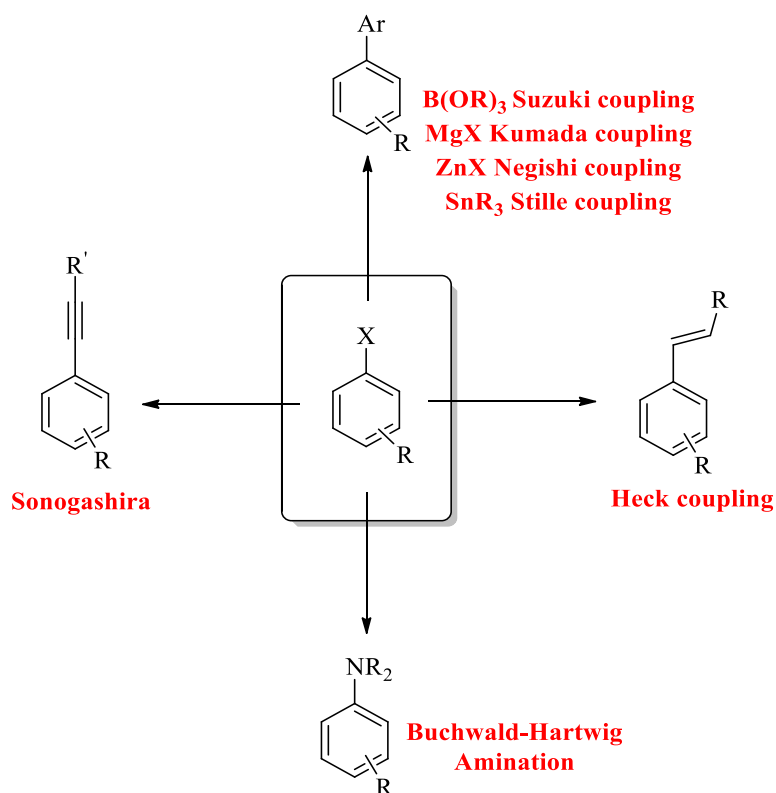
By choosing reaction components, catalysts, and conditions, most carbon-carbon single bonds can be constructed through this process. The utility of cross-couplings for the accessibility of bi-aryl, aryl-alkenyl, and aryl-alkynyl moieties has made these structures common synthetic intermediates for pharmacophores, numerous rationally designed drugs and clinical candidates as exemplified by Losartan, Naratriptan, and Singulair **Figure 1**.[14, 15]

Figure 1. Examples for application of cross-coupling reactions.

Losartan
Antihypertensive

Naratriptan
Antimigraine

Singulair
Antiasthmatic
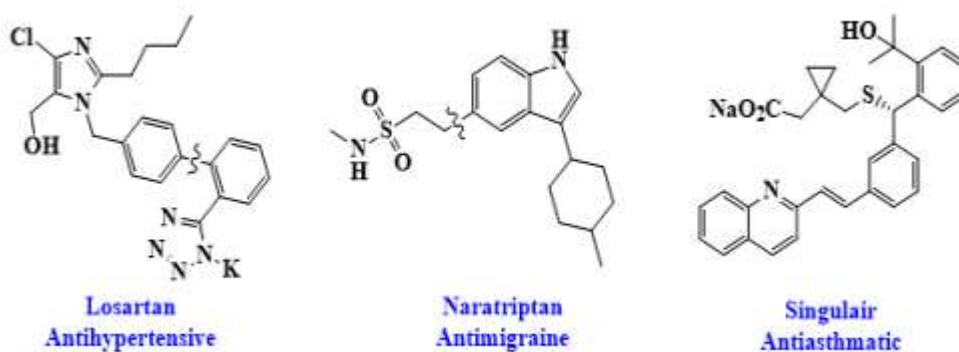
Since the 1970s, much attention has been paid to cross-coupling reactions. A large variety of electrophiles continued to be developed and extensively used in organic synthesis. In the early stages of this development, aryl iodides and bromides were successfully employed as electrophiles in cross-coupling reactions because of their relatively high reactivities.[16] New efficient catalytic systems are being developed to obtain the cross-coupled product utilizing the less-reactive aryl chlorides and fluorides. [17-20]

Scheme 2. Cross-coupling reaction of less reactive aryl chlorides.

X= 4-NO$_2$, CN, NH$_2$, CO$_2$Me, Me, OMe, 2-COMe, CF$_3$, C(O)Me, COH, CH$_2$CONCH$_2$

X= H, *p*-COMe, *p*-OMe, *o*-Me, pyridine
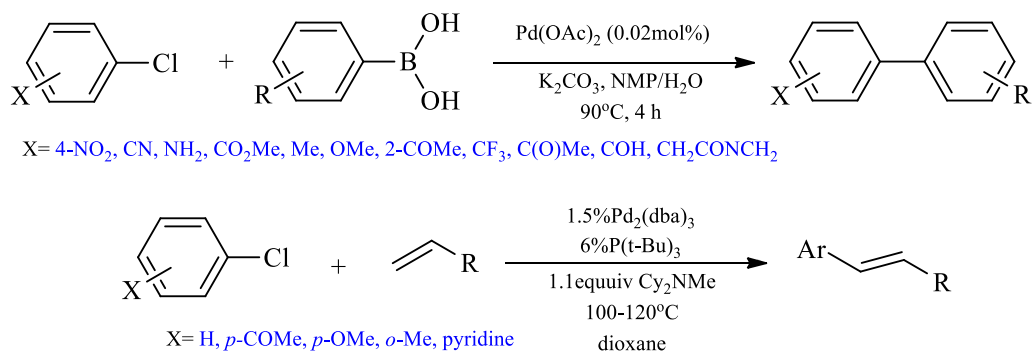
Compared with the electrophiles mentioned above, readily available phenol substrates and their derivatives provide an alternative route to C-C bond formation. As shown in **Scheme 3** aryl triflates have been successfully used as an efficient electrophile because of their relatively high reactivity.[21]

Scheme 3. Aryl triflates were successfully used as an efficient electrophile of cross-coupling reaction.

R = nBu, CO$_2$Hex, OEt, NO$_2$, CN, Ph
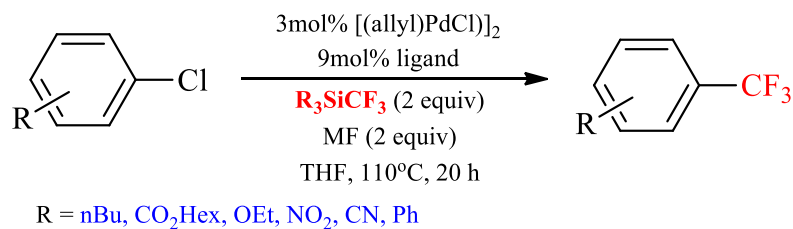
As shown in **Scheme 4** the phenolic anion is an excellent s-donor ligand, which could bind to the metal catalyst and impede the transition-metal-induced cleavage of the C-O bond.[22]

126

Scheme 4. Phenolic anion as a ligand for the cleavage of the C-O bond.
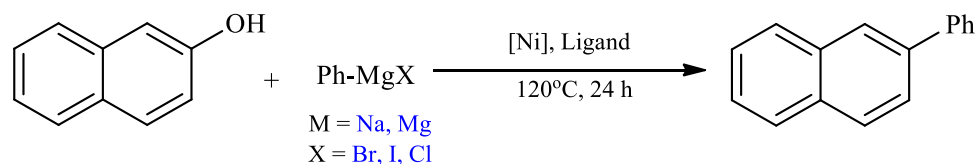
Significant progress has also been shown for the carbon-nitrile cross-coupling reaction. Asymmetric intramolecular olefin arylcyanations provide indanes with quaternary carbon stereogenic centers from readily available benzonitrile precursors with good yields and high enantioselectivities. [23-25]

Scheme 5. Asymmetric intramolecular olefin arylcyanation cross-coupling reaction.
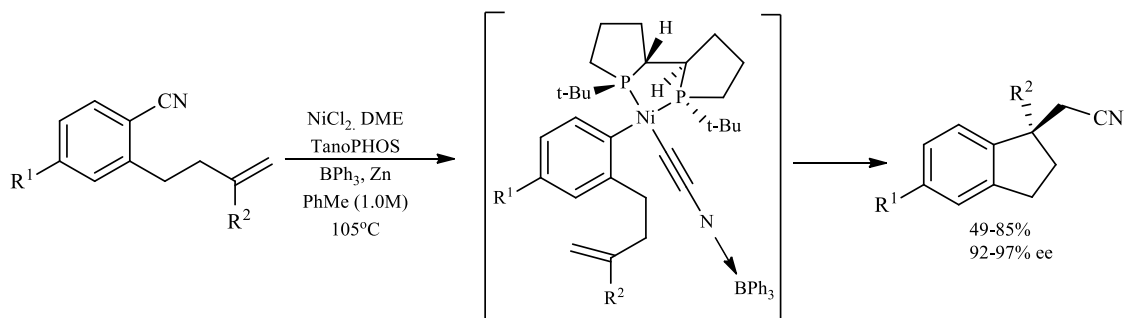
Aryl trimethylammonium triflates and tetrafluoroborates were found to be highly reactive electrophiles in the Pd-catalyzed cross-coupling with aryl Grignard reagents.[26] These advances have significantly increased the flexibility for incorporating a larger pool of commercially available materials into a synthesis.

Scheme 6. Pd-catalyzed cross-coupling with aryl Grignard reagents.

R = F, Cl, CO$_2$Et, OPiv, CN, SMe, OCF$_3$, NMe$_2$
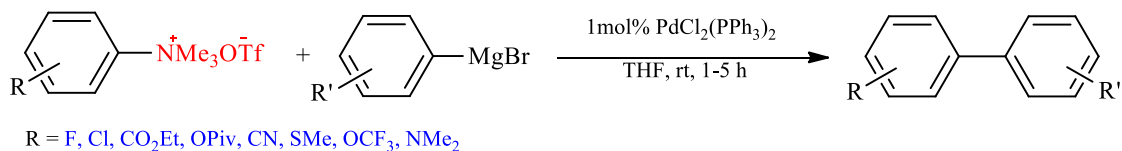
In addition to the advances made with the electrophiles, the nucleophile scope has also expanded to include carboxylic acids (decarboxylative couplings)[27], perfluorinated alkanes[28], and C–H insertions.[29] Progress was also made for enantioselective cross-couplings [30] to provide access to atropisomers, emerging as pharmacophores. [31] These advances in cross-couplings are growing exponentially, a trend that will add additional value to the chemical and pharmaceutical industries. These methodologies provide the robustness required for forming a large diversity of structures necessary for discovery and development. Some notable examples are shown in **Figure 2** the multibillion-dollar drugs Gleevec from Novartis, Abilify from Otsuka Pharmaceuticals, and Pfizer's Phase III candidate Torcetrapid, [32] An early classical example of Suzuki coupling in the pharmaceutical industry was Merck's synthesis of losartan 2, an angiotensin II receptor antagonist **Scheme 7**

Figure 2. Pharmaceutical application of heteroatom cross-coupling reaction.

Gleevec
(Imatinib)
Oncology

Abilify
(Aripiprazole)
Antidepressant

(Torcetrapid)
Dyslipidemia
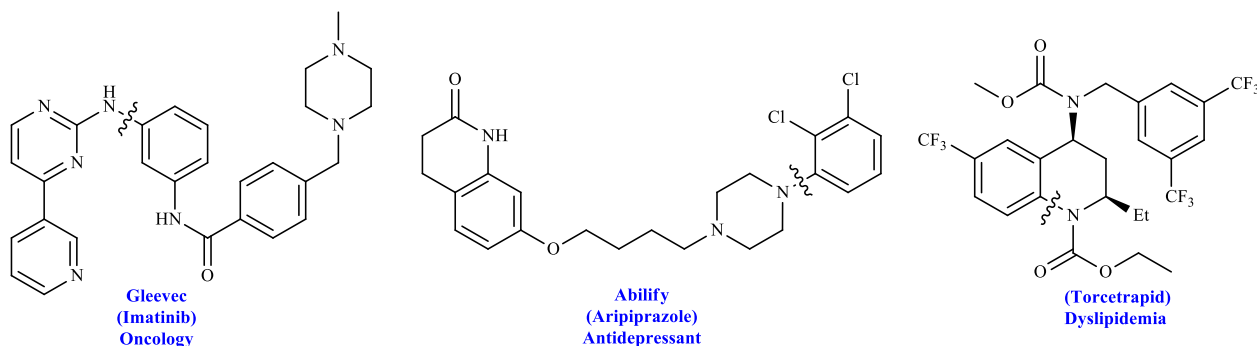
Scheme 7. Merck's synthesis of Losartan via Suzuki coupling.

n-BuLi, the B(O-iPr)$_3$, then IPA-NH$_4$Cl.H$_2$O
90%

54g (80 wt%)

1mol% Pd(OAc)$_2$, 4mol% PPh$_3$
2.5 equiv K$_2$CO$_3$, H$_2$O/THF/DME
Reflux

93%

15.5 g

Losartan
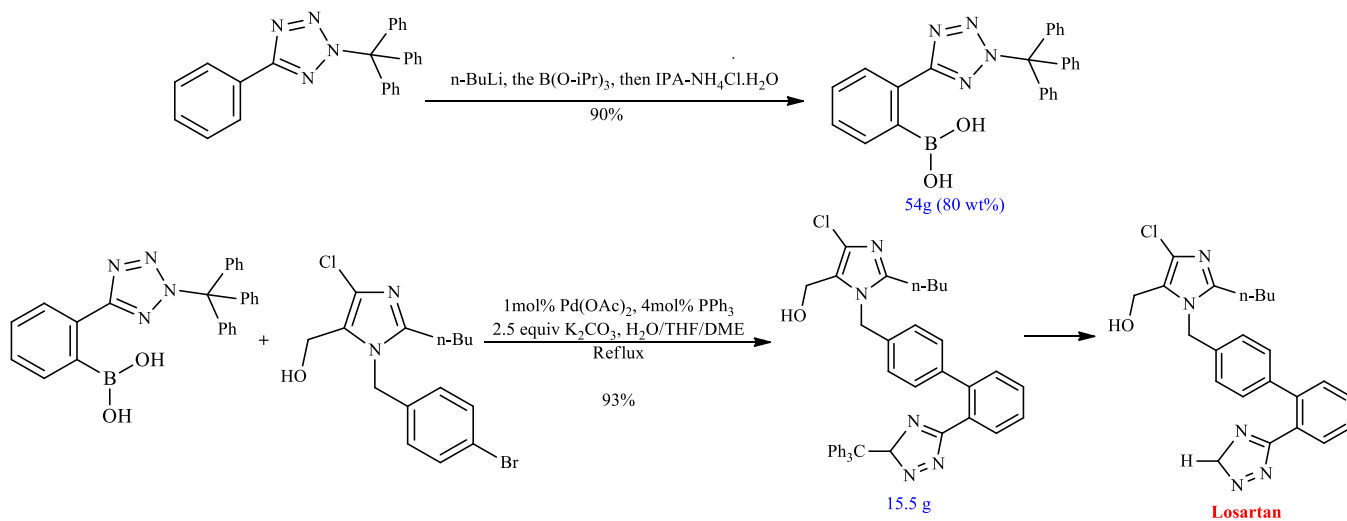
3.2.2 Cross-Couplings for the Formation of Carbon-Carbon Bonds

The core of cross-coupling reactions is the reductive elimination of two organic components from a high valent late transition metal for the formation of a C–C bond. [33] This reaction's utility was achieved by developing appropriate components for the selective formation of the mixed bis-organometallic

intermediate. There has been remarkable progress in the cross-coupling reaction of organometallic

reagents containing various nucleophiles such as B, Mg, Li, Sn, Al, Zn with unsaturated electrophiles

containing alkenyl, aryl, allyl, alkynyl groups. The general catalytic cycle involves oxidative addition of

the organic electrophile to a coordinatively unsaturated metal complex, followed by transmetallation from

the nucleophile to the intermediate species formed in the first step. Reductive elimination affords the

coupling product with the regeneration of the catalyst.

Scheme 8. A general mechanism for transition metal-catalyzed cross-coupling reaction.
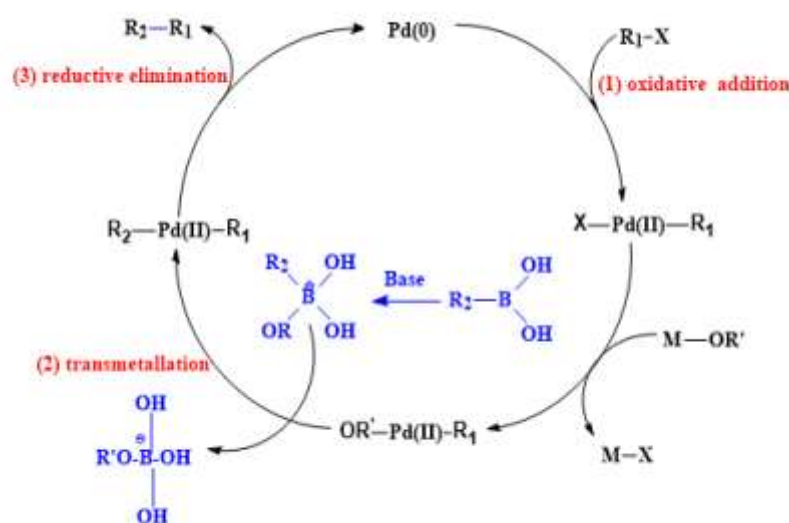
3.2.3   Palladium-catalyzed cross-coupling reactions

Awarding the 2010 Nobel Prize to Heck, Negishi, and Suzuki for "palladium-catalyzed cross-couplings in

organic synthesis" shows how significant the carbon-carbon bond formation. Palladium-catalyzed cross-

coupling reactions are pivotal steps in syntheses of agrochemicals, pharmaceuticals, and other fine

chemicals.[7, 34-38] Palladium catalysts are one of the most used transition metal catalysts due to their low toxicity and ease of handling. Palladium catalysts have many advantages over the use of non-precious metals like copper, nickel, and iron, even though the cost is lower for the 1st-row transition metals.[28, 39-44] These advantages can include higher reactivity facilitating the transformation of less reactive substrates [19, 45], performing at relatively low temperatures, and having a higher catalyst turnover number (TONs). [46] As a rule of thumb for fine chemicals production, significant catalyst turnover numbers (TONs) of >1000– 10000 are needed if the use of expensive metal complexes should be competitive with other routes. As initially developed, these reactions predominantly employ soluble Pd complexes with various organic and inorganic co-additives. **Figure 3** shows some examples of commonly used Pd/ligand systems used to catalyze cross-coupling reactions. $Pd(PPh_3)_4$ is the most frequently used, $PdCl_2(PPh_3)_2$, and $Pd(OAc)_2/PPh_3$ are also efficient as they are readily reduced to active Pd(0) complex. Various ligands such as dialkyl diphenylphosphine, ferrocenyl dialkyl phosphines, sterically hindered N-heterocyclic carbenes (NHCs) heteroaromatic phosphine ligands are used in cross-coupling reactions.[47-61]

Figure 3. Examples of homogeneous Pd/ligand complexes used in cross-coupling reaction.

Tetrakis(triphenylphosphine)
palladium(0)

Bis(triphenylphosphine)
palladium(II)diacetate

Bis(triphenylphosphine)
palladium(II)dichloride

R=Cy, tBu
R'=OMe, H, NMe2

Dialkylbiphenylphosphines
(Buchwald group)

R=Cy, tBu
R'=H, NMe2

Heteroaromaticphosphines
(Better group)

Ferrocenyldialkylphosphines
(Hartwig group)

N-heterocyclic carbenes (NHCs)
(Nolan group)
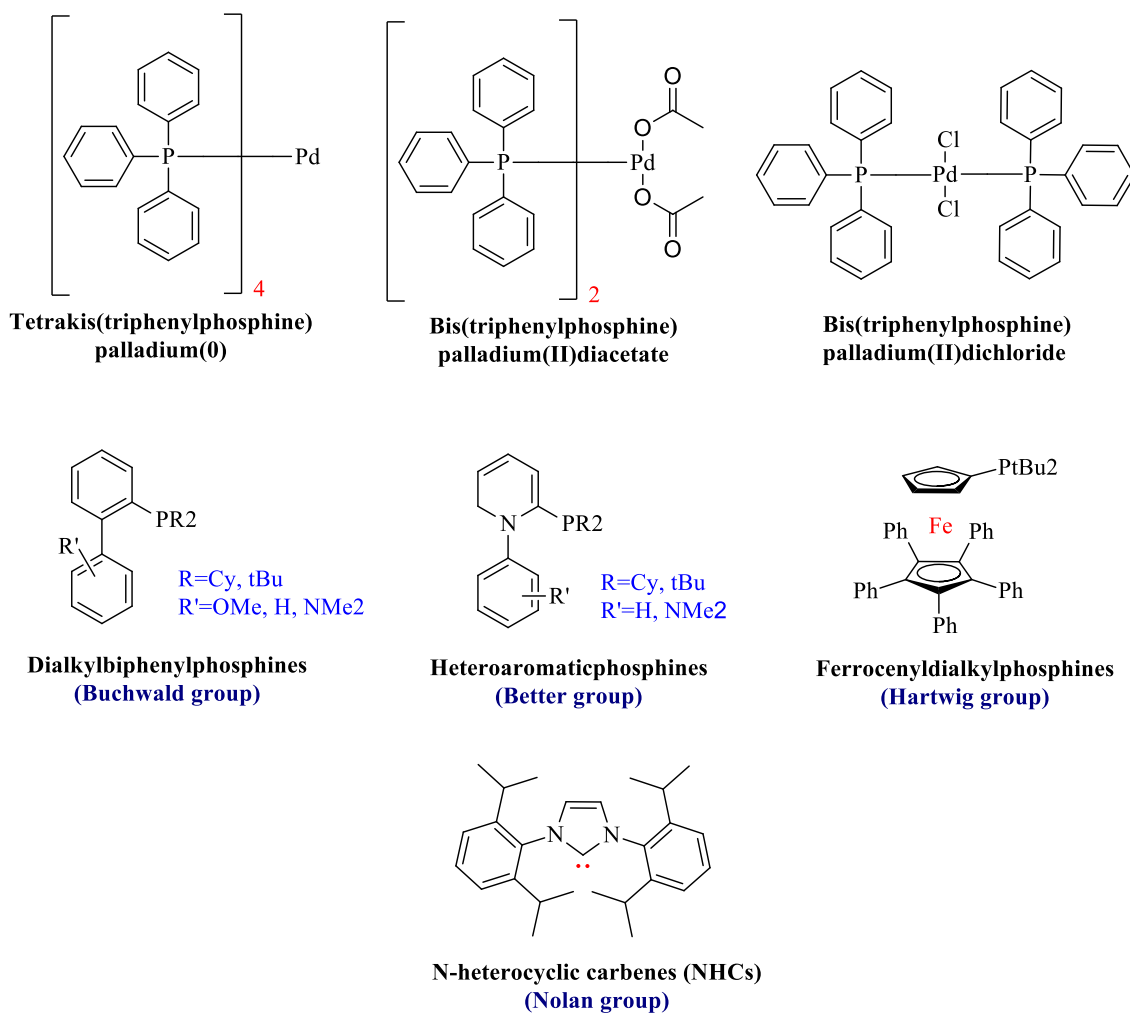
However, such complex homogenous reaction systems present several challenges for scale-up and industrial use, inhibit product purification (Pd removal), and have limited catalyst recyclability.[62-64] Efforts to convert homogenous Pd/ligand systems into similarly ligated Pd/ligand heterogeneous systems using insoluble supporting materials have had limited success.[65-70] When designing metal-ligand complexes, it is crucial to consider: **(i)** the productivity of the catalyst system, **(ii)** its activity, and **(iii)** its selectivity, as

well as **(iv)** the contamination of the product with metal and ligands.[4, 71]Also, the ligand price should be considered, especially with more complex structures.[13, 72] The catalytic system activity must be taken into account to minimize costs. Often, pharmaceutical intermediates synthesis can result in the formation of many by-products, so the metal catalyst selectivity is incredibly significant and must be addressed to cut cost. Also, the contamination of the product with the ligands and the metal can be another issue that needs to be considered, especially for pharmaceuticals. Usually, the amount of heavy metal must be controlled to levels below 10 ppm.[73] If higher, removal strategies must be developed, which adds to the overall cost.[74] The use of palladium to catalyze coupling reactions offers significantly shorter routes to the desired products, minimizing side products and waste. Recent studies aimed at the development of robust and recyclable Pd heterogeneous systems with catalytic activities comparable to homogeneous systems have focused on the potential use of Pd nanoparticles (Pd_NP)[75-78] Pd_NP-supported nanocomposite materials,[79-87] and Pd single-atom composite materials.[88, 89] Better et al. obtained 97% conversion in a Heck reaction of 4-bromoacetophenone and butyl acrylate at 140°C in the presence of 0.05 mol % of Pd colloids

Scheme 9.[90]

Scheme 9. Pd colloid catalyzed Heck reaction.

133
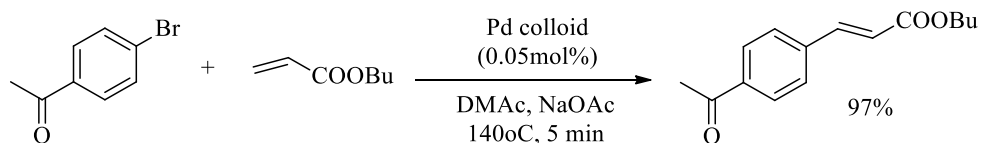
The main disadvantage of these procedures is the short lifetime of the catalyst tending to further

aggregate and form inactive Pd. The higher the Pd load is, the faster the deactivation relative to the

catalytic process occurs. Moreover, for challenging substrates like aryl chlorides or alkyl halides, ligands

are required. Reetz and co-workers were the first to report Pd and Pd/Ni nanoparticles' use stabilized by

tetrabutylammonium salts and PVP for the Suzuki coupling of aryl bromides and chlorides with

phenylboronic acid using 2 mol% of these catalysts shown in **Scheme 10**.[91] In 2000, a paper reported the

use of Pd_{NPs} stabilized by N-vinyl-2-pyrrolidone (PVP) (0.3 mol% of Pd) for Suzuki-Miyaura reaction in

water. [92] In 2004, Pd_{NPs} (2-5 nm) entrapped in SiO_2 gel (SiO_2/TEG/Pd) were reported to catalyze coupling

of aryl iodides and bromides with boronic acid using 0.75 mol% Pd catalyst [93], Pd^0-AmP-MCF catalyst

using amino-propyl-functionalized silicane foam with Pd_{NPs} for the coupling of aryl iodides and bromides

was reported by the Baclovall group.[94]

Scheme 10. The first example of Pd and Pd/Ni NPs catalyzed Suzuki coupling. [91]
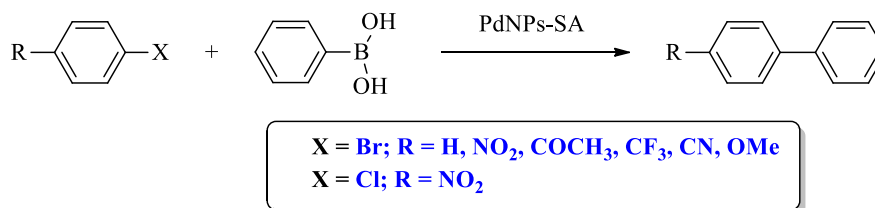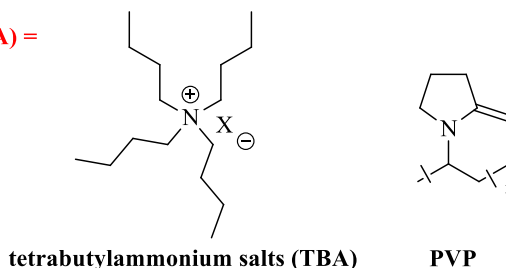
X = Br; R = H, NO₂, COCH₃, CF₃, CN, OMe
X = Cl; R = NO₂

Stablizing Agent (SA) =

tetrabutylammonium salts (TBA)   PVP

However, many of these systems suffer from low reactivity, thermal instability, metal leaching, metal agglomeration, and higher reaction temperatures. Therefore, new heterogeneous Pd systems are needed that offer high catalytic activity under ambient conditions, use benign chemical additives, are reactive in green solvent systems, can be easily recycled, and are cost-effective.

3.2.4 Transition Metal Nanoparticles

Modern transition metal nanoclusters exhibit several advantages over classical colloids and differ from them in several important aspects. They are usually smaller (1–10 nm in diameter) with narrower size dispersion, and their synthesis is reproducible with well-defined composition and clean surfaces.[95-98] They are isolable and re-dissolvable in aqueous and/or organic solvents. In terms of catalytic properties, transition metal nanoparticles are usually more active and display reproducible activities and often high selectivity. Nanocatalysis combines the advantages of easy separation, handling, and reuse, typical of heterogeneous catalysts, and the benefits of homogeneous catalysis, namely high selectivity and efficiency.[99] Furthermore, the use of supports for metals is of great interest for its potential to recover and reuse the catalyst and reduce metal usage.[99, 100]

3.2.5 Synthesis of Transition Metal Nanoparticles

Metal nanoparticles (M-NPs) designed for catalytic applications are usually synthesized through two methods: metal salts reduction and organometallic complexes decomposition.[96-98, 101-106] Although various techniques are used to synthesize nanoparticles, some features are common to all the methods. That is, the synthesis of nanoparticles requires the use of a device or process that fulfills the following conditions:

- control of particle size, size distribution, shape, crystal structure, and composition distribution

- improvement of the purity of nanoparticles (lower impurities)

- control of aggregation

- stabilization of physical properties, structures, and reactants

- higher reproducibility

- higher mass production, scale-up, and lower costs

Unsupported metal nanoparticles with well-defined surface structures and clean exposed facets are a simplified model for theoretical studies. However, the transfer from computational approaches and real catalysts is still a challenge. Because of their high-dispersed state, metal nanoparticles in solution tend to agglomerate and coagulate. Therefore spontaneously, they need to be stabilized by a protective agent to avoid bulk metal formation. Two types of stabilization can be achieved as illustrated in **Figure 4** depending on the nature of the protecting agents: **(i)** electrostatic stabilization can be obtained using ionic compounds as protecting agents; Adsorption of ions to the surface creates an electrical double layer which results in a coulombic repulsion force between individual particles. **(ii)** steric stabilization can be achieved by surrounding the metal center with layers of material that are sterically bulky molecules such as polymers.

Figure 4. Schematic representation of the electrostatic and steric stabilization in (M-NPs).

Electrostatic stabilization   Steric stabilization
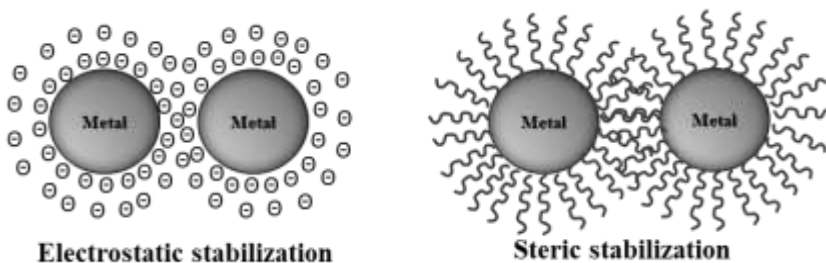
The nature and/or length of the sterically protecting agent will modify the thickness of the protecting layer and thus influence the stability/reactivity of the nanoparticles. Some examples include organic ligand shells (citrates, amines, thiols),[107-109] surfactants (CTAB),[110] polymers (PVA, PVP),[111] dendrimers,[112] and ionic liquids (hydroxy imidazolium chlorides).[113] **Figure 5** Capping agents do more than just preventing nanoparticle agglomeration, organic ligand modification of metal surface is a useful tool for increasing the compatibility with another phase or introducing additional functionalities.[114] Moreover, in supported metal nanoparticles, the capping agent can facilitate the anchoring onto the support resulting in a high metal dispersion.[115] Impact on the performances of M-NPs, mainly because of the hindered access of reactants to the catalyst surface. [116, 117]

Figure 5. Examples of capping agents.
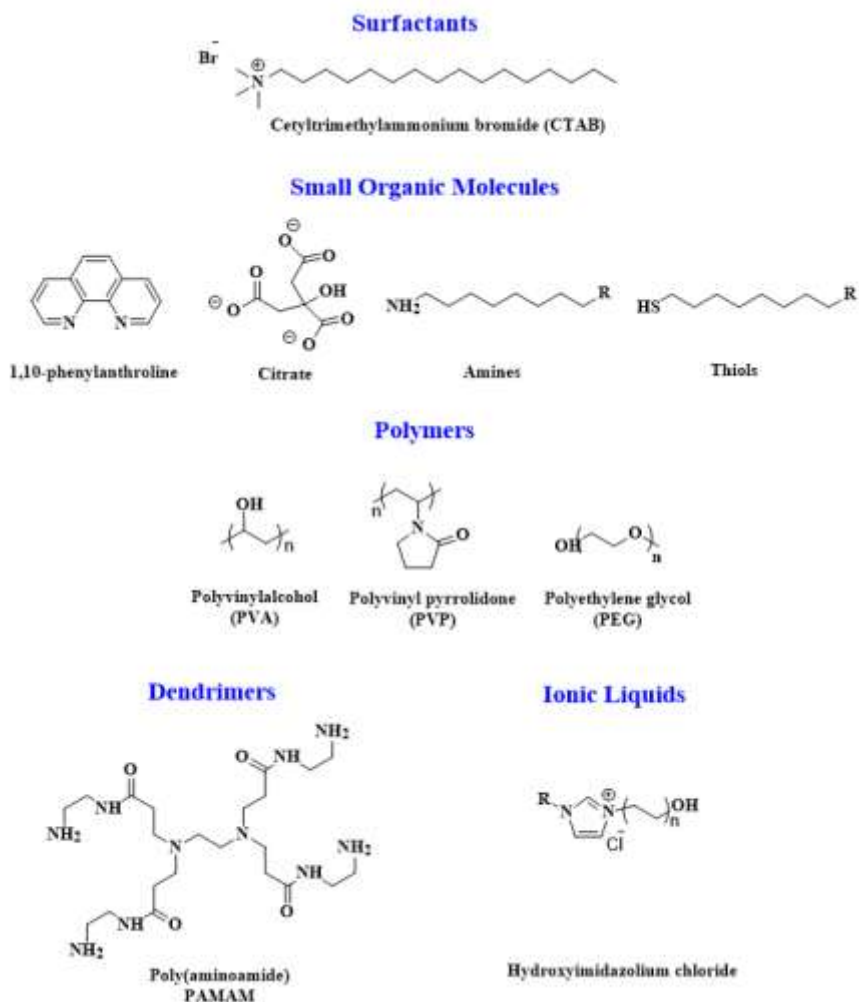
3.2.6 Immobilization of M-NPs on a Solid Support

The immobilization of colloidal M-NPs on a solid support is an exciting alternative since the catalyst can be recycled by simple filtration. Several approaches to the preparation of supported nanocatalysts have been reported, including conventional impregnation, coprecipitation and deposition–precipitation

138

techniques, photo deposition, sputtering, colloidal methods, and more [100, 118-122]. Recently, novel approaches have been presented, which improve the distribution of metal particles and the degree of dispersion on the support [123-126]. For example, Pd nanoparticles with controlled size and narrow size distribution were deposited on TiO_2 spheres containing many surface hydroxyl groups with the assistance of $SnCl_2$ [123]. Based on the surface redox reaction between the metal oxide support and metal ions, metal nanoparticles and metal alloys (e.g., Pt, Au, Ru, PtRu, etc.) were in situ deposited on the metal oxide support, resulting in metal/metal oxide or nanocatalysts with uniform metal particle size [126]. Palladium NPs immobilized on various supports have been applied as catalysts for cross-coupling reactions. The efficient immobilization of these nanocatalysts was mainly reported onto classical supports such as polymers,[127-130] resins, activated carbon,[131] carbon nanotubes[132], and various inorganic materials.[133, 134] Immobilizing M-NPs onto solid supports can minimize atom/ion leaching from the particles.

3.2.8   Halloysite as a Support

The kaolinite-related clay, halloysite (Hal), has been identified as solid support for numerous chemical applications. Halloysite is a dioctahedral 1:1 clay mineral and occurs in nature as a hydrate consisting of rolled aluminosilicate sheets.[135-137] The morphology of Hal particles is highly diverse, but the most common shapes are elongated, curled particles that form nanotubes or nanoscrolls. Hal nanoscrolls are generally 0.2–2 μm in length, having an inner diameter of 10–40 nm and an outer diameter of 40–70 nm.[137] Hal nanoscrolls are classified into two morphologies, having the stoichiometry Hal-(10 Å) $[Al_2Si_2O_5(OH)_4 \cdot 2H_2O]$ and dehydrated Hal-(7 Å) $[Al_2Si_2O_5(OH)_4]$. [137]

Figure 6. Halloysite nanoscroll.
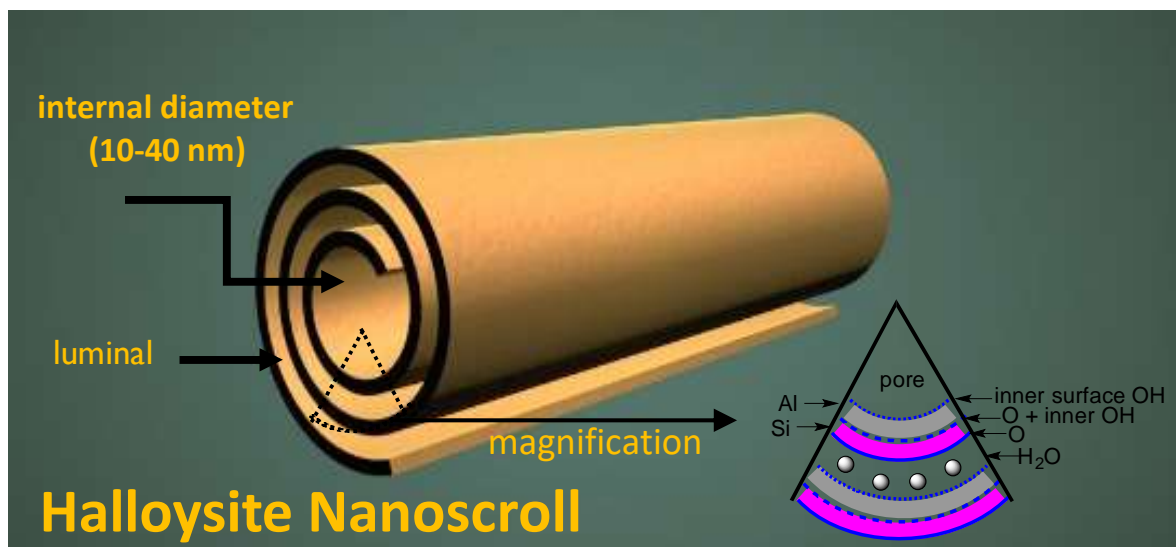
New synthetic methods for the formation of Pd_{NP} and Pd_{NP} nanocomposites with well-controlled size and shape are essential because of the crucial role it plays in many technologies and its usage in many industrial applications. Several Pd-halloysite heterogeneous systems have been reported in the recent literature,[138-142] based upon both Pd/ligand-halloysite and Pd_{NP}-Hal systems have been reported. In both systems, the palladium species were supported on the halloysite's scrolled framework. Although these systems afforded good yields of cross-coupled products, the catalysts suffered from similar issues typically associated with other heterogeneous systems (lower reactivity requiring raised reaction temperatures, leaching, and catalyst deactivation over multiple uses). Recent reports have described the preparation of an encapsulated gold, silver, and ruthenium nanoparticle-halloysite nanocomposites.[143, 144] Based on these studies, it became interesting to explore whether encapsulated Pd_{NP} in halloysite could offer greater stability and improved nanoparticle reactivity. To our knowledge, Pd_{NP} had not successfully been exclusively encapsulated in halloysite; thus, our initial focus was to develop a method for the synthesis of an encapsulated-Pd_{NP}-Hal nanocomposite material (Pd@Hal) then investigate this material as a catalyst for

cross-coupling reactions. Herein we describe a convenient and reliable synthesis of Pd@Hal and its remarkable catalytic activity for the Suzuki-Miyaura reaction.

3.3   Results and Discussion

Our approach initially produced monodispersed Pd_{NP} of appropriate size by reducing palladium (II) to achieve encapsulation with halloysite nanoscrolls.[75, 145-150] As summarized in **Table 1**, treatment of palladium acetate with sodium ascorbate afforded Pd_{NP} of appropriate size for encapsulation in halloysite.

Figure 7. Synthesis of Pd@Hal nanocomposite
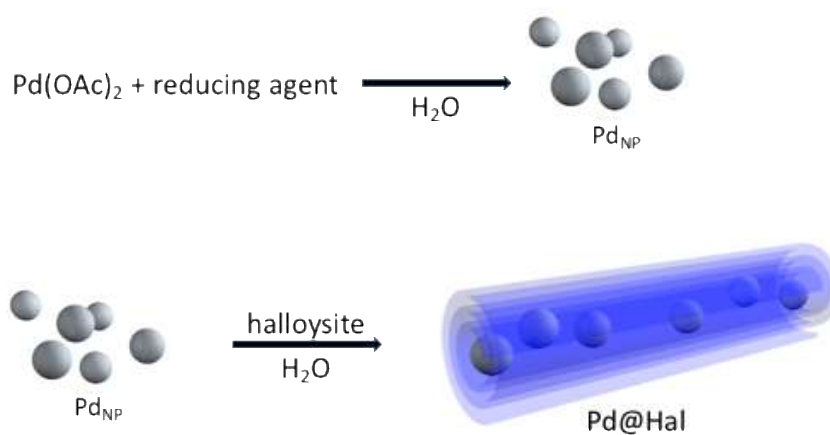
Table 1. Two-Step optimized encapsulation of Pd_{NP} in Halloysite.

Entry[a]	Pd(OAc)$_2$ (mmol)	Pd/Hal[b]	Reducing agent (mmol)	Capping agent (mmol)	Description (E, A)[c]
1	0.060	1:16	sodium ascorbate (10)	ascorbic acid (0.60)	E, A
2	0.060	1:16	sodium ascorbate (7.0)	ascorbic acid (0.60)	E, A
3	0.13	1:8	sodium ascorbate (7.0)	ascorbic acid (0.60)	E, A
4	0.13	1:8	sodium ascorbate (7.0)	ascorbic acid (1.4)	E, A
5	0.26	1:8	sodium ascorbate (7.0)	ascorbic acid (2.7)	E only
6	0.26	1:8	ascorbic acid (7.0)	ascorbic acid (2.7)	A only
7	0.26	1.8	ascorbic acid (4.0)	citric acid (2.7)	A only
8	0.60	1:1	sodium ascorbate (100)	trisodium citrate (6.0)	E only
9	0.60	1:1	sodium ascorbate (7.0)	trisodium citrate (1.2)	E only
10	0.60	1:1	sodium ascorbate (10)	trisodium citrate (0.60)	E only

[a]Results are based on 3 trials for each set of reaction conditions.
[b]Molar ratio of Pd(OAc)$_2$/halloysite.
[c]Encapulation inside the scroll (E). Agglomeration of nanoparticles outside of the scroll (A).

Table 1, entry 1
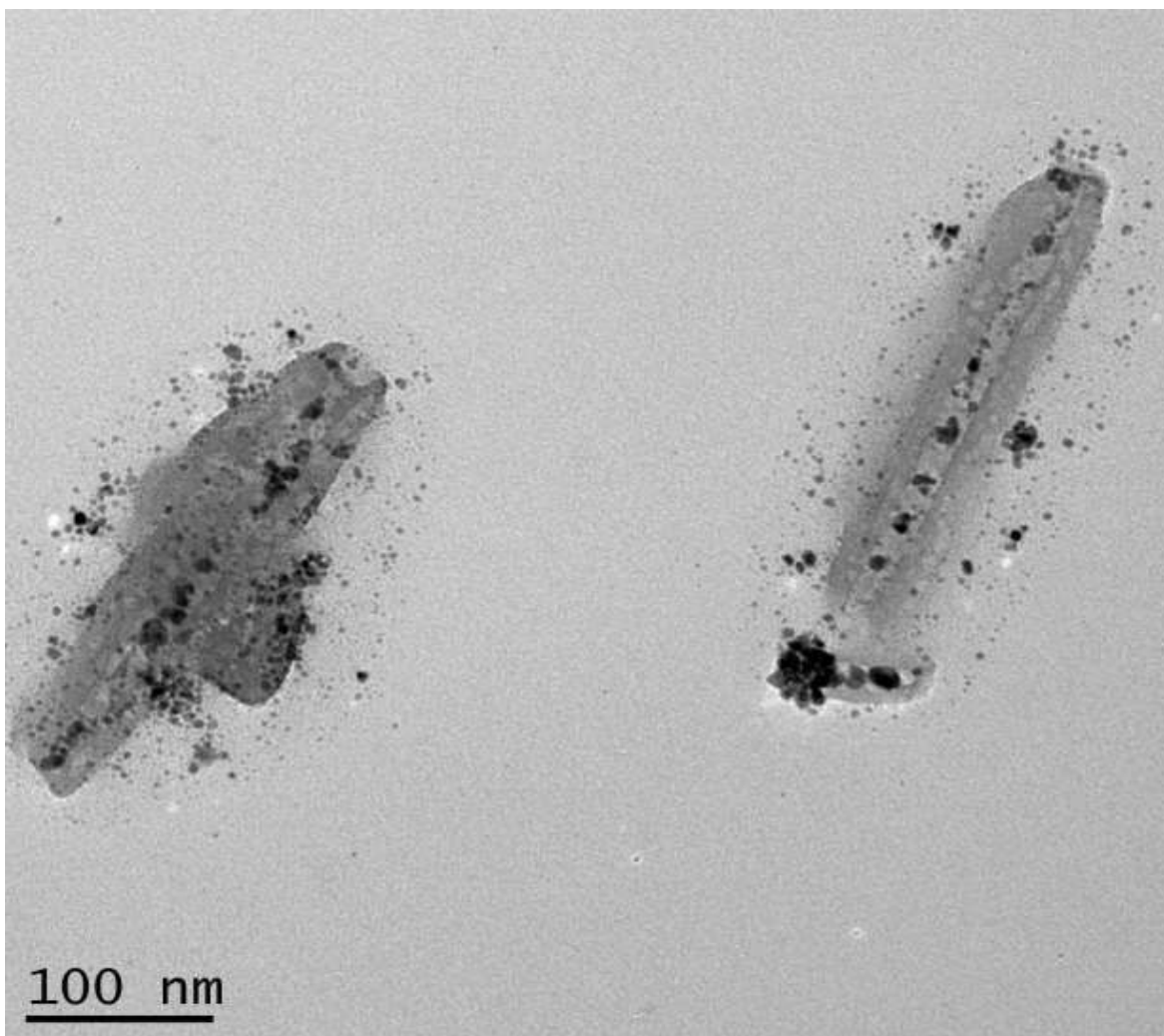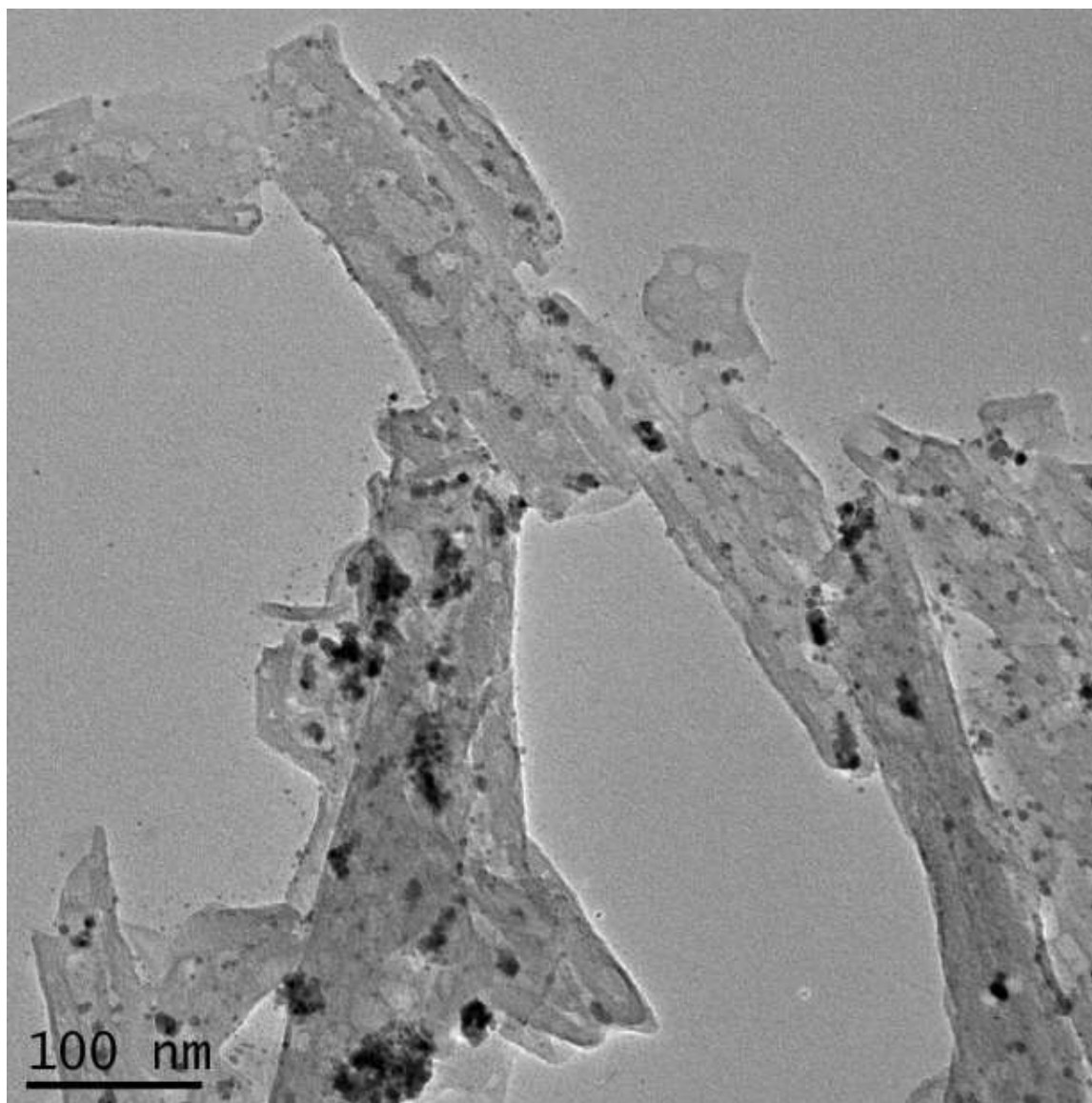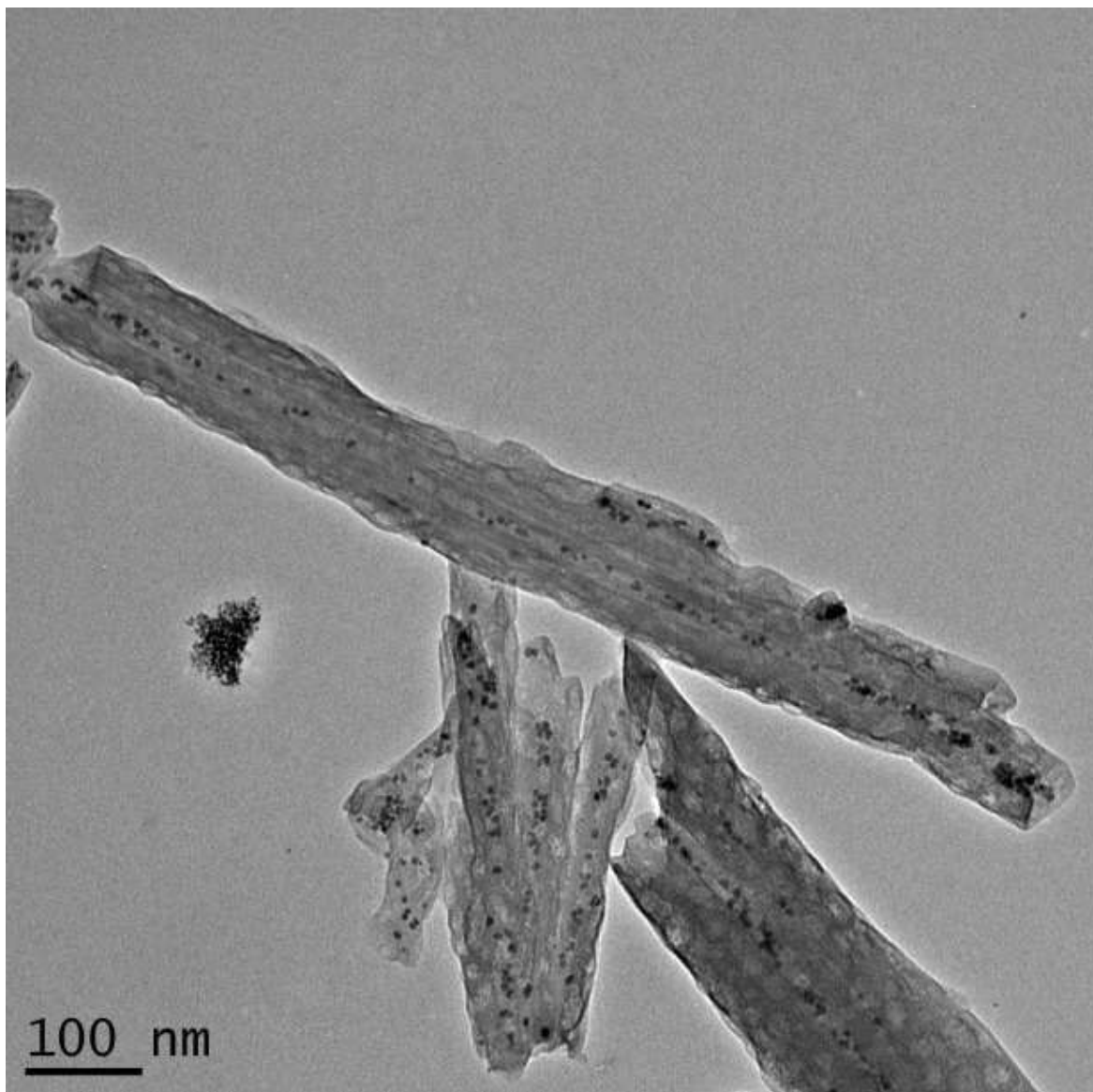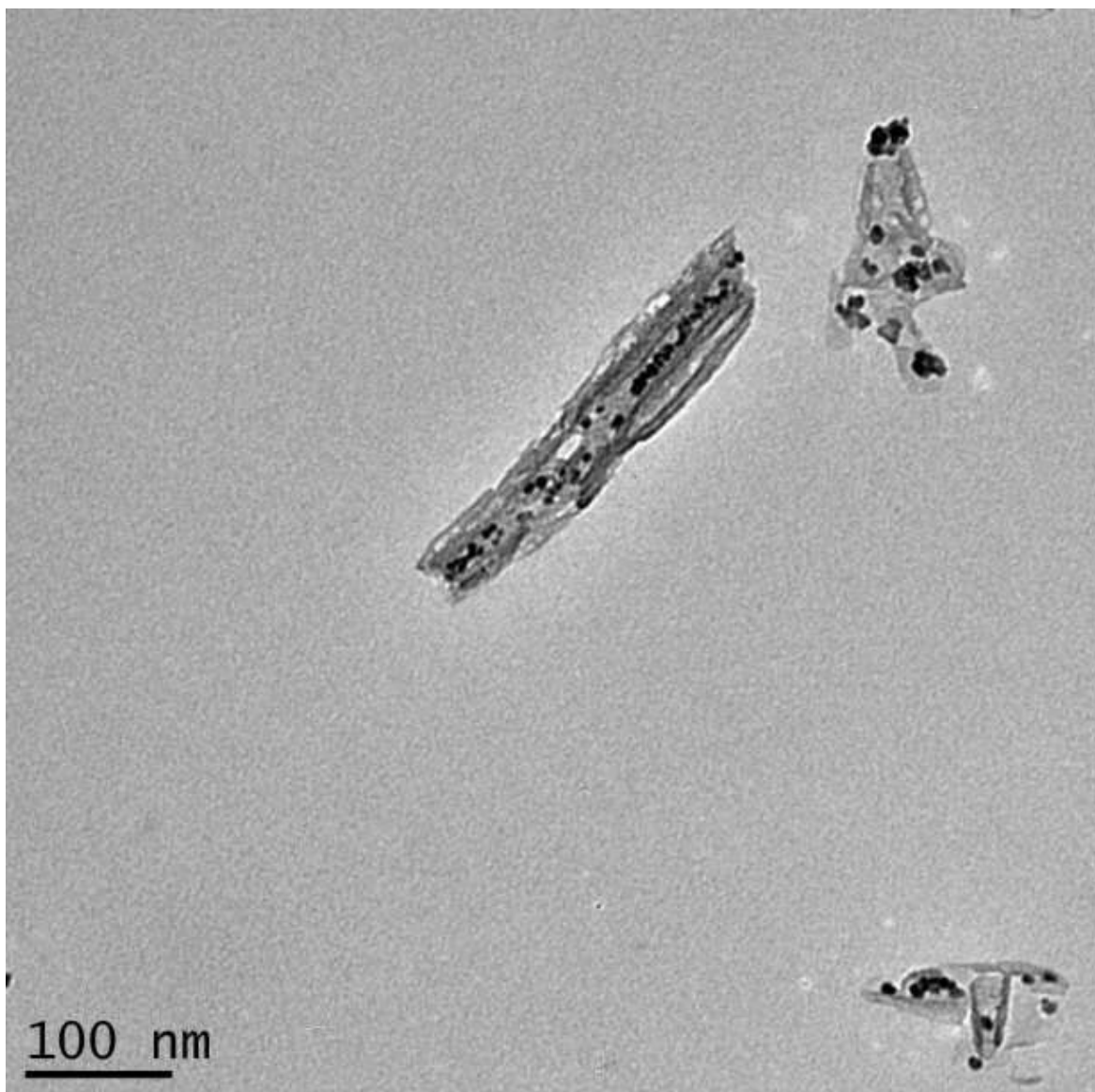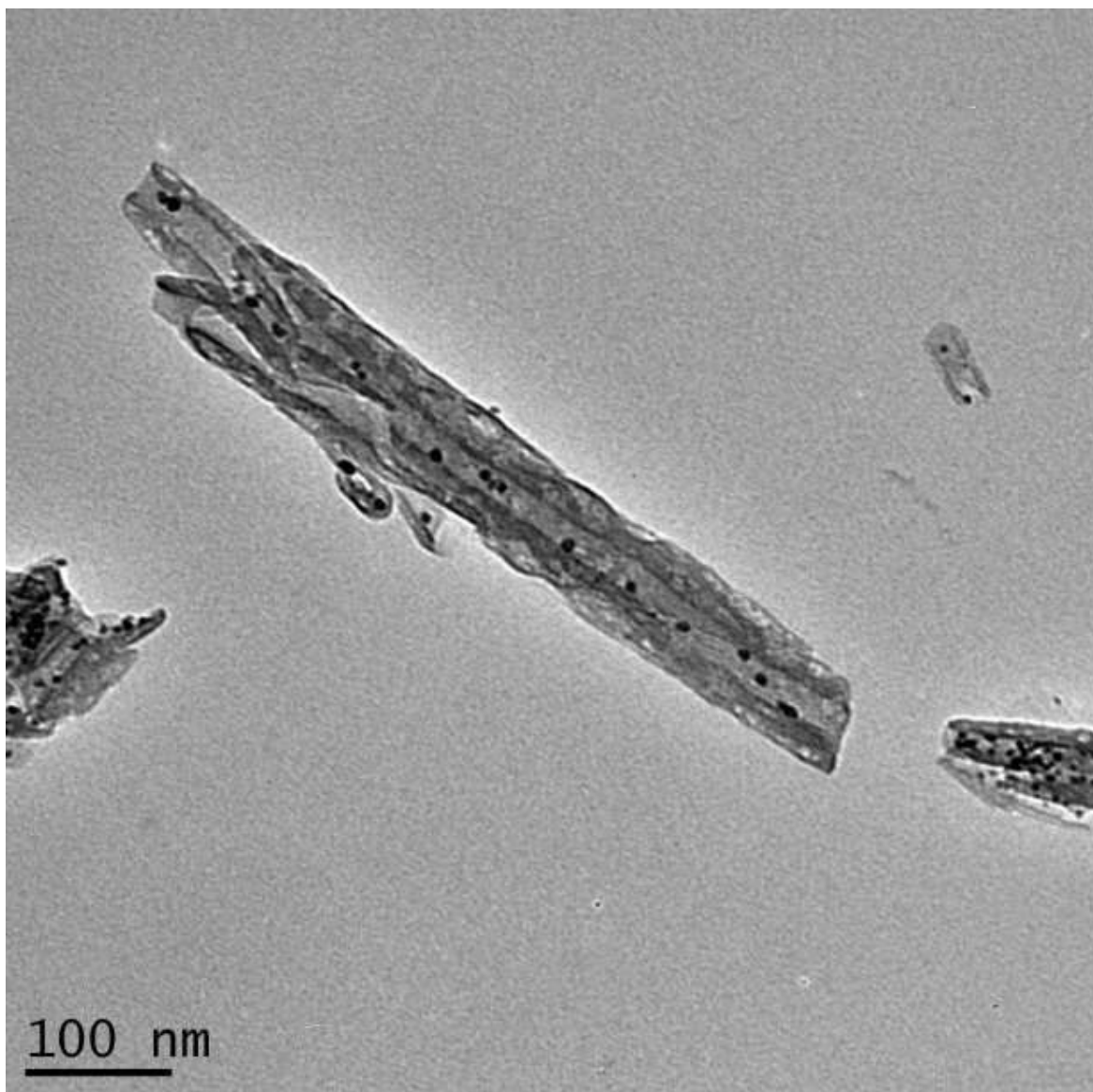
100 nm

Table 1, entry 2

100 nm

Table 1, entry 3

100 nm

Table 1, entry 4

100 nm

Table 1, entry 5

100 nm

Table 1, entry 6

100 nm

Table 1, entry 7

100 nm

Table 1, entry 8

100 nm

Table 1, entry 9

100 nm

Table 1, entry 10

100 nm
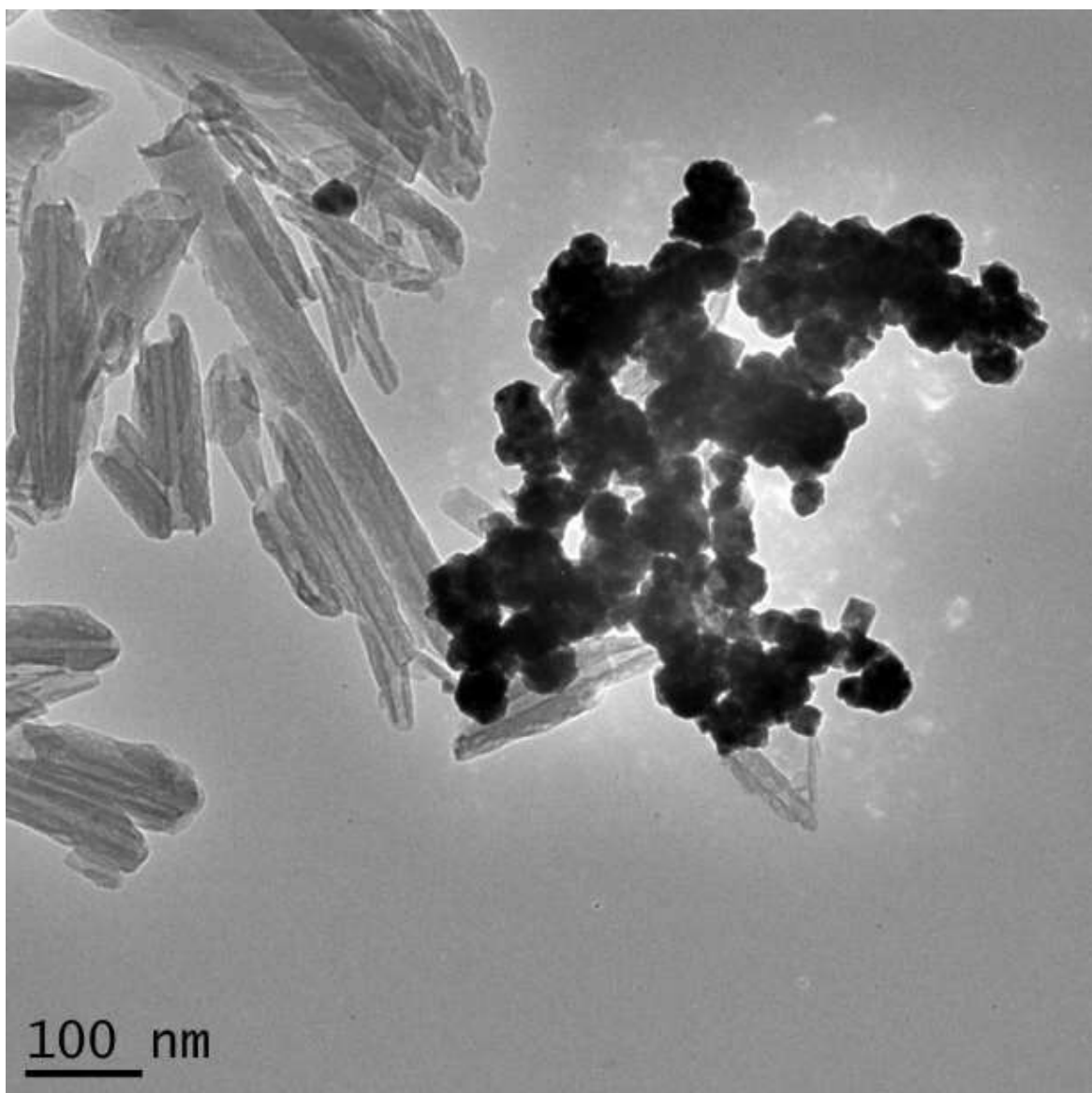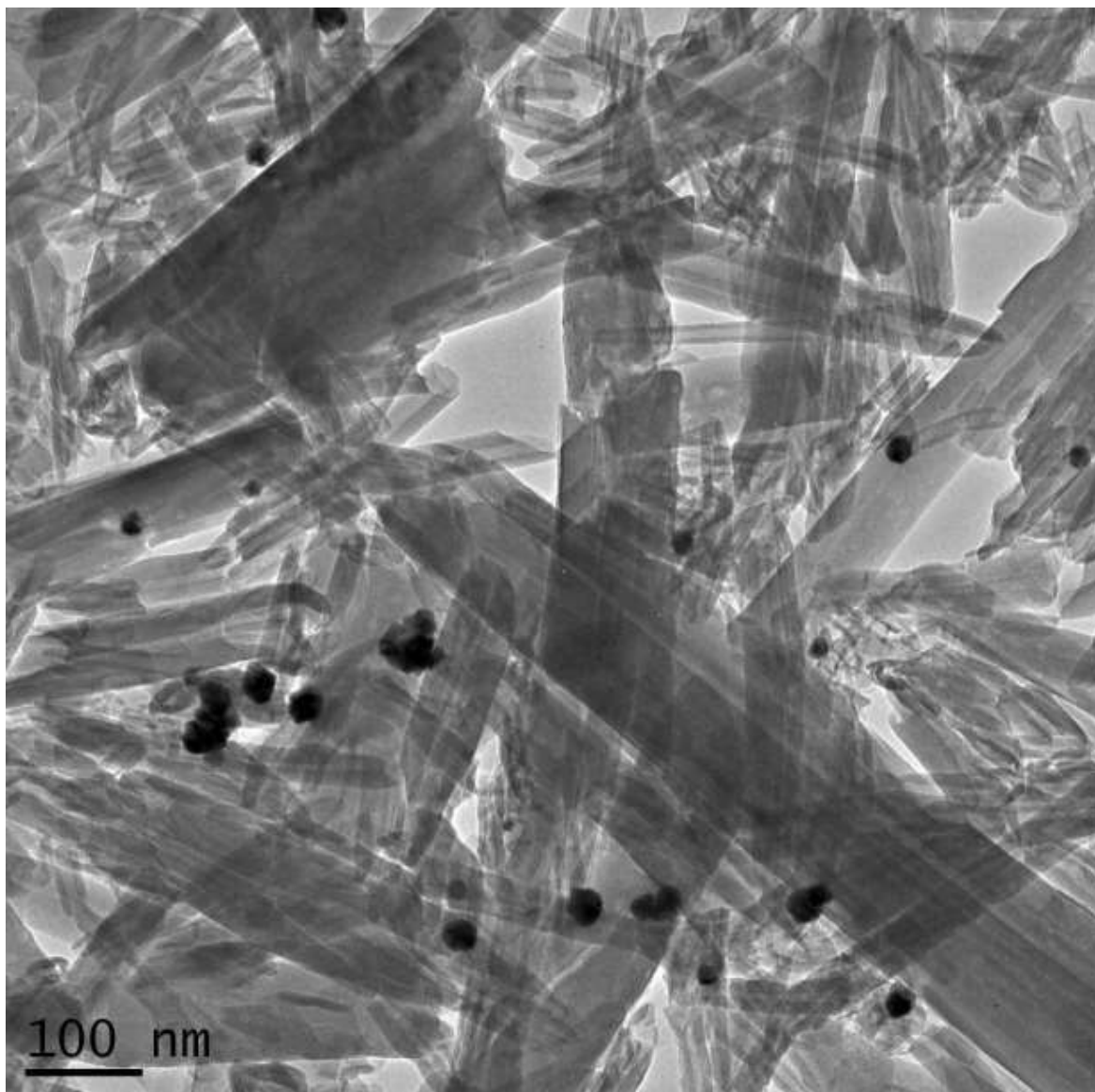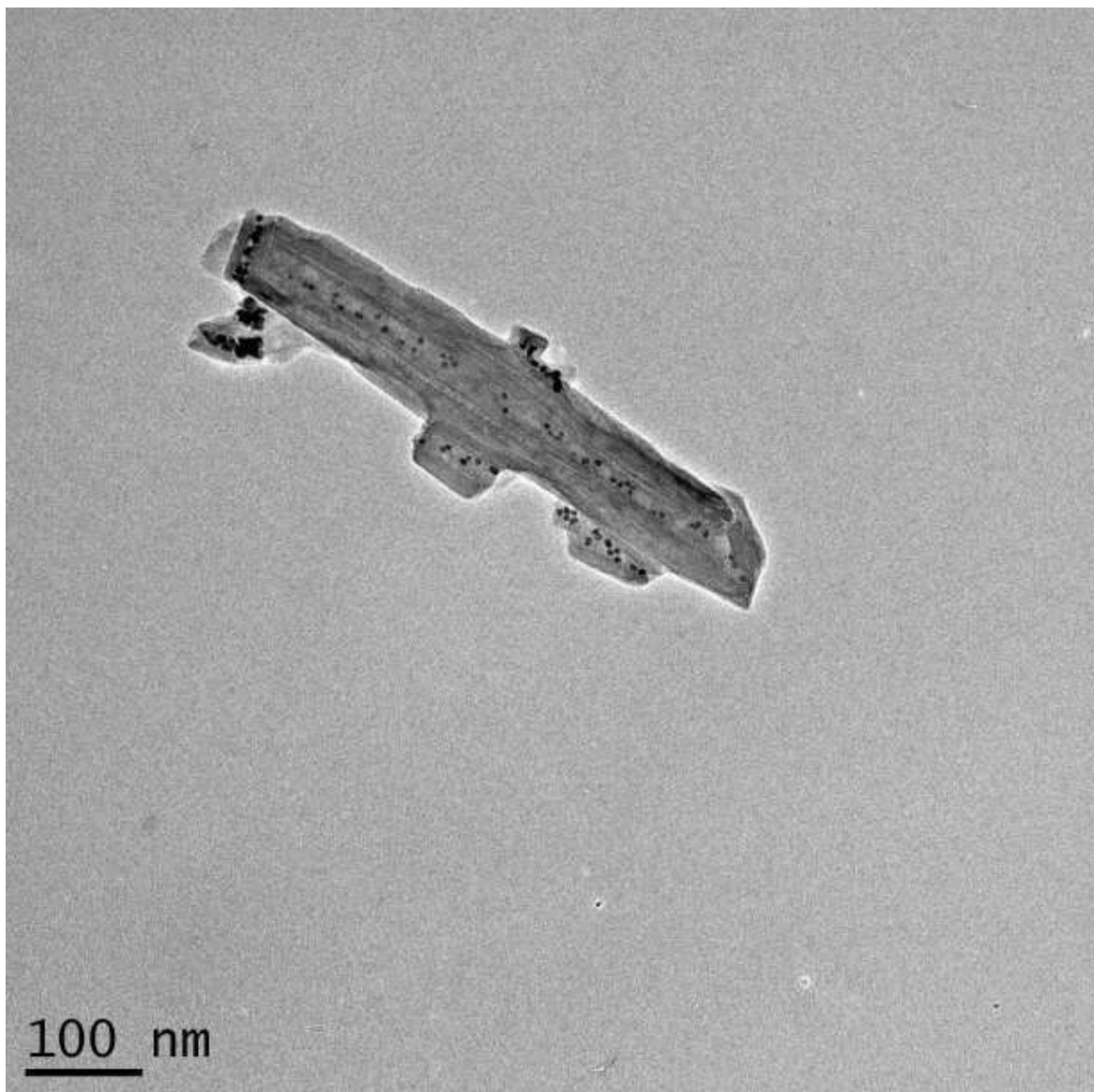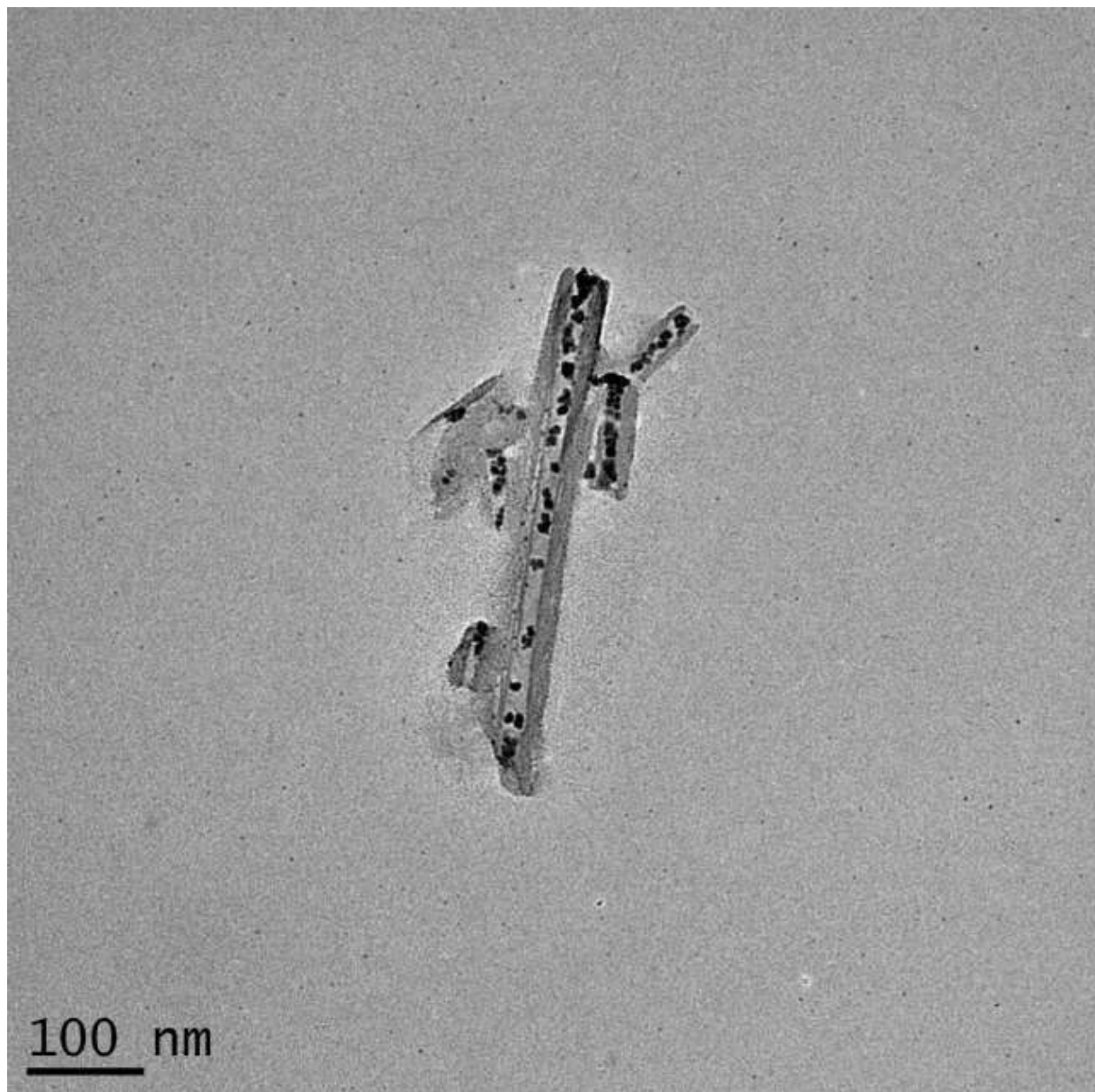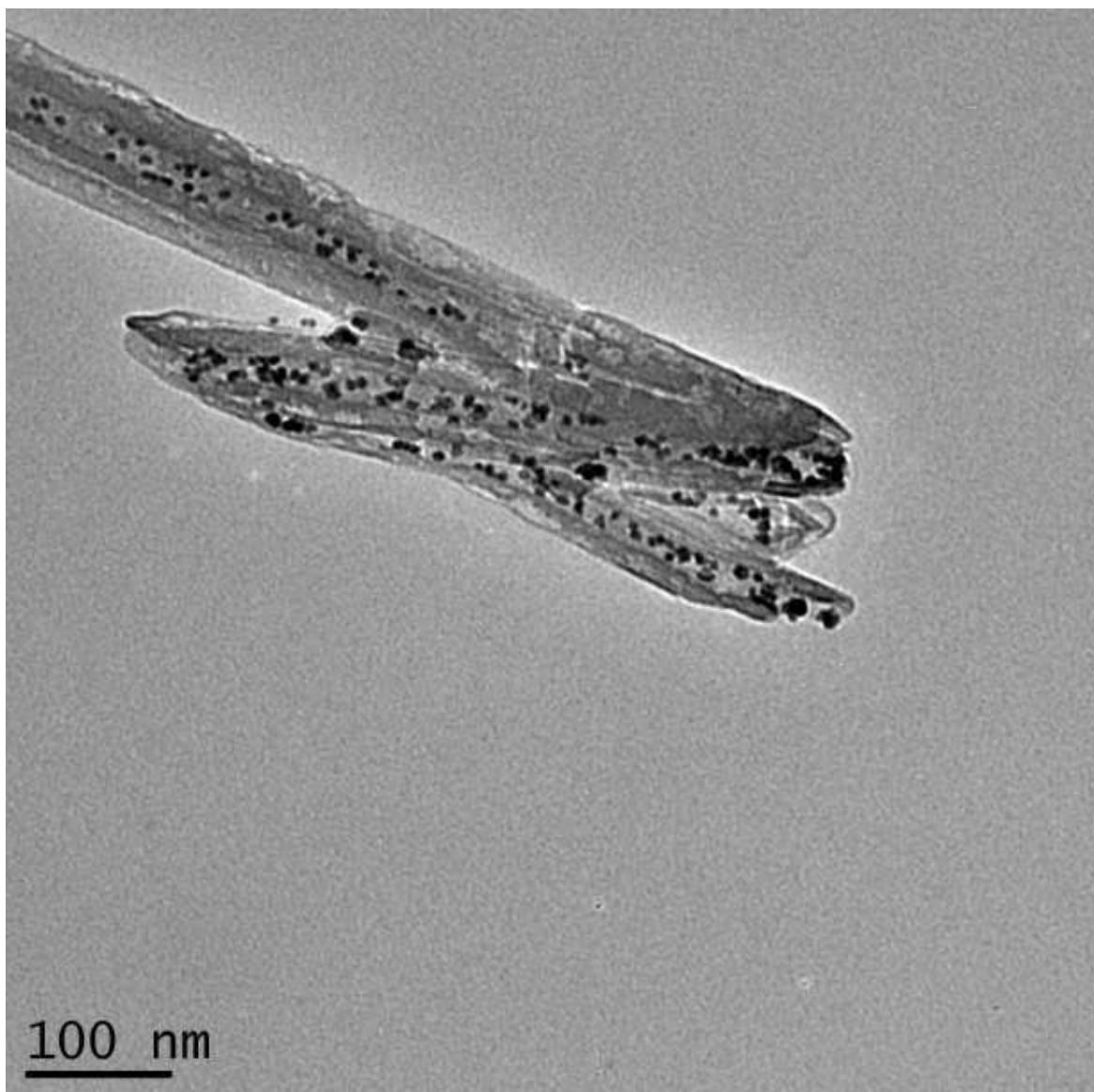
An aqueous suspension of the synthetic Pd_{NP}, when combined with halloysite, furnished the desired encapsulated Pd@Hal nanocomposite. The degree to which the Pd_{NP} were encapsulated versus agglomerated outside of the nanoscroll was determined from TEM images. Initial attempts to form a Pd@Hal nanocomposite material focused on a 1:16 molar ratio of Pd/Hal (entry 1, 10% wt/wt) with sodium ascorbate employed as the reducing agent for nanoparticle formation and citric acid was used as the capping agent to reduce nanoparticle agglomeration and control the size of the particles. This initial attempt resulted in good encapsulation of the Pd_{NP} in halloysite; however, there was a significant aggregation of the Pd_{NP} outside of the scrolls, resulting in incomplete encapsulation of Pd_{NP}. Decreasing the amount of the reducing agent did not improve encapsulation (**Table 1**, entry 2), and the use of ascorbic acid proved to be deleterious to Pd_{NP} encapsulation due to the formation of large nanoparticles that were incapable of entering the scroll (**Table 1**, entries 6 and 7). The use of a 1:8 molar ratio of Pd/Hal gave similar results (**Table 1**, entry 3) to the 1:16 ratio. It was not until the amount of capping agent was increased that improved encapsulation was observed. An optimum encapsulation was achieved with a 4.5-fold increase in the relative amount of citric acid (**Table 1**, entry 5). TEM images **Figure 8a** of the sample show that the bulk of Pd_{NP} were encapsulated, with no agglomeration on the halloysite surface or agglomerates outside of the scrolls. Encapsulated Pd_{NP} size averaged between 6-8 nm. This approach (**Table 1**, entry 5) resulted in 98% Pd loading (based on $Pd(OAc)_2$) to furnish a Pd@Hal nanocomposite that was 4% Pd content (%wt) as determined by ICP-AES analysis.

Figure 8. TEM Images of Pd@Hal nanocomposite. **(a)** Table 1, entry 5. **(b)** Table 1, entry 10.
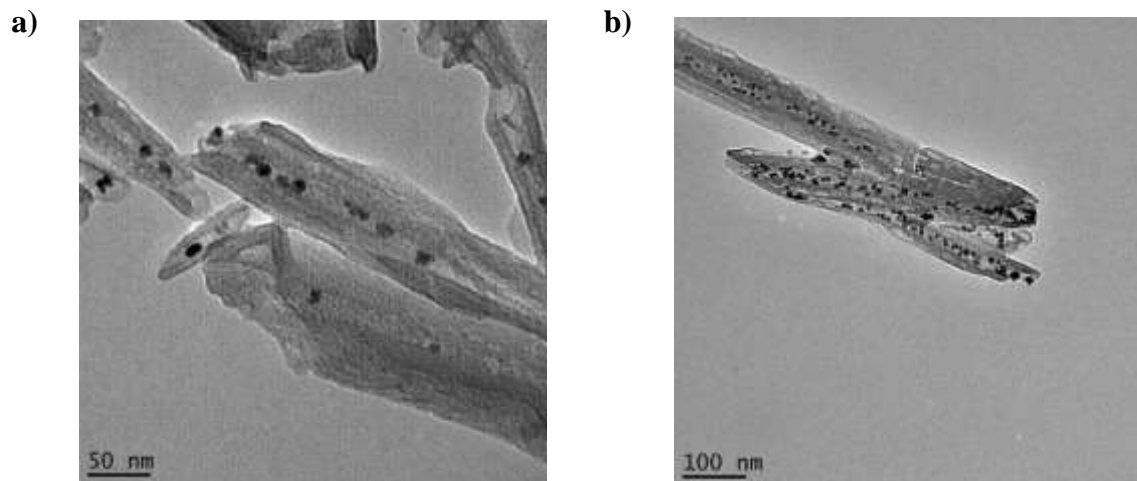
Having identified conditions for the successful encapsulation of Pd_{NP}, attention turned toward increasing the loading of encapsulated Pd_{NP}. In these studies, trisodium citrate was employed as the capping agent since it had been reported to control the aggregation of Pd_{NP} better than citric acid.[75, 150] Given the larger amount of palladium in the reaction, it was assumed that trisodium citrate would facilitate encapsulation over aggregation. Using a molar ratio of 1:1 Pd/Hal and trisodium citrate, higher encapsulation levels of the Pd_{NP} could be achieved. In addition, a large excess of sodium ascorbate was employed to promote the formation of small Pd_{NP} and facilitate the encapsulation into the halloysite (**Table 1**, entry 8); under these conditions, excellent encapsulation was observed; however, the Pd_{NP} were extremely small (1-2 nm). Decreasing sodium ascorbate gave larger nanoparticles (6-8 nm) and excellent encapsulation (**Table 1**, entries 9 and 10). Optimized conditions were established using a 1:1 molar ratio of Pd/Hal, with a 16-fold excess of sodium ascorbate and an equal molar amount of trisodium citrate (**Table 1**, entry 10). These conditions furnished a Pd@Hal nanocomposite with 98% encapsulation with no observable external scroll decoration **Figure 8b**. The palladium content of this

154

Pd@Hal nanocomposite was found to be 25% (wt) based upon ICP-AES analysis. Having produced quality Pd@Hal nanocomposites, attention turned toward the application of this new material in cross-coupling reactions. Initial optimization of Suzuki-Miyaura reaction conditions employed the 4% Pd@Hal nanocomposite material prepared previously (**Table 1**, entry 5). A catalyst loading of 10% (wt/wt) Pd@Hal nanocomposite was employed relative to the limiting reagent (aryl bromide). This corresponds to a metal loading of 5.6g Pd/mmol. The base was used in excess (2 equivalents) relative to the boronic acid. As summarized in **Table 2**, a survey of conditions was performed with 4-bromotoluene (**1**) and 4-methoxyphenylboronic acid (**2**) to identify optimized reaction conditions for cross-coupling to yield 4-methoxy-4'-methyl biphenyl (**3**). Traditional solvents used in Suzuki-Miyaura reactions (1,4-dioxane and toluene) gave low yields or complex mixtures of coupling products and homo-coupling by-products (Table 2, entries 1-7). [4, 47, 151] Homo-coupling by-products were observed when the reaction was performed in air (**Table 2**, entries 1-3) to prevent the homo-coupled formation by-products; the reactants and reaction mixtures were maintained under a nitrogen atmosphere until the reaction reached completion. [152] It was interesting that although the water was a poor solvent for the reaction (**Table 2**, entry 8), the addition of water to 1,4-dioxane or toluene (Table 2, entries 9 and 10) promoted the coupling reaction at room temperature. This prompted the use of the more polar solvent, *n*-propanol, as a co-solvent with water. Much to our surprise, an *n*-propanol/water (4:1) solvent mixture furnished the desired coupling products at room temperature in 93% yield within one hour (**Table 2**, entry 11). The coupling reaction proved highly efficient, requiring only a slight excess of boronic acid (**Table 2**, entry 12) with no homo-coupled by-product observed. A slight increase in the amount of water, *n*-propanol/water ratio to 5:2, gave optimum conditions for the coupling reaction and afforded the coupled product **3** in nearly quantitative yield (99%, **Table 2**, entry 13). Under these conditions' catalyst loading was evaluated. It was determined that 5% wt/wt loading of the 4%Pd@Hal was equally

effective, affording **3** in 98% yield within 1 h (**Table 2**, entry 14). This corresponds to a metal loading

of 2.8g Pd/mmol. Further reduction of the catalyst loading to 2% wt/wt required a longer reaction time

to achieve the same success but gave 3 in 95% yield after 8 h at room temperature (**Table 2**, entries 15-

16). Initially, Cs_2CO_3 (2 Equiv.) was used in these studies as the base. However, it was later found that

K_2CO_3 could successfully substitute for Cs_2CO_3. Using two equivalents of K_2CO_3 required a longer

reaction time; however, three equivalents of K_2CO_3 gave a comparable yield to the Cs_2CO_3 system

(**Table 2**, entries 17-19). In addition, to the mild and efficient nature of this reaction, it was extremely

satisfying to realize that the catalytic reaction was scalable without loss of yield at the ambient

conditions. Using 10% wt/wt 4% Pd@Hal, a 97% yield of **3** (0.96 g, 5 mmol scale) was obtained after 1

h (**Table 2**, entry 20). Similarly (**Table 2**, entry 22) 5% wt/wt 4% Pd@Hal, a 99% yield of **3** (2.27 g,

11.6 mmol scale) after 8 h.

The high reactivity of Pd@Hal is believed to be due to the synergy of the Pd_{NP} (large reaction

surface area) in halloysite (a confined amphiphilic environment) since control reactions showed that

neither Pd_{NP} nor halloysite alone exhibited catalytic activity in this reaction system. The catalytic effect

of halloysite encapsulated Pd_{NP} is believed to be similar to the micellar effects observed for various

metal-catalyzed reactions in aqueous-based systems.[153]

Table 2. Optimization of Suzuki-Miyaura reaction.
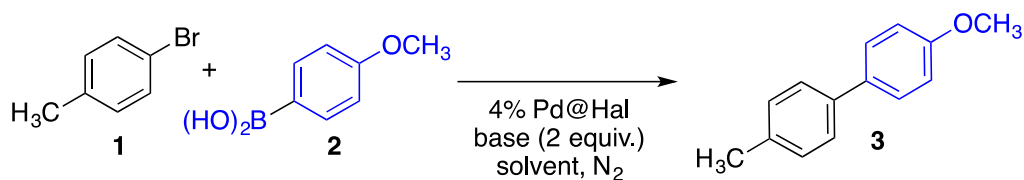
Entry	2:1 (mmol)	4% Pd@Hal loading[a]	solvent / (base, 2 equiv.)	T (°C), time, (h)	yield (%)[b]
1	1.5:1.0	10	1,4-dioxane (Cs$_2$CO$_3$)	80, 6	22[c,d]
2	1.5:1.0	10	1,4-dioxane (Cs$_2$CO$_3$)	80, 24	76[c,d]
3	1.5:1.0	10	1,4-dioxane (Cs$_2$CO$_3$)	reflux, 6	CM[c,e]
4	1.5:1.0	10	1,4-dioxane (Cs$_2$CO$_3$)	reflux, 24	CM[e]
5	1.5:1.0	10	toluene (Cs$_2$CO$_3$)	80, 24	NR[f]
6	1.5:1.0	10	toluene (Cs$_2$CO$_3$)	reflux, 24	CM[e]
7	1.5:1.0	10	toluene (Cs$_2$CO$_3$)	reflux, 8	65[d]
8	1.5:1.0	10	H$_2$O (Cs$_2$CO$_3$)	reflux, 8	NR[f]
9	1.5:1.0	10	toluene: H$_2$O [4:1]	rt, 24	CM[e]
10	1.5:1.0	10	1,4-dioxane: H$_2$O [4:1] (Cs$_2$CO$_3$)	rt, 24	CM[e]
11	1.5:1.0	10	n-PrOH: H2O [4:1] (Cs$_2$CO$_3$)	rt, 1	93
12	1.2:1.0	10	n-PrOH/H$_2$O [4:1] (Cs$_2$CO$_3$)	rt, 1	94
13	1.2:1.0	10	n-PrOH/H$_2$O [5:2] (Cs$_2$CO$_3$)	rt, 1	99
14	1.2:1.0	5	n-PrOH: H$_2$O [5:2] (Cs$_2$CO$_3$)	rt, 1	98
15	1.2:1.0	2	n-PrOH: H$_2$O [5:2] (Cs$_2$CO$_3$)	rt, 1	75
16	1.2:1.0	2	n-PrOH:H$_2$O [5:2] (Cs$_2$CO$_3$)	rt, 8	95
17	1.2:1.0	10	n-PrOH:H$_2$O [5:2] (K$_2$CO$_3$)	rt, 1	87
18	1.2:1.0	10	n-PrOH:H$_2$O [5:2] (K$_2$CO$_3$)	rt, 8	96
19	1.2:1.0	10	n-PrOH:H$_2$O [5:2] (K$_2$CO$_3$, 3 equiv.)	rt, 1	99
20[g]	5.7:5.0	10	n-PrOH:H$_2$O [5:2] (Cs$_2$CO$_3$)	rt, 1	97
21[h]	11.8:11.6	5	n-PrOH:H$_2$O [5:2] (Cs$_2$CO$_3$)	rt, 1	70
22[h]	11.8:11.6	5	n-PrOH:H$_2$O [5:2] (Cs$_2$CO$_3$)	rt, 8	98

[a]10% (wt/wt) of 4%Pd@Hal relative to bromotoluene (1) corresponds to 5.6g Pd/mmol 1). 5% (wt/wt) of 4%Pd@Hal relative to 1 corresponds to 2.8g Pd/mmol 1). 2% (wt/wt) of 4%Pd@Hal relative to 1 corresponds to 1.1g Pd/mmol 1). [b]Isolated yields based on at least three trials. [c]Sealed vial under air. [d]Isolated yield of coupling product and homo-coupling product also present. [e]CM: Complex mixture of starting material, coupling product, and homo-coupling product [f]NR: no reaction, only starting material. [g]5 mmol scale. [h]12 mmol scale.

The Pd@Hal catalyst was found to be durable and chemically robust. The catalyst could be recovered by simple centrifugation and filtration and reused without loss of activity or structural change to the Pd@Hal nanocomposite based upon TEM analysis.

Recycling Studies

Pd@Hal (cycle 1)
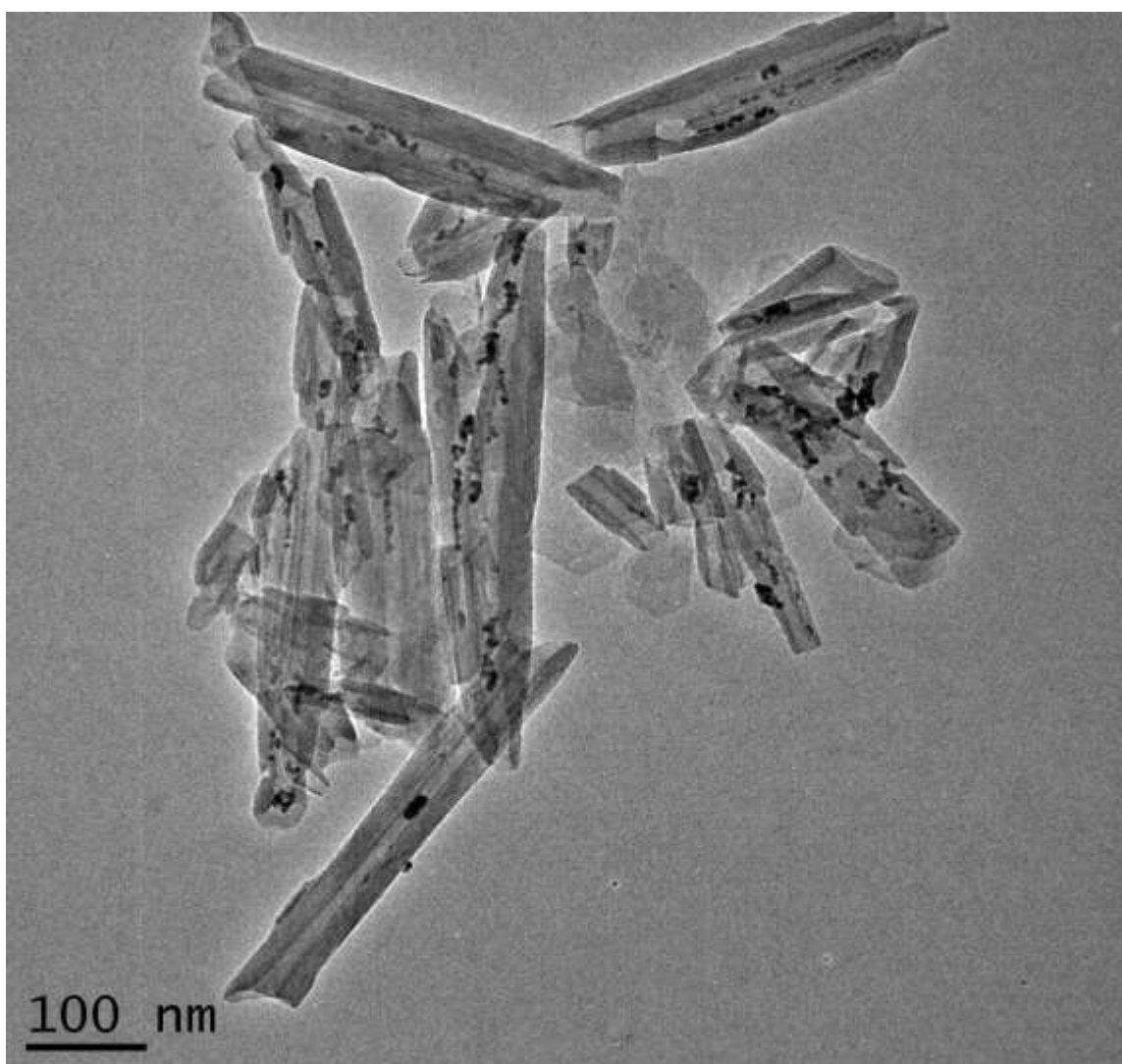
Pd@Hal (after three cycles)

100 nm
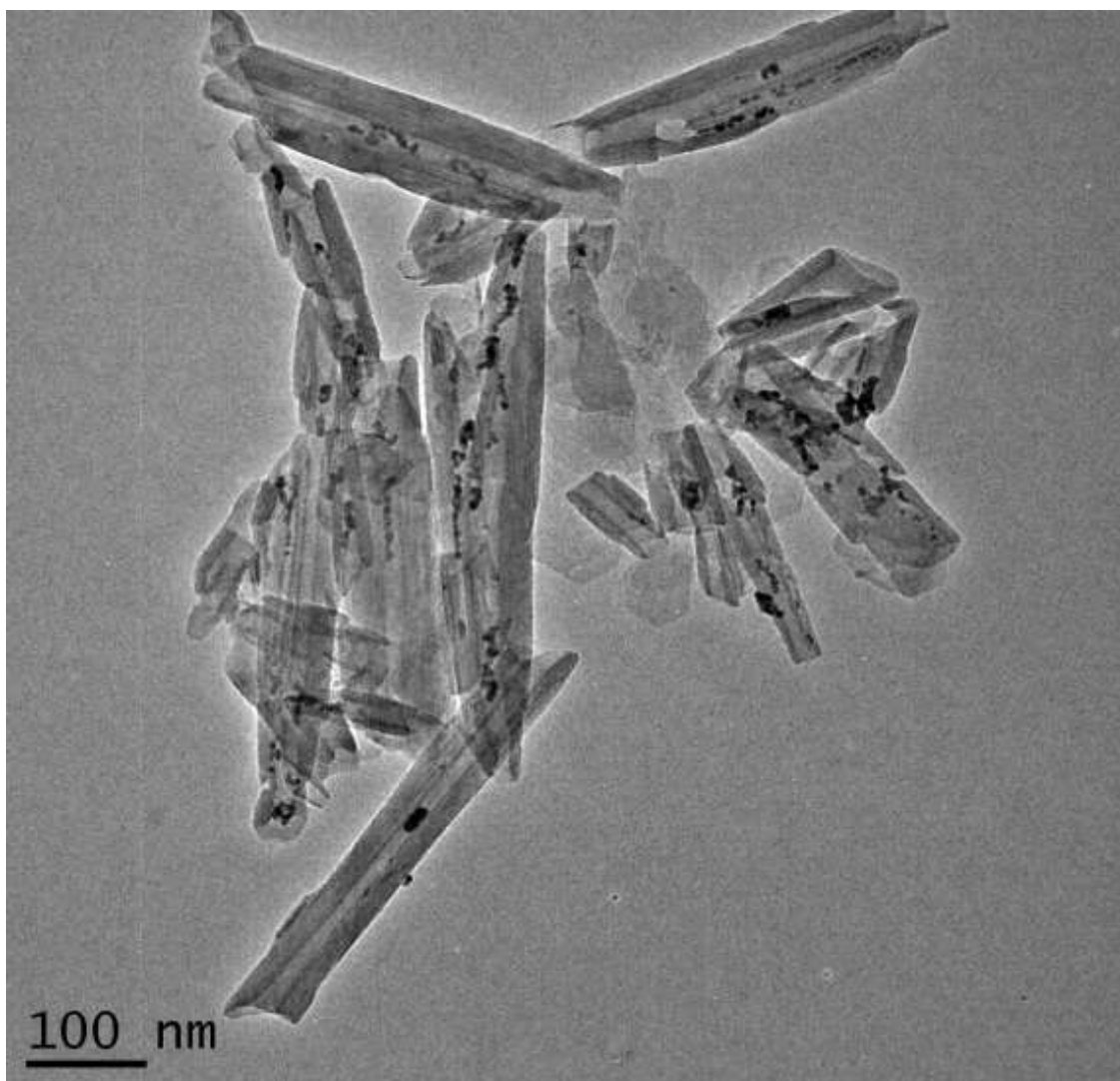
Moreover, the Pd@Hal nanocomposite could be stored for several months and used without loss of activity. As illustrated in **Figure 9**, recycling studies with 4% Pd@Hal (**Table 1**, entry 5) showed that the catalyst could be cycled through nine consecutive coupling reactions with no loss of activity and excellent isolated yields of the coupling product **3** in each trial. It was not until the ninth trial that the yield started to diminish. Further, the palladium content of the Pd@Hal catalyst was determined after five recycled reactions, and the ICP-AES analysis

indicated no significant palladium loss. It was also determined by ICP-AES analysis that some

residual Pd (6.4 ppm) was present in **3** after the first cycle of the study. It is unclear if this low-

level Pd residue is due to ionic Pd(II) or soluble Pd(0) species released during the reaction or the

recovery/work-up procedure.

Figure 9. Pd@Hal recycling studies.
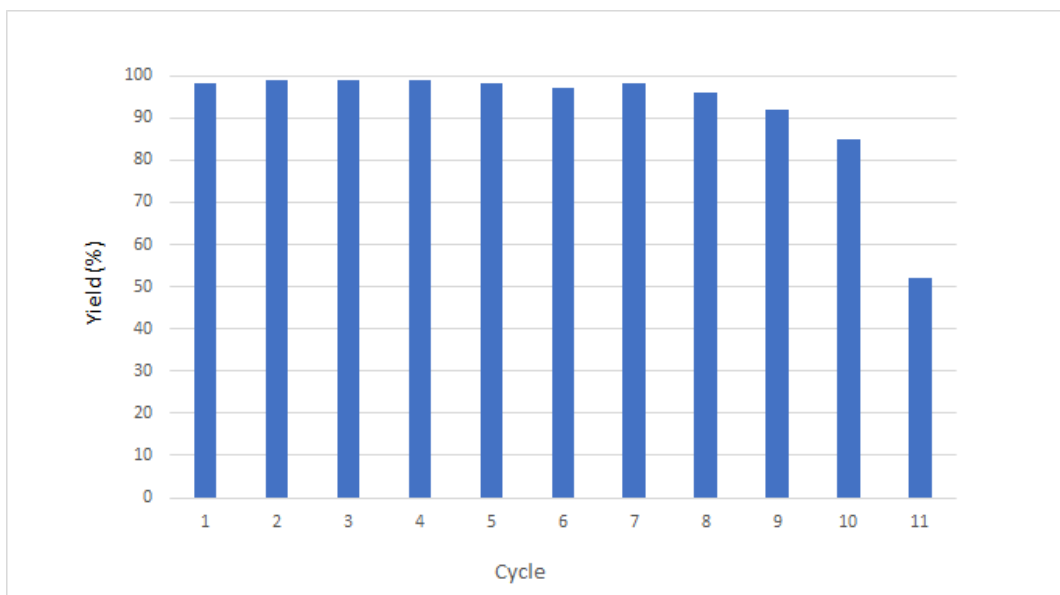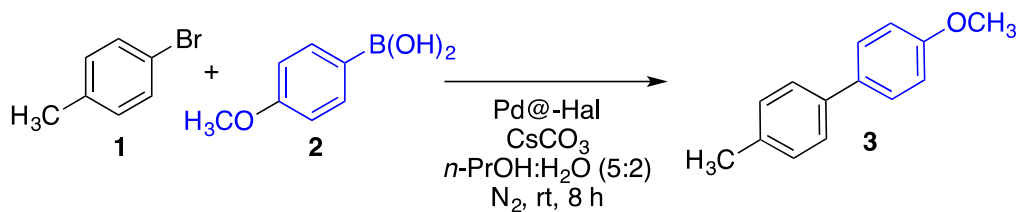
To further demonstrate this catalyst system's utility for the Suzuki-Miyaura cross-

coupling reaction, a series of aryl halides (4) and boronic acids (5) were investigated substrates

for cross-coupling. As summarized in **Scheme 11,** the Pd@Hal catalyst demonstrated high

reactivity in the presence of a variety of functional groups to afford cross-coupling products (**6**) in excellent yields under very mild conditions. In all examples, product formation began immediately, and within one h, the limiting reagent **4** was consumed entirely. The reaction conditions equally tolerated both hydrophobic and hydrophilic substrates. It is noteworthy that the hydrophilic cross-coupling products, 4-hydroxy-4'-methoxybiphenyl (**6m**, 97%) 4-amino-4'-methoxybiphenyl (**6n**, 92%), were obtained in high yield from the corresponding aryl bromides.

Scheme 11. Pd@Hal catalyzed Suzuki-Miyaura cross-coupling reactions.

6a, 98%   **6b**, 92%   **6c**, 97%

6d, 98%   **6e**, 96%   **6f**, 98%

6g, 96%   **6h**, 91%   **6i**, 94%

6j, 92%   **6k**, 97%   **6l**, 96%

6m, 97%   **6n**, 92%
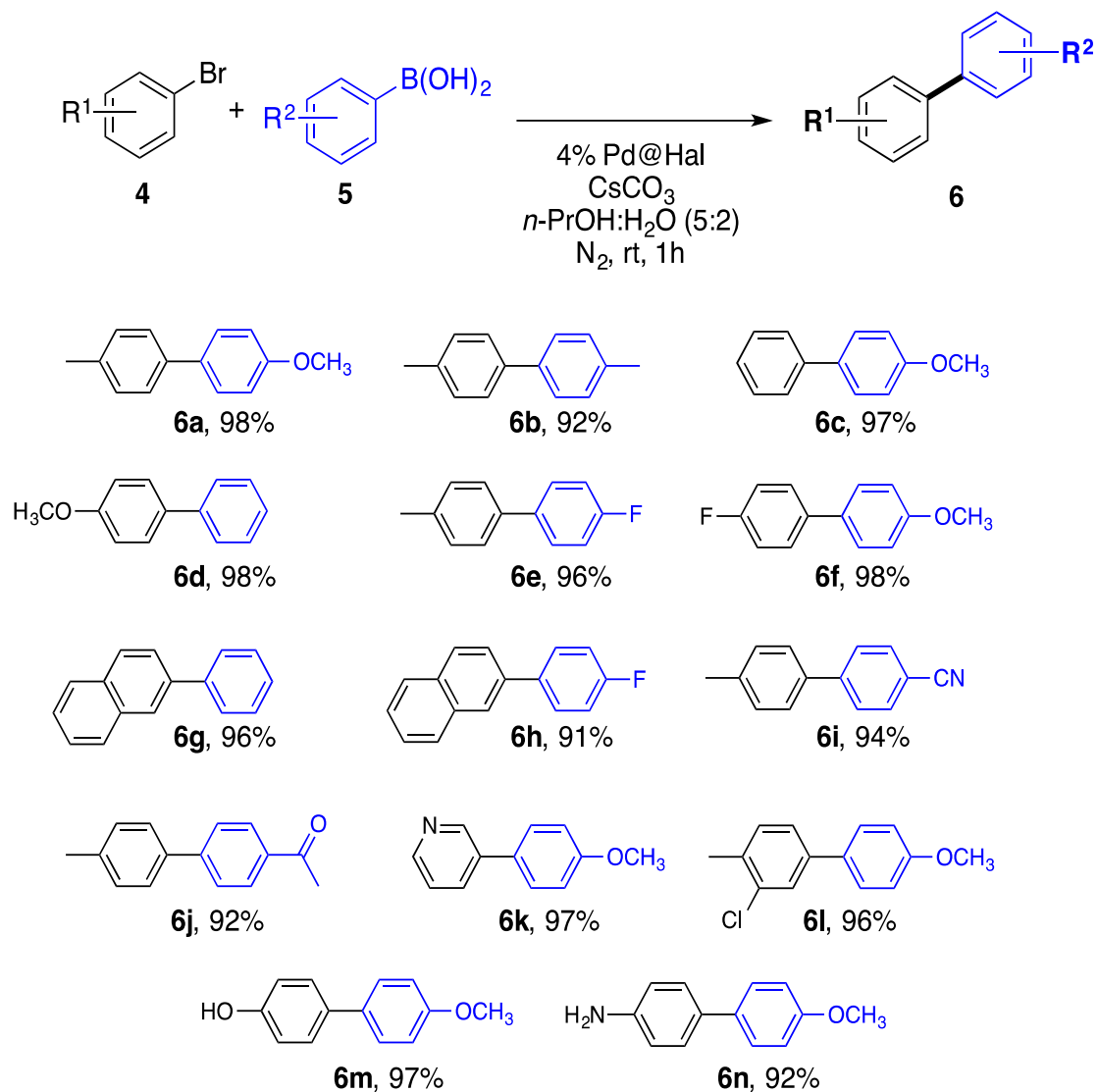
[a]Isolated yields based on a minimum of three trials

3.4   Conclusion

In summary, a new, extremely useful Pd@Hal nanocomposite catalyst for Suzuki-Miyaura cross-coupling reactions has been developed. This material produces high yields of a diverse array of coupling products within one hour at room temperature in n-PrOH: H_2O (5:2). The Pd@Hal catalytic system was remarkably effective with both hydrophobic and hydrophilic substrates. The Pd@Hal nanocomposite material is a cost-effective, highly efficient, and easily recyclable material. This newly developed nanocomposite presents a significant advance in heterogeneous catalysis, exploiting the nanoporous structure of halloysite.

3.5   Experimental

3.5.1   Materials and Methods

All reactions were carried out in oven-dried glassware under a N_2 atmosphere unless indicated otherwise. Halloysite clay was purchased from Sigma Aldrich. All other chemicals were purchased from Alfa Aesar, Sigma Aldrich, and VWR. Halloysite was purchased from Sigma Aldrich. All chemicals were used as received without further purification. ^{1}H and ^{13}C NMR spectra were recorded at r.t. in DMSO-$d6$ on a Bruker 400 MHz instrument operating at a frequency of 300 MHz for ^{1}H NMR and 75 MHz for ^{13}C NMR. [1]H chemical shifts were referenced to the DMSO solvent signal (2.50 ppm). [13]C chemical shifts were referenced to the DMSO solvent signal (39.51 ppm). Pd_{NP} size was determined from TEM images obtained on a JEOL 2010 equipped with an EDAX genesis energy dispersive spectroscopy (EDS) system, operated at an accelerating voltage of 200

kV an emission current of 109 μA. ICP- AES analysis of the Pd@Hal was performed by Galbraith Laboratories, Inc., Knoxville, TN.

3.5.2 Synthesis of 4% Pd@Hal.

A solution of Pd(OAc)$_2$ (60 mg, 0.26 mmol) in deionized water (10 mL) was prepared in a 50 mL Erlenmeyer flask. A solution of L-sodium ascorbate (1400 mg, 7.0 mmol) in deionized water (15 mL) was added to the palladium acetate solution, followed by the addition of a solution of trisodium citrate (570 mg, 2.7 mmol) in deionized water (10 mL). The combined solution was allowed to stir for 15 min at room temperature. During the first 10 min, the palladium acetate solution mixture's initial light orange color turned black, indicating Pd nanoparticle formation. After 15 min, no more color changes were observed, and the solution was left to rest at room temperature, open to air for 80 min. Halloysite (600 mg, 2.0 mmol) was added to the Pd nanoparticle solution, and the colloid mixture was stirred for 15 min. The mixture was then allowed to rest at room temperature for 10 min. The mixture was centrifuged (6000 rpm), and the liquid was decanted away from the solid residue. The residue was washed with deionized water (3 x 15 mL) and isopropyl alcohol (3 x 15 mL). The resultant powder was dried at room temperature for 24 h in a desiccator (CaSO$_4$) to afford 4% Pd@Hal as a gray powder (620 mg).

3.5.3 Synthesis of 25% Pd@Hal.

A solution of Pd(OAc)$_2$ (140 mg, 0.60 mmol) in deionized water (10 mL) was prepared in a 50 mL Erlenmeyer flask. A solution of L-sodium ascorbate (1900 mg, 10 mmol) in deionized water (15 mL) was added to the palladium acetate solution, followed by the addition of a solution of trisodium citrate (180 mg, 0.60 mmol) in deionized water (10 mL). The combined solution was allowed to stir for 15 min at room temperature. During the first 10 min, the palladium acetate solution mixture's initial light orange color turned black, indicating the formation of Pd$_{NP}$. After 15 min, no more color

changes were observed, and the solution was left to rest at room temperature open to air for 80 min. Halloysite (180 mg, 0.60 mmol) was added to the Pd_{NP} solution, and the colloid mixture was stirred for 15 min. The mixture was then allowed to rest at room temperature for 10 min. The mixture was centrifuged (6000 rpm), and the liquid was decanted away from the solid residue. The residue was washed with deionized water (3 x 15 mL) and isopropyl alcohol (2 x 15 mL). The resultant powder was dried at room temperature for 24 h in a desiccator ($CaSO_4$) to afford 25% Pd@Hal as a gray powder (310 mg).

3.5.4   General Procedure: Suzuki-Miyaura Cross-Coupling Reaction

To a 50 mL round bottom flask equipped with a magnetic stir bar and a nitrogen inlet balloon, the aryl halide (1.0, mmol 1.2 Equiv.) and the aryl boronic acid (1.2 mmol 1.2 Equiv.) was added. The reaction mixture was flushed with nitrogen, followed by the addition of *n*-propanol (10.0 mL) via syringe. The reaction mixture was allowed to stir for 5 min allowing the complete dissolution of all solids. Cs_2CO_3 (652 mg, 2.0 mmol) was dissolved in (2.0 mL) of DI water, then added to the reaction mixture via syringe. The 4% Pd@Hal (5% wt/wt) catalyst was dissolved in (2.0 mL) of DI water; the solution was sonicated (10 min) to ensure dispersion, then added to the reaction mixture via syringe. The reaction flask was sonicated for 10 mins then allowed to stir at room temperature. The reaction progress was monitored by TLC. Typically, after 1 h, the catalyst was recovered by vacuum filtration. The Pd@Hal was rinsed with ethyl acetate (20 mL) followed by DI water (20 mL) and dried in a desiccator ($CaSO_4$). The diluted reaction mixture was transferred to a separatory funnel, and the organic phase was removed and filtered through a 2 cm bed of silica gel. The silica gel was rinsed with several portions of hexanes: ethyl acetate (9:1). The organic portions were combined, and the solvent was removed under vacuum to afford **6**. TLC and NMR established purity. All products are known compounds unless otherwise indicated, and spectral data were identical to those

reported in the literature.

3.5.5 Large-Scale Procedure: Suzuki-Miyarua Cross-Coupling Reaction

To a 200 mL round bottom flask equipped with a magnetic stir bar and a nitrogen inlet balloon, the 4-bromtoluene (2.05 g 12.0 mmol, 1.0 equiv.) and the 4-methoxyphenylboronic acid (1.85 g, 12.2 mmol 1.2 Equiv.) was added. The reaction mixture was flushed with nitrogen, followed by the addition of 1-propanol (100 mL) via syringe. The reaction mixture was stirred for 10 min allowing the complete dissolution of all solids. Cs_2CO_3 (4.20g, 13.0 mmol) was dissolved in (20 mL) of DI water, then added to the reaction mixture via syringe. The Pd@Hal catalyst (0.100 g, 5 %wt/wt) was dissolved in (20 mL) of DI water; the solution was sonicated (10 min) to ensure dispersion, then added to the reaction mixture via syringe. The reaction flask was sonicated for 10 mins then allowed to stir at room temperature. The reaction progress was monitored by TLC (9:1, hexanes: ethyl acetate). The reaction was determined to be complete by the consumption of the bromotoluene, and the catalyst was recovered by vacuum filtration. The Pd@Hal was rinsed with ethyl acetate (40 mL) followed by DI water (40 mL) and dried in a desiccator $(CaSO_4)$. The diluted reaction mixture was transferred to a separatory funnel, and the organic phase was removed and filtered through a 2 cm bed of silica gel. The silica gel was rinsed with several portions of (9:1, hexanes: ethyl acetate). The organic portions were combined, and the solvent was removed under vacuum to afford **3**. (2.29g, 98%). Purity was established by TLC, melting point, and NMR. Product **3** is a known compound, and spectral data were identical to those reported in the literature.[1,2]

3.5.6 Recycling Studies

The Large-scale procedure was used for Cycle 1.

Pd@Hal recovery procedure:

The Pd@Hal was removed from the filter paper and added to a beaker with EtOH (20 mL), then sonicated for 10 mins. The solid was then centrifuged down and then washed again with (15 mL) DI water followed by (15 mL) isopropyl alcohol. The solid was dried in a desiccator ($CaSO_4$) overnight or in an oven at 120° for 20 mins before each subsequent cycle.

Cycles 2-11

Due to loss of material during each cycle's recovery procedure, it was necessary to adjust the reagent amounts. A consistent catalyst was loading of 5% (wt/wt) Pd@Hal/4 Bromotoluene was maintained.

Cycle	Yield (%)
1	98
2	99
3	99
4	99
5	98
6	97
7	98
8	96
9	92
10	85
11	52

3.5.7 Characterization of Coupling Products (Scheme 11).

All the products are known compounds, and the spectral data and melting points were identical to those reported in the literature. ^{1}H NMR is shown below each entry to illustrate the purity of the sample.

4-methoxy-4'-methyl-1,1'-biphenyl (6a)

OCH₃— (biphenyl structure diagram)
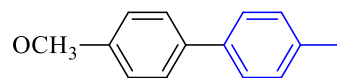
White solid (0.195 g, 98%); mp 109-110 °C. [Lit. mp 107.9-108.1 °C][1]

^{1}H NMR (400 MHz, DMSO-d_6) δ: 7.55 (d, J = 8.8 Hz, 2H), 7.48 (d, J = 8.0 Hz, 2H), 7.21 (d, J = 7.6 Hz, 2H), 6.98 (d, J = 8.4 Hz, 2H), 3.76 (s, 3H), 2.30 (s, 3H). Identical to ^{1}H NMR reported in the literature.[2]
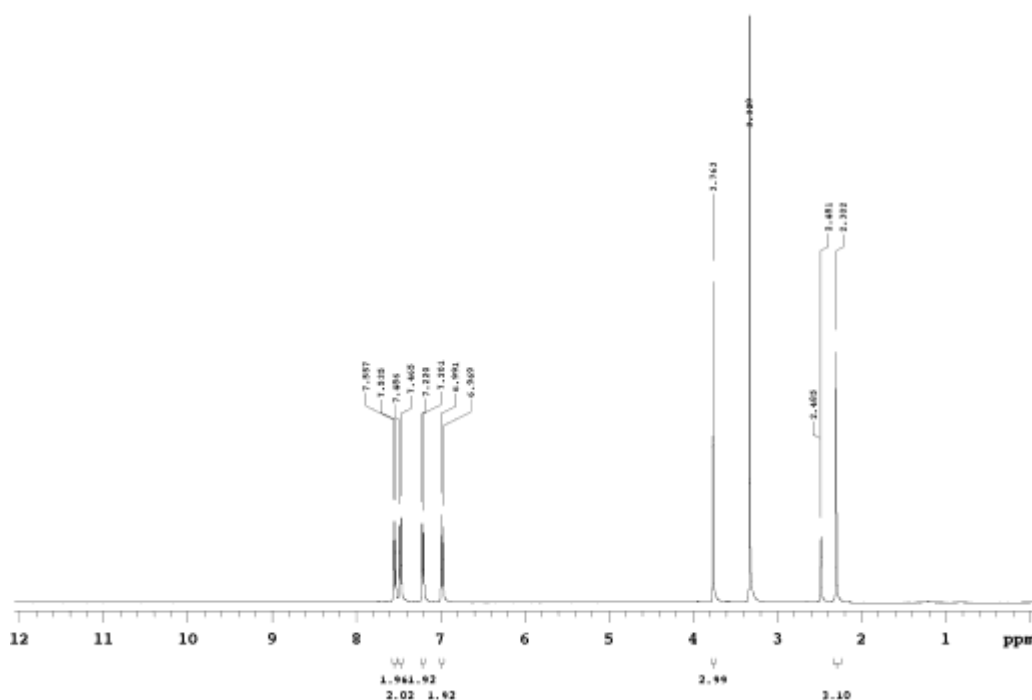
[1]Ackermann, L.; Althammer, A. *Org. Lett.* **2006,** *8(16)*, 3457-3460.
[2]Lu, B.; Fu, C.; Ma, S. *Tetrahedron Lett*, **2010**, *51(9),* 1284-6

4,4'-dimethyl-1,1'-biphenyl (6b)
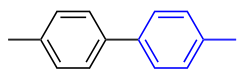
White solid (0.168 g, 92%); mp 118-119.5 °C. [Lit. mp 121.5-122.0 °C][1]

^{1}H NMR (400 MHz, DMSO-d_6) δ: 7.50 (d, J = 8.4 Hz, 4H), 7.23 (d, J = 8.0 Hz, 4H), 2.31 (s, 6H). Identical to ^{1}H NMR reported in the literature.[1]
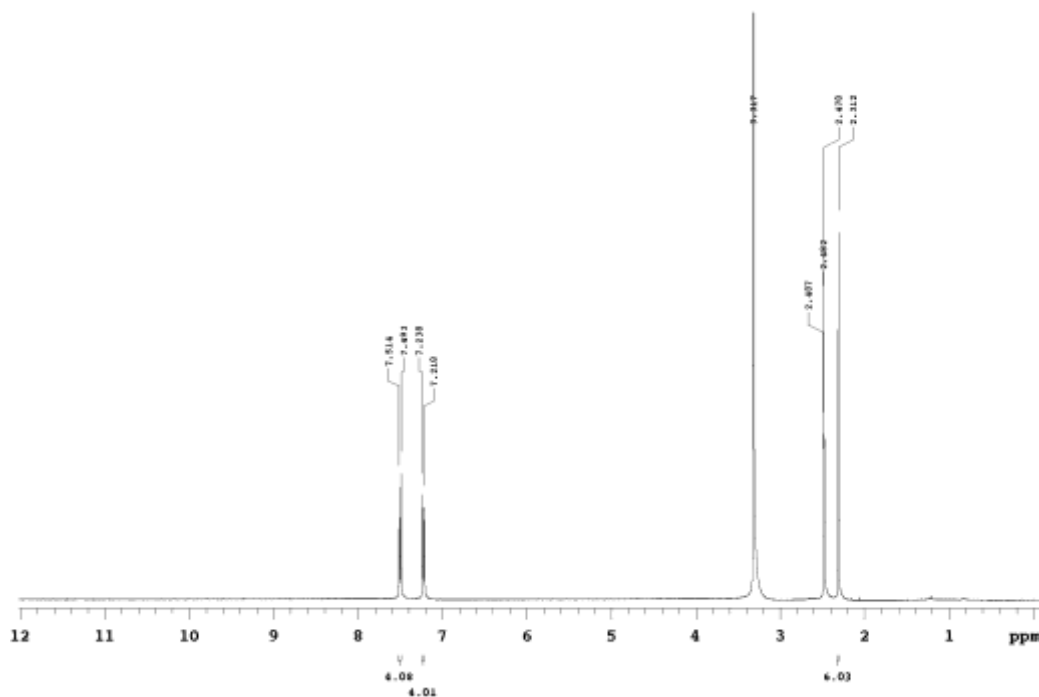
[1]Cepanec, I.; Litvic, M.; Udikovic, J.; Pogorelic, I.; Lovric, M. *Tetrahedron* **2007**, *63 (25),* 5614-5621.

4-methoxy-1,1'-biphenyl (6c/6d)

H₃CO—⟨benzene⟩—⟨benzene⟩

White solid (0.178 g/0.180, 97%/98%); mp 89.2-91.1 °C. [Lit. mp 85.3-85.7°C][1]

^{1}H NMR (400 MHz, DMSO-d_6) δ: 7.58 (dd, J = 8.4, 1.6 Hz, 4H), 7.41 (t, J = 7.6 Hz, 2H), 7.29 (t, J = 7.2 Hz, 1H), 7.01 (d, J = 8.8 Hz, 2H), 3.78 (s, 3H). Identical to ^{1}H NMR reported in the literature.[2]
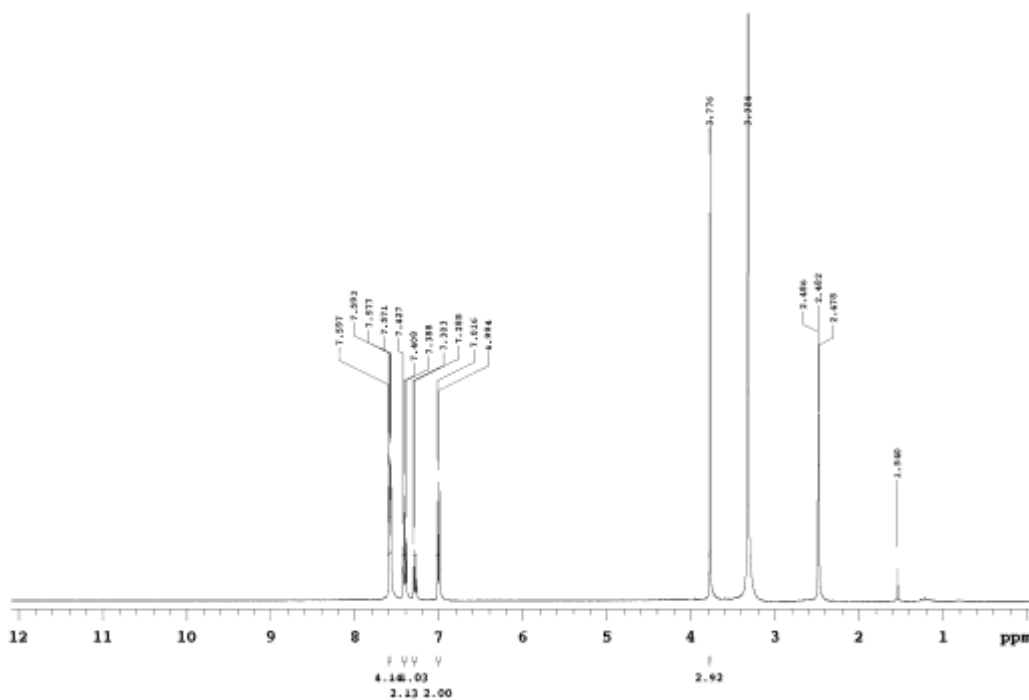
[1]Ackermann, L.; Althammer, A. *Org. Lett.* **2006,** *8(16)*, 3457-3460.
[2]Alacid, E.; Najera, C. *Org. Lett.* **2008**, *10(21),* 5011-5014

4-fluoro-4'-methyl-1,1'-biphenyl (6e)
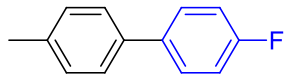
White solid (0.178 g, 96%); mp 76.5-77.1°C {Lit. mp 78-79}[1]

^{1}H NMR (400 MHz, DMSO-d_6) δ: 7.65 (dd, J = 8.8, 5,6 Hz, 2H), 7.51 (d, J = 7.6 Hz, 2H), 7.27- 7.22 (m, 4H), 2.48 (s, 3H). Identical to ^{1}H NMR reported in the literature.[2]
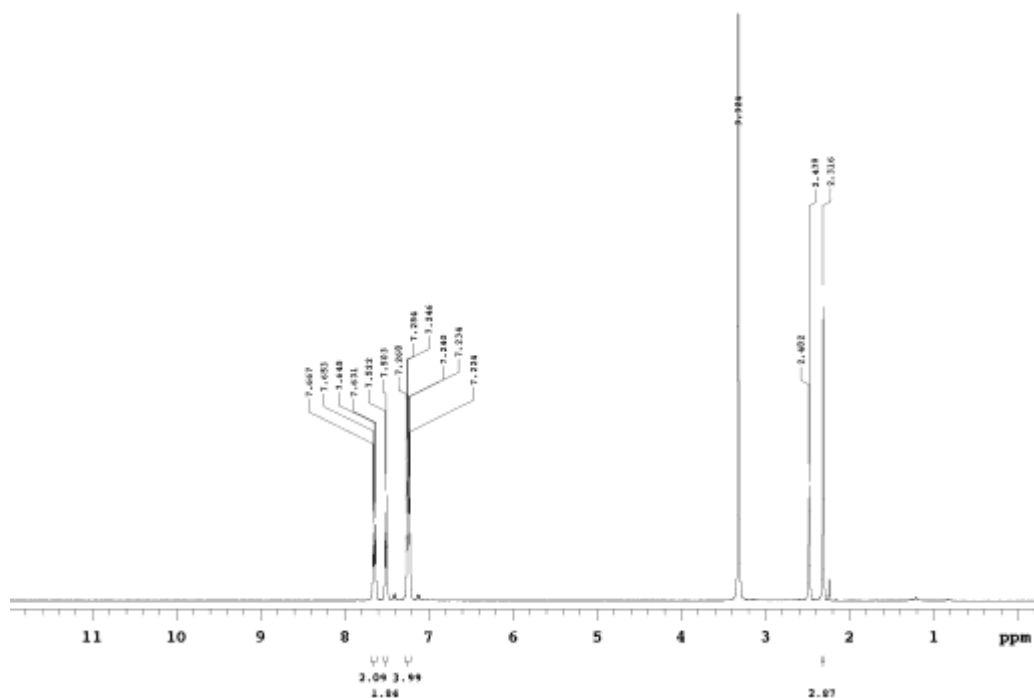
`[1]Kuriyama, M.; Shimazawa, R.; Shirai, R. *Tetrahedron* **2007**, *63(38),* 9393-9400.
[2]Roy, A. Hartwig, J. F. *J. Am. Chem. Soc*. **2003**, *125*, 8704-5.

4-fluoro-4'-methoxy-1,1'-biphenyl (6f)
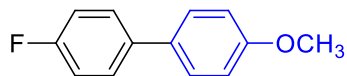
White solid (0.198 g, 98%); mp 88.6-89.5 °C [Lit. mp: 87.3-87.8 °C][1]

^{1}H NMR (400 MHz, DMSO-d_6) δ: 7.64-7.60 (m, 2H), 7.56 (d, J = 8.8 Hz, 2H), 7.23 (t, J = 8.8 Hz, 2 H), 7.00 (d, J = 8.8 Hz, 2H), 3.77 (s, 3H). Identical to ^{1}H NMR reported in the literature.[2]
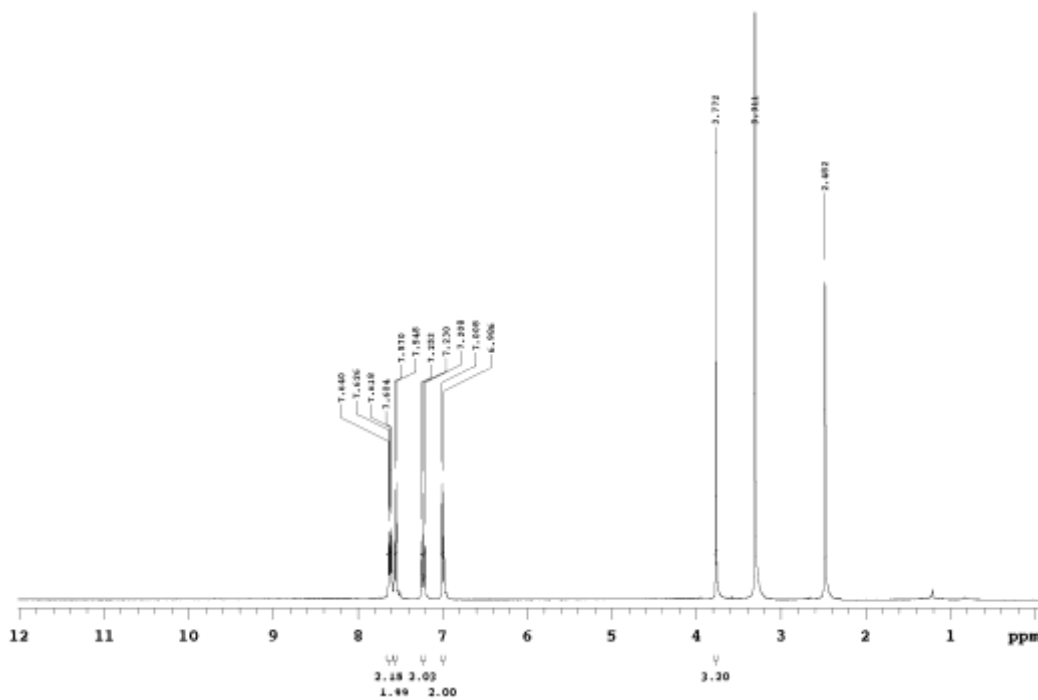
`[1]Ackermann, L.; Althammer, A. *Org. Lett.* **2006,** *8(16)*, 3457-3460.
[2]Doebele, M.; Vanderheiden, S.; Jung, N.; Brase, S. *Angew. Chemie, Int. Ed.* **2010**, *49*, 5986-5988.

2-phenyl-naphthalene (6g)
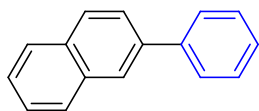
White solid (0.197 g, 96%); mp 102.5-103. 8°C [Lit. mp 101 °C].[1]

^{1}H NMR (300 MHz, DMSO-d_6) δ: 8.19 (d, J = 7.2Hz, 1 H), 7.99-7.91 (m, 3 H), 7.88-7.77 (m, 3 H), 7.64-7.49 (m, 4 H), 7.40-7.35 (m, 1 H). Identical to ^{1}H NMR reported in the literature.[2]
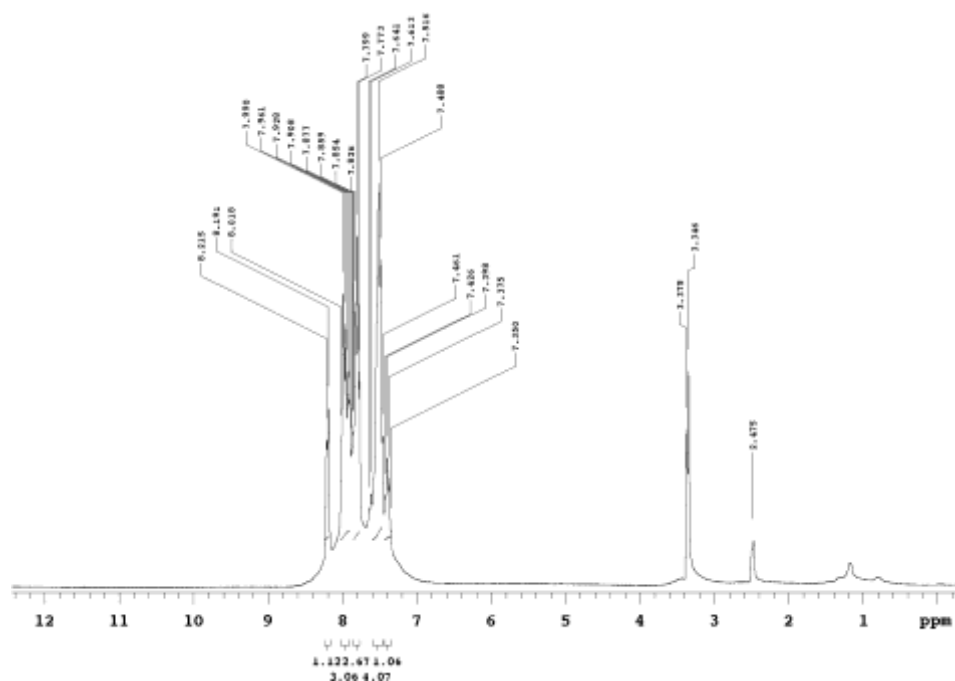
`[1]Alvarez-Bercedo, P.; Martin, R. *J. Am. Chem. Soc*. **2010**, *132*, 17352-17353.
[2]Guan, B.-T.; Wang, Y.; Li, B.J.; Yu, D.-G.; Shi, Z.-J. *J. Am. Chem Soc*. **2008**, *130*, 14468-70.

2-(4-fluorophenyl)naphthalene (6h)
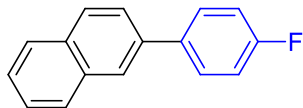
White solid (0.202 g, 91%); mp 101.1-103.2

^{1}H NMR (300 MHz, DMSO-d_6) δ: 8.19 (s, 1H), 8.00-7.92 (m, 3H), 7.86-7.80 (m, 3H), 7.53-7.50 (m, 2H), 7.39 (t, J = 8.7 Hz, 2H). Identical to ^{1}H NMR reported in the literature.[1]
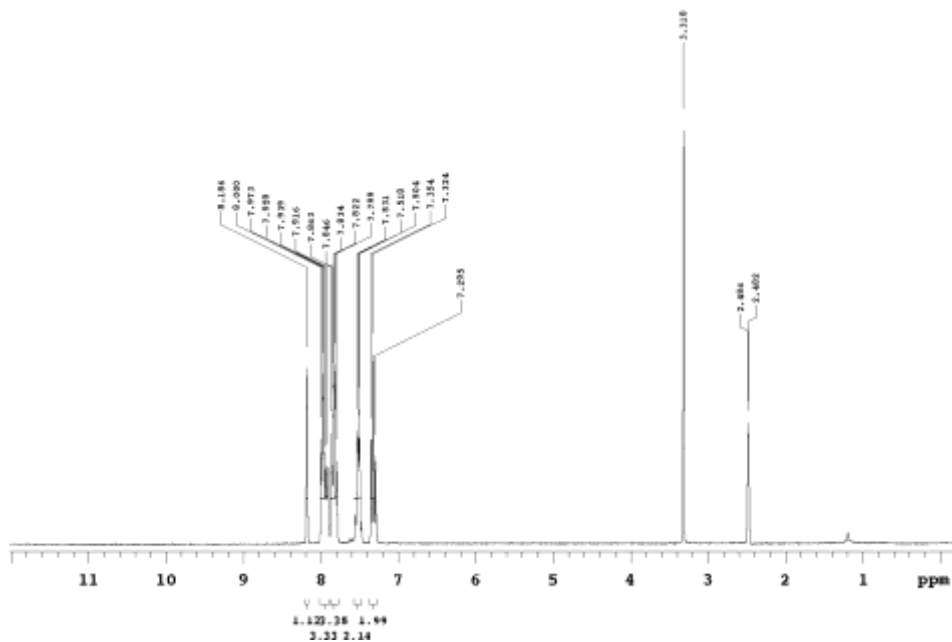
[1]Guan, B.-T.; Wang, Y.; Li, B.J.; Yu, D.-G.; Shi, Z.-J. *J. Am. Chem Soc*. **2008**, *130*, 14468-14470.

4'-methyl-biphenyl-4-carbonitrile (6i)
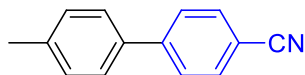
White solid (0.182 g, 94%); mp 110.6-111.8°C [Lit. mp 110-111 °C][1]

^{1}H NMR (400 MHz, DMSO-d_6) δ: 7.89 (d, J = 8.4 Hz, 2H), 7.84 (d, J = 8.4 Hz, 2H), 7.64 (d, J = 8.0 Hz, 2H), 7.31 (d, J = 7.6 Hz, 2H), 2.34 (s, 3H). Identical to ^{1}H NMR reported in the literature.[2]
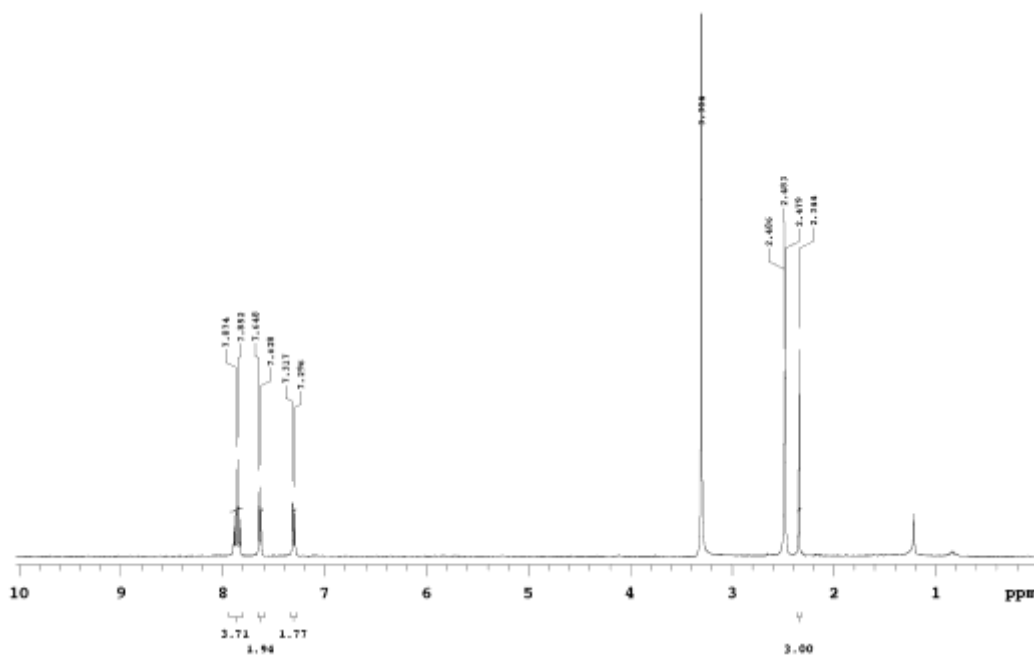
[1]Wang, L.; Wang, Z.-X. *Org. Lett.* **2007**, *9(21),* 4335-4338.
[2]Yu, D.-G.; Yu, M.; Guan, B.-T.; Li, B.-j.; Zheng, Y.; Wu, Z.-H.; Shi, Z.-J. *Org. Lett.* **2009**, *11(15),* 3374- 3377.

.

1-(4'-Methyl[1,1'-biphenyl]-4-yl)ethanone (6j)
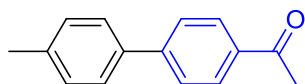
White solid (0.194 g, 92%); mp 120.3-122.1 °C [Lit. mp 122-124 °C][1]

^{1}H NMR (300 MHz, DMSO-d_6) δ: 8.00 (d, J = 6.0 Hz, 2H), 7.78 (d, J = 6.0 Hz, 2H), 7.63 (d, J = 6.0 Hz, 2H), 7.29 (d, J = 5.7 Hz, 2H), 2.58 (s, 3H), 2.34 (s, 3H). Identical to ^{1}H NMR reported in the literature.[1]
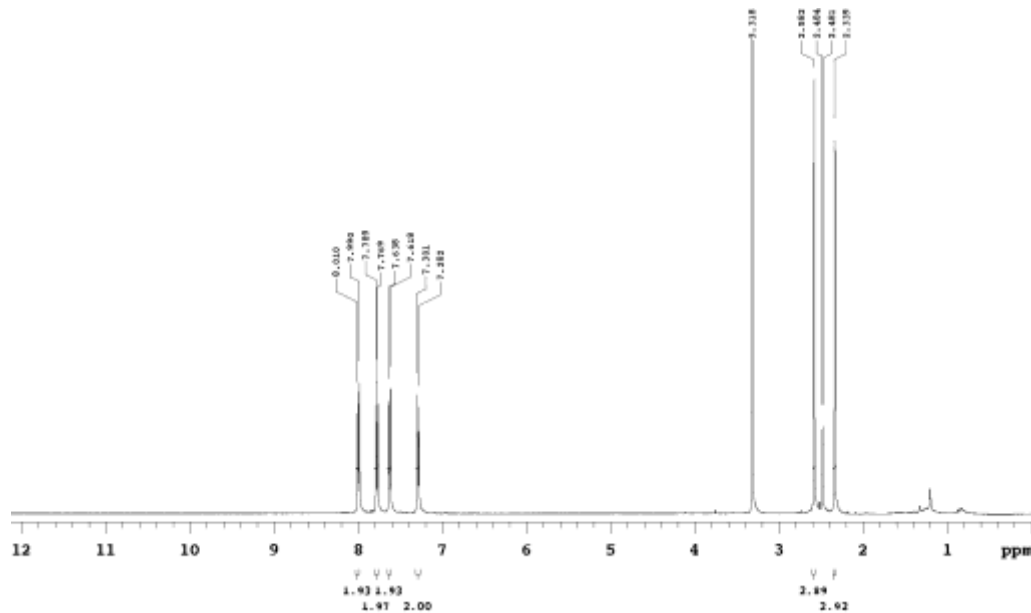
[1]Molander, G. A.; Iannazzo, L. *J. Org. Chem.* **2011**, *76 (21),* 9182-7.

3-(4-methoxyphenyl) pyridine (6k)
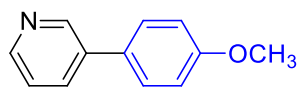
Light yellow solid (0.178 g, 97%); mp 61.5-63.1 °C [Lit. mp 62-63 °C].[1]

^{1}H NMR (400 MHz, DMSO-d_6) δ: 8.83 (s, 1H), 8.49 (d, J = 4.0 Hz, 1H), 8.00 (d, J = 8.4 Hz, 1H), 7.66 (d, J = 8.4 Hz, 2H), 7.43 (m, 1H), 7.04 (d, J = 8.4 Hz, 2H), 3.79 (s, 3H). Identical to ^{1}H NMR reported in the literature.[1]
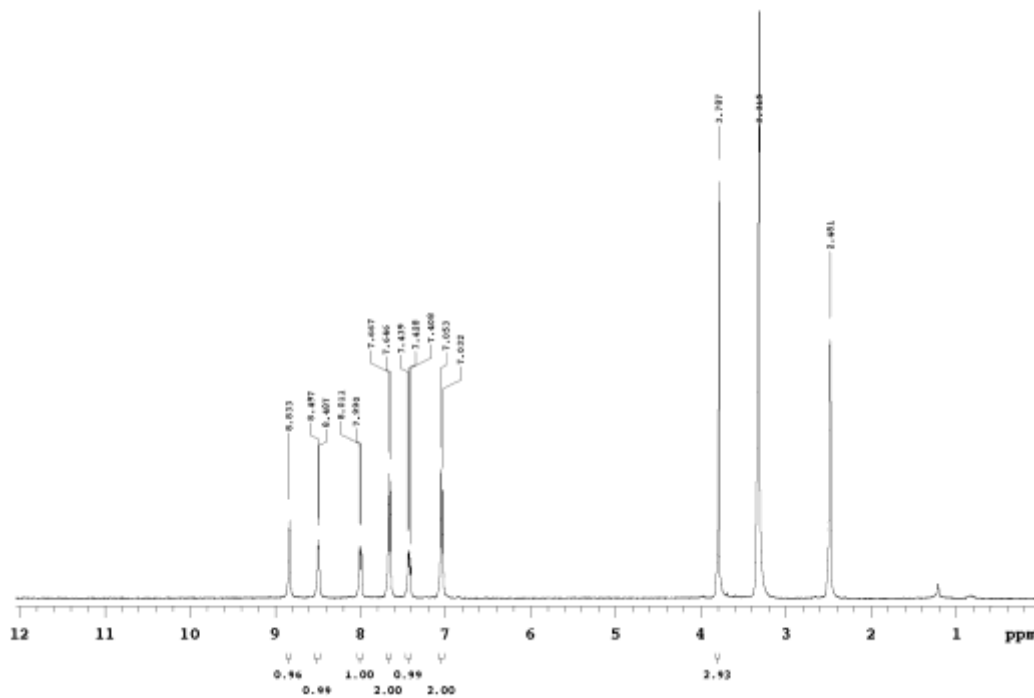
[1]Gavryushin, A.; Kofink, C.; Manolikakes, G.; Knochel, P. *Org. Lett.* **2005**, *7(22),* 4871-4

3-chloro-4'-methoxy-4-methyl-1,1'-biphenyl (6l)
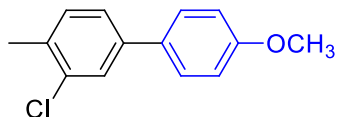
Colorless oil (0.223 g, 96%)

^{1}H NMR (400 MHz, DMSO-d_6) δ: 7.63-7.59 (m, 3H), 7.48 (d, J = 8.0 Hz, 1H), 7.37 (d, J = 7.6 Hz, 1H), 6.99 (d, J = 8.4 Hz, 2H), 3.77 (s, 3H), 2.33 (s, 3H).

Anal. Calcd for C$_{14}$H$_{13}$ClO: C, 72.26; H, 5.63. Found: 72.18; H, 5.70.
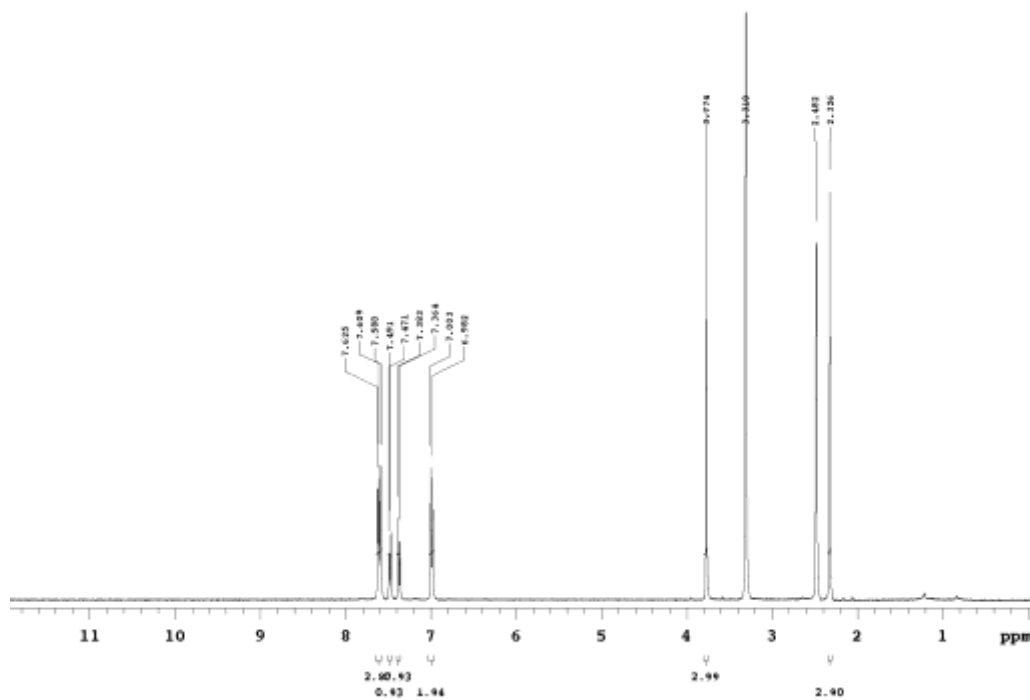
4-(4'-Methoxyphenyl) phenol (6m)

HO—⟨benzene⟩—⟨benzene⟩—OCH$_3$
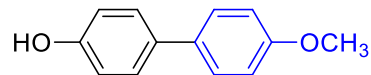
White solid (0.194 g, 97%); mp 181.5-182.2 °C [Lit. mp 180-181°C].[1]

^{1}H NMR (300 MHz, DMSO-d_6) δ: 9.41 (s, 1H), 7.47 (d, J = 8.1 Hz, 2H), 7.39 (d, J = 8.7, 2H), 6.95 (d, J = 8.7 Hz, 2H), 6.79 (d, J = 9.0 Hz, 2H), 3.75 (s, 3H). Identical to ^{1}H NMR reported in the literature.[2]
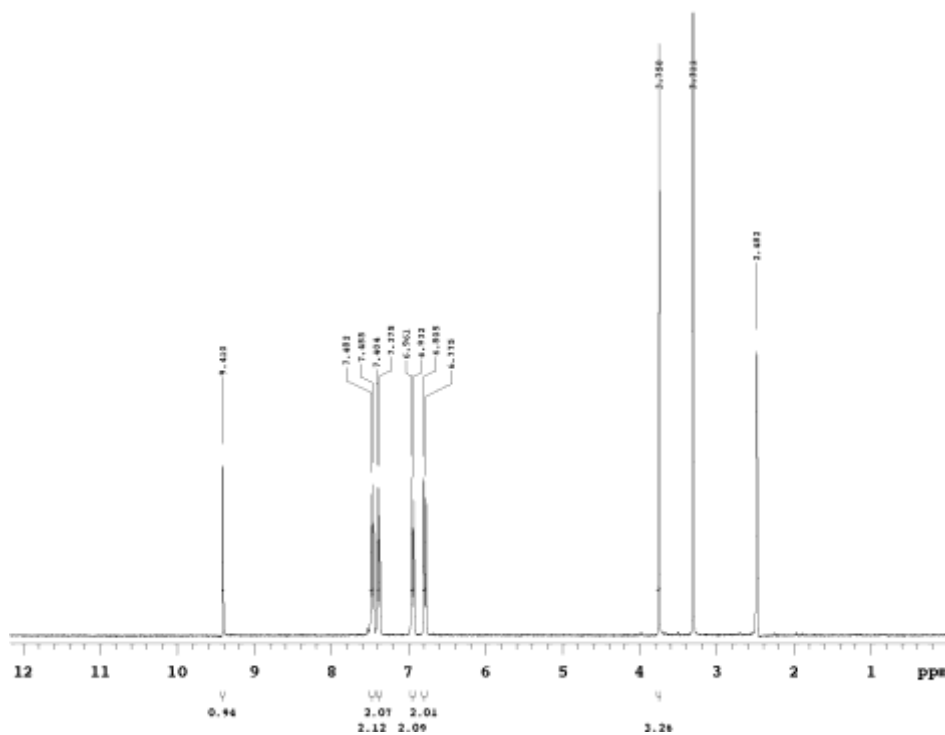
[1]Abramovitch, R. A.; Alvernhe, G.; Bartnik, R.; Dassanayake, N. L.; Inbasekaran, M. N.; Kato, S. *J. Am.Chem. Soc.* **1981**, *103(15),* 4558-65.
[2]Razler, T. M.; Hsiao, Y.; Qian, F.; Fu, R.; Khan, R. K.; Doubleday, W. *J. Org. Chem.* **2009**, *74(3),* 1381-4.

(4-methoxyphenyl) aniline (6n)

H_2N—⬡—⬡—OCH_3
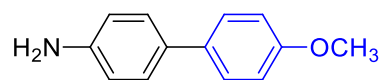
Light yellow solid (0.184 g, 92%); mp 144.8-145.2 °C [Lit. mp 147°C][15]

^{1}H NMR (300 MHz, DMSO-d_6) δ: 7.42 (d, J = 7.8 Hz, 2H), 7.26 (d, J = 7.2 Hz, 2H) 6.91 (d, J = 7.8 Hz, 2H), 6.60 (d, J = 6.9 Hz, 2H), 5.10 (s, 2H), 3.74 (s, 3H). Identical to ^{1}H NMR reported in the literature.[16]
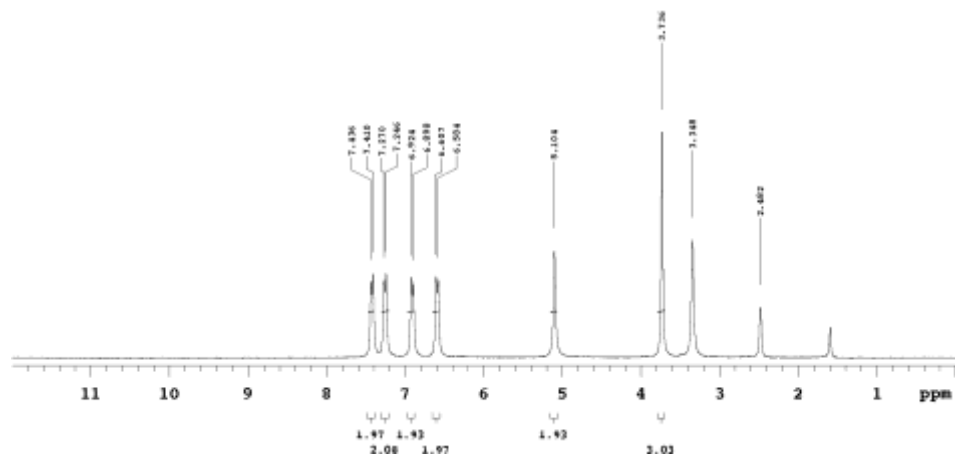
[1]Razler, T. M.; Hsiao, Y.; Qian, F.; Fu, R.; Khan, R. K.; Doubleday, W. *J. Org. Chem.* **2009**, *74(3)*, 1381-4.
[2]Scheuermann, G. M.; Rumi, L.; Steurer, P.; Bannwarth, W.; Mulhaupt, R. *J. Am. Chem. Soc.* **2009**, *131(23)*, 8262-8270.

3.6   References

1.   Seyferth, D., The Grignard Reagents. *Organometallics* **2009,** *28* (6), 1598-1605.

2.   Gregoritza, M.; Brandl, F. P., The Diels–Alder reaction: A powerful tool for the design of drug delivery systems and biomaterials. *European Journal of Pharmaceutics and Biopharmaceutics* **2015,** *97*, 438-453.

3.   Shah, S.; Protasiewicz, J. D., 'Phospha-variations' on the themes of Staudinger and Wittig: phosphorus analogs of Wittig reagents. *Coordination Chemistry Reviews* **2000,** *210* (1), 181-201.

4.   Miyaura, N.; Suzuki, A., Palladium-Catalyzed Cross-Coupling Reactions of Organoboron Compounds. *Chemical Reviews* **1995,** *95* (7), 2457-2483.

5.   Söderberg, B. C. G., Transition metals in organic synthesis: Highlights for the year 2004. *Coordination Chemistry Reviews* **2006,** *250* (19), 2411-2490.

6.   Trost, B. M., Basic Aspects of Organic Synthesis with Transition Metals. In *Transition Metals for Organic Synthesis*, 2004; pp 2-14.

7.   Vlaar, T.; Ruijter, E.; Orru, R. V. A., Recent Advances in Palladium-Catalyzed Cascade Cyclizations. *Advanced Synthesis & Catalysis* **2011,** *353* (6), 809-841.

8.   Tamura, M.; Kochi, J. K., Vinylation of Grignard reagents. Catalysis by iron. *Journal of the American Chemical Society* **1971,** *93* (6), 1487-1489.

9.   Tamao, K.; Sumitani, K.; Kumada, M., Selective carbon-carbon bond formation by cross-coupling of Grignard reagents with organic halides. Catalysis by nickel-phosphine complexes. *Journal of the American Chemical Society* **1972,** *94* (12), 4374-4376.

10.   Denmark, S. E.; Regens, C. S., Palladium-Catalyzed Cross-Coupling Reactions of Organosilanols and Their Salts: Practical Alternatives to Boron- and Tin-Based Methods. *Accounts of Chemical Research* **2008,** *41* (11), 1486-1499.

11.   Farina, V.; Krishnamurthy, V.; Scott, W. J., The Stille Reaction. In *Organic Reactions*, pp 1-652.

12.   Stille, J. K., The Palladium-Catalyzed Cross-Coupling Reactions of Organotin Reagents with Organic Electrophiles [New Synthetic Methods (58)]. *Angewandte Chemie International Edition in English* **1986,** *25* (6), 508-524.

13.   Knochel, P.; Singer, R. D., Preparation and reactions of polyfunctional organozinc reagents in organic synthesis. *Chemical Reviews* **1993,** *93* (6), 2117-2188.

14. Quan, M. L.; DeLucca, I.; Boswell, G. A.; Chiu, A. T.; Wong, P. C.; Wexler, R. R.; Timmermans, P. B. M. W. M., Imidazolinones as nonpeptide angiotensin II receptor antagonists. *Bioorganic & Medicinal Chemistry Letters* **1994,** *4* (12), 1527-1530.

15. Labelle, M.; Belley, M.; Gareau, Y.; Gauthier, J. Y.; Guay, D.; Gordon, R.; Grossman, S. G.; Jones, T. R.; Leblanc, Y.; McAuliffe, M.; McFarlane, C.; Masson, P.; Metters, K. M.; Ouimet, N.; Patrick, D. H.; Piechuta, H.; Rochette, C.; Sawyer, N.; Xiang, Y. B.; Pickett, C. B.; Ford-Hutchinson, A. W.; Zamboni, R. J.; Young, R. N., Discovery of MK-0476, a potent and orally active leukotriene D4 receptor antagonist devoid of peroxisomal enxyme induction. *Bioorganic & Medicinal Chemistry Letters* **1995,** *5* (3), 283-288.

16. Alimardanov, A.; Schmieder-van de Vondervoort, L.; de Vries, A. H. M.; de Vries, J. G., Use of "Homeopathic" Ligand-Free Palladium as Catalyst for Aryl-Aryl Coupling Reactions. *Advanced Synthesis & Catalysis* **2004,** *346* (13-15), 1812-1817.

17. Littke, A. F.; Fu, G. C., A versatile catalyst for Heck reactions of aryl chlorides and aryl bromides under mild conditions. *Journal of American Chemical Society* **2001,** *123* (29), 6989-7000.

18. Testa, C.; Roger, J.; Fleurat-Lessard, P.; Hierso, J.-C., Palladium-Catalyzed Electrophilic C–H-Bond Fluorination: Mechanistic Overview and Supporting Evidence. *European Journal of Organic Chemistry* **2019,** *2019* (2-3), 233-253.

19. Littke, A. F.; Fu, G. C., Palladium-catalyzed coupling reactions of aryl chlorides. *Angewandte Chemie International Edition* **2002,** *41* (22), 4176-211.

20. Littke, A. F.; Fu, G. C., A Convenient and General Method for Pd-Catalyzed Suzuki Cross-Couplings of Aryl Chlorides and Arylboronic Acids. *Angewandte Chemie International Edition* **1998,** *37* (24), 3387-3388.

21. Cho, E. J.; Senecal, T. D.; Kinzel, T.; Zhang, Y.; Watson, D. A.; Buchwald, S. L., The palladium-catalyzed trifluoromethylation of aryl chlorides. *Science* **2010,** *328* (5986), 1679-81.

22. Yu, D. G.; Li, B. J.; Zheng, S. F.; Guan, B. T.; Wang, B. Q.; Shi, Z. J., Direct application of phenolic salts to nickel-catalyzed cross-coupling reactions with aryl Grignard reagents. *Angewandte Chemie International Edition* **2010,** *49* (27), 4566-70.

23. Watson, M. P.; Jacobsen, E. N., Asymmetric Intramolecular Arylcyanation of Unactivated Olefins via C−CN Bond Activation. *Journal of the American Chemical Society* **2008,** *130* (38), 12594-12595.

24. Stuart, D. R.; Fagnou, K., The catalytic cross-coupling of unactivated arenes. *Science* **2007,** *316* (5828), 1172-5.

25.   Bergman, R. G., C–H activation. *Nature* **2007,** *446* (7134), 391-393.

26.   Reeves, J. T.; Fandrick, D. R.; Tan, Z.; Song, J. J.; Lee, H.; Yee, N. K.; Senanayake, C. H., Room temperature palladium-catalyzed cross-coupling of aryltrimethylammonium triflates with aryl Grignard reagents. *Organic Letters* **2010,** *12* (19), 4388-91.

27.   Goossen, L. J.; Zimmermann, B.; Knauber, T., Palladium/copper-catalyzed decarboxylative cross-coupling of aryl chlorides with potassium carboxylates. *Angewandte Chemie International Edition* **2008,** *47* (37), 7103-6.

28.   Senecal, T. D.; Parsons, A. T.; Buchwald, S. L., Room Temperature Aryl Trifluoromethylation via Copper-Mediated Oxidative Cross-Coupling. *The Journal of Organic Chemistry* **2011,** *76* (4), 1174-1176.

29.   Chen, X.; Engle, K. M.; Wang, D. H.; Yu, J. Q., Palladium(II)-catalyzed C-H activation/C-C cross-coupling reactions: versatility and practicality. *Angewandte Chemie International Edition* **2009,** *48* (28), 5094-115.

30.   Ros, A.; Estepa, B.; Bermejo, A.; Álvarez, E.; Fernández, R.; Lassaletta, J. M., Phosphino Hydrazones as Suitable Ligands in the Asymmetric Suzuki–Miyaura Cross-Coupling. *The Journal of Organic Chemistry* **2012,** *77* (10), 4740-4750.

31.   LaPlante, S. R.; Edwards, P. J.; Fader, L. D.; Jakalian, A.; Hucke, O., Revealing atropisomer axial chirality in drug discovery. *Chemical Medicianl Chemistry* **2011,** *6* (3), 505-13.

32.   Busacca, C. A.; Fandrick, D. R.; Song, J. J.; Senanayake, C. H., Transition Metal Catalysis in the Pharmaceutical Industry. In *Applications of Transition Metal Catalysis in Drug Discovery and Development*, pp 1-24.

33.   Slagt, V. F.; de Vries, A. H. M.; de Vries, J. G.; Kellogg, R. M., Practical Aspects of Carbon−Carbon Cross-Coupling Reactions Using Heteroarenes. *Organic Process Research & Development* **2010,** *14* (1), 30-47.

34.   Devendar, P.; Qu, R.-Y.; Kang, W.-M.; He, B.; Yang, G.-F., Palladium-Catalyzed Cross-Coupling Reactions: A Powerful Tool for the Synthesis of Agrochemicals. *Journal of Agricultural and Food Chemistry* **2018,** *66* (34), 8914-8934.

35.   Kapdi, A. R.; Prajapati, D., Regioselective palladium-catalyzed cross-coupling reactions: a powerful synthetic tool. *RSC Advances* **2014,** *4* (78), 41245-41259.

36.   Lundgren, R. J.; Stradiotto, M., Addressing Challenges in Palladium-Catalyzed Cross-Coupling Reactions Through Ligand Design. *Chemistry-A European Journal* **2012,** *18* (32), 9758-9769.

37.   Blom, C.; Cross-Coupling Reactions. *Organic Letters* **2012,** *14* (12), 2925-2928.

38.   Torborg, C.; Beller, M., Recent Applications of Palladium-Catalyzed Coupling Reactions in the Pharmaceutical, Agrochemical, and Fine Chemical Industries. *Advanced Synthesis & Catalysis* **2009,** *351* (18), 3027-3043.

39.   Buchwald, S. L.; Bolm, C., On the Role of Metal Contaminants in Catalyses with $FeCl_3$. *Angewandte Chemie International Edition* **2009,** *48* (31), 5586-5587.

40.   Ikeda, S., Nickel-catalyzed intermolecular domino reactions. *Accounts of Chemical Research* **2000,** *33* (8), 511-9.

41.   Fürstner, A., From Oblivion into the Limelight: Iron (Domino) Catalysis. *Angewandte Chemie International Edition* **2009,** *48* (8), 1364-1367.

42.   Correa, A.; García Mancheño, O.; Bolm, C., Iron-catalysed carbon-heteroatom and heteroatom–heteroatom bond-forming processes. *Chemical Society Reviews* **2008,** *37* (6), 1108-1117.

43.   Lipshutz, B. H.; Yamamoto, Y., Introduction: Coinage metals in organic synthesis. *Chemical Review* **2008,** *108* (8), 2793-5.

44.   Montgomery, J., Nickel-Catalyzed Cyclizations, Couplings, and Cycloadditions Involving Three Reactive Components. *Accounts of Chemical Research* **2000,** *33* (7), 467-473.

45.   Frisch, A. C.; Beller, M., Catalysts for cross-coupling reactions with non-activated alkyl halides. *Angewandte Chemie International Edition* **2005,** *44* (5), 674-88.

46.   Farina, V., High-Turnover Palladium Catalysts in Cross-Coupling and Heck Chemistry: A Critical Overview. *Advanced Synthesis & Catalysis* **2004,** *346* (13-15), 1553-1582.

47.   Martin, R.; Buchwald, S. L., Palladium-catalyzed Suzuki-Miyaura cross-coupling reactions employing dialkylbiaryl phosphine ligands. *Accounts of Chemical Research* **2008,** *41* (11), 1461-1473.

48.   Barder, T. E.; Buchwald, S. L., Efficient Catalyst for the Suzuki−Miyaura Coupling of Potassium Aryl Trifluoroborates with Aryl Chlorides. *Organic Letters* **2004,** *6* (16), 2649-2652.

49.   Walker, S. D.; Barder, T. E.; Martinelli, J. R.; Buchwald, S. L., A rationally designed universal catalyst for Suzuki-Miyaura coupling processes. *Angewandte Chemie International Edition* **2004,** *43* (14), 1871-6.

50. Barder, T. E.; Walker, S. D.; Martinelli, J. R.; Buchwald, S. L., Catalysts for Suzuki-Miyaura coupling processes: scope and studies of the effect of ligand structure. *Journal of American Chemical Society* **2005,** *127* (13), 4685-96.

51. Stambuli, J. P.; Kuwano, R.; Hartwig, J. F., Unparalleled rates for the activation of aryl chlorides and bromides: coupling with amines and boronic acids in minutes at room temperature. *Angewandte Chemie International Edition* **2002,** *41* (24), 4746-8.

52. Hamann, B. C.; Hartwig, J. F., Palladium-Catalyzed Direct α-Arylation of Ketones. Rate Acceleration by Sterically Hindered Chelating Ligands and Reductive Elimination from a Transition Metal Enolate Complex. *Journal of the American Chemical Society* **1997,** *119* (50), 12382-12383.

53. Liu, D.; Gao, W.; Dai, Q.; Zhang, X., Triazole-Based Monophosphines for Suzuki−Miyaura Coupling and Amination Reactions of Aryl Chlorides. *Organic Letters* **2005,** *7* (22), 4907-4910.

54. Zapf, A.; Jackstell, R.; Rataboul, F.; Riermeier, T.; Monsees, A.; Fuhrmann, C.; Shaikh, N.; Dingerdissen, U.; Beller, M., Practical synthesis of new and highly efficient ligands for the Suzuki reaction of aryl chlorides. *Chemical Communications* **2004,** (1), 38-39.

55. Guram, A. S.; Wang, X.; Bunel, E. E.; Faul, M. M.; Larsen, R. D.; Martinelli, M. J., New Catalysts for Suzuki−Miyaura Coupling Reactions of Heteroatom-Substituted Heteroaryl Chlorides. *The Journal of Organic Chemistry* **2007,** *72* (14), 5104-5112.

56. Zapf, A.; Beller, M., The development of efficient catalysts for palladium-catalyzed coupling reactions of aryl halides. *Chemical Communications* **2005,** (4), 431-440.

57. Bedford, R. B., Palladacyclic catalysts in C–C and C–heteroatom bond-forming reactions. *Chemical Communications* **2003,** (15), 1787-1796.

58. Bedford, R. B.; Hazelwood, S. L.; Limmert, M. E., Extremely high activity catalysts for the Suzuki coupling of aryl chlorides: the importance of catalyst longevity. *Chemical Communications* **2002,** (22), 2610-2611.

59. Özdemir, İ.; Çetinkaya, B.; Demir, S.; Gürbüz, N., Palladium-Catalyzed Suzuki–Miyaura Reaction Using Saturated N-Heterocarbene Ligands. *Catalysis Letters* **2004,** *97* (1), 37-40.

60. Bedford, R. B.; Blake, M. E.; Butts, C. P.; Holder, D., The Suzuki coupling of aryl chlorides in TBAB–water mixtures. *Chemical Communications* **2003,** (4), 466-467.

61. Grasa, G. A.; Viciu, M. S.; Huang, J.; Zhang, C.; Trudell, M. L.; Nolan, S. P., Suzuki−Miyaura Cross-Coupling Reactions Mediated by Palladium/Imidazolium Salt Systems. *Organometallics* **2002,** *21* (14), 2866-2873.

62.   McGlacken, G. P.; Fairlamb, I. J. S., Palladium-Catalysed Cross-Coupling and Related Processes: Some Interesting Observations That Have Been Exploited in Synthetic Chemistry. *European Journal of Organic Chemistry* **2009,** *2009* (24), 4011-4029.

63.   Pink, C. J.; Wong, H.-t.; Ferreira, F. C.; Livingston, A. G., Organic Solvent Nanofiltration and Adsorbents; A Hybrid Approach to Achieve Ultra Low Palladium Contamination of Post Coupling Reaction Products. *Organic Process Research & Development* **2008,** *12* (4), 589-595.

64.   Karami, K.; Abedanzadeh, S.; Hervés, P., Synthesis and characterization of functionalized titania-supported Pd catalyst deriving from new orthopalladated complex of benzophenone imine: catalytic activity in the copper-free Sonogashira cross-coupling reactions at low palladium loadings. *RSC Advances* **2016,** *6* (96), 93660-93672.

65.   Wei, Y.-L.; Li, Y.; Chen, Y.-Q.; Dong, Y.; Yao, J.-J.; Han, X.-Y.; Dong, Y.-B., Pd(II)-NHDC-Functionalized UiO-67 Type MOF for Catalyzing Heck Cross-Coupling and Intermolecular Benzyne–Benzyne–Alkene Insertion Reactions. *Inorganic Chemistry* **2018,** *57* (8), 4379-4386.

66.   Nagai, D.; Goto, H., Effective Heterogeneous Catalyst for Suzuki-Miyaura Cross-Coupling in Aqueous Media: Melamine Cyanurate Complex Containing Pd Species. *Bulletin of the Chemical Society of Japan* **2018,** *91* (2), 147-152.

67.   Manjunatha, K.; Koley, T. S.; Kandathil, V.; Dateer, R. B.; Balakrishna, G.; Sasidhar, B. S.; Patil, S. A.; Patil, S. A., Magnetic nanoparticle-tethered Schiff base–palladium(II): Highly active and reusable heterogeneous catalyst for Suzuki–Miyaura cross-coupling and reduction of nitroarenes in aqueous medium at room temperature. *Applied Organometallic Chemistry* **2018,** *32* (4), e4266.

68.   Yu, L.; Han, Z.; Ding, Y., Gram-Scale Preparation of Pd@PANI: A Practical Catalyst Reagent for Copper-Free and Ligand-Free Sonogashira Couplings. *Organic Process Research & Development* **2016,** *20* (12), 2124-2129.

69.   Diebold, C.; Becht, J.-M.; Lu, J.; Toy, P. H.; Le Drian, C., An Efficient and Reusable Palladium Catalyst Supported on a Rasta Resin for Suzuki–Miyaura Cross-Couplings. *European Journal of Organic Chemistry* **2012,** *2012* (5), 893-896.

70.   Rangel Rangel, E.; Maya, E. M.; Sánchez, F.; de la Campa, J. G.; Iglesias, M., Palladium-heterogenized porous polyimide materials as effective and recyclable catalysts for reactions in water. *Green Chemistry* **2015,** *17* (1), 466-473.

71.   Butters, M.; Catterick, D.; Craig, A.; Curzons, A.; Dale, D.; Gillmore, A.; Green, S. P.; Marziano, I.; Sherlock, J. P.; White, W., Critical assessment of pharmaceutical processes--A rationale for changing the synthetic route. *Chemical Review* **2006,** *106* (7), 3002-27.

72.   Messerle, L., Applied Homogeneous Catalysis with Organometallic Compounds. A Comprehensive Handbook in Two Volumes Edited by B. Cornils (Hoechst AG Germany) and W. A. Herrmann (Tech. University München, Germany). VCH: Weinheim. 1996. 1246 pp. DM 598. ISBN 3-527-29286-1. *Journal of the American Chemical Society* **1998,** *120* (9), 2209-2210.

73.   Heck, R. F., Palladium-Catalyzed Vinylation of Organic Halides. In *Organic Reactions*, pp 345-390.

74.   Bryndza, H. E.; Tam, W., Monomeric metal hydroxides, alkoxides, and amides of the late transition metals: synthesis, reactions, and thermochemistry. *Chemical Reviews* **1988,** *88* (7), 1163-1188.

75.   Bej, A.; Ghosh, K.; Sarkar, A.; Knight, D. W., Palladium nanoparticles in the catalysis of coupling reactions. *RSC Advances* **2016,** *6* (14), 11446-11453.

76.   Deraedt, C.; Astruc, D., "Homeopathic" Palladium Nanoparticle Catalysis of Cross Carbon-Carbon Coupling Reactions. *Accounts of Chemical Research* **2014,** *47* (2), 494-503.

77.   Balanta, A.; Godard, C.; Claver, C., Pd nanoparticles for C–C coupling reactions. *Chemical Society Reviews* **2011,** *40* (10), 4973-4985.

78.   Tsuji, Y.; Fujihara, T., Homogeneous Nanosize Palladium Catalysts. *Inorganic Chemistry* **2007,** *46* (6), 1895-1902.

79.   Pourjavadi, A.; Habibi, Z., Palladium nanoparticle-decorated magnetic pomegranate peel-derived porous carbon nanocomposite as an excellent catalyst for Suzuki–Miyaura and Sonogashira cross-coupling reactions. *Applied Organometallic Chemistry* **2018,** *32* (10), e4480.

80.   Chen, Y.; Wang, M.; Zhang, L.; Liu, Y.; Han, J., Poly(o-amino thiophenol)-stabilized Pd nanoparticles as efficient heterogenous catalysts for Suzuki cross-coupling reactions. *RSC Advances* **2017,** *7* (74), 47104-47110.

81.   Veerakumar, P.; Thanasekaran, P.; Lu, K.-L.; Liu, S.-B.; Rajagopal, S., Functionalized Silica Matrices and Palladium: A Versatile Heterogeneous Catalyst for Suzuki, Heck, and Sonogashira Reactions. *ACS Sustainable Chemistry & Engineering* **2017,** *5* (8), 6357-6376.

82.   Shaikh, M. N., Pd nanoparticles on green support as dip-catalyst: a facile transfer hydrogenation of olefins and N-heteroarenes in water. *RSC Advances* **2019,** *9* (48), 28199-28206.

83.   Sá, S.; Gawande, D. M.; Velhinho, A.; Veiga, J. P.; Bundaleski, N.; Trigueiro, J.; Tolstogouzov, A.; Teodoro, O.; Zboril, R.; Varma, R.; Branco, P., Magnetically recyclable magnetite–palladium (Nanocat-Fe–Pd) nanocatalyst for the Buchwald–Hartwig reaction. *Green Chemistry* **2014,** *16*.

84.   Kalbasi, R. J.; Mosaddegh, N., Palladium Nanoparticles Supported on Poly(2-hydroxyethyl methacrylate)/KIT-6 Composite as an Efficient and Reusable Catalyst for Suzuki–Miyaura Reaction in Water. *Journal of Inorganic and Organometallic Polymers and Materials* **2012,** *22* (2), 404-414.

85.   Kalbasi, R. J.; Mosaddegh, N., Synthesis, characterization and catalytic activity studies of Pd-based supported nanoparticle catalyst anchoring on poly(N-vinyl-2-pyrrolidone) modified CMK-3. *Materials Chemistry and Physics* **2011,** *130* (3), 1287-1293.

86.   Das, P.; Sharma, D.; Shil, A. K.; Kumari, A., Solid-supported palladium nano and microparticles: an efficient heterogeneous catalyst for ligand-free Suzuki–Miyaura cross coupling reaction. *Tetrahedron Letters* **2011,** *52* (11), 1176-1178.

87.   Zhi, J.; Song, D.; Li, Z.; Lei, X.; Hu, A., Palladium nanoparticles in carbon thin film-lined SBA-15 nanoreactors: efficient heterogeneous catalysts for Suzuki–Miyaura cross-coupling reaction in aqueous media. *Chemical Communications* **2011,** *47* (38), 10707-10709.

88.   Zhang, H.; Lu, X. F.; Wu, Z.-P.; Lou, X. W. D., Emerging Multifunctional Single-Atom Catalysts/Nanozymes. *ACS Central Science* **2020,** *6* (8), 1288-1301.

89.   Wang, Q.; Li, J.; Tu, X.; Liu, H.; Shu, M.; Si, R.; Ferguson, C. T. J.; Zhang, K. A. I.; Li, R., Single Atomically Anchored Cobalt on Carbon Quantum Dots as Efficient Photocatalysts for Visible Light-Promoted Oxidation Reactions. *Chemistry of Materials* **2020,** *32* (2), 734-743.

90.   Iranpoor, N.; Firouzabadi, H.; Moghadam, K. R.; Motavalli, S., First reusable ligand-free palladium-catalyzed C–P bond formation of aryl halides with trialkylphosphites in neat water. *RSC Advances* **2014,** *4* (99), 55732-55737.

91.   Reetz, M. T.; Breinbauer, R.; Wanninger, K., Suzuki and Heck reactions catalyzed by preformed palladium clusters and palladiumnickel bimetallic clusters. *Tetrahedron Letters* **1996,** *37* (26), 4499-4502.

92.   Li, Y.; Hong, X. M.; Collard, D. M.; El-Sayed, M. A., Suzuki Cross-Coupling Reactions Catalyzed by Palladium Nanoparticles in Aqueous Solution. *Organic Letters* **2000,** *2* (15), 2385-2388.

93.   Kim, M.; Heo, E.; Kim, A.; Park, J. C.; Song, H.; Park, K. H., Synthesis of Pd/SiO2 Nanobeads for Use in Suzuki Coupling Reactions by Reverse Micelle Sol–gel Process. *Catalysis Letters* **2012,** *142*.

94.   Shakeri, M.; Tai, C.-w.; Göthelid, E.; Oscarsson, S.; Bäckvall, J.-E., Small Pd Nanoparticles Supported in Large Pores of Mesocellular Foam: An Excellent Catalyst for Racemization of Amines. *Chemistry-A European Journal* **2011,** *17* (47), 13269-13273.

95.   Widegren, J. A.; Finke, R. G., A review of soluble transition-metal nanoclusters as arene hydrogenation catalysts. *Journal of Molecular Catalysis A: Chemical* **2003,** *191* (2), 187-207.

96.   Roucoux, A., Stabilized Noble Metal Nanoparticles: An Unavoidable Family of Catalystsfor Arene Derivative Hydrogenation. In *Surface and Interfacial Organometallic Chemistry and Catalysis*, Copéret, C.; Chaudret, B., Eds. Springer Berlin Heidelberg: Berlin, Heidelberg, 2005; pp 261-279.

97.   Roucoux, A.; Schulz, J.; Patin, H., Reduced Transition Metal Colloids: A Novel Family of Reusable Catalysts? *Chemical Reviews* **2002,** *102* (10), 3757-3778.

98.   Gual, A.; Godard, C.; Castillón, S.; Claver, C., Soluble transition-metal nanoparticles-catalysed hydrogenation of arenes. *Dalton Transactions* **2010,** *39* (48), 11499-11512.

99.   Schauermann, S.; Nilius, N.; Shaikhutdinov, S.; Freund, H. J., Nanoparticles for heterogeneous catalysis: new mechanistic insights. *Accounts of Chemical Research* **2013,** *46* (8), 1673-81.

100.   Astruc, D.; Lu, F.; Aranzaes, J. R., Nanoparticles as recyclable catalysts: the frontier between homogeneous and heterogeneous catalysis. *Angewandte Chemie International Edition* **2005,** *44* (48), 7852-72.

101.   Jacimovic, Z.; Evans, I.; Howard, J.; Jevtovic, V.; Leovac, V., Synthesis and characterizations of new binuclear Cu I , Cu II and Co II complexes with 3,5-dimethyl-1-thiocarboxamide pyrazole. *Acta Crystallographica Section A-***2004,** *60*.

102.   Bönnemann, H.; Braun, G.; Brijoux, W.; Brinkmann, R.; Tilling, A. S.; Seevogel, K.; Siepen, K., Nanoscale colloidal metals and alloys stabilized by solvents and surfactants Preparation and use as catalyst precursors. *Journal of Organometallic Chemistry* **1996,** *520* (1), 143-162.

103.   Yu, W.; Liu, M.; Liu, H.; Zheng, J., Preparation of Polymer-Stabilized Noble Metal Colloids. *Journal of Colloid Interface Science* **1999,** *210* (1), 218-221.

104.   Liu, M.; Yu, W.; Liu, H., Selective hydrogenation of o-chloronitrobenzene over polymer-stabilized ruthenium colloidal catalysts. *Journal of Molecular Catalysis A: Chemical* **1999,** *138* (2), 295-303.

105. Legrand, J.; Gota, S.; Guittet, M. J.; Petit, C., Synthesis and XPS Characterization of Nickel Boride Nanoparticles. *Langmuir* **2002,** *18* (10), 4131-4137.

106. Jansat, S.; Gómez, M.; Philippot, K.; Muller, G.; Guiu, E.; Claver, C.; Castillón, S.; Chaudret, B., A Case for Enantioselective Allylic Alkylation Catalyzed by Palladium Nanoparticles. *Journal of the American Chemical Society* **2004,** *126* (6), 1592-1593.

107. Villa, A.; Dimitratos, N.; Chan-Thaw, C. E.; Hammond, C.; Veith, G. M.; Wang, D.; Manzoli, M.; Prati, L.; Hutchings, G. J., Characterisation of gold catalysts. *Chemical Society Reviews* **2016,** *45* (18), 4953-94.

108. Morsbach, E.; Spéder, J.; Arenz, M.; Brauns, E.; Lang, W.; Kunz, S.; Bäumer, M., Stabilizing catalytically active nanoparticles by ligand linking: toward three-dimensional networks with high catalytic surface area. *Langmuir* **2014,** *30* (19), 5564-73.

109. Villa, A.; Schiavoni, M.; Prati, L., Material science for the support design: a powerful challenge for catalysis. *Catalysis Science & Technology* **2012,** *2* (4), 673-682.

110. Smith, D. K.; Korgel, B. A., The importance of the CTAB surfactant on the colloidal seed-mediated synthesis of gold nanorods. *Langmuir* **2008,** *24* (3), 644-9.

111. Baygazieva, E.; Yesmurzayeva, N.; Tatykhanova, G.; Mun, G.; Khutoryanskiy, V.; Kudaibergenov, S., Polymer Protected Gold Nanoparticles: Synthesis, Characterization , and Application in Catalysis. *International Journal of Biology and Chemistry* **2014,** *7*.

112. Crooks, R. M.; Zhao, M.; Sun, L.; Chechik, V.; Yeung, L. K., Dendrimer-encapsulated metal nanoparticles: synthesis, characterization, and applications to catalysis. *Accounts of Chemical Research* **2001,** *34* (3), 181-90.

113. Yan, N.; Yang, X.; Fei, Z.; Li, Y.; Kou, Y.; Dyson, P., Solvent-Enhanced Coupling of Sterically Hindered Reagents and Aryl Chlorides using Functionalized Ionic Liquids. *Organometallics* **2009,** *28*.

114. Neouze, M.-A.; Schubert, U., Surface Modification and Functionalization of Metal and Metal Oxide Nanoparticles by Organic Ligands. *Monatshefte für Chemie - Chemical Monthly* **2008,** *139* (3), 183-195.

115. Prati, L.; Villa, A., Gold colloids: from quasi-homogeneous to heterogeneous catalytic systems. *Accounts of Chemical Research* **2014,** *47* (3), 855-63.

116. Li, D.; Wang, C.; Tripkovic, D.; Sun, S.; Markovic, N. M.; Stamenkovic, V. R., Surfactant Removal for Colloidal Nanoparticles from Solution Synthesis: The Effect on Catalytic Performance. *American Chemical Society: Catalysis* **2012,** *2* (7), 1358-1362.

117. Campisi, S.; Chan-Thaw, C. E.; Wang, D.; Villa, A.; Prati, L., Metal nanoparticles on carbon-based supports: The effect of the protective agent removal. *Catalysis Today* **2016,** *278*, 91-96.

118. Yan, W.; Ma, Z.; Mahurin, S.; Jiao, J.; Hagaman, E.; Overbury, S.; Dai, S., Novel $Au/TiO_2/Al_2O_3 \cdot xH_2O$ catalysts for CO oxidation. *Catalysis Letters* **2008,** *121*, 209-218.

119. Chen, J. I.; Loso, E.; Ebrahim, N.; Ozin, G. A., Synergy of slow photon and chemically amplified photochemistry in platinum nanocluster-loaded inverse titania opals. *Journal of American Chemical Society* **2008,** *130* (16), 5420-1.

120. Albers, P.; Seibold, K.; McEvoy, A. J.; Kiwi, J., High-dispersion d.c. sputtered platinum-titania powder catalyst active in ethane hydrogenolysis. *The Journal of Physical Chemistry* **1989,** *93* (4), 1510-1515.

121. Li, J.; Zeng, H. C., Preparation of Monodisperse Au/TiO2 Nanocatalysts via Self-Assembly. *Chemistry of Materials* **2006,** *18* (18), 4270-4277.

122. Lin, C.-H.; Chao, J.-H.; Liu, C.-H.; Chang, J.-C.; Wang, F.-C., Effect of Calcination Temperature on the Structure of a Pt/TiO2 (B) Nanofiber and It's Photocatalytic Activity in Generating H2. *Langmuir* **2008,** *24* (17), 9907-9915.

123. Niu, F.; Liu, C.-C.; Cui, Z.-M.; Zhai, J.; Jiang, L.; Song, W.-G., Promotion of organic reactions by interfacial hydrogen bonds on hydroxyl group rich nano-solids. *Chemical Communications* **2008,** (24), 2803-2805.

124. Peng, K. Q.; Hu, J. J.; Yan, Y. J.; Wu, Y.; Fang, H.; Xu, Y.; Lee, S. T.; Zhu, J., Fabrication of Single-Crystalline Silicon Nanowires by Scratching a Silicon Surface with Catalytic Metal Particles. *Advanced Functional Materials* **2006,** *16* (3), 387-394.

125. Peng, K.-Q.; Yan, Y.-J.; Gao, S.-P.; Zhu, J., Synthesis of Large-Area Silicon Nanowire Arrays via Self-Assembling Nanoelectrochemistry. *Advanced Materials* **2002,** *14* (16), 1164-1167.

126. Liu, Z.; Sun, Z., Green solvent-based approaches for synthesis of nanomaterials. *Science China Chemistry* **2010,** *53* (2), 372-382.

127. Zhang, Q.; Su, H.; Luo, J.; Wei, Y., "Click" magnetic nanoparticle-supported palladium catalyst: a phosphine-free, highly efficient, and magnetically recoverable catalyst for Suzuki–Miyaura coupling reactions. *Catalysis Science & Technology* **2013,** *3* (1), 235-243.

128. Wang, J.; Song, G.; Peng, Y., Reusable Pd nanoparticles immobilized on functional ionic liquid co-polymerized with styrene for Suzuki reactions in water-ethanol solution. *Tetrahedron Letters* **2011,** *52* (13), 1477-1480.

129. Yu, Y.; Hu, T.; Chen, X.; Xu, K.; Zhang, J.; Huang, J., Pd nanoparticles on a porous ionic copolymer: a highly active and recyclable catalyst for Suzuki–Miyaura reaction under air in water. *Chemical Communications* **2011,** *47* (12), 3592-3594.

130. Kashin, A. N.; Panchuk, D. A.; Yarysheva, L. M.; Volynskii, A. L.; Beletskaya, I. P., Preparation of an active Suzuki-Miyaura catalyst from nanoparticles obtained by deposition of palladium onto a polyvinyl alcohol support. *Russian Journal of Organic Chemistry* **2011,** *47* (1), 48-53.

131. Narayanan, R.; El-Sayed, M. A., Carbon-supported spherical palladium nanoparticles as potential recyclable catalysts for the Suzuki reaction. *Journal of Catalysis* **2005,** *234* (2), 348-355.

132. Mahouche Chergui, S.; Ledebt, A.; Mammeri, F.; Herbst, F.; Carbonnier, B.; Ben Romdhane, H.; Delamar, M.; Chehimi, M. M., Hairy carbon nanotube@nano-Pd heterostructures: design, characterization, and application in Suzuki C-C coupling reaction. *Langmuir : the ACS journal of Surfaces and Colloids* **2010,** *26* (20), 16115-16121.

133. Bernini, R.; Cacchi, S.; Fabrizi, G.; Forte, G.; Petrucci, F.; Prastaro, A.; Niembro, S.; Shafir, A.; Vallribera, A., Perfluoro-tagged, phosphine-free palladium nanoparticles supported on silica gel: application to alkynylation of aryl halides, Suzuki–Miyaura cross-coupling, and Heck reactions under aerobic conditions. *Green Chemistry* **2010,** *12* (1), 150-158.

134. Moradi, R.; Ziarani, G.; Badiei, A.; Mohajer, F., Synthesis and characterization of mesoporous organosilica supported palladium (SBA-Pr-NCQ-Pd) as an efficient nanocatalyst in the Mizoroki–Heck coupling reaction. *Applied Organometallic Chemistry* **2020,** *34*.

135. Liu, M.; ZhixinJia; Jia, D.; Zhou, C., Recent Advance in Research on Halloysite Nanotubes-Polymer Nanocomposite. *Progress in Polymer Science* **2014,** *39*.

136. Saif, M. J.; Asif, H. M.; Naveed, M., Properties and Modification Methods of Halloysite Nanotubes: A State-of-the-Art Review.*Journal of the Chilean Chemical Society* **2018,** *63*, 4109-4125.

137. Joussein, E.; Petit, S.; Churchman, J.; Theng, B.; Righi, D.; Delvaux, B., Halloysite clay minerals — a review. *Clay Minerals* **2005,** *40* (4), 383-426.

138. Sadjadi, S.; Malmir, M.; Lazzara, G.; Cavallaro, G.; Heravi, M. M., Preparation of palladated porous nitrogen-doped carbon using halloysite as porogen: disclosing its utility as a hydrogenation catalyst. *Scientific Reports* **2020,** *10* (1), 2039.

139. Sadjadi, S.; Akbari, M.; Monflier, E.; Heravi, M. M.; Leger, B., Pd nanoparticles immobilized on halloysite decorated with a cyclodextrin modified melamine-based polymer: a promising heterogeneous catalyst for hydrogenation of nitroarenes. *New Journal of Chemistry* **2018,** *42* (19), 15733-15742.

140. Massaro, M.; Colletti, C. G.; Buscemi, G.; Cataldo, S.; Guernelli, S.; Lazzara, G.; Liotta, L. F.; Parisi, F.; Pettignano, A.; Riela, S., Palladium nanoparticles immobilized on halloysite nanotubes covered by a multilayer network for catalytic applications. *New Journal of Chemistry* **2018,** *42* (16), 13938-13947.

141. Zhang, H., Selective modification of inner surface of halloysite nanotubes: a review. *Nanotechnology Reviews* **2017,** *6* (6), 573-581.

142. Asadi, S.; Sedghi, R.; Heravi, M. M., Pd Nanoparticles Immobilized on Supported Magnetic GO@PAMPS as an Auspicious Catalyst for Suzuki–Miyaura Coupling Reaction. *Catalysis Letters* **2017,** *147* (8), 2045-2056.

143. Rostamzadeh, T.; Islam Khan, M. S.; Riche', K.; Lvov, Y. M.; Stavitskaya, A. V.; Wiley, J. B., Rapid and Controlled In Situ Growth of Noble Metal Nanostructures within Halloysite Clay Nanotubes. *Langmuir* **2017,** *33* (45), 13051-13059.

144. Glotov, A.; Levshakov, N.; Stavitskaya, A.; Artemova, M.; Gushchin, P.; Ivanov, E.; Vinokurov, V.; Lvov, Y., Templated self-assembly of ordered mesoporous silica on clay nanotubes. *Chemical Communications* **2019,** *55* (38), 5507-5510.

145. Cookson, J., The Preparation of Palladium Nanoparticles. *Platinum Metals Review* **2012,** *56* (2), 83-98.

146. Graham, L.; Collins, G.; Holmes, J. D.; Tilley, R. D., Synthesis and catalytic properties of highly branched palladium nanostructures using seeded growth. *Nanoscale* **2016,** *8* (5), 2867-2874.

147. Stolaś, A.; Darmadi, I.; Nugroho, F. A. A.; Moth-Poulsen, K.; Langhammer, C., Impact of Surfactants and Stabilizers on Palladium Nanoparticle–Hydrogen Interaction Kinetics: Implications for Hydrogen Sensors. *ACS Applied Nano Materials* **2020,** *3* (3), 2647-2653.

148. Kim, H.-s.; Seo, Y. S.; Kim, K.; Han, J. W.; Park, Y.; Cho, S., Concentration Effect of Reducing Agents on Green Synthesis of Gold Nanoparticles: Size, Morphology, and Growth Mechanism. *Nanoscale Research Letters* **2016,** *11* (1), 230.

149. Zhang, L.; Wang, L.; Jiang, Z.; Xie, Z., Synthesis of size-controlled monodisperse Pd nanoparticles via a non-aqueous seed-mediated growth. *Nanoscale research letters* **2012,** *7* (1), 312-312.

150. Kim, S.-W.; Park, J.; Jang, Y.; Chung, Y.; Hwang, S.; Hyeon, T.; Kim, Y. W., Synthesis of Monodisperse Palladium Nanoparticles. *Nano Letters* **2003,** *3* (9), 1289-1291.

151. Johansson Seechurn, C. C.; Kitching, M. O.; Colacot, T. J.; Snieckus, V., Palladium-catalyzed cross-coupling: a historical contextual perspective to the 2010 Nobel Prize. *Angewandte Chemie International Edition* **2012,** *51* (21), 5062-85.

152. Miller, W. D.; Fray, A. H.; Quatroche, J. T.; Sturgill, C. D., Suppression of a Palladium-Mediated Homocoupling in a Suzuki Cross-Coupling Reaction. Development of an Impurity Control Strategy Supporting Synthesis of LY451395. *Organic Process Research & Development* **2007,** *11* (3), 359-364.

153. La Sorella, G.; Strukul, G.; Scarso, A., Recent advances in catalysis in micellar media. *Green Chemistry* **2015,** *17* (2), 644-683.

Chapter 4

Pd@Hal Nanocomposite as A Catalyst for the Hydrogenation of Alkenes/Alkynes, and Nitro Compounds

4.1 Abstract

Pd@Hal (Pd content was 4.3% wt/wt) was shown to be useful as a hydrogenation catalyst for the selective reduction of aromatic nitro compounds. Preliminary studies with cinnamic acid and diphenyl acetylene afforded the hydrogenation products at ambient temperature and pressure (1 atm H_2) in ethanol: water (2:4). A catalyst loading of the Pd@Hal 10% wt/wt relative to the alkene/alkyne (0.4% Pd/starting material, %wt/wt) afforded the corresponding saturated analogs in nearly quantitative yields. The Pd@Hal catalyst was easily recovered and recycled with minimum loss of catalytic activity. Subsequent studies demonstrated that Pd@Hal catalyzed the hydrogenation of a series of aromatic nitro compounds to furnish the corresponding aromatic amino compounds in high yield.

4.2   Introduction

4.2.1   Hydrogenation of Nitro Compounds

Aromatic and heterocyclic amines are fundamental building blocks in industrial-scale organic synthesis, as they are extensively used as intermediates for the production of various dyes, pharmaceuticals, pigments, and polymers.[1, 2] Nitro compounds are versatile building blocks in organic transformations, as shown in **Figure 1**.[3-6]

Figure 1. Nitro compound platforms in organic synthesis.
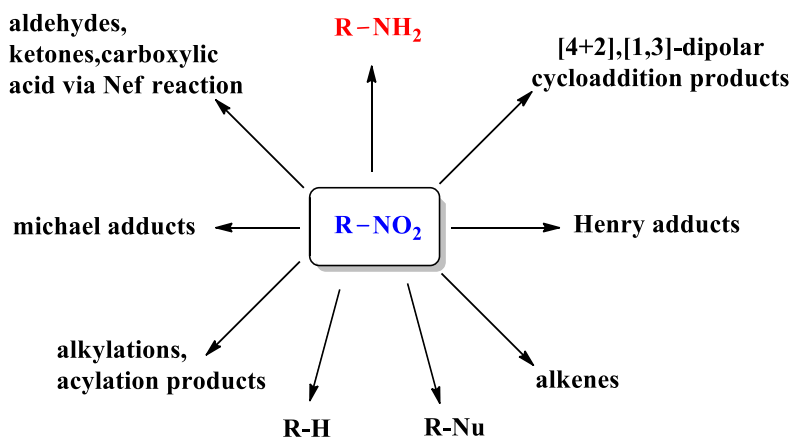
Reduction of nitro compounds to amines have been carried out under hydrogenation, electron-transfer, electrochemical, and hydride-transfer conditions.[7] Classical methods for the preparation of amines involve the reduction of the corresponding nitro compounds by the use of stoichiometric Fe^{8-10} or $Zn^{11, 12}$ reagents in the presence of various proton sources, or by other catalytic protocols employing toxic reducing agents, such as H_2S,[13] N_2H_4,[14-16] or $NaBH_4$.[17-19]

During the past decades, catalytic hydrogenation protocols utilizing Pd/C, Pt/C, or Raney Ni as catalysts have become the methods of choice for the reduction of nitro compounds.[20] Palladium on charcoal catalyzed hydrogenation of nitro compounds using triethylammonium formate as the hydrogen source at elevated reaction temperatures **Scheme 1**.[21]

Scheme 1 Reduction of aromatic nitro compounds with triethylammonium formate.
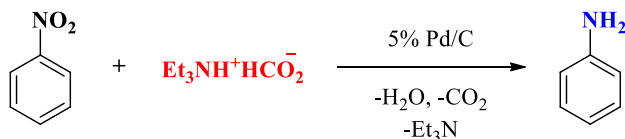
Hydrogenation of mono- and poly- nitroaromatics can also be achieved in high yields using Pd/C catalyst via hydrogen transfer from cyclohexene in ethanol under reflux conditions **Scheme 2**.[22]

Scheme 2. Nitro compounds reduced by transfer hydrogenation.
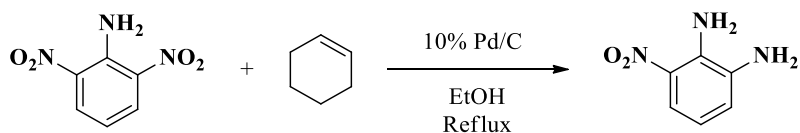
Recently, Shi *et al*. have reported the reduction of nitroarenes over nickel-iron mixed oxide catalyst using hydrazine hydrate under reflux conditions **Scheme 3**.[23, 24] A facile selective reduction of nitro compounds catalyzed by $HCOONH_4$-Cu nanoparticles (NPs) has also appeared in the recent literature. [24]

Scheme 3. Reduction of nitro compounds using Fe and Cu NPs.

R = CHO, COMe, CO$_2$Me, COOH, CONH$_2$, CN, N$_3$, Br, Cl, SCN
These easily reducible functionalities remained unaffected
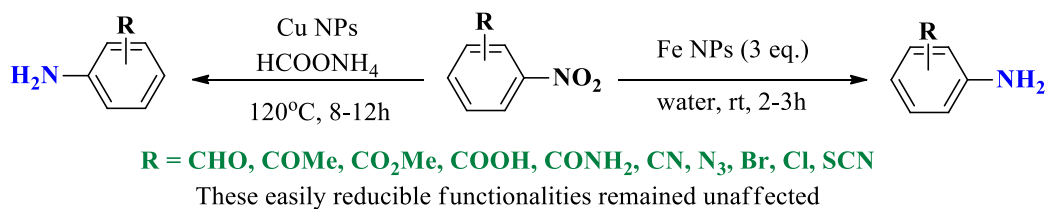
However, one critical limitation of these processes is that the active catalysts are flammable and can readily ignite, making them air sensitive. This limitation can also present additional handling problems. Although these heterogeneous catalysts generally display good nitro group reduction, they are unfortunately associated with chemoselectivity issues if other reducible groups are present in the substrate. In addition, the reduction of aromatic nitro compounds often stops at an intermediate stage, yielding hydroxylamines, hydrazines, and azoarene products.[25] Thus, high temperatures, high pressures, and longer reaction times typically accompany the reductions of the nitro compounds to drive the reactions to the corresponding amines. Therefore, significant attention has been dedicated to the development of new catalytic hydrogenation systems that display higher selectivity towards the complete and efficient reduction of nitro functionality. [20, 26-28]

4.2.2   Nanoparticle-Based Hydrogenation Catalysts

More recently, metal-nanoparticle-based catalysts have emerged as attractive and green alternatives for the hydrogenation of nitro compounds. These systems have exhibited excellent activities and selectivity under mild reaction conditions and low H$_2$ pressures.[29-32] In addition, heterogeneously supported nanocatalysts offer several practical advantages, such as more

straightforward procedures for separation and recycling of the catalyst and reduced levels of metal impurities in the final products, making these catalysts attractive from an economic and environmental point view. It is well known that the catalytic properties of heterogeneous catalysts depend on the metal particle size and the support surface structure.[33-35] Several research groups have reported the catalytic activities of various palladium and other transition metal nanostructured materials [36-40] supported mainly on polymeric matrixes, which have superior or at least comparable catalytic activities to bulk metal catalysts. Vehro coworkers recently reported developing a heterogeneous catalyst comprised of Pd nanoparticles immobilized on amino-functionalized siliceous mesocellular foam (Pd0 – AmP–MCF) and its successful application in a wide range of organic transformations.[29, 41, 42] In all cases, the Pd nanocatalyst exhibited excellent activity and recyclability. The reduction of nitrobenzene to aniline using (polymer-anchored anthranilic acid-PdCl$_2$ complexes) under high pressures of 500–800 psi at 70–100°C was reported in the literature.[43-45] As illustrated in **Scheme 4**, Pt nanoparticles on CNFs (Pt/CNFs) were reported to be efficient hydrogenation catalysts for the reduction of nitroarenes to anilines without affecting the reduction of halogen or other functional groups.[46]

Scheme 4. Reduction of nitroarenes to anilines using Pt NPs on CNFs support.

X = Br, Cl, I, CONH$_2$, CO$_2$R, COR, OH, OBn
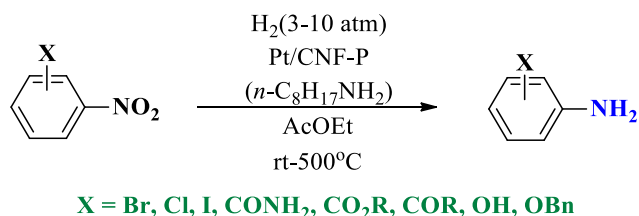
Despite the wide use of several such procedures, environmental concerns, the demands of combinatorial syntheses, and/or functional group compatibility issues continue to drive the development of new reduction methods. In this respect, there is a strong motivation to develop new simple, efficient, easily handled procedures that can allow the for highly chemo- and regioselective reduction of the nitro group under mild conditions.

4.3   Result and Discussion

4.3.1   Pd@Hal Hydrogenation of Cinnamic Acid/Dihenylacetylene

As summarized in **Table 1**, preliminary studies with cinnamic acid and diphenylacetylene afforded quantitative yields of hydrogenation products at ambient temperature using and pressure (1 atm H_2) in various solvents, including ethanol and water. The Pd@Hal nanocomposite Pd content was 4.3%, and the loading of nanocomposite used was 10% wt/wt relative to the alkene/alkyne (0.4% Pd/alkene, %wt/%wt). The hydrogenations were equally effective using water or ethanol as the solvent.

Table 1. Preliminary studies with cinnamic acid and diphenylacetylene.
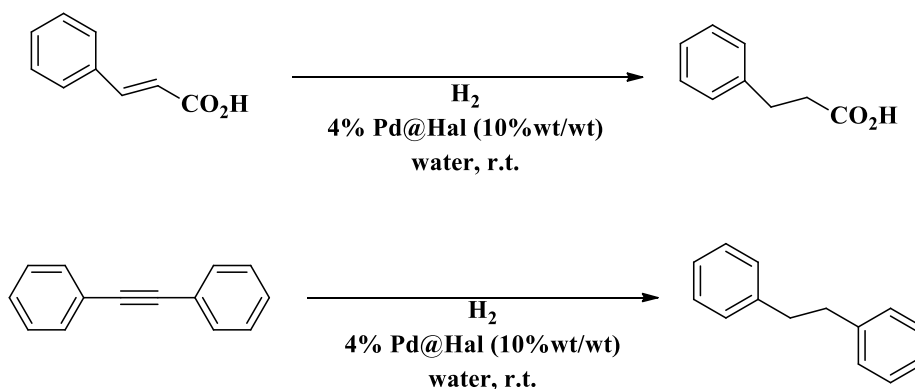
Entry	Alkene/Alkyne	Solvent	Yield (%)
1	Cinnamic acid	EtOH	100
2	Cinnamic acid	Water	98
3	Diphenylacetylene	EtOH	97
4	Diphenylacetylene	Water	88

4.3.2   Recycling Investigation

After the initial hydrogenation of cinnamic acid and diphenylacetylene, the Pd@Hal catalyst was recovered by simple filtration. The catalyst was washed and dried. It could then be reused without loss of activity or structural change to the nanocomposite. **Table 2**. summarizes the recycling studies. In both reactions, the catalyst could recycle with minimum loss of catalytic activity. It was not until the in-5th cycle that significantly diminished yields were observed for each compound.

Table 2. Hydrogenation recycling investigation.

alkene/alkyne/solvent	cycle	conversion (%)
cinnamic acid/H_2O	1	100
	2	98
	3	95
	4	86
	5	82
diphenylacetylene/H_2O	1	97
	2	92
	3	87
	4	87
	5	84

Figure 2. TEM image of Pd@Hal nanocomposite before use
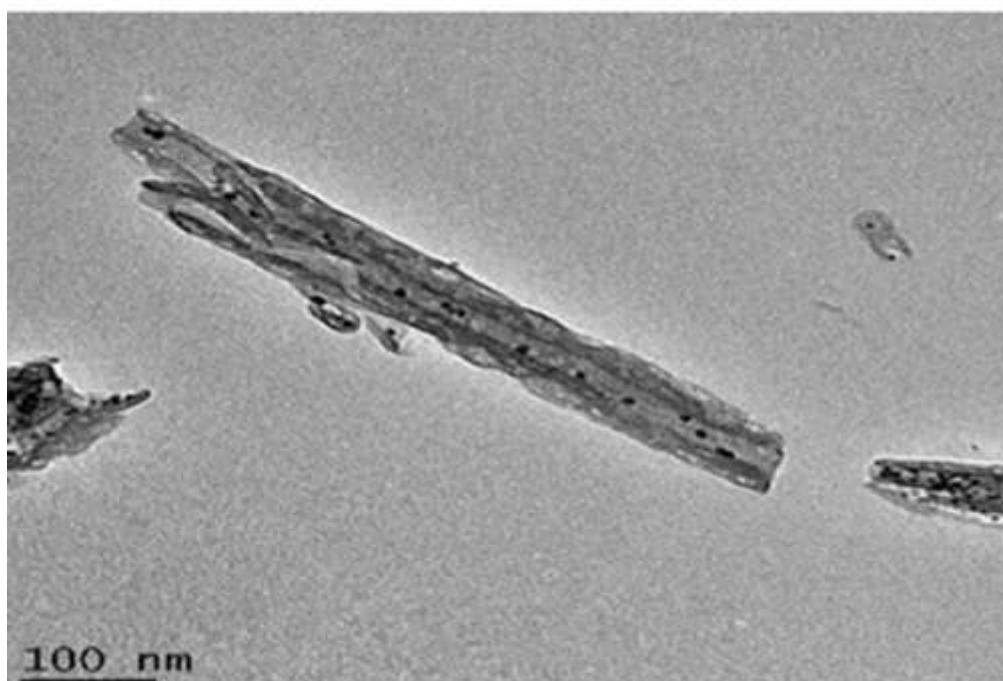
Figure 3. TEM image of Pd@Hal nanocomposite after use
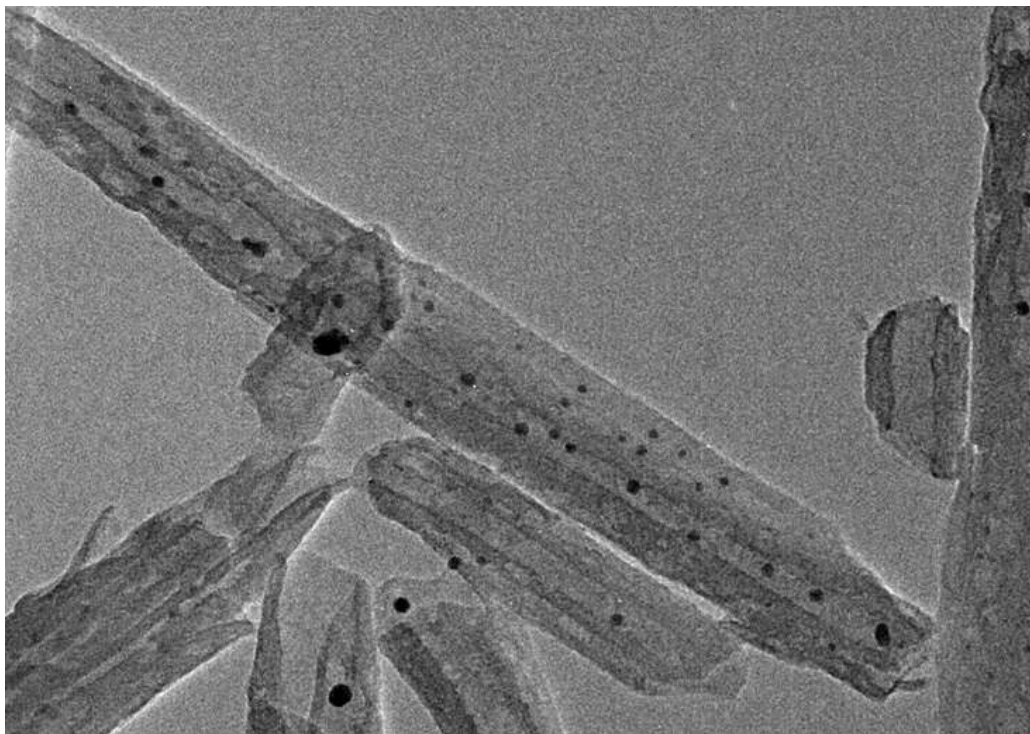
To further demonstrate this utility of the Pd@Hal catalyst system for the hydrogenation reaction, the reduction of a series of substituted nitrobenzenes was investigated. As summarized in **Scheme 5**, the Pd@Hal catalyst demonstrated high reactivity and selectivity in the presence of a variety of functional groups to afford the substituted anilines in excellent yields under very mild conditions. In all examples, product formation began immediately, and within 8h, the starting nitro group was fully reduced to the amine. The reaction conditions equally tolerated both hydrophobic and hydrophilic substrates. It is noteworthy that the reduction of the nitro group proceeded without affecting the reduction of halogen or other functional groups.

Scheme 5. Nitro-compound hydrogenation using Pd@Hal.

compound	product	yield (%)	compound	product	yield (%)
		99			99
		86			99
		92			91
		99			99
		99			98
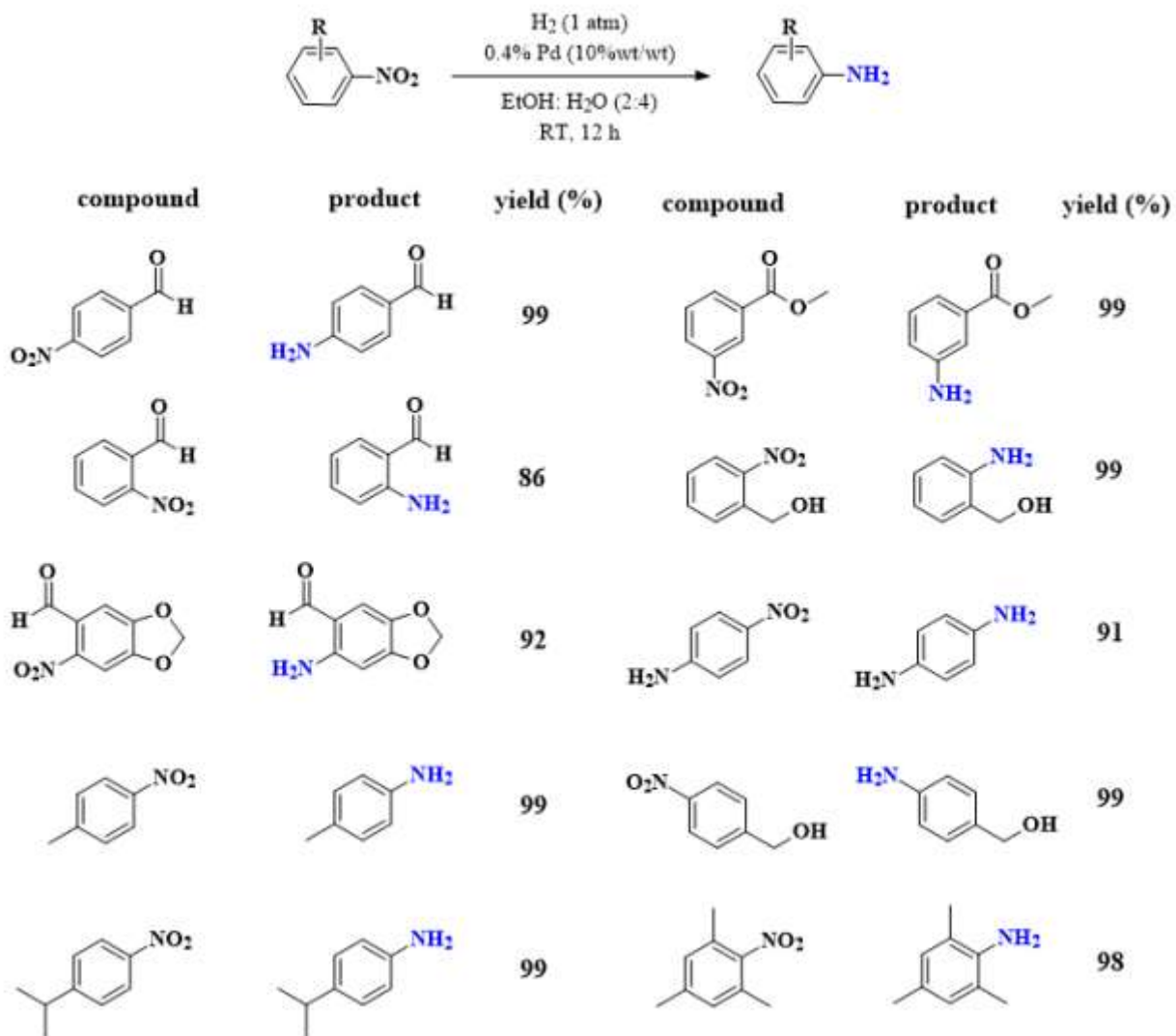
4.4   Conclusion

In conclusion, a reproducible method for the preparation of a new transition metal catalyst system based on Pd@halloysite nanocomposites has been developed. These nanocomposite materials are an efficient catalyst for the hydrogenation of various aromatic nitro compounds under ambient conditions. The catalyst is recoverable and recyclable without significant loss of catalytic activity. Furthermore, the catalyst proved to be robust and stable. The Pd@Hal nanocomposite is a new heterogenous catalyst for palladium-catalyzed reactions. This nanocomposite material is a cost-effective, highly efficient, recyclable, and environmentally friendly prototypical transition metal nanoparticle catalyst with a broadening scope of synthetic utility.

4.5   Experimental

4.5.1   Materials and Methods

All reactions were carried out in oven-dried glassware under a H_2 atmosphere unless indicated otherwise. Halloysite clay was purchased from Sigma Aldrich. All other chemicals were purchased from Alfa Aesar, Sigma Aldrich, and VWR. Halloysite was purchased from Sigma Aldrich. All chemicals were used as received without further purification. ^{1}H and ^{13}C NMR spectra were recorded at r.t. in $CDCl_3$ on a Bruker 300 MHz instrument operating at a frequency of 300 and 400 MHz for ^{1}H NMR and 75 MHz for ^{13}C NMR. ^{1}H chemical shifts were referenced to the $CDCl_3$ solvent signal (7.26 ppm). ^{13}C chemical shifts were referenced to the $CDCl_3$ solvent signal (77.0 ppm). Pd_{NP} size was determined from TEM images obtained on a

JEOL 2010 equipped with an EDAX genesis energy dispersive spectroscopy (EDS) system, operated at an accelerating voltage of 200 kV an emission current of 109 μA. ICP- AES analysis of the Pd@Hal was performed by Galbraith Laboratories, Inc., Knoxville, TN.

4.5.2   Synthesis of 4% Pd@Hal.

A solution of $Pd(OAc)_2$ (60 mg, 0.26 mmol) in deionized water (10 mL) was prepared in a 50 mL Erlenmeyer flask. A solution of L-sodium ascorbate (1400 mg, 7.0 mmol) in deionized water (15 mL) was added to the palladium acetate solution, followed by the addition of a solution of trisodium citrate (570 mg, 2.7 mmol) in deionized water (10 mL). The combined solution was allowed to stir for 15 min at room temperature. During the first 10 minutes, the palladium acetate solution mixture's initial light orange color turned black, indicating Pd nanoparticles' formation. After 15 min, no more color changes were observed, and the solution was left to rest at room temperature, open to air for 80 min. Halloysite (600 mg, 2.0 mmol) was added to the Pd nanoparticle solution, and the colloid mixture was stirred for 15 min. The mixture was then allowed to rest at room temperature for 10 min. The mixture was centrifuged (6000 rpm), and the liquid was decanted away from the solid residue. The residue was washed with deionized water (3 x 15 mL) and isopropyl alcohol (3 x 15 mL). The resultant powder was dried at room temperature for 24 h in a desiccator ($CaSO_4$) to afford 4% Pd@Hal as a gray powder (620 mg).

4.5.3   General Procedure for Hydrogenation of Nitro-Compounds

To a 10 mL round bottom flask equipped with a magnetic stir bar and a nitrogen inlet balloon, the nitro compound (1.0, mmol) was added. The reaction mixture was flushed with nitrogen, followed by the addition of EtOH (4.0 mL) via syringe. The reaction mixture was allowed to stir for 5 min allowing the complete dissolution of all solids. The

4% Pd@Hal (0.4% wt/wt) catalyst was dissolved in (2.0 mL) of DI water; the solution was sonicated (10 min) to ensure dispersion, then added to the reaction mixture via syringe. The reaction was placed under H_2 (1 atm). The reaction flask was sonicated for 10 mins then allowed to stir at room temperature. The reaction progress was monitored by TLC. Typically, after 8 h, the catalyst was recovered by vacuum filtration. The Pd@Hal was rinsed with EtOH (10 mL) followed by DI water (4.0 mL) and dried in a desiccator ($CaSO_4$). The solvent was removed under vacuum to afford reduced aniline product. TLC and NMR established purity. All products are known compounds unless otherwise indicated, and spectral data were identical to those reported in the literature.

4.5.4   Pd@Hal Recovery Procedure:

The Pd@Hal was removed from the filter paper and added to a beaker with EtOH (20 mL), then sonicated for 10 mins. The solid was then centrifuged down and then washed again with (15 mL) DI water followed by (15 mL) isopropyl alcohol. The solid was dried in a desiccator ($CaSO_4$) overnight or in an oven at 120° for 20 mins before each subsequent cycle.

Due to loss of material during each cycle's recovery procedure, it was necessary to adjust the reagent amounts. A consistent catalyst was loading of 4% (wt/wt) Pd@Hal/alkene/alkyne was maintained.

4.5.5.   Characterization of Hydrogenation Products (Scheme 5).

All the products are known compounds, and the spectral data were identical to those reported in the literature. ^{1}H NMR spectra were identical to spectra in the Spectral Database for organic compounds. SDBSWeb: https://sdbs.db.aist.go.jp (National Institute of Advanced Industrial Science and Technology)

4-toluidine [106-49-0]
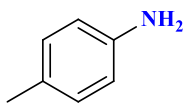
Light yellow solid (89 mg, 83%).

^{1}H NMR (400 MHz, CDCl$_3$) δ: 7.04 (d, J = 7.5 Hz, 2H), 6.67 (d, J= 6.7 Hz, 2H), 3.56 (s, 2H, -NH2), 2.32 (s, 3H)

Cumidine [99-88-7]
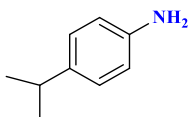
Light yellow solid (156 mg, 99%).

^{1}H NMR (400 MHz, CDCl$_3$) δ: 7.02 (d, J=8.0 Hz, 2H), 6.63 (d, J=8.0 Hz, 2H), 3.27 (s, 2H), 2.84 – 2.75 (m, 1H), 1.20 (d, J=6.8 Hz, 6H)

4-amino benzaldehyde [556-18-3]
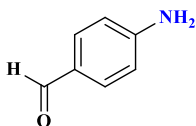
Orange solid (125 mg, 99%).

^{1}H NMR (300 MHz, CDCl$_3$) δ: 6.66 (d, J = 8.4 Hz, 2H), 7.57 (d, J = 8.4 Hz, 2H), 9.61 (s,1H).

1,4-benzenediamine [106-50-3]
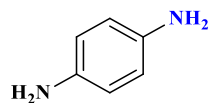
Dark purple solid (83 mg, 77%).

^{1}H NMR (400 MHz, CDCl$_3$) δ: 6.57 (s, 4H), 3.32 (s, 4H).

6-Amino-1,3-benzodioxole-5-carbaldehyde [23126-68-3]
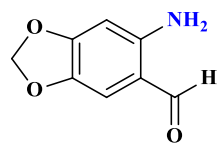
Red solid (152 mg, 92%).

^{1}H NMR (300 MHz, CDCl$_3$) δ: 9.53 (s, 1H), 6.74 (s, 1H), 6.22 (s, 2H), 6.07 (s, 1H), 5.85 (s, 2H).

Methyl 3-aminobenzoate [4518-10-9]
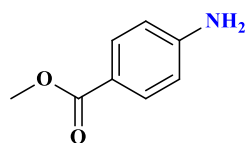
Light orange solid (182 mg, 99%).

^{1}H NMR (300 MHz, CDCl$_3$) δ: 7.43 (d, J = 7.7 Hz, 1H), 7.36 (s, 1H), 7.28 – 7.15 (m, 1H), 6.87 (d, J = 10.3 Hz, 1H), 3.89 (s, 3H), 3.14 (s, 2H).

2-amino benzyl alcohol [5344-90-1]
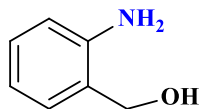
Light orange solid (134 mg, 99%).

^{1}H NMR (400 MHz, DMSO-d_6) δ: 4.40 (d, J = 5.4 Hz, 2H), 4.91 (s, 2H), 5.01 (t, J = 5.4 Hz, 1H), 6.54 (t, J = 7.4 Hz, 1H), 6.64 (d, J = 7.4 Hz, 1H), 6.98 (t, J = 7.4 Hz, 1H), 7.07 (d, J = 7.4 Hz, 1H).

4-amino benzyl alcohol [623-04-1]
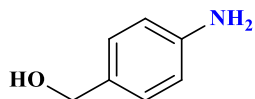
Dark orange solid (192 mg, 99%).

^{1}H NMR (400 MHz, DMSO-d_6) δ: 4.31 (d, J= 5.87 Hz, 2H), 4.82 (t, J= 5.6 Hz, 1H), 4.95 (s, 2H), 6.52 (d, J= 8.2 Hz, 2H), 6.98 (d, J= 8.2 Hz, 2H).

Mesodine [88-05-1]
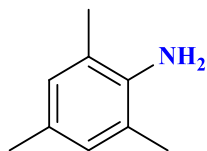
Light orange solid (132 mg, 98%).

^{1}H NMR (400 MHz, CDCl$_3$) δ: 6.76 (s, 2H), 3.43 (s, 2H), 2.20 (s, 3H), 2.15 (s, 6H).

4.6   References

1.   Downing, R. S.; Kunkeler, P. J.; van Bekkum, H., Catalytic syntheses of aromatic amines. *Catalysis Today* **1997,** *37* (2), 121-136.

2.   Besson, M.; Pinel, C., Diastereoselective Heterogeneous Catalytic Hydrogenation of Aromatic or Heteroaromatic Compounds. *Topics in Catalysis* **2003,** *25* (1), 43-61.

3.   The Nitro Group in Organic Synthesis N. Ono. Wiley-VCH: Weinheim. 2001. 372 pp. DM 315. ISBN 0-471-31611-3. *Organic Process Research & Development* **2001,** *5* (6), 668-668.

4.   Pinnick, H. W., The Nef Reaction. In *Organic Reactions*, pp 655-792.

5.   Williams, D. R.; Brugel, T. A., Intramolecular Diels−Alder Cyclizations of (E)-1-Nitro-1,7,9-decatrienes: Synthesis of the AB Ring System of Norzoanthamine. *Organic Letters* **2000,** *2* (8), 1023-1026.

6.   Trost, B. M.; Yeh, V. S. C.; Ito, H.; Bremeyer, N., Effect of Ligand Structure on the Zinc-Catalyzed Henry Reaction. Asymmetric Syntheses of (−)-Denopamine and (−)-Arbutamine. *Organic Letters* **2002,** *4* (16), 2621-2623.

7.   Basu, B.; Das, P.; Das, S., Transfer hydrogenation using recyclable polymer-supported formate (PSF): Efficient and chemoselective reduction of nitroarenes. *Molecular Diversity* **2005,** *9* (4), 259-262.

8.   Liu, Y.; Lu, Y.; Prashad, M.; Repič, O.; Blacklock, T. J., A Practical and Chemoselective Reduction of Nitroarenes to Anilines Using Activated Iron. *Advanced Synthesis & Catalysis* **2005,** *347* (2-3), 217-219.

9.   Desai, D. G.; Swami, S. S.; Dabhade, S. K.; Ghagare, M. G., FeS-NH$_4$Cl-CH$_3$OH-H$_2$O: An Efficient and Inexpensive System for Reduction of Nitroarenes to Anilines. *Synthetic Communications* **2001,** *31* (8), 1249-1251.

10.   Wang, L.; Li, P.; Wu, Z.; Yan, J.; Wang, M.; Ding, Y., Reduction of Nitroarenes to Aromatic Amines with Nanosized Activated Metallic Iron Powder in Water. *Synthesis* **2003,** *2003* (13), 2001-2004.

11.   Kelly, S. M.; Lipshutz, B. H., Chemoselective Reductions of Nitroaromatics in Water at Room Temperature. *Organic Letters* **2014,** *16* (1), 98-101.

12.   Khan, F. A.; Dash, J.; Sudheer, C.; Gupta, R. K., Chemoselective reduction of aromatic nitro and azo compounds in ionic liquids using zinc and ammonium salts. *Tetrahedron Letters* **2003,** *44* (42), 7783-7787.

13. Ratcliffe, C. T.; Pap, G., Catalytic reduction of dinitroaromatic compounds with hydrogen sulphide–carbon monoxide. A novel, low-cost replacement for elemental hydrogen. *Chemical Communications* **1980,** (6), 260-261.

14. Cantillo, D.; Moghaddam, M. M.; Kappe, C. O., Hydrazine-mediated reduction of nitro and azide functionalities catalyzed by highly active and reusable magnetic iron oxide nanocrystals. *Journal of Organic Chemistry* **2013,** *78* (9), 4530-42.

15. Huang, L.; Wang, Z.; Geng, L.; Chen, R.; Xing, W.; Wang, Y.; Huang, J., Selective and recyclable rhodium nanocatalysts for the reductive N-alkylation of nitrobenzenes and amines with aldehydes. *RSC Advances* **2015,** *5* (70), 56936-56941.

16. Kim, S.; Kim, E.; Kim, B. M., Fe3O4 Nanoparticles: A Conveniently Reusable Catalyst for the Reduction of Nitroarenes Using Hydrazine Hydrate. *Chemistry – An Asian Journal* **2011,** *6* (8), 1921-1925.

17. Petkar, D. R.; Kadu, B. S.; Chikate, R. C., Highly efficient and chemoselective transfer hydrogenation of nitroarenes at room temperature over magnetically separable Fe–Ni bimetallic nanoparticles. *RSC Advances* **2014,** *4* (16), 8004-8010.

18. Li, L.; Chen, Z.; Zhong, H.; Wang, R., Urea-Based Porous Organic Frameworks: Effective Supports for Catalysis in Neat Water. *Chemistry-A European Journal* **2014,** *20* (11), 3050-3060.

19. Layek, K.; Kantam, M. L.; Shirai, M.; Nishio-Hamane, D.; Sasaki, T.; Maheswaran, H., Gold nanoparticles stabilized on nanocrystalline magnesium oxide as an active catalyst for reduction of nitroarenes in aqueous medium at room temperature. *Green Chemistry* **2012,** *14* (11), 3164-3174.

20. Blaser, H.-U.; Steiner, H.; Studer, M., Selective Catalytic Hydrogenation of Functionalized Nitroarenes: An Update. *Chemistry Europe Academic Journals: ChemCatChem* **2009,** *1* (2), 210-221.

21. Cortese, N. A.; Heck, R. F., Palladium-catalyzed reductions of halo- and nitroaromatic compounds with triethylammonium formate. *The Journal of Organic Chemistry* **1977,** *42* (22), 3491-3494.

22. Entwistle, I. D.; Johnstone, R. A. W.; Povall, T. J., Selective, rapid transfer-hydrogenation of aromatic nitro-compounds. *Journal of the Chemical Society, Perkin Transactions 1* **1975,** (13), 1300-1301.

23. Dey, R.; Mukherjee, N.; Ahammed, S.; Ranu, B. C., Highly selective reduction of nitroarenes by iron(0) nanoparticles in water. *Chemical Communications* **2012,** *48* (64), 7982-7984.

24. Saha, A.; Ranu, B., Highly Chemoselective Reduction of Aromatic Nitro Compounds by Copper Nanoparticles/Ammonium Formate. *The Journal of Organic Chemistry* **2008,** *73* (17), 6867-6870.

25. Yu, C.; Liu, B.; Hu, L., Samarium(0) and 1,1'-Dioctyl-4,4'-Bipyridinium Dibromide: A Novel Electron-Transfer System for the Chemoselective Reduction of Aromatic Nitro Groups. *The Journal of Organic Chemistry* **2001,** *66* (3), 919-924.

26. Jagadeesh, R. V.; Surkus, A. E.; Junge, H.; Pohl, M. M.; Radnik, J.; Rabeah, J.; Huan, H.; Schünemann, V.; Brückner, A.; Beller, M., Nanoscale Fe2O3-based catalysts for selective hydrogenation of nitroarenes to anilines. *Science* **2013,** *342* (6162), 1073-6.

27. Cárdenas-Lizana, F.; de Pedro, Z. M.; Gómez-Quero, S.; Keane, M. A., Gas phase hydrogenation of nitroarenes: A comparison of the catalytic action of titania supported gold and silver. *Journal of Molecular Catalysis A: Chemical* **2010,** *326* (1), 48-54.

28. Chernichenko, K.; Madarász, A.; Pápai, I.; Nieger, M.; Leskelä, M.; Repo, T., A frustrated-Lewis-pair approach to catalytic reduction of alkynes to cis-alkenes. *Nature Chemistry* **2013,** *5* (8), 718-23.

29. Verho, O.; Gustafson, K. P. J.; Nagendiran, A.; Tai, C.-W.; Bäckvall, J.-E., Mild and Selective Hydrogenation of Nitro Compounds using Palladium Nanoparticles Supported on Amino-Functionalized Mesocellular Foam. *Chemistry Europe Academic Journals: ChemCatChem* **2014,** *6* (11), 3153-3159.

30. Li, Z.; Li, J.; Liu, J.; Zhao, Z.; Xia, C.; Li, F., Palladium Nanoparticles Supported on Nitrogen-Functionalized Active Carbon: A Stable and Highly Efficient Catalyst for the Selective Hydrogenation of Nitroarenes. *Chemistry Europe Academic Journals*: *ChemCatChem* **2014,** *6* (5), 1333-1339.

31. Furukawa, S.; Yoshida, Y.; Komatsu, T., Chemoselective Hydrogenation of Nitrostyrene to Aminostyrene over Pd- and Rh-Based Intermetallic Compounds. *American Chemcial Society: Catalysis* **2014,** *4* (5), 1441-1450.

32. Pandarus, V.; Ciriminna, R.; Béland, F.; Pagliaro, M., A New Class of Heterogeneous Platinum Catalysts for the Chemoselective Hydrogenation of Nitroarenes. *Advanced Synthesis & Catalysis* **2011,** *353* (8), 1306-1316.

33. Vanden Bout, D. A., Metal Nanoparticles: Synthesis, Characterization, and Applications Edited by Daniel L. Feldheim (North Carolina State University) and Colby A. Foss, Jr. (Georgetown University). Marcel Dekker, Inc.: New York and Basel. 2002. ISBN: 0-8247-0604-8. *Journal of the American Chemical Society* **2002,** *124* (26), 7874-7875.

34. Stiles, A. B., *Catalyst Supports and Supported Catalysts*. Butterworth Publishers,Stoneham, MA: 1987; Pages: 320.

35.   Boudart, M.; Davis, B. H.; Heinemann, H., Introduction. In *Handbook of Heterogeneous Catalysis*, 1997; pp 1-48.

36.   Bönnemann, H.; Brijoux, W.; Brinkmann, R.; Fretzen, R.; Joussen, T.; Köppler, R.; Korall, B.; Neiteler, P.; Richter, J., Preparation, characterization, and application of fine metal particles and metal colloids using hydrotriorganoborates. *Journal of Molecular Catalysis* **1994,** *86* (1), 129-177.

37.   Klabunde, K. J.; Tanaka, Y., The building of a Catalytic metal particle one atom at a time: solvated metal atom dispersed Catalysts. *Journal of Molecular Catalysis* **1983,** *21* (1), 57-79.

38.   Bradley, J. S.; Millar, J. M.; Hill, E. W., Surface chemistry on colloidal metals: a high-resolution NMR study of carbon monoxide adsorbed on metallic palladium crystallites in colloidal suspension. *Journal of the American Chemical Society* **1991,** *113* (10), 4016-4017.

39.   Seregina, M. V.; Bronstein, L. M.; Platonova, O. A.; Chernyshov, D. M.; Valetsky, P. M.; Hartmann, J.; Wenz, E.; Antonietti, M., Preparation of Noble-Metal Colloids in Block Copolymer Micelles and Their Catalytic Properties in Hydrogenation. *Chemistry of Materials* **1997,** *9* (4), 923-931.

40.   Schmid, G.; Emde, S.; Maihack, V.; Meyer-Zaika, W.; Peschel, S., Synthesis and catalytic properties of large ligand stabilized palladium clusters. *Journal of Molecular Catalysis A: Chemical* **1996,** *107* (1), 95-104.

41.   Verho, O.; Nagendiran, A.; Johnston, E. V.; Tai, C.-w.; Bäckvall, J.-E., Nanopalladium on Amino-Functionalized Mesocellular Foam: An Efficient Catalyst for Suzuki Reactions and Transfer Hydrogenations. *Chemistry Europe academic journals ChemCatChem* **2013,** *5* (2), 612-618.

42.   Verho, O.; Nagendiran, A.; Tai, C.-W.; Johnston, E. V.; Bäckvall, J.-E., Nanopalladium on Amino-Functionalized Mesocellular Foam as an Efficient and Recyclable Catalyst for the Selective Transfer Hydrogenation of Nitroarenes to Anilines. *Chemistry Europe Academic Journals ChemCatChem* **2014,** *6* (1), 205-211.

43.   Baralt, E.; Holy, N., Hydrogenation of nitro compounds with an anthranilic acid polymer-bound catalyst. *The Journal of Organic Chemistry* **1984,** *49* (14), 2626-2627.

44.   Banerjee, T. K.; Sen, D., Homogeneous reduction of aromatic nitro compounds by a triphenylphosphine complex of palladium. *Journal of Chemical Technology and Biotechnology* **1981,** *31* (1), 676-682.

45.   Mukkanti, K.; Subba Rao, Y. V.; Choudary, B. M., Selective and sequential reduction of nitroaromatics by montmorillonitesilylaminepalladium(II) complex. *Tetrahedron Letters* **1989,** *30* (2), 251-252.

46.   Takasaki, M.; Motoyama, Y.; Higashi, K.; Yoon, S.-H.; Mochida, I.; Nagashima, H.,
        Chemoselective Hydrogenation of Nitroarenes with Carbon Nanofiber-Supported
        Platinum and Palladium Nanoparticles. *Organic Letters* **2008,** *10* (8), 1601-1604.

Chapter 5

Ambient Pressure Ir@Hal Catalyzed Hydrogenation of Phenol, Aldehydes, and Ketones

5.1 ABSTRACT

A reliable method for encapsulating iridium nanoparticles (6-8 nm particles) in halloysite furnished the Ir@Hal catalyst with over 97% of the Ir nanoparticles exclusively captured within the clay nanoscroll. The Ir@Hal nanocomposite was found to be a highly efficient catalyst for the hydrogenation and transfer hydrogenation of phenol to furnish cyclohexanol (93-95% yield) at ambient pressure at 50 °C. The catalytic system was also effective for hydrogenating aldehydes and ketones with a broad scope of substrates. Further, the catalyst was easily recovered and recycled without significant loss of catalytic activity over multiple trials.

5.2   Introduction

5.2.1   Sustainable Production

The green and sustainable production of chemical feedstocks has been an essential focus of the biorefinery industry over the past decade.[1, 2] Various strategies for converting biomass into different platform chemicals have been developed to reduce dependence on fossil-fuel-derived chemicals.[3-8] However, to fully achieve the product manufacturing environmentally-friendly goals, the development of green and sustainable methods for converting biomass-derived platform chemicals into fine intermediate chemicals and building blocks remains a fundamental challenge to the chemical industry.

Cyclohexanol is an essential intermediate industrial chemical obtained from the lignan-biomass platform chemical phenol.[9, 10] The hydrogenation of phenol is a preferable process for cyclohexanol production over cyclohexane oxidation methods. The hydrogenation methods are generally more energy-efficient and produce less waste than oxidation methods.[11, 12] Thus, a wide range of materials have been explored for the hydrogenation of phenol. These include various solid-supported transition metal catalysts (Pd[12-24], Pt[25], Ru[26], Rh[27-29], Ni[30-32], and Ir[33]. Different Palladium systems have exhibited good selectivity for the formation of either cyclohexanone or cyclohexanol from phenol hydrogenation in aqueous media[16, 19, 20]. However, phenol hydrogenation's selectivity was also shown to depend upon the chemical nature of the solid support. Supports like SiO_2 and Al_2O_3 favored cyclohexanone formation, while oxophilic supports like ZnO_2 have been reported to suppress cyclohexanone and cyclohexanol formation instead of conversion to benzene[19, 21, 32, 33].

As part of a program aimed at the elucidation of the chemical utility of the natural scrolled clay halloysite (Hal)[34-36] as solid support for transition metal nanoparticles, it was of interest to investigate the reactivity of transition metal nanoparticle halloysite nanocomposites (M@Hal) as catalysts for the hydrogenation of phenol. As an aluminosilicate, halloysite would be expected to favor cyclohexanone or cyclohexanol formation over the formation of benzene. Previous work with Pd@Hal in cross-coupling reactions and the hydrogenation of alkenes and nitro compounds demonstrated the nanocomposite exhibited high catalytic activity levels in aqueous media with excellent recyclability.[37] Therefore, it was envisaged that a M@Hal nanocomposite could be developed for the ambient hydrogenation of phenol. To this end, an iridium system was envisaged as a target due to the greater oxophilicity of iridium relative to other noble metals.[38] Herein, we describe the synthesis and catalytic activity of an Ir@Hal valuable nanocomposite for the selective conversion of phenol into cyclohexanol.

5.3   Results and Discussion

5.3.1 Synthesis and Characterization of Ir@Hal

Intending to prepare a nanocomposite material consisting of iridium nanoparticles (Ir$_{NP}$) encapsulated in halloysite (Ir@Hal), our initial focus was synthesizing appropriately sized Ir$_{NP}$. There have been several reports describing the preparation of IrNP; however, it was necessary to use a process compatible with encapsulation in halloysite in water. Previous work with palladium nanoparticles had identified trisodium citrate as an ideal capping agent for halloysite encapsulation.[37] Thus, the synthesis of Ir$_{NP}$ was explored with iridium

219

chloride and various reducing agents (ascorbic acid, sodium ascorbate, sodium cyanoborohydride, and sodium borohydride) trisodium citrate as the capping agent in water. It was found that $IrCl_3$/$NaBH_4$/trisodium citrate in the molar ratio 1.0/1.3/1.2 in water gave monodispersed Ir_{NP} (Figure 1) of appropriate size for encapsulation. For a comparison, Ir_{NP} were also prepared from iridium chloride/$NaBH_4$ using PVP or CTAB as the capping agent. However, as anticipated, the Ir_{NP} prepared under these conditions was too large to ultimately fit within the halloysite nanoscroll.

To achieve encapsulation of the Ir_{NP} within the halloysite, our initial approach was to use the preformed monodispersed Ir_{NP} obtained from the conditions described above. However, this two-step approach was unsuccessful and only afforded agglomerated material when combined with halloysite (**Table 1**, entries 1 - 2). We then attempted a one-step preparation of Ir@Hal, in which the Ir_{NP} were formed in the presence of halloysite. As summarized in **Table 1** (entries 3-9), increasing the amount of reducing agent ($NaBH_4$) and capping agent (trisodium citrate) relative to iridium chloride in an aqueous suspension of halloysite led to the encapsulation of the Ir_{NP}.

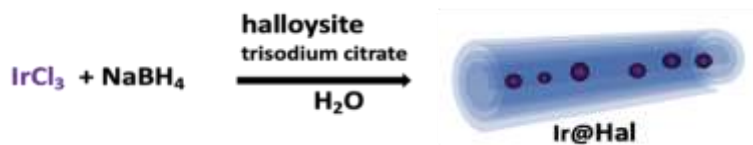**Figure 1.** Optimized synthesis of Ir@Hal

Table 1. Optimized synthesis of Ir@Hal

Entry	IrCl$_3$ (mmol)	Hal (mmol)	trisodium citrate (mmol)	NaBH$_4$ (mmol)	Results
1	0.60	1.2	1.2	0.80	No encapsulation Agglomeration[a]
2	0.60	1.2	1.6	0.80	No encapsulation Agglomeration[a]
3	0.60	1.2	2.4	0.80	Encapsulation/ Agglomeration[b]
4	0.60	0.60	2.4	0.80	Encapsulation/ Agglomeration[b]
5	0.12	0.12	2.4	1.2	Encapsulation/ Agglomeration[b]
6	0.60	0.60	6.0	2.4	Encapsulation[b]
7	1.2	1.2	6.0	2.4	Encapsulation[b]
8	0.60	0.60	12.0	2.4	Encapsulation[b]
9	0.60	0.60	20.0	2.4	Encapsulation[b]
10	0.60	0.60	6.0	2.4	Encapsulation[a]

[a]Conditions: Preformed Ir$_{NP}$ added to Hal (two-step process).
[b]Conditions: Ir$_{NP}$ formed in the presence of Hal (one-step process).

The degree to which the Ir$_{NP}$ were encapsulated versus agglomerated outside of the nanoscroll was determined from TEM images. Initial attempts to form an Ir@Hal nanocomposite material focused on a 1:2 IrCl$_3$:Hal molar ratio (**Table 1**, entry 3) with a four-fold excess of trisodium citrate. This initial attempt resulted in good encapsulation of the Ir$_{NP}$ in halloysite; however, there was significant agglomeration of the Ir$_{NP}$ outside of the scrolls, resulting in incomplete encapsulation of Ir$_{NP}$. Decreasing the amount of the halloysite did not improve encapsulation (**Table 1**, entry 4). Decreasing the reagent concentrations (**Table 2**, entry 5) also did not increase the amount of encapsulated Ir$_{NP}$ relative to agglomeration. It was not until the amount of capping agent was significantly increased that improved encapsulation was observed. An optimum level

of encapsulation was achieved with a 10-fold increase in the relative amount of trisodium citrate and a four-fold increase of the reducing agent NaBH$_4$. (**Table 1**, entry 6). TEM images (**Fig. 1a**) of the sample show that the bulk of Ir$_{NP}$ was encapsulated, with no agglomeration on the halloysite surface or agglomerates outside of the scrolls. The size of encapsulated Ir$_{NP}$ averaged between 8 - 9nm. This approach (**Table 1**, entry 6) resulted in 98% Ir loading [based on IrCl$_3$] to furnish an Ir@Hal nanocomposite that was 15% Ir content (weight percent) as determined by ICP-AES analysis.

It was subsequently determined that encapsulation could be scaled up to a 1.2 mmol scale to afford fully encapsulated Ir@Hal (**Table 1**, entry 7). Using higher amounts of trisodium citrate also afforded excellent encapsulation (**Table 1**, entries 8-9). However, it was later determined that the excess capping agent present in these nanocomposites decreased the catalytic activity.

The results of the one-step encapsulation studies revealed the importance of the capping agent for the nanoparticle to be drawn into the halloysite lumen. To establish that the trisodium citrate concentration was an essential component of the encapsulation process, the two-step process was repeated using the conditions that successfully led to the encapsulation of the Ir$_{NP}$ (**Table 1**, entry 6). As indicated in **Table 1**, entry 10, monodispersed Ir$_{NP}$ were prepared separately with a 10-fold excess of trisodium citrate and four-fold excess of sodium borohydride. The Ir$_{NP}$ were then dispersed in an aqueous solution of halloysite. In contrast to our initial attempt (**Table 1**, entry 1), all the Ir$_{NP}$ were encapsulated with little agglomeration observed (**Fig. 1b**).

Characterization of the Ir@Hal by XRD confirmed the presence of the Ir(0) nanoparticles (Figs. 2). XRD spectrum shows the presence of broad reflection lines indicating the diffraction by very small crystals. The four diffraction peaks were assigned as corresponding to the Ir(0) (111),

(200), (220), and (311) reflection planes. The Ir sample's diffraction pattern peaks appeared at

2Θ angles of 44.12, 46.78, 69.67, and 76.57 and were consistent with previous reports.[39-45]

Figure 2. TEM image of Ir@Hal prepared using conditions described in (a) Table 1, entry 6; (b) Table 1, entry 10.
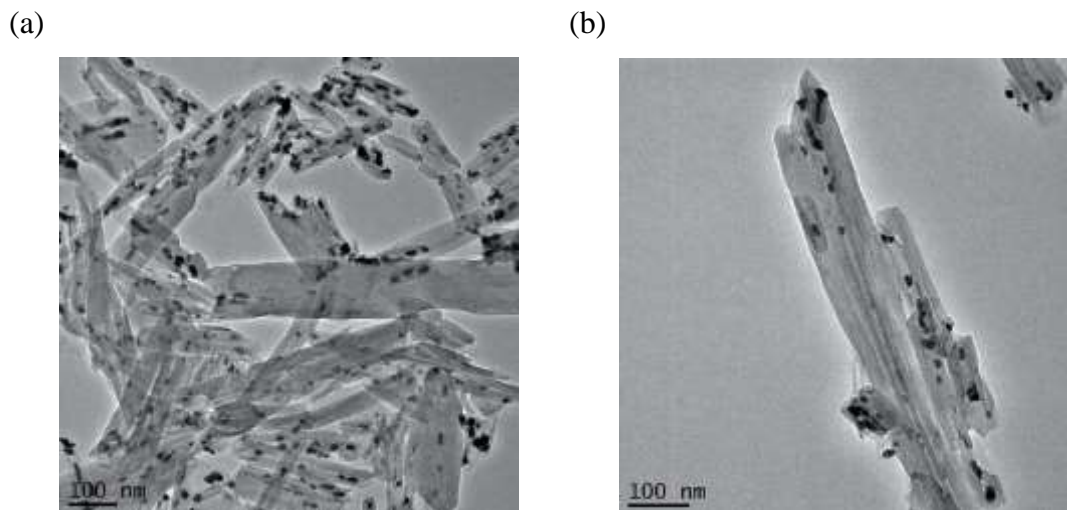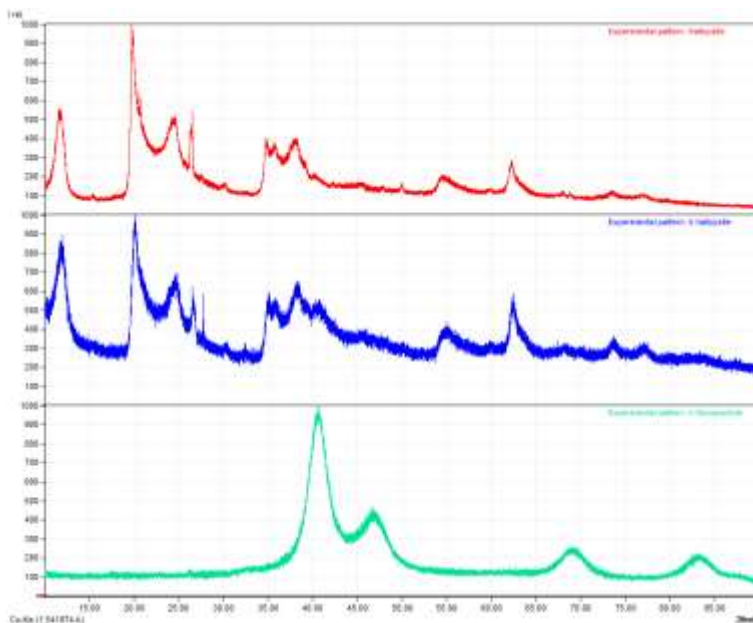
(a)   (b)

Figure 3. XRD spectrum of Ir@Hal (red) raw halloysite (blue) Ir@Hal nanocomposite (green) Ir (0) nanoparticles.

5.3.2 Hydrogenation of Phenol with Ir@Hal Catalyst

With the Ir@Hal in hand, our attention turned to the evaluation of the nanocomposite as a catalyst for the hydrogenation of phenol. As summarized in **Table 2**, a series of reaction conditions were explored with various solvents and hydrogen sources to convert phenol into cyclohexanol. Using hydrogen (1 atm, balloon), the reduction of phenol to afford cyclohexanol was readily achieved in aqueous isopropanol (iPrOH:H_2O, 5:2) at 50°C, 12 h (**Table 2**, entry 3). The reaction proceeded with 100% conversion of phenol and 95% isolated yield of cyclohexanol. Under these conditions, 10%wt of the Ir@Hal nanocomposite (1.5% Ir metal) was used relative to phenol. The hydrogenation did not occur in water alone nor at temperatures below 50°C (**Table 2**, entries 1-2). Decreasing the catalyst loading from 10 wt% Ir@Hal to 5 wt% or 1 wt% Ir@Hal relative to phenol (**Table 2**, entries 4-5) only slightly decreased the yield but significantly lengthened the reaction times with incomplete conversion of phenol.

It was noteworthy that the reaction did proceed without hydrogen, using only iPrOH as the hydrogen source.[46] While the hydrogen transfer conditions proceeded to give cyclohexanol in high yield (93%), the reaction times were significantly longer for complete conversion Attempts to use formic acid or sodium formate as the hydrogen source were unsuccessful (**Table 2**, entries 7-8). Under acidic conditions, decomposition of the Ir@Hal catalyst was observed, while sodium formate in aqueous ethanol gave no observable reduction products.

Table 2. Optimized hydrogenation of phenol to cyclohexanol

Entry	Ir@Hal (wt%)	hydrogen source	solvent	T(°C), time (h)	Yield (%)
1	10	H$_2$ (1 atm)	H$_2$O	25-90 °C, 24 h	NR
2	10	H$_2$ (1 atm)	iPrOH:H$_2$O (5:2)	25 °C, 12 h	NR
3	10	H$_2$ (1 atm)	iPrOH:H$_2$O (5:2)	50 °C, 12 h	95
4	5	H$_2$ (1 atm)	iPrOH:H$_2$O (5:2)	50 °C, 48 h	88
5	1	H$_2$ (1 atm)	iPrOH:H$_2$O (5:2)	50 °C, 72 h	72
6	10	iPrOH	iPrOH:H$_2$O (5:2)	50 °C, 24 h	93
7	10	HCO$_2$H	iPrOH:H$_2$O (5:2)	50 °C, 24 h	DR
8	10	HCO$_2$Na	EtOH:H$_2$O (5:2)	25-50 °C, 24 h	NR
9	10	H$_2$ (1 atm)	hexane	50 °C, 24 h	NR
10	10	H$_2$ (1 atm)	hexane:iPrOH (1:1)	50 °C, 24 h	40

In addition, attempts to do the reduction in a non-polar solvent (hexane) caused the Ir@Hal to aggregate and was inactive. Some catalyst activity could be achieved in a mixture of hexane:iPrOH, but poor dispersion resulted in low conversion and poor yields.

5.3.3 Hydrogenation of Aldehydes and Ketones with Ir@Hal Catalyst

The highly selective conversion of phenol into cyclohexanol suggested that the Ir@Hal nanocomposite was very reactive toward hydrogenation of the keto/enol forms cyclohexanone that have been postulated as intermediates in the overall reduction process.[13, 16, 47] The fact that cyclohexanone was never observed in the product mixture indicated that the hydrogenation of keto/enol intermediate resulting from the aromatic ring's initial reduction occurred readily upon formation. Several heterogenous iridium systems have been reported as effective catalysts for the reduction of ketones and aldehydes.[48, 49] Therefore, it was interesting to explore the catalytic activity of Ir@Hal to reduce cyclohexanone and other carbonyl compounds.

As summarized in **Table 3**, a series of aldehydes and ketones were easily reduced to alcohols using Ir@Hal in aqueous isopropanol. Initially, cyclohexanone was reduced to cyclohexanol in nearly quantitative yield (99%, **Table 3**, entry 1) under a balloon of hydrogen at 50°C. However, as anticipated, the highly reactive nanocomposite afforded cyclohexanol in similar yield at room temperature (99%, **Table 3**, entry 2). In addition, transfer-hydrogenation was equally effective at room temperature with aqueous isopropanol and elevated temperature with sodium formate in aqueous ethanol (99%, **Table 3**, entry 1).

Table 3. Ir@Hal catalyzed hydrogenation of carbonyl compounds

Entry	carbonyl compound	alcohol	conditions[a]	yield (%)
1 2 3 4			A B C D	99 99 97 98
5 6			A B	96 < 5[b]
7 8 9			A B C	90 < 5[b] 92[c]
10 11 12			A B C	80 < 5[b] < 5[b]
13 14 15			A B C D	91 93 90 NR
16 17 18 19			A B C D	98 93 < 5[b] NR
20 21 22			A B C	98 < 5[b] NR
23 24 25 26			A B C D	99 98 97 97
27			A	70

[a]Conditions. **A**: Ir@Hal (10% wt), H_2 (1 atm), iPrOH/H_2O, 50 °C, 12 h. **B**: Ir@Hal (10% wt), H_2 (1 atm), r.t., 12 h.
C: Ir@Hal (10% wt), iPrOH/H_2O, 50 °C, 8 h. **D**: Ir@Hal (10% wt), HCO_2Na, EtOH/H_2O, 50 °C, 8 h.
[b]Less than 5% conversion after 24 h.
[c]24 h reaction time.
NR: No reaction, no product observed by NMR after 24 h.

Aryl ketones were also reduced at ambient hydrogen pressure at 50 °C in high yield (**Table 3**, entries 7 and 10). However, low conversion was observed at room temperature (entries 8 and 11). Benzophenone could be reduced using transfer-hydrogenation with isopropanol (entry 9) but was unreactive with sodium formate in ethanol. Alkyl and aryl aldehydes typically resistant to hydrogenation were also conveniently reduced at ambient pressures.[50-56] Electron-rich aryl aldehydes could be hydrogenated at room temperature, and 3,4,5-trimethoxybenzaldehyde could also be efficiently reduced in high yield under transfer-hydrogenation conditions with isopropanol or with sodium formate in ethanol. The deactivated 4-chlorobenzaldehyde required a higher temperature (50 °C) for efficient conversion to 4-chlorobenzyl alcohol.

The successful reduction of the aliphatic ketones to alcohols using the Ir@Hal nanocomposite prompted an investigation of the nanocomposite's potential use for the conversion of biomass-derived levulinic acid to the value-added derivative g-valerolactone (GVL).[57, 58] As shown in **Table 3**, treatment of levulinic acid (entry 27) with hydrogen (1 atm, balloon) in aqueous isopropanol (iPrOH:H_2O, 5:2) at 50°C, 12 h with a catalyst loading of 10% wt/wt afforded GVL in 70% isolated yield. Longer reaction time or higher reaction temperature did not improve the yields of GVL. Also, transfer-hydrogenation conditions were not adequate for this conversion. Nevertheless, the high yield of GVL under these mild hydrogenation conditions indicates that Ir@Hal nanocomposites may help produce this biomass-derived platform chemical.

5.3.4 Recycling Studies with Ir@Hal Catalyst.

As illustrated in Figure 3, recycling studies with Ir@Hal showed that the catalyst could be cycled through consecutive hydrogenation reactions without loss of activity and excellent isolated yields of the corresponding alcohols.

Figure 4. Recycling studies with Ir@Hal.
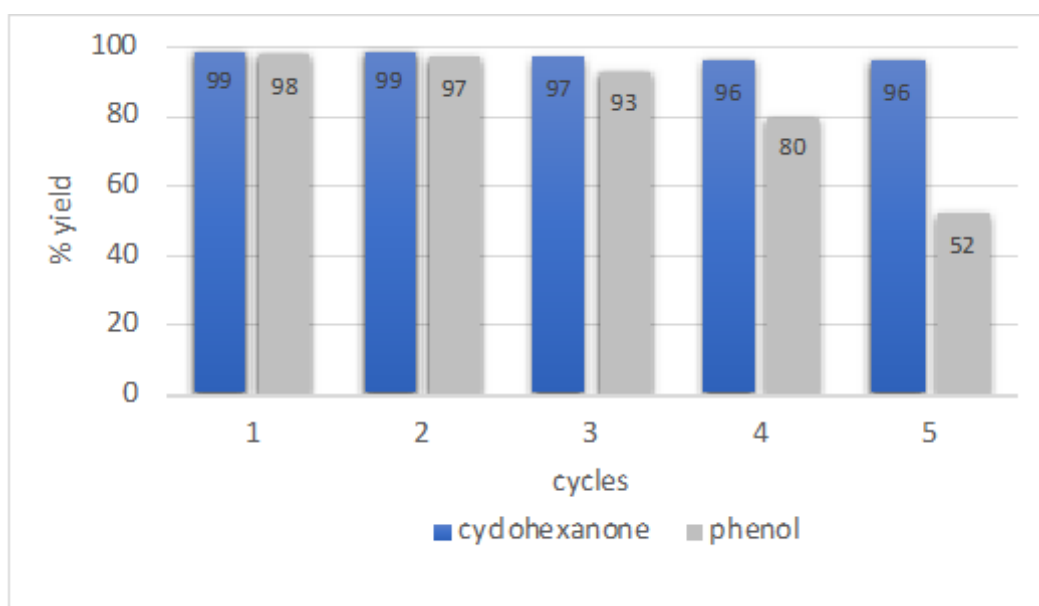
For cyclohexanone's hydrogenation at ambient pressure and temperature (**Table 3**, entry 2, conditions B), the catalyst was used through five cycles with no reduction in yield. Cyclohexanol was isolated in > 95% yield in each trial. For the hydrogenation of phenol at 50 °C (**Table 2**, entry 3), the catalyst was used through three cycles without a decrease in the yield of cyclohexanol (> 93%). However, the fourth trial observed the fifth trial observed a reduction in yield and a more significant reduction. The diminished catalyst lifetime for phenol

hydrogenation over that observed for cyclohexanone suggests that the nanocomposite has some thermal instability over prolonged usage at elevated temperatures.

5.4   Conclusions

In conclusion, a reliable method for encapsulation of iridium nanoparticles (6-8 nm particles) in halloysite furnished the Ir@Hal catalyst with over 97% of the Ir nanoparticles exclusively captured within the clay nanoscroll. The Ir@Hal nanocomposite was found to be a highly efficient catalyst for the hydrogenation and transfer hydrogenation of phenol to furnish cyclohexanol (93-95% yield) at ambient pressure at 50 °C. The catalytic system was also effective for hydrogenating aldehydes and ketones with a broad scope of substrates and provided high yields of the corresponding alcohols. In addition, the catalyst was easily recovered and recycled without significant loss of catalytic activity over multiple cycles. This new Ir@Hal nanocomposite demonstrates further the utility of halloysite as a support for the development of transition metal-based nanocomposites for heterogeneous catalysis for future investigations; the substrate scope of the hydrogenation reaction and transfer-hydrogenation reaction will be expanded. Furthermore, the development of new Ir@Hal nanocomposites is explored for the efficient high-yielding conversion of levulinic acid into GVL.

5.5 Experimental

5.5.1 Materials and Methods

All reactions were carried out in oven-dried glassware under a N_2 atmosphere unless indicated otherwise. Halloysite clay was purchased from Sigma Aldrich. All other chemicals were purchased from Alfa Aesar, Sigma Aldrich, and VWR. Halloysite was purchased from Sigma Aldrich. All chemicals were used as received without further purification. ^1H and ^{13}C NMR spectra were recorded at r.t. in DMSO-d_6 on a Bruker 400 MHz instrument operating at a frequency of 300 MHz for ^1H NMR and 75 MHz for ^{13}C NMR. ^1H chemical shifts were referenced to the DMSO solvent signal (2.50 ppm). ^{13}C chemical shifts were referenced to the DMSO solvent signal (39.51 ppm). Pd_{NP} size was determined from TEM images obtained on a JEOL 2010 equipped with an EDAX genesis energy dispersive spectroscopy (EDS) system, operated at an accelerating voltage of 200 kV an emission current of 109 μA. ICP-AES analysis of the Ir@Hal was performed by Galbraith Laboratories, Inc., Knoxville, TN.

5.5.2 Synthesis of Ir@Hal. Preformation of Ir_{NP}

A solution of $IrCl_3$ (0.18 g, 0.60 mmol) in deionized water (10 mL) was prepared in a 250 mL Erlenmeyer flask. A trisodium citrate solution (1.76 g, 6.00 mmol) in deionized water (10 mL) was added to the iridium chloride solution. The mixture was sonicated for 10 mins then placed in an ice bath while continuing to stir as the prepared solution of sodium borohydride (100 mg, 2.4 mmol) in deionized water (10 mL) was added dropwise via pipet over 15 minutes. The combined solution was allowed to stir for 15 min at room temperature. During the first 10 minutes, the initial light yellowish/green color of the iridium chloride solution mixture turned

black, indicating Ir nanoparticles' formation. After 15 min, no more color changes were observed, and the solution was left to rest at room temperature, open to air for 80 min. Halloysite (0.18g, 0.60 mmol) was added to the Ir nanoparticle solution, and the colloid mixture was stirred for 15 min. The mixture was then allowed to rest at room temperature for 10 min. The mixture was centrifuged (6000 rpm), and the liquid was decanted away from the solid residue. The residue was washed with deionized water (3 x 15 mL) and isopropyl alcohol (2 x 15 mL). The resultant powder was dried at room temperature for 24 h in a desiccator ($CaSO_4$) to afford Ir@Hal a black powder.

5.5.3   Synthesis of Ir@Hal. In Situ Formation and Encapsulation of Ir$_{NP}$.

A solution of $IrCl_3$ (180 mg, 0.60 mmol) in deionized water (10 mL) was prepared in a 250 mL Erlenmeyer flask. A trisodium citrate solution (1760 mg, 6.0 mmol) in deionized water (10 mL) was added to the iridium chloride solution. Halloysite (176 mg, 0.60 mmol) dispersed in water (10 mL) was added to the Iridium chloride solution, and the mixture was stirred and sonicated for 15 min. The mixture was then placed in an ice bath while continuing to stir as the prepared solution of sodium borohydride (100 mg, 2.4 mmol) in deionized water (10 mL) was added dropwise via pipet over 15 minutes. The combined solution was allowed to stir for 15 min at room temperature. During the first 10 minutes, the initial light yellowish/green color of the iridium chloride solution mixture turned black, indicating Ir nanoparticles' formation. After 15 min, no more color changes were observed, and the solution was left to rest at room temperature, open to air for 80 min. The mixture was sonicated for 10 minutes before washing. The mixture was centrifuged (6000 rpm), and the liquid was decanted away from the solid residue. The residue was washed with deionized water (3 x 15 mL) and isopropyl alcohol (2 x 15 mL). The

resultant powder was dried at room temperature for 24 h in a desiccator ($CaSO_4$) to afford 15% Ir@Hal as a black powder.

5.5.4   Hydrogenation of Phenol

To a 10 mL round bottom flask equipped with a magnetic stir bar was added the phenol (1.00 mmol), the Ir@Hal (10% wt/wt) followed by the addition of isopropyl alcohol: water (5:2). The mixture was placed under hydrogen atmosphere (1 atm) and sonicated for 5 minutes, then allowed to stir at 70°C (oil bath) overnight. The reaction progress was monitored by TLC (8:2, hexanes: ethyl acetate). The Ir@Hal catalyst was recovered by vacuum filtration. The Ir@Hal was rinsed using (10 mL) of isopropyl followed by DI water (5 mL). The solvent was removed under vacuum to afford the purified product. TLC and NMR verified product purity.

5.5.5   Hydrogenation of Aldehydes and Ketones

5.5.5.1 General Conditions A

To a 10 mL round bottom flask equipped with a magnetic stir bar was added the aldehyde or ketone (1.00 mmol), the Ir@Hal (10% wt/wt) followed by the addition of isopropyl alcohol: water (5:2). The mixture was placed under hydrogen atmosphere (1 atm) and sonicated for 5 minutes, then allowed to stir at 50°C (oil bath) overnight. The reaction progress was monitored by TLC (8:2, hexanes: ethyl acetate). The Ir@Hal catalyst was recovered by vacuum filtration. The Ir@Hal was rinsed using (10 mL) of isopropyl followed by DI water (5 mL). The solvent was removed under vacuum to afford the purified product. TLC and NMR verified product purity.

5.5.5.2 General Conditions B

To a 10 mL round bottom flask equipped with a magnetic stir bar was added the aldehyde or ketone (1.00 mmol), the Ir@Hal (10% wt/wt) followed by the addition of isopropyl alcohol: water (5:2). The mixture was placed under hydrogen atmosphere (1 atm) and sonicated for 5 minutes, then allowed to stir at 25°C overnight. The reaction progress was monitored by TLC (8:2, hexanes: ethyl acetate). The Ir@Hal catalyst was recovered by vacuum filtration. The Ir@Hal was rinsed using (10 mL) of isopropyl followed by DI water (5 mL). The solvent was removed under vacuum to afford the purified product. TLC and NMR verified product purity.

5.5.5.3 General Conditions C

To a 10 mL round bottom flask equipped with a magnetic stir bar was added the aldehyde or ketone (1.00 mmol), the Ir@Hal (10% wt/wt) followed by the addition of isopropyl alcohol: water (5:2). The mixture was placed under hydrogen atmosphere (1 atm) and sonicated for 5 minutes, then allowed to stir at 50°C 8 hours. The reaction progress was monitored by TLC (8:2, hexanes: ethyl acetate). The Ir@Hal catalyst was recovered by vacuum filtration. The Ir@Hal was rinsed using (10 mL) of isopropyl followed by DI water (5 mL). The solvent was removed under vacuum to afford the purified product. TLC and NMR verified product purity.

5.5.5.4 General Conditions D

To a 10 mL round bottom flask equipped with a magnetic stir bar was added, the aldehyde or ketone (1.00 mmol), sodium formate, the Ir@Hal (10% wt/wt) followed by the addition of EtOH: water (5:2). The mixture was placed under hydrogen atmosphere (1 atm) and sonicated for 5 minutes, then allowed to stir at 50°C overnight. The reaction progress was monitored by TLC (8:2, hexanes: ethyl acetate). The Ir@Hal catalyst was recovered by vacuum filtration. The

Ir@Hal was rinsed using (10 mL) of isopropyl followed by DI water (5 mL). The solvent was removed under vacuum to afford the purified product. TLC and NMR verified product purity.

5.5.6   Recycling Experiments

The Ir@Hal was removed from the filter paper and added to a beaker with EtOH (20 mL), then sonicated for 10 mins. The solid was then centrifuged down and then washed again with (15 mL) DI water followed by (15 mL) isopropyl alcohol. The solid was dried in a desiccator ($CaSO_4$) overnight or in an oven at 120° for 20 mins before each subsequent cycle.

5.5.7 ^{1}H NMR Characterization of hydrogenated products (Table 3)

All the products are known compounds. ^{1}H NMR spectra were identical to spectra in the Spectral Database for organic compounds. SDBSWeb: https://sdbs.db.aist.go.jp (National Institute of Advanced Industrial Science and Technology)

Cyclohexanol [108-93-0]

OH
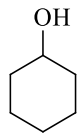
Colorless liquid (99%)

^{1}H NMR (300 MHz, CDCl$_3$) δ: 3.98 (p, J = 6.0 Hz, 1H), 3.57 (s, 1H), 2.01 (s, 1H), 1.86 (s, 1H), 1.69 (s, 1H), 1.54 – 1.47 (m, 1H), 1.18 (s, 6H).

2-heptanol [543-49-7]

OH
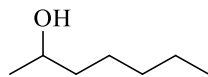
Colorless liquid (96%)

^{1}H NMR (300 MHz, CDCl$_3$) δ: 3.78 (s, 1H), 1.73 – 1.18 (m, 12H), 0.88 (s, 3H).

benzhydrol [91-01-0]

OH
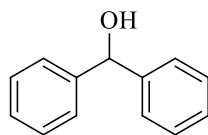
A colorless solid of mp 65-66 °C. Lit mp (65-66°C) (90%)

^{1}H NMR (300 MHz, CDCl$_3$) δ: 2.19 (1H, d, J = 4.0 Hz), 5.86 (1H, d, J = 4.0 Hz), 7.25-7.28 (2H, m), 7.32-7.35 (4H, m), 7.38-7.40 (4H, m).

fluorenone [486-25-9]

OH
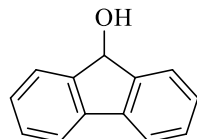
A white solid of mp 80.2-81.1°C. Lit mp (80-83°C) (80%)

^{1}H NMR (300 MHz, DMSO-d_6) δ: 7.76 (d, J = 7.2 Hz, 2H), 7.57 (d, J = 7.2 Hz, 2H), 7.33 (dt, J = 21.0, 7.3 Hz, 4H), 5.86 – 5.73 (m, 1H), 5.51 – 5.39 (m, 1H).

benzyl alcohol [100-51-6]
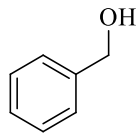
Colorless liquid (93%)

^{1}H NMR (400 MHz, CDCl$_3$) δ: 7.37-7.38 (m, 5H), 4.70 (s, 2H).

4-methoxy benzyl alcohol [105-13-5]
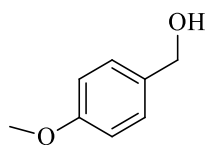
Pale yellow liquid (98%)

^{1}H NMR (300 MHz, CDCl$_3$) δ: 7.38 – 7.29 (d, J=8.6 Hz, m, 2H), 6.93 (d, J = 8.6 Hz, 2H), 4.51 (s, 2H), 3.83 (s, 3H), 2.59 (s, 1H).

4-chloro benzyl alcohol [873-76-7]
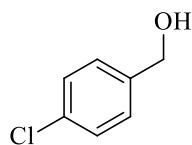
Pale yellow liquid (98%)

^{1}H NMR (300 MHz, CDCl$_3$) δ: 7.32 (s, 4H), 4.68 (s, 2H), 1.60 (s, 1H).

3,4,5-trimethoxy benzyl alcohol [3840-31-1]
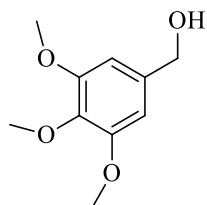
Pale yellow liquid (99%)

^{1}H NMR (300 MHz, CDCl$_3$) δ: 6.53 (s, 2H), 4.55 (s, 2H), 3.78 (d, J = 4.5 Hz, 9H), 2.69 (s, 1H).

5.6 References

1. Ragauskas, A. J.; Williams, C. K.; Davison, B. H.; Britovsek, G.; Cairney, J.; Eckert, C. A.; Frederick, W. J., Jr.; Hallett, J. P.; Leak, D. J.; Liotta, C. L.; Mielenz, J. R.; Murphy, R.; Templer, R.; Tschaplinski, T., The path forward for biofuels and biomaterials. *Science* **2006,** *311* (5760), 484-9.

2. Cherubini, F., The biorefinery concept: Using biomass instead of oil for producing energy and chemicals. *Energy Conversion and Management* **2010,** *51* (7), 1412-1421.

3. Ghadiryanfar, M.; Rosentrater, K.; Keyhanii, A.; Omid, M., Corrigendum to "A review of macroalgae production, with potential applications in biofuels and bioenergy" [Renew Sustain Energy Rev 54 (2016) 473–481]. *Renewable and Sustainable Energy Reviews* **2018,** *96*.

4. Tye, Y.; Peng, L. C.; Lee, K. T.; Wan Nadiah, W., Non-wood Lignocellulosic Biomass for Cellulosic Ethanol Production: Effects of Pretreatment on Chemical Composition in Relation to Total Glucose Yield. *Journal of the Japan Institute of Energy* **2017,** *96*, 503-508.

5. Huber, G. W.; Iborra, S.; Corma, A., Synthesis of Transportation Fuels from Biomass: Chemistry, Catalysts, and Engineering. *Chemical Reviews* **2006,** *106* (9), 4044-4098.

6. Corma, A.; Iborra, S.; Velty, A., Chemical Routes for the Transformation of Biomass into Chemicals. *Chemical Reviews* **2007,** *107* (6), 2411-2502.

7. Jing, Y.; Guo, Y.; Xia, Q.; Liu, X.; Wang, Y., Catalytic Production of Value-Added Chemicals and Liquid Fuels from Lignocellulosic Biomass. *Chemistry* **2019,** *5* (10), 2520-2546.

8. Bomtempo, J. V.; Chaves Alves, F.; de Almeida Oroski, F., Developing new platform chemicals: what is required for a new bio-based molecule to become a platform chemical in the bioeconomy? *Faraday Discuss* **2017,** *202*, 213-225.

9. Musser, M. T., Cyclohexanol and Cyclohexanone. In *Ullmann's Encyclopedia of Industrial Chemistry*.

10. Ma, H.; Li, H.; Zhao, W.; Li, X.; Long, J., Production of oxygen-containing fuel from lignin bio-oil: Guaiacol as the model compound. *Energy Procedia* **2019,** *158*, 370-375.

11. Yang, C.; Li, K.; Wang, J.; Zhou, S., Selective hydrogenation of phenol to cyclohexanone over Pd nanoparticles encaged hollow mesoporous silica catalytic nanoreactors. *Applied Catalysis A: General* **2021,** *610*, 117961.

12. Li, H.; Liu, J.; Xie, S.; Qiao, M.; Dai, W.; Lu, Y.; Li, H., Vesicle-Assisted Assembly of Mesoporous Ce-Doped Pd Nanospheres with a Hollow Chamber and Enhanced Catalytic Efficiency. *Advanced Functional Materials* **2008,** *18* (20), 3235-3241.

13. Hu, S.; Yang, G.; Jiang, H.; Liu, Y.; Chen, R., Selective hydrogenation of phenol to cyclohexanone over Pd@CN (N-doped porous carbon): Role of catalyst reduction method. *Applied Surface Science* **2018,** *435*, 649-655.

14. Zhang, J.; Zhang, C.; Jiang, H.; Liu, Y.; Chen, R., Highly Efficient Phenol Hydrogenation to Cyclohexanone over Pd@CN-rGO in Aqueous Phase. *Industrial & Engineering Chemistry Research* **2020,** *59* (23), 10768-10777.

15. Liu, Y.; Dong, Z.; Li, X.; Le, X.; Zhang, W.; Ma, J., Aqueous-phase hydrodechlorination and further hydrogenation of chlorophenols to cyclohexanone in water over palladium nanoparticles modified dendritic mesoporous silica nanospheres catalyst. *RSC Advances* **2015,** *5* (27), 20716-20723.

16. Chen, H.; He, Y.; Pfefferle, L. D.; Pu, W.; Wu, Y.; Qi, S., Phenol Catalytic Hydrogenation over Palladium Nanoparticles Supported on Metal-Organic Frameworks in the Aqueous Phase. *Chemistry Europe Academic Journals: ChemCatChem* **2018,** *10* (12), 2558-2570.

17. Liu, H.; Jiang, T.; Han, B.; Liang, S.; Zhou, Y., Selective Phenol Hydrogenation to Cyclohexanone Over a Dual Supported Pd–Lewis Acid Catalyst. *Science* **2009,** *326* (5957), 1250-1252.

18. Chen, H.; He, Y.; Pfefferle, L. D.; Pu, W.; Wu, Y.; Qi, S., Front Cover: Phenol Catalytic Hydrogenation over Palladium Nanoparticles Supported on Metal-Organic Frameworks in the Aqueous Phase *Chemistry Europe Academic Journals*: *ChemCatChem* **2018,** *10* (12), 2505-2505.

19. Nelson, N. C.; Manzano, J. S.; Sadow, A. D.; Overbury, S. H.; Slowing, I. I., Selective Hydrogenation of Phenol Catalyzed by Palladium on High-Surface-Area Ceria at Room Temperature and Ambient Pressure. *ACS Catalysis* **2015,** *5* (4), 2051-2061.

20. Wang, Y.; Yao, J.; Li, H.; Su, D.; Antonietti, M., Highly Selective Hydrogenation of Phenol and Derivatives over a Pd@Carbon Nitride Catalyst in Aqueous Media. *Journal of the American Chemical Society* **2011,** *133* (8), 2362-2365.

21. Teles, C. A.; Rabelo-Neto, R. C.; Jacobs, G.; Davis, B. H.; Resasco, D. E.; Noronha, F. B., Hydrodeoxygenation of Phenol over Zirconia-Supported Catalysts: The Effect of Metal Type on Reaction Mechanism and Catalyst Deactivation. *Chemistry Europe Academic Journals: ChemCatChem* **2017,** *9* (14), 2850-2863.

22.   de Souza, P. M.; Rabelo-Neto, R. C.; Borges, L. E. P.; Jacobs, G.; Davis, B. H.; Sooknoi, T.; Resasco, D. E.; Noronha, F. B., Role of Keto Intermediates in the Hydrodeoxygenation of Phenol over Pd on Oxophilic Supports. *American Chemical Society: Catalysis* **2015,** *5* (2), 1318-1329.

23.   de Souza, P. M.; Rabelo-Neto, R. C.; Borges, L. E. P.; Jacobs, G.; Davis, B. H.; Graham, U. M.; Resasco, D. E.; Noronha, F. B., Effect of Zirconia Morphology on Hydrodeoxygenation of Phenol over Pd/ZrO2. *American Chemical Society: Catalysis* **2015,** *5* (12), 7385-7398.

24.   Dong, Z.; Le, X.; Liu, Y.; Dong, C.; Ma, J., Metal-organic framework derived magnetic porous carbon composite supported gold and palladium nanoparticles as highly efficient and recyclable catalysts for reduction of 4-nitrophenol and hydrodechlorination of 4-chlorophenol. *Journal of Materials Chemistry A* **2014,** *2* (44), 18775-18785.

25.   Yang, X.; Yu, X.; Long, L.; Wang, T.; Ma, L.; Wu, L.; Bai, Y.; Li, X.; Liao, S., Pt nanoparticles entrapped in titanate nanotubes (TNT) for phenol hydrogenation: the confinement effect of TNT. *Chemical Communications* **2014,** *50* (21), 2794-2796.

26.   El Sayed, S.; Bordet, A.; Weidenthaler, C.; Hetaba, W.; Luska, K. L.; Leitner, W., Selective Hydrogenation of Benzofurans Using Ruthenium Nanoparticles in Lewis Acid-Modified Ruthenium-Supported Ionic Liquid Phases. *American Chemical Society: Catalysis* **2020,** *10* (3), 2124- 2130.

27.   Song, Y.; Gutiérrez, O. Y.; Herranz, J.; Lercher, J. A., Aqueous phase electrocatalysis and thermal catalysis for the hydrogenation of phenol at mild conditions. *Applied Catalysis B: Environmental* **2016,** *182*, 236-246.

28.   Park, I. S.; Kwon, M. S.; Kang, K. Y.; Lee, J. S.; Park, J., Rhodium and Iridium Nanoparticles Entrapped in Aluminum Oxyhydroxide Nanofibers: Catalysts for Hydrogenations of Arenes and Ketones at Room Temperature with Hydrogen Balloon. *Advanced Synthesis & Catalysis* **2007,** *349* (11-12), 2039-2047.

29.   Schulz, J.; Roucoux, A.; Patin, H., Unprecedented efficient hydrogenation of arenes in biphasic liquid-liquid catalysis by re-usable aqueous colloidal suspensions of rhodium. *Chemical Communications* **1999,** (6), 535-536.

30.   Yoon, Y.; Rousseau, R.; Weber, R. S.; Mei, D.; Lercher, J. A., First-principles study of phenol hydrogenation on Pt and Ni catalysts in aqueous phase. *Journal of American Chemical Society* **2014,** *136* (29), 10287-98.

31.   Xiang, Y.; Ma, L.; Lu, C.; Zhang, Q.; Li, X., Aqueous system for the improved hydrogenation of phenol and its derivatives. *Green Chemistry* **2008,** *10* (9), 939-943.

32.   Li, Y.; Fu, J.; Chen, B., Highly selective hydrodeoxygenation of anisole, phenol, and guaiacol to benzene over nickel phosphide. *RSC Advances* **2017,** *7* (25), 15272-15277.

33.   Teles, C.; Rabelo Neto, R.; Duong, N.; Quiroz, J.; Camargo, P.; Jacobs, G.; Resasco, D.; Noronha, F., Role of the Metal-Support Interface in the Hydrodeoxygenation Reaction of Phenol. *Applied Catalysis B Environmental* **2020,** *277*, 119238.

34.   Duce, C.; Vecchio, S.; Ghezzi, L.; Ierardi, V.; Tiné, M., Thermal behavior study of pristine and modified halloysite nanotubes: A modern kinetic study. *Journal of Thermal Analysis and Calorimetry* **2015,** *121*.

35.   Hillier, S.; Brydson, R.; Delbos, E.; Fraser, T.; Gray, N.; Pendlowski, H.; Phillips, I.; Robertson, J.; Wilson, I., Correlations among the mineralogical and physical properties of halloysite nanotubes (HNTs). *Clay Minerals* **2016,** *51* (3), 325-350.

36.   Hamdi, J.; Diehl, B. N.; Kilgore, K.; Lomenzo, S. A.; Trudell, M. L. Halloysite-Catalyzed Esterification of Bio-Mass Derived Acids *American Chemical Society: Omega*, 2019, p. 19437-19441.

37.   Hamdi, J.; Blanco, A. A.; Diehl, B.; Wiley, J. B.; Trudell, M. L., Room-Temperature Aqueous Suzuki–Miyaura Cross-Coupling Reactions Catalyzed via a Recyclable Palladium@Halloysite Nanocomposite. *Organic Letters* **2019,** *21* (10), 3471-3475.

38.   Thomas, J. M., Handbook Of Heterogeneous Catalysis. 2., completely revised and enlarged Edition. Vol. 1–8. Edited by G. Ertl, H. Knözinger, F. Schüth, and J. Weitkamp. *Angewandte Chemie International Edition* **2009,** *48* (19), 3390-3391.

39.   Li, J.; Pan, Z.; Zhou, K., Enhanced photocatalytic oxygen evolution activity by the formation of Ir@IrOx(OH)y core-shell heterostructure. *Nanotechnology* **2018,** *29* (40), 405705.

40.   Rojas, J. V.; Castano, C. H., Radiation-assisted synthesis of iridium and rhodium nanoparticles supported on polyvinylpyrrolidone. *Journal of Radioanalytical and Nuclear Chemistry* **2014,** *302* (1), 555-561.

41.   Goel, A.; Rani, N., Effect of PVP, PVA, and POLE surfactants on the size of iridium nanoparticles. *Open Journal of Inorganic Chemistry* **2012,** *02*.

42.   Zahmakiran, M., Iridium nanoparticles stabilized by metal-organic frameworks (IrNPs@ZIF-8): synthesis, structural properties, and catalytic performance. *Dalton Transactions* **2012,** *41* (41), 12690-12696.

43.   Rueping, M.; Koenigs, R. M.; Borrmann, R.; Zoller, J.; Weirich, T. E.; Mayer, J., Size-Selective, Stabilizer-Free, Hydrogenolytic Synthesis of Iridium Nanoparticles Supported on Carbon Nanotubes. *Chemistry of Materials* **2011,** *23* (8), 2008-2010.

44. Fonseca, G. S.; Machado, G.; Teixeira, S. R.; Fecher, G. H.; Morais, J.; Alves, M. C. M.; Dupont, J., Synthesis, and characterization of catalytic iridium nanoparticles in imidazolium ionic liquids. *Journal of Colloid and Interface Science* **2006,** *301* (1), 193-204.

45. Özkar, S.; Finke, R. G., Iridium(0) Nanocluster, Acid-Assisted Catalysis of Neat Acetone Hydrogenation at Room Temperature: Exceptional Activity, Catalyst Lifetime, and Selectivity at Complete Conversion. *Journal of the American Chemical Society* **2005,** *127* (13), 4800-4808.

46. Wang, D.; Astruc, D., The Golden Age of Transfer Hydrogenation. *Chemical Reviews* **2015,** *115* (13), 6621-6686.

47. Wang, Y.; Yao, J.; Li, H.; Su, D.; Antonietti, M., Highly selective hydrogenation of phenol and derivatives over a Pd@carbon nitride catalyst in aqueous media. *Journal of American Chemical Society* **2011,** *133* (8), 2362-5.

48. De bruyn, M.; Coman, S.; Bota, R.; Parvulescu, V. I.; De Vos, D. E.; Jacobs, P. A., Chemoselective Reduction of Complex α,β-Unsaturated Ketones to Allylic Alcohols over Ir-Metal Particles on β Zeolites. *Angewandte Chemie International Edition* **2003,** *42* (43), 5333-5336.

49. Jiang, H. Y.; Yang, C. F.; Li, C.; Fu, H. Y.; Chen, H.; Li, R. X.; Li, X. J., Heterogeneous enantioselective hydrogenation of aromatic ketones catalyzed by cinchona- and phosphine-modified iridium catalysts. *Angewandte Chemie International Edition* **2008,** *47* (48), 9240-4.

50. Gladiali, S.; Alberico, E., Asymmetric transfer hydrogenation: chiral ligands and applications. *Chemical Society Reviews* **2006,** *35* (3), 226-236.

51. Miecznikowski, J. R.; Crabtree, R. H., Hydrogen Transfer Reduction of Aldehydes with Alkali-Metal Carbonates and Iridium NHC Complexes. *Organometallics* **2004,** *23* (4), 629-631.

52. Yang, J. W.; Hechavarria Fonseca, M. T.; List, B., A metal-free transfer hydrogenation: organocatalytic conjugate reduction of alpha,beta-unsaturated aldehydes. *Angewandte Chemie International Edition* **2004,** *43* (48), 6660-2.

53. N'Ait Ajjou, A.; Pinet, J.-L., The Biphasic Transfer Hydrogenation of Aldehydes and Ketones With Isopropanol Catalyzed by Water-Soluble Rhodium Complexes. *Journal of Molecular Catalysis A-chemical* **2004,** *214*, 203-206.

54. Naskar, S.; Bhattacharjee, M., Ruthenium cationic species for transfer hydrogenation of aldehydes: Synthesis and catalytic properties of $[(PPh_3)_2Ru(CH_3CN)_3Cl]+[A]-$ {A=BPh_4 or ClO_4} *Journal of Organometallic Chemistry* **2005,** *690* (21), 5006-5010.

55. Nomura, K., Transition metal-catalyzed hydrogenation or reduction in water. *Journal of Molecular Catalysis A: Chemical* **1998,** *130* (1), 1-28.

56. Joó, F.; Kathó, Á., Recent developments in aqueous organometallic chemistry and catalysis. *Journal of Molecular Catalysis A: Chemical* **1997,** *116* (1), 3-26.

57. Ledoux, A.; Sandjong Kuigwa, L.; Framery, E.; Andrioletti, B., A highly sustainable route to pyrrolidone derivatives – direct access to biosourced solvents. *Green Chemistry* **2015,** *17* (6), 3251-3254.

58. Du, X.; Liu, Y.; Wang, J.; Cao, Y.; Fan, K., Catalytic conversion of biomass-derived levulinic acid into γ-valerolactone using iridium nanoparticles supported on carbon nanotubes. *Chinese Journal of Catalysis* **2013,** *34* (5), 993-1001.

Conclusion

In summary, this research on halloysite nanotubes led to the development of new nanocomposite systems with tunable properties. These novel nanocomposite systems were successfully employed as highly active heterogeneous catalysts, possessing a greener chemical impact compared to catalysts currently in use. It is reasonable to foresee that Halloysite nanomaterials will emerge as a valuable new heterogeneous catalyst and be employed in many organic transformations in the near future.

With the unique tubular nanostructure, raw halloysite exhibited remarkable chemical reactivity superior to other clays in the esterification of biomass-derived carboxylic acids. Raw halloysite was also effective in the esterification of various aromatic and non-aromatic carboxylic acids. These results indicated that halloysite has the potential utility as a "Green" heterogeneous catalyst for a broad scope of esterification applications.

Extremely useful transition metal@halloysite nanocomposites were developed. A novel Pd@Hal nanocomposite was synthesized under ambient conditions. The newly prepared catalyst was applied to the widely used Suzuki-Miyaura cross-coupling reaction. This nanocomposite material produced exceptionally high yields under ambient conditions. Complete product conversion was obtained with no byproducts using an alcohol: water solvent system at room temperature. It showed excellent results with both hydrophobic/ hydrophilic substrates. The Pd@Hal nanocomposite was also utilized in the hydrogenation reaction of nitro compounds. It exhibited high reaction yields of the corresponding aniline derivatives under very ambient conditions. The catalyst was shown to be recoverable and recyclable in both reaction systems without significant loss of catalytic activity.

In addition, a reliable method was also developed for the preparation of the Ir@Hal nanocomposite. The Ir@Hal catalyst was very efficient for the hydrogenation and transfer hydrogenation of phenol to furnish cyclohexanol. Also, Ir@Hal effectively hydrogenated various aldehydes and ketones with a broad scope of substrates under very ambient conditions. The catalyst was shown to be recoverable and recyclable without significant loss of catalytic activity for both the hydrogenation of phenol and cyclohexanone to yield cyclohexanol.

These M@Hal nanocomposites proved to be robust and stable under a variety of reaction conditions. Furthermore, as catalysts, these M@Hal nanocomposites afforded high yields, were amenable to scalable conditions, and exhibited incredible rate enhancement for various organic transformations. In addition, These M@Hal nanocomposites demonstrated the further utility of halloysite as a support for the development of transition metal-based nanocomposite for heterogeneous catalysis having all the advantages of easy separation, easy recovery, and excellent solubility/dispersion. These novel heterogeneous materials undoubtedly have a fundamental role in the development of new sustainable industrial and pharmaceutical processes.

Vita

The author is originally from Damascus, Syria. She was born in Riyadh, Saudi Arabia, on November 25, 1986. She migrated to the United States in 1999. She graduated high school from Broadmoor High in 2004. She received her Bachelor of Science degree in Chemistry from The University of New Orleans, New Orleans, in 2015. With love for chemistry and a passion for teaching and research, she ultimately attended the University of New Orleans, obtaining a Master of Science in Chemistry in 2019. She continued her graduate studies and completed the Doctor of Philosophy in Organic Chemistry requirements in May 2021 under the supervision of Distinguished Professor Dr. Mark L Trudell.